Exotic Phenomenology of DFSZ Axion Models

Dissertation submitted for the award of the title
"Doctor of Natural Sciences"
to the Faculty of Physics, Mathematics and Computer Science of
Johannes Gutenberg University Mainz

Julien Laux
born in Boppard, Germany

Mainz, August 23, 2023

JOHANNES GUTENBERG UNIVERSITÄT MAINZ

JG|U

Date of submission: 23.08.2023
Date of examination: 18.01.2024

For my family

"Sapere aude! - Dare to know!"

Immanuel Kant

"A physicist is just an atom's way of looking at itself."

Niels Bohr

"The ultimate answer to life, the universe and everything is ... 42!"

Douglas Adams, The Hitchhiker's Guide to the Galaxy

Abstract

In this thesis we introduce exotic properties of the highly motivated axion particle which lead to a better accessibility in experimental searches. The axion is an essential ingredient of theories beyond the Standard Model of particle physics (SM) which aim to solve the strong CP problem manifesting in the absence of an electric dipole moment of the neutron (nEDM).

The axion is mainly characterized by its mass m_a and its coupling to SM particles with a special emphasis on the axion-diphoton coupling $G_{a\gamma\gamma}$. Our focus lies on axion models which fall into the class of the Dine-Fischler-Srednicki-Zhitnitsky (DFSZ) construction which is specified by direct axion-fermion couplings. This is in contrast to the Kim-Shifman-Vainshtein-Zakharov model which only accounts for axion couplings to gauge bosons.

While the first part of this work is dedicated to new effects which arise in the axion potential with an influence on m_a, the second part deals with new interactions described within an effective field theory framework. These interactions comprise enhanced axion fermion couplings induced by a Dark Matter scalar field as well as axion couplings to the Higgs and Z boson which are generated through kinetic mixing effects in gauged $U(1)'$ extensions.

On one hand, the axion potential is sensitive to corrections by instanton and QCD effects, leading to a constant shift in the axion mass. On the other hand, additional operators which explicitly break the global Peccei-Quinn symmetry associated to the axion have a more severe impact. We show that these operators can lead to a much lighter axion mass than expected from traditional models. Taking into account current nEDM bounds, we estimate the maximal extent of the DFSZ-line in the $\{m_a, G_{a\gamma\gamma}\}$-plane. Under the use of a UV completion we provide an example which naturally induces these effects.

Heavy new particles induce effective axion interactions at energies below their mass scale which we calculate in a general framework accounting for possible flavor-changing effects in the fermion couplings. We show that these effective operators can be generated from a heavy Dark Matter field and lead to a chiral enhancement in the fermion couplings. Constraining our parameter space under the use of Dark Matter effects, we find that the axion interactions to charged leptons and heavy up-type quarks can naturally be enhanced by a factor of order $\mathcal{O}(10-100)$ while couplings to light quarks and neutrinos are barely enhanced.

Finally, we present non-trivial mixing effects between axions and additional $U(1)'$ gauge bosons, leading to a reduced parameter space as the mass of the additional gauge boson $m_{Z'}$ depends on the properties of the axion field. We demonstrate the phenomenological consequences in a gauged baryon number extension and constrain the parameter space in the mass vs. coupling planes on the basis of collider data from ATLAS and CMS.

List of Publications

This thesis is based on the following list of projects, of which three papers [1–3] are already published and two in preparation [4, 5]. We provide a brief overview of the topics and highlight the authors's contributions.

[1] A. Kivel, J. Laux and F. Yu, *Supersizing axions with small size instantons*, *JHEP* **11** (2022) 088 [2207.08740].

At collider scales, the QCD axion in its canonical form is already excluded. Nevertheless, effects from additional $SU(N)$ gauge groups which confine at a high energy scale can lead to small size instanton (SSI) effects. These SSI effects affect the relation between the axion mass m_a and the decay constant f_a allowing for a shift of the QCD axion band to higher masses for fixed f_a. This includes a region which is accessible by collider experiments.

In our work we calculate these effects quantitatively with a new approach by using the t'Hooft determinantal operator. The calculation involves the diagonalization of the mass matrix of the pseudoscalar particles such as the axion, the pion, the η', and an additional axieta. We present our results in the mass vs. diphoton coupling-plane with two bands for the axion and the axieta covering the parameter space for collider searches. The author constructed an order by order analysis for the eigenvalues and derived several limiting cases to compare with established results and to point out the main dependences on our parameters.

[2] A. Kivel, J. Laux and F. Yu, *Axion couplings in gauged U(1)' extensions of the Standard Model*, *JHEP* **03** (2023) 078 [2211.12155].

The Standard Model Lagrangian is invariant under two anomalous global $U(1)$ symmetries related to baryon number conservation and lepton number conservation. These symmetries can be protected by being gauged, involving a new gauge boson which we call Z'. Since anomalous symmetries cannot be gauged, we need to introduce new heavy fermions which cancel the gauge anomalies and are therefore called anomalons.

The author constructed a UV completion which gives both, a Z' from gauged baryon number, as well as a DFSZ-type axion-like particle (ALP) which is characterized by its direct coupling to SM fermions through a two Higgs doublet model. Integrating out the heavy anomalons leads to an effective theory of the ALP which contains new and enhanced operators such as an ALP coupling to photon and Z' or to Higgs and Z boson. The author was also responsible for performing the calculations in a general way accounting for possible flavor-violating ALP couplings and defining a basis which is invariant under chiral fermion transformations. In the end, we constrain our model by comparing simulated cross sections with recent LHC measurements. Here, the author provided the calculation for the branching ratios of the ALP and Z' decays as well as the `FeynRules` model which was implemented in `MadGraph5_aMC@NLO` for our simulation.

[3] F. Elahi, G. Elor, A. Kivel, J. Laux, S. Najjari and F. Yu, *Lighter QCD axion from anarchy*, *Phys. Rev. D* **108** (2023) L031701 [2301.08760].

A problem which many axion models must face is the axion quality problem: In order to solve the strong CP problem exactly, we cannot have additional terms which break the associated anomalous, global Peccei-Quinn (PQ) symmetry. However, for example, gravity effects would break global symmetries and lead therefore to a misalignment in the strong CP phase, spoiling the axion solution to the strong CP problem.

In this work, we explore the effects of a term which breaks the PQ symmetry softly but is still consistent with current nEDM measurements. We find in the case of the DFSZ model that this leads to changes in the low m_a region of the QCD axion band, allowing us to find the axion at a lower mass for constant f_a, and to set an upper bound on f_a. In this project, the author constructed a general potential for a toy model as well as for the DFSZ model. In addition, the author calculated the mass basis of the Goldstone bosons and pointed out the new f_a dependence. Finally, we implemented the result into the axion diphoton coupling.

[4] J. Laux, S. Najjari and F. Yu, *in preparation.*

Besides the axion-diphoton coupling, experimental data also provide constraints for other axion couplings, especially axion couplings to fermions. Analogously to the theoretical approaches to solve the muon g-2 tension, we can consider chirally enhanced axion-fermion couplings by introducing an additional heavy fermion and heavy scalar.

We work out the manifestations of chiral enhancement in KSVZ and DFSZ models and use constraints from colliders and Dark Matter (DM) observables for the heavy scalar to identify new parameter space. The author's part was to define the corresponding model and to describe the chiral enhancement as well as flavor changing effects. In addition, the author estimated the chiral enhancement in the DFSZ model accounting for DM effects and tested an alternative model involving neutrino masses.

[5] A. Kivel, J. Laux and F. Yu, *in preparation.*

We discovered in our project [3] that PQ-breaking operators can lead to a much lighter axion than in traditional approaches. However, our solution was still subject to the axion quality problem, since we only achieved a sizable deviation from the canonical QCD axion band for extreme values of the CP-violating parameters in the UV.

In this project, we construct a UV completion for the anarchic axion model which avoids generating a new fine-tuning problem under the help of a Nelson-Barr model extension. In addition, we present possible origins of the additional PQ-breaking operator. The author helped identifying the required field content and constructed a mechanism which provided the additional PQ-breaking operator.

If not stated otherwise, the figures presented in this thesis were created by the author himself. Figures which were produced by collaborators refer to the respective paper. Some figures were recreated to achieve a uniform color scheme and plot layout. Feynman

diagrams in this thesis were produced using `JaxoDraw` [6]. We performed our calculations primarily with the help of `Mathematica` [7] where we used the packages `Package X` [8] and `FeynRules` [9]. We simulated collider and DM data using `MadGraph5_aMC@NLO` [10] and `micrOMEGAS-5.3` [11].

Contents

Prologue

CHAPTER I

Introduction

Over the last century, our understanding of the universe and its tiniest constituents has undergone remarkable progress. We learned that atoms were composed out of elementary particles which interact via fundamental force carriers and that radiation from the depths of our universe provides information about the origins of our universe. Furthermore, we gained the knowledge to reproduce the conditions of the early universe in experiments like the Large Hadron Collider (LHC).

All these achievements would not have been possible without an underlying theory as a mathematical description that allows us to formulate our expectations as measurable observables. The most successful theory which explains the processes in the atom with incredible precision was constructed more than fifty years ago and is called the Standard Model (SM) of particles physics. One of the most important predictions of the SM was the existence of the Higgs boson, which was finally observed in 2012 at the LHC [12, 13].

Despite its tremendous success, there is various evidence of an incompleteness of the SM. Phenomena that are observed but not described by the SM include, for example, gravity, Dark Matter (DM), Dark Energy, neutrino masses, or the asymmetry between matter and anti-matter. On the other hand, there are phenomena that are generally expected in the SM but are not observed in nature. One important example is the absence of an electric dipole moment of the neutron (nEDM).

The nEDM is an observable associated with the behavior of the strong nuclear force under charge conjugation C and parity inversion P. The SM incorporates two mechanisms, instantons and chiral fermion transformations, which lead to an asymmetry under a CP transformation, quantified by a CP violating angle $\bar{\theta}$. This angle induces an nEDM and is constrained to $\bar{\theta} < 10^{-10}$ [14]. Hence, the two contributions from instantons and chiral fermion transformations cancel out, hinting toward a new symmetry beyond the SM.

The most extensively studied solution to this strong CP problem was proposed by Roberto Peccei and Helen Quinn in 1977 [15, 16] and is therefore called the Peccei-Quinn (PQ) mechanism. It is based on a spontaneously broken global symmetry at high energies that renders $\bar{\theta}$ dynamically to zero. Of particular interest in this mechanism is the prediction of a new particle, the axion [17, 18].

The axion is characterized by its mass m_a and its decay constant f_a which follow the constant relation $m_a^2 f_a^2 \equiv \Lambda_{\mathrm{QCD}}^4$ determined by effects from quantum chromodynamics (QCD), the theory of the strong nuclear interactions. The couplings of the axion to the fundamental particles of the SM are described by two classes of models, which are called Kim-Shifman-Vainshtein-Zakharov (KSVZ) and Dine-Fischler-Srednicki-Zhitnitsky (DFSZ). In KSVZ constructions [19, 20] the axion only couples to the force carriers of

the SM with special attention on the axion-diphoton coupling $G_{a\gamma\gamma}$, which is inversely proportional to f_a. On the other hand, DFSZ models [21,22] include additional interactions with the fermionic matter fields in the SM.

Since the axion was proposed, there has been an extensive effort to prove its existence in the laboratory and with astronomical observations. Various experiments search for the axion in the sun (Helioscopes), in the local DM density (Haloscopes), behind walls ("Light-shining-through-wall"), or at colliders. The challenges of all these experiments are, on one hand that the axion can acquire masses within the whole mass range from almost massless up to collider scale masses. On the other hand, the couplings to SM particles become much weaker for small axion masses due to their inverse f_a scaling.

This brings us to ask the following question, whether these challenges are generic for the axion or whether other known effects beyond the SM modify our expectations, leading to better accessibility of the axion in experiments. In this thesis, we pursue this question within the DFSZ axion model, where we present different methods to either change the axion mass or its couplings.

In order to find possible modifications of the axion mass, we want to investigate the impact of additional operators which break the PQ-symmetry explicitly. These kinds of operators are in general expected from gravity effects and change the potential in such a way, that the minimum is moved out of the CP conserving phase, leading to a quality problem of the axion [23]. In our work, we pursue the idea that these operators could also change the canonical axion mass relation as long as the residual CP violating phase is still consistent with the nEDM bound.

In the second project, we intend to learn about enhancement effects in axion-fermion couplings. We address the question of whether axions are sensitive to chiral enhancement effects, which were analogously motivated to solve the tension in the muon magnetic dipole moment. In particular, we want to know whether a heavy DM scalar or heavy right-handed neutrinos can induce such effects and how we can estimate the enhancement.

Lastly, we search for new effects arising in axion models that also involve an additional $U(1)'$ gauge symmetry. We aim to include kinetic mixing effects and incorporate effective interactions induced by heavy fermions, which are needed to cancel gauge anomalies and are therefore called anomalons. In order to constrain the associated observables, we apply our results to collider data from LHC experiments.

We organize this thesis in the following way: First, we present in Chapter II the theoretical background of our work, where we introduce the SM and the original axion extensions. We then move on with part I about modifications of the axion potential. In this part, we first provide in Chapter III a general discussion about contributions to the axion potential from complex scalar fields, Yukawa interaction to fermions, and instanton effects. Afterwards, we use this description in Chapter IV to define a class of axions with exceptionally light masses that solve the strong CP problem with in current nEDM bounds.

The second part of this thesis dedicates exotic axion couplings primarily induced by new heavy particles. Hence, we describe the resulting interactions in an effective field theory (EFT) framework and calculate the respective Wilson coefficients in Chapter V. In Chapter VI we derive one-loop effects which chirally enhance axion-fermion couplings and constrain the parameter space by using DM bounds on the heavy fields. Another application of the EFT framework is presented in Chapter VII where we introduce a new Z' gauge boson associated with a gauged version of baryon number along with heavy anomalons generating new axion couplings to various bosons. Finally, we conclude our work in Chapter VIII.

CHAPTER II

Theoretical Background

In this chapter we present the context and motivation of this thesis within the field of high-energy physics. The research which is pursued in the field is driven by the questions of how the world works in its smallest components and how the universe evolved to provide an environment in which stars and planets can form to pave the way for a habitable earth.

There are two main concepts which allow us to find the answers to these questions at high energies: special relativity and quantum mechanics. Special relativity postulates that light travels with a constant velocity $c \equiv 299792458\text{m/s}$, such that cosmic radiation opens a window to the past as the light we see now was emitted at an earlier stage of the universe. Observations like the cosmic microwave background (CMB) lead to the conclusion, that the universe used to be at a much denser and hotter stage, a stage of high energies.

Quantum mechanics on the other hand tells us that there is a minimal uncertainty between the measurements of distances and momenta, $\Delta x \times \Delta p \geq \hbar/2$, set by Planck's constant $2\pi\hbar \equiv 6.62607015 \times 10^{-34}\text{Js}$. Together with the relation between energy, mass, and momentum in special relativity, $E^2 = p^2c^2 + m^2c^4$, it signifies that phenomena at very small distances can only be described by theories at very high energies. Since relativistic effects play an important role at these energies, we use the framework of a relativistic quantum field theory (QFT) to formulate a theory of high-energy physics, describing the behavior of physical particles as quantum fields.

The model which describes the behavior of the known fundamental particles best is called the Standard Model of particle physics (SM). In fact, it is so successful that precision experiments have not been able to rule out the SM so far, but observations showed an incompleteness in multiple aspects. The research area which aims to find completions of the SM is called physics beyond the Standard Model (BSM).

In order to test the SM and search for new building blocks of a more complete theory of high energy physics, there are two ways of building up experiments. The first option is to use signals which nature provides from the depths of the universe. For this purpose we can use telescopes which capture the light from distant stars and galaxies as well as primordial radiation like the CMB. More recently we can also use earth based detectors to detect gravitational waves and cosmic particles like neutrinos as messengers from the early universe.

On the other hand, we can invent technical machines which produce and accelerate particles at very high energies, therefore simulating the conditions which were present in the beginnings of the universe. The facility which reaches the highest particle energies up to now was built in Geneva by the European Organization for Nuclear Research (CERN) and is called the Large Hadron Collider (LHC).

In the following we present in section II.1 the historical evolution of the SM and the state of the art in high-energy physics introducing open problems which can not be solved within the framework of the SM. In section II.2 we then build up the formal description of the SM as a QFT on the Lagrangian level. Finally, in section II.3 we introduce the BSM theory of an axion which was invented originally to solve the strong CP problem of the SM.

II.1 The Standard Model of Particle Physics

The field of particle physics began to evolve when Ernest Rutherford discovered in 1911 [24] that atoms are composed out of a heavy nucleus and a light shell consisting of subatomic particles. The force which binds the two components together is given by the electric force between the positively charged protons (p) in the nucleus and the negatively charged electrons (e) in the shell. This force is mediated by photons (γ) which also transmit energy between different atoms through their role as electromagnetic radiation observed as visible light in the optical frequency spectrum.

The atomic nucleus is characterized by two numbers, the nuclear charge number Z and the atomic mass number A. These two numbers provide information of the content of subatomic particles in the nucleus: The number of positively charged protons (p^+) is given by Z, while the difference $A-Z$ specifies the number of electrically neutral neutrons (n^0). Since neutrons are slightly heavier than protons, they can decay via the β-decay into a proton and an electron, hence increasing Z by one unit.

The behavior of the nucleus required an explanation involving two new forces. The "strong" nuclear forces binds protons and neutrons together. It is mediated by pions (π) and was first described by Hideki Yukawa in 1935 [25]. The "weak" nuclear force mediates the β-decay and was theorized by Enrico Fermi in 1933 [26, 27] as a contact interaction involving an additional charge- and mass-less particle, the neutrino (ν). Both new particles could later be experimentally observed, the pion in 1947 [28] and the neutrino in 1956 [29].

The next step was to formulate the nuclear forces within the framework of a QFT. The underlying theory of the strong force is called quantum chromodynamics (QCD). It postulates that the nucleons p^+, n^0 as well as the pions consist of fundamental particles, the quarks (q) [30, 31]. Quarks are characterized by two properties, color and flavor. Color is responsible for binding quarks together and is mediated by mass-less gluons (g), whereas flavor categorizes masses and electrical charges of quarks. Up-type quarks have an electrical charge of $2/3$ and are called up, charme and top (u, c, t) ordered by increasing mass, while down, strange and bottom (d, s, b) represent down-type quarks with a charge of $-1/3$.

The weak force was unified with the electric force to an electroweak force coming along with three new mediator particles, the electrically charged $W^\pm$ bosons and the neutral Z^0 boson [32]. These weak mediators have high masses, and therefore energies which are much heavier than the momentum transfer in the β-decay. An external observer is therefore not able to resolve their impact, leading to the aforementioned description of Fermi's theory as a contact interaction. The mathematical procedure of removing high-energy modes from a low-energy theory is called "integrating out" the heavy fields and the the resulting theory is described as an effective field theory (EFT).

The weak interaction is able to change the flavor of quarks through the charged W interaction. It also couples to three generations of leptons, which comprise the electrically charged electron, muon and tau (e, μ, τ) as well as three respective neutrinos $(\nu_e, \nu_\mu, \nu_\tau)$.

However, in 1956 Chien-Shiung Wu demonstrated that the weak interaction violates parity by only coupling to neutrinos with a spin-projection opposite to the momentum direction [33]. Hence, the weak interaction effects only particles with left-handed chirality and possible right-handed neutrinos remained unobservable.

The chiral behavior and the short range of the weak interaction were difficult to explain within the framework of a QFT, since matter fields (fermions) with chiral interactions and mediator fields (gauge bosons) were considered to be massless to preserve a gauge symmetry in the QFT. In order to solve this problem, three independent groups proposed a new particle which gives a mass to both, fermions and gauge bosons, while breaking the gauge symmetry of the QFT [34–36]. This particle was later named Higgs particle (h) after one of the inventors.

With this new ingredient, Steven Weinberg and Abdus Salam were able to finalize the electroweak theory [37, 38] which then together with QCD formed the Standard Model of Particle Physics (SM). The discovery of the Higgs particle by the ATLAS and CMS collaborations at the Large Hadron Collider (LHC) in 2012 [12, 13] completed the particle spectrum of the SM, leaving the SM as the most successful theory in high-energy physics, which still is consistent with the overwhelming majority of precision measurements.

fermions $s = \frac{1}{2}$	leptons $Q = 0$	ν_e $m_{\nu_e} < 1.0$ eV/c^2	ν_μ $m_{\nu_\mu} < 0.19$ MeV/c^2	ν_τ $m_{\nu_\tau} < 18.2$ MeV/c^2
	leptons $Q = -1$	e $m_e = 0.511$ MeV/c^2	μ $m_\mu = 105.658$ MeV/c^2	τ $m_\tau = 1.776$ GeV/c^2
	quarks $Q = \frac{2}{3}$	u $m_u = 2.16$ MeV/c^2	c $m_c = 1.27$ GeV/c^2	t $m_t = 172.69$ GeV/c^2
	quarks $Q = -\frac{1}{3}$	d $m_d = 4.67$ MeV/c^2	s $m_s = 93.4$ MeV/c^2	b $m_b = 4.18$ GeV/c^2
bosons $s = 0, 1$	electroweak $s = 1$	γ $m_\gamma = 0$	Z^0 $m_Z = 91.188$ GeV/c^2	$W^\pm$ $m_W = 80.377$ GeV/c^2
	gluons $s = 1$	g $m_g = 0$	Higgs $s = 0$	h $m_h = 124.97$ GeV/c^2
bound states	baryons $s = \frac{1}{2}$	n^0 $m_n = 0.939$ GeV/c^2	p^+ $m_p = 0.938$ GeV/c^2	...
	mesons $s = 0$	π^0 $m_\pi = 134.976$ MeV/c^2	$\pi^\pm$ $m_{\pi^\pm} = 139.570$ MeV/c^2	...

Table II.1: Overview of SM particles and light QCD bound states. The table contains mass m, electric charge Q and spin s of all SM fermions and gauge bosons as well as the lightest baryons and mesons which are composed out of up- and down-quarks. The masses are given up to three decimal places and can be found in reference [39].

Table II.1 gives an overview of the particles of the SM and some noteworthy low-energy bound states. It contains the masses of the particles as well as their electrical charge and spin. We express masses of particles in units of eV, referring to the kinetic energy of a single electron with elementary charge $1\text{e} \equiv 1.602176634 \times 10^{-19}\text{C}$ which is accelerated from rest in an electric potential of 1V. Hence, the conversion factor into the International System of Units (SI) is given by $1\text{eV}/c^2 = 1.78266192 \times 10^{-36}\text{kg}$. For the remainder of the thesis we use natural units, for which we set the fundamental constants to $c = 1 = \hbar$.

II.1.1 Open Problems and New Physics

Although precision measurements strongly support the SM, there are several observations which hint towards an incompleteness of the SM. First of all, there is the simple observation that there is gravity [40]. The gravitational force has not yet been described by the SM and has its own fundamental theory called general relativity (GR) [41]. It is widely believed that in agreement with the weakness of the gravitational force, quantum effects would play an important role at energies above the Planck mass $M_{\mathrm{Pl}} \approx 1.2209 \times 10^{19}$ GeV [39], where a theory of quantum gravity is needed.

Important applications of GR comprise the description of gravitational waves as well as the expansion of the universe through a cosmological constant. It also gives a prediction for the rotation curves of galaxies which is in tension with the observations. This leads to the conclusion that there are matter particles which do not have interactions described by the SM and are therefore called Dark Matter (DM).

Another area which reveals open problems of the SM is the cosmological evolution of the universe. One important source of information in this field is the CMB, which was emitted 380000 years after the Big Bang. It shows temperature anisotropies in the angular power spectrum which can be fitted under the use of the ΛCDM model [42], where Λ represents the cosmological constant and CDM stands for cold Dark Matter. It not only supports the existence of DM and a cosmological constant but also gives an estimate of the energy budget of the universe. Within this energy budget, ordinary (mainly baryonic) matter makes up 4.9%, Dark Matter provides 26.8% and dark energy given by the cosmological constant contributes with 68.3% [39].

It is also evident that there is an asymmetry between matter and anti-matter, since we predominantly observe matter particles in nature but not their corresponding anti-particles. To account for this asymmetry, the cosmological evolution of the universe has to fulfill the Sakharov conditions [43] which include the violation of baryon number B, CP violation and interactions out of thermal equilibrium. The process which leads to the asymmetry between matter and anti-matter is called baryogenesis and relies on BSM extensions, since there is not enough B and CP violation within the SM.

Lastly, there are problems concerning parameters which are predicted by the SM but are observed differently. Most relevant for this thesis is the strong CP problem concerning the absence of CP violation in QCD manifesting in an apparently vanishing electric dipole moment (EDM) of the neutron [14]. This is surprising as the SM contains two mechanisms which lead to a CP violation in the strong sector as we will see in subsection II.2.2.

Another contradiction was found in neutrino physics. Since right-handed neutrinos are unobserved, the neutrinos remain as the only purely left-handed particles and are described mass-less within the SM. However, the observed phenomenon of neutrino oscillations [44] can only be explained by having massive neutrinos, which require BSM extensions with additional particle content.

A discrepancy is also present for the anomalous magnetic dipole moment of the muon. Recent studies show a deviation between theoretical expectation and experimental observation of 4.2σ [45]. This gap provides room for BSM theories involving heavy fields which are integrated out. Of course there are many more open problems, but to mention all of them would clearly lead far beyond the scope of this thesis.

II.2 Formalism of the Standard Model

In order to calculate measurable observables we formulate our models as field theories, characterized by their Lagrangian. The fundamental Lagrangian of a theory contains all possible operators $\mathcal{O}_i$ of interactions between particles respecting the gauge symmetry which are renormalizable for four space-time dimensions,

$$\mathcal{L} \supset \sum_{d\leq 4} \sum_i \frac{C_i}{\Lambda^{d-4}} \mathcal{O}_i^{\dim=d} \,, \tag{II.1}$$

with dimensionless couplings C_i and mass scale Λ. Higher dimensional operators ($d \geq 5$) will be regarded as effective interactions, which are suppressed by a UV mass scale $\Lambda \gg m_t$. A renormalizable theory at the corresponding UV mass scale is called a UV completion of the effective theory.

We distinguish three types of particles, varying by their spin properties. Fermions are spin-1/2 particles which are formally represented by spinors ψ. In the case of the SM these are quarks and leptons. Gauge bosons are spin-1 particles, described by 4-vectors in space-time A_μ^a, where the group index a refers to the generators of the corresponding gauge group. These vector bosons respect a gauge symmetry, where the physics is invariant under a transformation $A_\mu \to A_\mu + \partial_\mu \alpha$ in the case of a $U(1)$ gauge group. Massless gauge bosons as photons and gluons have two transversal polarization modes, while massive gauge bosons as W and Z bosons have a third, longitudinal mode. Finally, spin-0 particles like the Higgs boson are expressed by (in general complex) scalar fields Φ.

For example, for a theory containing a fermion ψ with mass m respecting an $SU(N)$ gauge symmetry with gauge coupling g, the (classical) Lagrangian can be written as

$$\mathcal{L} \supset \bar{\psi}(i\not{D} - m)\psi - \frac{1}{4} F^a_{\mu\nu} F^{a\mu\nu} \,, \tag{II.2}$$

where $D_\mu = \partial_\mu + igt^a A^a_\mu$ is the covariant derivative and $F^a_{\mu\nu} = \partial_\mu A^a_\nu - \partial_\nu A^a_\mu + g f^{abc} A^b_\mu A^c_\nu$ the field strength tensor. The structure constants f^{abc} depend on the generators t^a of the gauge group and vanish in the abelian $U(1)$ case. We implicitly sum over Lorentz indices and group indices by using the Einstein sum convention.

Physical observables can then be calculated with a path integral, which gives the vacuum expectation value of the time-ordered product of an operator $\mathcal{O}$ via

$$\langle \Omega | \, T\{\mathcal{O}(x_1, ..., x_n)\} \, | \Omega \rangle = \frac{1}{Z[0]} \int \mathcal{D}\psi \int \mathcal{D}\bar{\psi} \int \mathcal{D}A^a_\mu \mathcal{O}(x_1, ..., x_n) \exp(iS) \,, \tag{II.3}$$

where Ω denotes the physical vacuum and $S = \int d^4x \mathcal{L}$ describes the action. The generating functional Z is defined by

$$Z[\eta, \bar{\eta}, J^a_\mu] = \int \mathcal{D}\psi \int \mathcal{D}\bar{\psi} \int \mathcal{D}A^a_\mu \exp\left(iS[\psi, \bar{\psi}, A^a_\mu] + i \int d^4x (\bar{\psi}\eta + \bar{\eta}\psi + J^a_\mu A^{a\mu}) \right) ,$$

where η, $\bar{\eta}$ and J^a_μ represent classical source fields.

We notice that symmetries of the classical Lagrangian are not necessarily symmetries of the quantized theory. Especially, the total derivative of the Chern-Simons current [46]

$$K^\mu = 2\epsilon^{\mu\nu\alpha\beta} (A^a_\nu \partial_\alpha A^a_\beta + \frac{g}{3} f^{abc} A^a_\nu A^b_\alpha A^c_\beta) \tag{II.4}$$

can change the action by a topological winding number

$$\delta S = \frac{g^2}{32\pi^2}\int d^4x \partial_\mu K^\mu \quad \Rightarrow \quad \delta\mathcal{L} = \frac{g^2}{32\pi^2}\frac{1}{2}\epsilon^{\mu\nu\alpha\beta}F^a_{\mu\nu}F^a_{\alpha\beta} = \frac{g^2}{32\pi^2}F^a_{\mu\nu}\tilde{F}^{a\mu\nu}\,. \tag{II.5}$$

A gauge field configuration which changes the winding number is called an instanton. The true vacuum is given by a superposition of all possible classes of instanton configurations and is parametrized by an angle $\theta \in \{0, 2\pi\}$, giving an effective term $\theta \times \delta\mathcal{L}$ in the Lagrangian.

The same term can be generated through anomalous fermion transformations of the form

$$\psi \to e^{-i\frac{X}{2}\alpha\gamma_5}\psi, \quad \bar{\psi} \to \bar{\psi}e^{-i\frac{X}{2}\alpha\gamma_5}\,. \tag{II.6}$$

This transformation changes the fermionic path integral measure in the partition function. The resulting Jacobian factor has to be regularized following Fujikawas method [47], which leads to a shift proportional to $\delta\mathcal{L}$ in the Lagrangian.

In particular, the fermionic part of the Lagrangian changes after such an anomalous transformation to

$$\bar{\psi}(i\partial\!\!\!/ - m)\psi \to \bar{\psi}i\gamma^\mu\partial_\mu\psi + \frac{X}{2}(\partial_\mu\alpha)\bar{\psi}\gamma^\mu\gamma_5\psi - \bar{\psi}me^{-iX\alpha\gamma_5}\psi - 2\alpha\mathcal{A}_{XQQ}\times\delta\mathcal{L}\,, \tag{II.7}$$

where $\mathcal{A}_{XQQ}$ denotes the anomaly coefficient

$$\mathcal{A}_{XQQ} = T(R)(X_L Q_L^2 - X_R Q_R^2) = \begin{cases} XQ^2 & U(1) \\ X/2 & SU(N) \end{cases}\,. \tag{II.8}$$

Here, we considered the fermion to transform vector-like under the gauge symmetries ($Q_L = Q_R$) and $T(R)$ represents the Dynkin index [48] of a representation R, $\mathrm{tr}\left[T^a_R T^b_R\right] \equiv T(R)\delta^{ab}$. In section V.1 we will generalize the anomalous transformations to multiple flavors and different chiralities.

II.2.1 Standard Model Lagrangian

In order to analyze the interactions of the different particles in the SM, we split the Lagrangian of the SM into four parts,

$$\mathcal{L}^{\mathrm{SM}} \supset \mathcal{L}^{\mathrm{SM}}_{\mathrm{gauge}} + \mathcal{L}^{\mathrm{SM}}_{\mathrm{scalar}} + \mathcal{L}^{\mathrm{SM}}_{\mathrm{fermion}} + \mathcal{L}^{\mathrm{SM}}_{\mathrm{Yukawa}}\,, \tag{II.9}$$

where $\mathcal{L}^{\mathrm{SM}}_{\mathrm{gauge}}$ describes the kinetic part of the gauge bosons, $\mathcal{L}^{\mathrm{SM}}_{\mathrm{scalar}}$ the kinetic part and potential of the scalar Higgs boson, $\mathcal{L}^{\mathrm{SM}}_{\mathrm{fermion}}$ the kinetic part of the fermions and $\mathcal{L}^{\mathrm{SM}}_{\mathrm{Yukawa}}$ the Yukawa interactions between the fermions and the Higgs.

The underlying gauge symmetry of the SM is given by

$$\mathcal{G}^{\mathrm{SM}}_{\mathrm{gauge}} = SU(3)_C \times SU(2)_L \times U(1)_Y\,, \tag{II.10}$$

where $SU(3)_C$ represents the color gauge group of QCD and $SU(2)_L \times U(1)_Y$ the electroweak gauge group containing the left-handed gauge group and hypercharge Y.

For each subgroup of the SM gauge group we have a set of gauge bosons, one for each generator. The kinetic terms including possible self-interactions can then be written under the use of the field strength tensors

$$\mathcal{L}^{\mathrm{SM}}_{\mathrm{gauge}} \supset -\frac{1}{4}B_{\mu\nu}B^{\mu\nu} - \frac{1}{4}W^a_{\mu\nu}W^{a\mu\nu} - \frac{1}{4}G^a_{\mu\nu}G^{a\mu\nu} + \theta_{\mathrm{QCD}}\frac{g_s^2}{32\pi^2}G^a_{\mu\nu}\tilde{G}^{a\mu\nu}\,, \tag{II.11}$$

with $\tilde{G}^{a\mu\nu} = 1/2\epsilon^{\mu\nu\alpha\beta}G^a_{\alpha\beta}$. We neglect possible θ terms for $SU(2)_L$ and $U(1)_Y$ since they appear to be unphysical as we will see in the next subsection.

Next, we have the scalar part of the SM Lagrangian, consisting of the kinetic part which is described by a covariant derivative $D_{H,\mu}$ containing gauge interactions, and a quartic potential with coupling λ,

$$\mathcal{L}^{\text{SM}}_{\text{scalar}} \supset |D_{H,\mu}H|^2 - \lambda\left(|H|^2 - \frac{v^2}{2}\right)^2 . \tag{II.12}$$

We account for gauge invariance by only having absolute value squares in the scalar Lagrangian. The quartic potential has its minima away from $|H| = 0$ leading to a vacuum expectation value (vev) $\langle|H|\rangle = v/\sqrt{2}$. This vev breaks the gauge symmetry as we will see in the next subsection.

We describe the fermions as chiral fields in the Weyl representation, such that we can treat the gauge interactions for left- and right-handed fields separately. The kinetic terms including the gauge interactions then read

$$\mathcal{L}^{\text{SM}}_{\text{fermion}} \supset i\bar{Q}^i_L \not{D}^{ij}_Q Q^j_L + i\bar{L}^i_L \not{D}^{ij}_L L^j_L + i\bar{u}^i_R \not{D}^{ij}_u u^j_R + i\bar{d}^i_R \not{D}^{ij}_d d^j_R + i\bar{e}^i_R \not{D}^{ij}_e e^j_R \,, \tag{II.13}$$

where $L_L = (\nu_L, e_L)^T$ and $Q_L = (u_L, d_L)^T$ represent the left-handed doublets which transform under the left-handed $SU(2)_L$ gauge group.

Each fermion has a flavor index $i \in 1, 2, 3$ which runs over the number of fermion generations N_g. Each generation has the same quantum numbers and transformation properties, shown in Table II.2.

	$SU(3)_C$	$SU(2)_L$	$U(1)_Y$
Q^i_L	3	2	1/6
u^i_R	3	1	2/3
d^i_R	3	1	-1/3
L^i_L	1	2	-1/2
e^i_R	1	1	-1
H	1	2	1/2

Table II.2: Fermionic and scalar field content of the SM. Shown are the transformation properties under the SM gauge groups for three generations of Weyl fermions with flavor index i. Quarks transform fundamentally under the color gauge group $SU(3)_C$, denoted by a "3", while left handed fields transform fundamentally ("2") under the weak gauge group $SU(2)_L$. The last column contains the hypercharges Y of the fields.

This means the Lagrangian possesses at this stage a global symmetry of the form

$$\mathcal{G}^{\text{SM}}_{\text{global}} = U(3)_Q \times U(3)_u \times U(3)_d \times U(3)_L \times U(3)_e \,, \tag{II.14}$$

meaning that we can transform each Weyl fermion individually under a global $U(3)$ group.

From Table II.2 we can now deduce the covariant derivatives for the fermions and the Higgs, giving

$$D^{ij}_{Q,\mu} = \left(\partial_\mu - i\frac{g_Y}{6}B_\mu - ig_L\tau^a W^a_\mu - ig_s\lambda^a G^a_\mu\right)\delta^{ij} \,,$$
$$D^{ij}_{L,\mu} = \left(\partial_\mu + i\frac{g_Y}{2}B_\mu - ig_L\tau^a W^a_\mu\right)\delta^{ij} \,,$$

$$D^{ij}_{f,\mu} = \left(\partial_\mu - iY_f g_Y B_\mu - i(1-\delta_{fe}) g_s \lambda^a G^a_\mu\right) \delta^{ij}\,, \quad f \in \{e,u,d\}\,,$$
$$D_{H,\mu} = \partial_\mu - i\frac{g_Y}{2} B_\mu - i g_L \tau^a W^a_\mu\,, \tag{II.15}$$

with τ^a and λ^a being the generators of the respective gauge groups. Due to the global symmetry the gauge interactions are flavor-conserving, which will change in the broken phase of the SM.

Finally, there are the Yukawa interactions of the fermions to the Higgs boson,

$$\mathcal{L}^{\text{SM}}_{\text{Yukawa}} \supset -y^{ij}_u \bar{Q}^i_L \tilde{H} u^j_R - y^{ij}_d \bar{Q}^i_L H d^j_R - y^{ij}_e \bar{L}^i_L H e^j_R + \text{h.c.}\,, \tag{II.16}$$

with $\tilde{H}_a = \epsilon_{ab} H^*_b$ describing the Higgs doublet contracted with the totally anti-symmetric tensor of $SU(2)_L$. The Higgs vev will introduce masses to the fermions which also breaks the global symmetry explicitly.

II.2.2 Electroweak Symmetry Breaking

Having introduced the ingredients of the SM, we can now discuss the effects of the vev v of the Higgs field, defined by its scalar potential. In particular, the symmetry under which H transforms is broken by the vev to its diagonal subgroup, $SU(2)_L \times U(1)_Y \to U(1)_Q$, where $U(1)_Q$ denotes the gauge group of QED with the electric charge Q.

In order to study the changes in the Lagrangian we express the Higgs doublet in its non-linear form

$$H = \exp\left(i\frac{\varphi^a \sigma^a}{v}\right) \begin{pmatrix} 0 \\ \frac{v+h}{\sqrt{2}} \end{pmatrix}\,, \tag{II.17}$$

where h denotes the radial mode of the Higgs field and φ^a the angular modes contracted with the $SU(2)$ Pauli matrices σ^a.

The scalar potential can then be expanded using the radial and angular modes by

$$\begin{aligned}\mathcal{L}^{\text{SM}}_{\text{scalar}} \to & \frac{1}{2}(\partial_\mu h)^2 - \lambda v^2 h^2 - \lambda v h^3 - \frac{\lambda}{4} h^4 \\ & + \frac{g_L^2 (v+h)^2}{4}\left(\left|W^+_\mu - \frac{D_\mu \varphi^+}{m_W}\right|^2 + \frac{1}{2\cos^2\theta_W}\left(Z_\mu - \frac{\partial_\mu \varphi^0}{m_Z}\right)^2\right)\,,\end{aligned} \tag{II.18}$$

where we used the weak mixing angle $\tan\theta_W = g_Y/g_L$. The fields $W^\pm_\mu$ and Z_μ are the mass eigenstates of the electroweak gauge bosons with masses $m_W = g_L v/2$ and $m_Z = m_W/c_W$. We can express these fields in terms of the original fields via

$$\begin{pmatrix} A_\mu \\ Z_\mu \end{pmatrix} = \begin{pmatrix} \cos\theta_W & \sin\theta_W \\ -\sin\theta_W & \cos\theta_W \end{pmatrix} \begin{pmatrix} B_\mu \\ W^3_\mu \end{pmatrix}\,, \quad W^\pm_\mu = \frac{W^1_\mu \mp i W^2_\mu}{\sqrt{2}}\,. \tag{II.19}$$

The angular modes $\varphi^\pm$ are constructed analogously. We see, that the field A_μ does not appear quadratically in the scalar Lagrangian, such that A_μ does not get a mass, describing the massless photon of QED.

In order to factor out the fermion mass matrices we remove the angular modes from the Yukawa potential by performing chiral rotations of the left-handed fermions and successively a vector-like rotation to account for the mixing of B_μ and W^3_μ,

$$F^i_L \to \exp\left(i\frac{\varphi^a \sigma^a}{v}\right) F^i_L\,, \quad F \in \{L,Q\}\,, \quad f^i \to \exp\left(-i s^2_W Q_f \frac{\varphi^0}{v}\right) f^i\,, \quad f \in \{e,u,d\}\,, \tag{II.20}$$

which leads to the desired form of the Yukawa potential,

$$\mathcal{L}^{\text{SM}}_{\text{Yukawa}} \to -\frac{v+h}{\sqrt{2}}\bar{\mathbf{u}}_L \mathbf{Y}_u \mathbf{u}_R - \frac{v+h}{\sqrt{2}}\bar{\mathbf{d}}_L \mathbf{Y}_d \mathbf{d}_R - \frac{v+h}{\sqrt{2}}\bar{\mathbf{e}}_L \mathbf{Y}_e \mathbf{e}_R + \text{h.c.}\,, \tag{II.21}$$

where the Yukawa matrices are still in general non-diagonal and complex and fermions are represented as vectors in flavor-space.

The transformation in equation (II.20) changes the kinetic part of the fermionic Lagrangian as well. Expressing the gauge interactions in terms of their conserved fermionic currents J^μ we get

$$\begin{aligned}\mathcal{L}^{\text{SM}}_{\text{fermion}} \to & i\bar{u}^i \partial\!\!\!/ u^i + i\bar{d}^i \partial\!\!\!/ d^i + i\bar{e}^i \partial\!\!\!/ e^i + i\bar{\nu}^i_L \partial\!\!\!/ \nu^i_L + eA_\mu J^\mu_{\text{QED}} + g_s G^a_\mu J^{a,\mu}_{\text{QCD}} \\ & + \frac{e}{s_W c_W}\left(Z_\mu - \frac{\partial_\mu \varphi^0}{m_Z}\right) J^\mu_Z + \frac{e}{\sqrt{2}s_W}\left(\left(W^+_\mu - \frac{D_\mu \varphi^+}{m_W}\right) J^{-\mu}_W + \text{h.c.}\right)\,, \end{aligned} \tag{II.22}$$

where $e = g_L/s_W = g_Y/c_W$ is now the electromagnetic coupling constant and $f^i \equiv f^i_L + f^i_R$ denote Dirac spinors with $f \in \{e, u, d\}$.

We notice that in both, the scalar and fermionic Lagrangian the massive gauge bosons $W^\pm_\mu$ and Z_μ appear in the same way in respect to the angular modes $\varphi^\pm$ and φ^0. Hence, we can use the gauge freedom of the original symmetry to shift the fields by

$$Z_\mu \to Z_\mu + \frac{\partial_\mu \varphi^0}{m_Z}\,, \quad W^+_\mu \to W^+_\mu + \frac{D_\mu \varphi^+}{m_W}\,, \quad W^-_\mu \to W^-_\mu + \frac{D_\mu \varphi^-}{m_W}\,. \tag{II.23}$$

This fixes the gauge to the so-called unitary gauge, which means, that the gauge symmetry is broken. The angular fields of the Higgs are therefore called the Goldstone bosons of the broken gauge symmetry and are absorbed ("eaten") as longitudinal modes of the massive gauge bosons. Note, that $\mathcal{L}^{\text{SM}}_{\text{gauge}}$ stays invariant under this transformation.

Finally, we want to diagonalize the Yukawa terms in order to obtain mass eigenstates of the fermions. Hence we use the $U(3)$ transformations of the original global symmetry to bring the Yukawa matrices into a real and diagonal form $\mathbf{Y}_{D,f}$. We express the transformations in terms of the unitary matrices $\mathbf{U}_f$ for the left-handed fields and $\mathbf{V}_f$ for the right-handed fields,

$$\mathbf{f}_L \to \mathbf{U}_f \mathbf{f}_L\,, \quad \mathbf{f}_R \to \mathbf{V}_f \mathbf{f}_R\,, \quad \mathbf{U}^\dagger_f \mathbf{U}_f = \mathbb{1} = \mathbf{V}^\dagger_f \mathbf{V}_f\,, \quad \mathbf{Y}_{D,f} = \mathbf{U}^\dagger_f \mathbf{Y}_f \mathbf{V}_f\,, \tag{II.24}$$

such that we get diagonal fermion mass matrices of the form $\mathbf{M}_f = \mathbf{Y}_{D,f} v/\sqrt{2}$.

These chiral transformations have two effects on the remaining SM parameters. On one hand, the weak gauge current becomes flavor-changing,

$$J^{-\mu}_W = \bar{u}^i_L \gamma^\mu \delta^{ij} d^j_L \to \bar{u}^i_L \gamma^\mu V^{ij}_{\text{CKM}} d^j_L\,, \tag{II.25}$$

where the flavor-changing CKM matrix $\mathbf{V}_{\text{CKM}} \equiv \mathbf{U}^\dagger_u \mathbf{U}_d$ also contains a CP-violating phase.

On the other hand, the θ term changes due to the anomalous nature of the chiral transformation,

$$\theta_{\text{QCD}} \to \bar{\theta}_{\text{SM}} = \theta_{\text{QCD}} - \arg\left(\frac{\det(\mathbf{U}_u \mathbf{U}_d)}{\det(\mathbf{V}_u \mathbf{V}_d)}\right) = \theta_{\text{QCD}} - \arg\left(\det(\mathbf{Y}_u \mathbf{Y}_d)\right)\,. \tag{II.26}$$

Since the other gauge groups, $SU(2)_L$ and $U(1)_Y$ are chiral, a corresponding transformation would not contain a matching number of phases of the matrices $\mathbf{U}_f$ and $\mathbf{V}_f$. Hence,

we can always use one matrix to cancel the corresponding θ terms, while keeping the total phase differences, making the θ terms for $SU(2)_L \times U(1)_Y$ unphysical.

The CP-violating parameter $\bar{\theta}_{\text{SM}}$ feeds linearly into the nEDM, which constrains $\bar{\theta}_{\text{SM}} < 10^{-10}$ [14]. Hence, θ_{QCD} and $\arg(\det(\mathbf{Y}_u \mathbf{Y}_d))$ would need to cancel almost exactly, hinting towards a new symmetry. This is called the strong CP problem and will be discussed in section II.3.

II.2.3 Chiral Symmetry Breaking

The gauge coupling g_s of the remaining gauge symmetry $SU(3)_C$ grows for larger distances, leading to confinement of quarks, such that we can not detect free quarks at measurable distances. Hence, the quarks form a so-called quark condensate for energies below the QCD confinement scale, which we can write as a vacuum expectation value $\langle \bar{q}q \rangle = v_\chi^3$. This vev breaks the chiral symmetry of QCD under which the light quarks u, d (and s) transform independently for left- and right-handed fields.

In particular, the up- and down-quarks form left- and right-handed doublets $(u_L, d_L)^T$ and $(u_R, d_R)^T$ transforming under a global $SU(2)_L \times SU(2)_R$ symmetry. The vev v_χ breaks this symmetry to its diagonal subgroup $SU(2)_I$, called isospin.

The Goldstone bosons of this spontaneous symmetry breaking can be combined as a field $\mathbf{\Sigma}$ containing the pions π^a,

$$\mathbf{\Sigma} = \frac{v_\pi}{\sqrt{2}} \exp\left(i \frac{\pi^a \sigma^a}{f_\pi} \right) , \tag{II.27}$$

which transforms as a bifundamental under $SU(2)_L \times SU(2)_R$. The parameter $f_\pi = \sqrt{2} v_\pi$ represents the pion decay constant.

Since the up- and down-quarks are not exactly massless, the chiral symmetry is broken also explicitly by the mass matrix $\mathbf{M} = \text{diag}(m_u, m_d)$. Hence, the pions acquire a mass and are therefore called pseudo-Nambu-Goldstone bosons. Treating the Mass matrix as a spurion which transforms as a bifundamental as well, we can construct the chiral Lagrangian as

$$\begin{aligned} \mathcal{L}_{\text{chiral}} \supset & \operatorname{Tr}(|D_{\Sigma,\mu} \mathbf{\Sigma})|^2) + \frac{v_\chi^3}{f_\pi} \operatorname{Tr}(\mathbf{M\Sigma} + \text{h.c.}) + \mathcal{O}\left(\frac{\pi^3}{f_\pi^3} \right) \\ = & \frac{1}{2} (\partial_\mu \pi^0)^2 + |D_\mu \pi^+|^2 + v_\chi^3 (m_u + m_d) \\ & - \frac{v_\chi^3 (m_u + m_d)}{2} \frac{(\pi^0)^2 + (\pi^+)^2 + (\pi^-)^2}{f_\pi^2} + \mathcal{O}\left(\frac{\pi^3}{f_\pi^3} \right) , \end{aligned} \tag{II.28}$$

where we neglect higher order interactions.

We see, that the pions indeed get a mass, leading to the Gell-Mann-Oakes-Renner relation [49] between pion mass and pion decay constant

$$m_\pi^2 f_\pi^2 = v_\chi^3 (m_u + m_d) . \tag{II.29}$$

We remark, that including the strange quark as well as corrections from higher order QCD effects add further mesons and correct the pion masses, leading to slightly different masses between neutral and charged pions.

II.3 Axions and Axion-like Particles

In order to solve the strong CP-Problem there are multiple attempts to introduce new symmetries, which either forbid such a CP-violating term (i.e. Nelson-Barr mechanism [50, 51]) or render it dynamically to zero (i.e. Peccei-Quinn mechanism [15, 16]). In this thesis we mainly focus on the latter. The Peccei-Quinn mechanism introduces a global $U(1)_{\text{PQ}}$ symmetry which is broken at a high mass scale v_a and dynamically cancels the $\bar{\theta}_{\text{SM}}$ parameter. The corresponding Goldstone boson was identified by Weinberg and Wilczek in [17, 18] and is called the axion a.

The $U(1)_{\text{PQ}}$ symmetry can be realized as the internal continuous shift symmetry of the angular mode of a complex scalar field

$$\Phi = \frac{v_\Phi + h_\Phi}{\sqrt{2}} \exp\left(i\frac{a_\Phi}{v_\Phi}\right), \quad \frac{a_\Phi}{v_\Phi} \sim \frac{a}{v_a}, \tag{II.30}$$

where h_Φ denotes the radial mode and a_Φ the angular mode which is mainly aligned with the axion. The vev v_Φ breaks the PQ symmetry, leaving a discrete shift symmetry for the axion. For a sufficiently high mass scale, v_Φ dominates the PQ breaking scale v_a which is related to the axion decay constant f_a via $f_a = X v_a$, where X is the PQ charge of the field Φ.

Writing $\mathcal{A}_{gg} = \sum_f N_g^f (X_L^f - X_R^f)/(2X)$ as the canonically normalized anomaly coefficient for the $U(1)_{\text{PQ}} \times SU(3)_C^2$ anomaly with N_g^f being the number of generations of fermion type f, we acquire a CP-conserving term at dimension 5 of the form

$$\mathcal{L}_{agg} \supset -\frac{g_s^2}{32\pi^2}\left(2X\mathcal{A}_{gg}\frac{a}{f_a} - \bar{\theta}_{\text{SM}}\right) G^a_{\mu\nu}\tilde{G}^{a\mu\nu}, \tag{II.31}$$

which also respects a discrete shift symmetry of the axion, since the path integral does not change for $\delta S \to \delta S + 2\pi$. We see, that the axion cancels the $\bar{\theta}_{\text{SM}}$ term exactly if it acquires a vev

$$\langle a \rangle = \frac{\bar{\theta}_{\text{SM}} f_a}{2X\mathcal{A}_{gg}}. \tag{II.32}$$

In subsection II.3.4 we will show that this is indeed the true minimum of the axion potential as long as the $G\tilde{G}$ term is the only term which breaks the discrete shift symmetry of the axion. In the following we mainly consider the canonical form of $\mathcal{L}_{agg}$, where we use the canonical PQ charge normalization $X = (2\mathcal{A}_{gg})^{-1}$.

There are two types of models which generate $\mathcal{L}_{agg}$ from the complex scalar Φ. A KSVZ model contains an additional heavy quark, which can be anomalously transformed to generate $\mathcal{L}_{agg}$, while a DFSZ model contains a second Higgs doublet, such that anomalous transformations of the SM fermions generate $\mathcal{L}_{agg}$ due to a mixing of the angular modes of the scalar fields. In the following we will present both types of models.

II.3.1 KSVZ Axion

In the KSVZ Model [19, 20] the PQ Anomaly is mediated by an additional heavy quark q, with its mass generated through a Yukawa coupling to the complex scalar Φ. An additional gloabal Z_n symmetry with $n > 4$ forbids polynomials of Φ in the scalar potential which would break the PQ symmetry explicitly. The corresponding field content is shown in Table II.3.

Since the neutral angular mode of the Higgs doublet is entirely absorbed by the Z boson, the axion aligns exactly with the angular mode a_Φ of the complex scalar. Hence,

	$SU(3)_C$	$SU(2)_L$	$U(1)_Y$	$\mathbb{Z}_n$	$U(1)_{PQ}$
Q_L^i	3	2	1/6	0	X_Q
u_R^i	3	1	2/3	0	X_Q
d_R^i	3	1	-1/3	0	X_Q
L_L^i	1	2	-1/2	0	X_L
e_R^i	1	1	-1	0	X_L
H	1	2	1/2	0	0
q_L	3	1	Y_q	0	$-X/2$
q_R	3	1	Y_q	n-1	$X/2$
Φ	1	1	0	1	$-X$

Table II.3: Fermionic and scalar field content of the KSVZ model. In addition to the SM we have a heavy quark field q and a gauge singlet complex scalar Φ. Both fields are charged under a $\mathbb{Z}_n$ symmetry which protects a global PQ symmetry.

the Higgs doublet is not charged under the global PQ symmetry and the SM fermions are only charged vector-like under $U(1)_{\text{PQ}}$ such that they do not contribute to the PQ Anomaly.

The Yukawa and scalar Lagrangians extend to

$$\begin{aligned}\mathcal{L}^{\text{KSVZ}}_{\text{scalar}} \supset& \mathcal{L}^{\text{SM}}_{\text{scalar}} + |\partial_\mu \Phi|^2 - \lambda_\Phi \left(|\Phi|^2 - \frac{v_\Phi^2}{2}\right)^2 - \lambda_{H\Phi}\left(|H|^2 - \frac{v^2}{2}\right)\left(|\Phi|^2 - \frac{v_\Phi^2}{2}\right), \\ \mathcal{L}^{\text{KSVZ}}_{\text{Yukawa}} \supset& \mathcal{L}^{\text{SM}}_{\text{Yukawa}} - y_q \bar{q}_L \Phi q_R + \text{h.c.}\,,\end{aligned} \tag{II.33}$$

with the scalar Potential only effecting the radial modes of the complex fields.

Performing an axial transformation on the heavy quarks,

$$q \to \exp\left(-i\frac{X}{2}\frac{a}{f_a}\gamma_5\right) q\,, \tag{II.34}$$

generates the PQ anomaly in the CP conserving $\mathcal{L}_{agg}$ interaction. The corresponding anomaly coefficient and PQ charge normalization evaluate to

$$\mathcal{A}_{gg}^{\text{KSVZ}} = \frac{1}{2} \quad \Rightarrow \quad X^{\text{KSVZ}} = 1\,. \tag{II.35}$$

We show the electromagnetic PQ anomaly in subsection II.3.4.

II.3.2 DFSZ Axion

In contrast to the KSVZ model, the DFSZ model [21, 22] relies on a two Higgs doublet description, where down-like quarks acquire their mass through the Yukawa interaction with a Higgs doublet H_d and up-like quarks through the interaction with a second Higgs doublet H_u. While H_d has the same gauge properties as the SM Higgs doublet H, H_u transforms like $\tilde{H}$.

A $\mathbb{Z}_n$ symmetry with $n > 4$ ensures that the quarks only have Yukawa couplings to their respective Higgs fields and that no polynomials in Φ break the PQ symmetry explicitly. The corresponding field content is shown in Table II.4.

We choose the $\mathbb{Z}_n$ charges for a Type II two Higgs doublet model [52] in which the charged leptons couple to H_d, such that the Yukawa Lagrangian becomes

$$\mathcal{L}^{\text{DFSZ}}_{\text{Yukawa}} \supset -y_u^{ij}\bar{Q}_L^i H_u u_R^j - y_d^{ij}\bar{Q}_L^i H_d d_R^j - y_e^{ij}\bar{L}_L^i H_d e_R^j + \text{h.c.}\,. \tag{II.36}$$

	$SU(3)_C$	$SU(2)_L$	$U(1)_Y$	$\mathbb{Z}_n$	$U(1)_{PQ}$
Q_L^i	3	2	1/6	0	X_Q
u_R^i	3	1	2/3	1	X_Q-X_u
d_R^i	3	1	-1/3	0	X_Q-X_d
L_L^i	1	2	-1/2	0	X_L
e_R^i	1	1	-1	0	X_L-X_d
H_u	1	2	-1/2	n-1	X_u
H_d	1	2	1/2	0	X_d
Φ	1	1	0	1	-X

Table II.4: Fermionic and scalar field content of the DFSZ model. The model contains two Higgs fields H_u and H_d which break the electroweak symmetry as well as an additional gauge singlet Φ. A $\mathbb{Z}_n$ defines the Higgs couplings to fermions and protects a global PQ symmetry.

Contracting $SU(2)_L$ indices implicitly, the scalar Lagrangian of this model reads

$$\begin{aligned}\mathcal{L}_{\text{scalar}}^{\text{DFSZ}} \supset & |D_{\tilde{H},\mu} H_u|^2 + |D_{H,\mu} H_d|^2 + |\partial_\mu \Phi|^2 - \mu_u^2 |H_u|^2 - \mu_d^2 |H_d|^2 - \mu_\Phi^2 |\Phi|^2 \\ & - \lambda_u |H_u|^4 - \lambda_d |H_d|^4 - \lambda_\Phi |\Phi|^4 - \lambda_{ud} |H_u|^2 |H_d|^2 - \lambda'_{ud} |H_u H_d|^2 \\ & - \lambda_{u\Phi} |H_u|^2 |\Phi|^2 - \lambda_{d\Phi} |H_d|^2 |\Phi|^2 - \mu_A H_u H_d \Phi + \text{h.c.}\,, \end{aligned} \tag{II.37}$$

where the term proportional to μ_A leads to a mixing between the neutral angular modes of H_u, H_d and Φ, providing a mass for one linear combination A and leaving the axion as the massless linear combination which is not absorbed by the Z boson.

The mixing of angular modes leads to a direct coupling of the SM fermions to the axion which also manifests in their non-vanishing axial PQ charges. Hence, in the DFSZ model the PQ anomaly $\mathcal{L}_{agg}$ is generated via an axial transformation of the SM fermion,

$$u^i \to \exp\left(-i \frac{X_u}{2} \frac{a}{f_a} \gamma_5\right) u^i\,, \quad d^i \to \exp\left(-i \frac{X_d}{2} \frac{a}{f_a} \gamma_5\right) d^i\,, \quad e^i \to \exp\left(-i \frac{X_d}{2} \frac{a}{f_a} \gamma_5\right) e^i\,, \tag{II.38}$$

with $X_u + X_d = X$, such that the DFSZ model does not require an additional heavy quark.

The resulting anomaly coefficient and PQ charge normalization are

$$\mathcal{A}_{gg}^{\text{DFSZ}} = \frac{N_g}{2} \quad \Rightarrow \quad X^{\text{DFSZ}} = \frac{1}{N_g}\,. \tag{II.39}$$

The electromagnetic anomaly is shown in subsection II.3.4.

Besides the mixing of the angular modes the DFSZ model also introduces a mixing between radial modes, since it relies on a two Higgs doublet models. The three additional scalar degrees of freedom are H^0 and $H^\pm$. The neutral boson is defined as the orthogonal combination to the SM Higgs field h in the Higgs basis. It is aligned with the SM vev v such that the mixing matrix reads

$$\begin{pmatrix} h \\ H^0 \end{pmatrix} \equiv \begin{pmatrix} s_\beta & c_\beta \\ c_\beta & -s_\beta \end{pmatrix} \begin{pmatrix} h_u \\ h_d \end{pmatrix}\,, \tag{II.40}$$

where β describes the mixing angle between v_u and v_d. We assume that H^0 and $H^\pm$ are much heavier than the electroweak scale, such that further mass mixing between H^0 and h is suppressed.

II.3.3 Axion Potential

In both, the KSVZ- and DFSZ-type models we can write the axion Lagrangian after anomalous transformation of the fermions as

$$\begin{aligned}\mathcal{L}_{\text{axion}} \supset & \frac{1}{2}(\partial_\mu a)^2 + \frac{\partial_\mu a}{f_a} J^\mu_{\text{PQ}} - \frac{g_s^2}{32\pi^2}\left(2X\mathcal{A}_{gg}\frac{a}{f_a} - \bar{\theta}_{\text{SM}}\right) G^a_{\mu\nu}\tilde{G}^{a\mu\nu} \\ & - X\mathcal{A}_{\gamma\gamma}\frac{e^2}{(4\pi)^2}\frac{a}{f_a}F_{\mu\nu}\tilde{F}^{\mu\nu} + \mathcal{O}\left(h, Z_\mu, W^\pm_\mu\right) , \end{aligned} \tag{II.41}$$

where we neglect for now all couplings to the heavy fields h, Z_μ and $W^\pm_\mu$. We see, that the axion coupling to fermions in this basis is given by the global PQ current J^μ_{PQ}. This has the advantage, that integrating out the fermions does not give additional contributions to the anomalous axion-gauge boson couplings. On the other hand, taking the opposite limit of light fermion masses in respect to the axion mass will change the anomalous axion-gauge boson couplings.

Of special interest for experimental searches is the axion-diphoton coupling, which under canonical charge normalization $X = (2\mathcal{A}_{gg})^{-1}$ is given by

$$\mathcal{L}_{a\gamma\gamma} \supset -X\mathcal{A}_{\gamma\gamma}\frac{e^2}{(4\pi)^2}\frac{a}{f_a}F_{\mu\nu}\tilde{F}^{\mu\nu} \equiv -\frac{G_{a\gamma\gamma}}{4}aF_{\mu\nu}\tilde{F}^{\mu\nu} , \quad G_{a\gamma\gamma} = \frac{e^2}{8\pi^2}\frac{1}{f_a}\frac{\mathcal{A}_{\gamma\gamma}}{\mathcal{A}_{gg}} . \tag{II.42}$$

The anomaly coefficients $\mathcal{A}_{gg}$ and $\mathcal{A}_{\gamma\gamma} = \sum_f N_g^f N_c^f (X_L^f (Q_L^f)^2 - X_R^f (Q_R^f)^2)/X$ with N_c^f being the number of colors of fermion f are model dependent and differ therefore in KSVZ and DFSZ models.

In order to determine the axion mass, we can use the chiral Lagrangian of the pions for a leading order result. Therefore, we remove the axion from the $G\tilde{G}$ operator and shift it into the mass matrix of up- and down quark via the transformation

$$u \to \exp\left(i\frac{X'_u}{2}\left(\frac{a}{f_a} - \bar{\theta}_{\text{SM}}\right)\gamma_5\right) u , \quad d \to \exp\left(i\frac{X'_d}{2}\left(\frac{a}{f_a} - \bar{\theta}_{\text{SM}}\right)\gamma_5\right) d , \tag{II.43}$$

where the global charges fulfil $X'_u + X'_d = 1$. The resulting quark mass matrix becomes

$$\mathbf{M} \to \text{diag}\left(m_u \exp\left(iX'_u\left(\frac{a}{f_a} - \bar{\theta}_{\text{SM}}\right)\right), m_d \exp\left(iX'_d\left(\frac{a}{f_a} - \bar{\theta}_{\text{SM}}\right)\right)\right) , \tag{II.44}$$

where the axion field couples exponentially to the masses.

Choosing $X'_u = m_d/(m_u + m_d)$ and $X'_d = m_u/(m_u + m_d)$, the chiral Lagrangian changes to

$$\mathcal{L}_{\text{chiral}} \to -\frac{v_\chi^3(m_u + m_d)}{2}\left(\frac{(\pi^0)^2 + (\pi^+)^2 + (\pi^-)^2}{f_\pi^2} + \frac{m_d m_u}{(m_d + m_u)^2}\left(\frac{a}{f_a} - \bar{\theta}_{\text{SM}}\right)^2\right) , \tag{II.45}$$

where the choice of the global charges X'_u and X'_d prevented any mixing of the axion with the neutral pion. Here, we neglected the kinetic part of the fields as well as higher order interactions.

For the axion mass we now get a relation

$$m_a^2 f_a^2 = \frac{m_d m_u}{(m_d + m_u)^2} m_\pi^2 f_\pi^2 \equiv \Lambda^4_{\text{QCD}} , \tag{II.46}$$

where we introduced Λ^4_{QCD} as the mass contribution from QCD. We note, that higher order QCD corrections as well as instanton contributions will correct this result. For the vanilla KSVZ and DFSZ model, these corrections can be taken to be small. We refer to the case that the $m_a f_a$ relationship is a free parameter as an axion-like particle (ALP) which does not have its origin in the strong CP problem.

Since we neglect higher order interactions of the axion, we can regard the axion potential as a leading order approximation of a cosine potential

$$V_{\text{axion}} = -\Lambda^4_{\text{QCD}} \cos\left(\frac{a}{f_a} - \bar{\theta}_{\text{SM}}\right) + \mathcal{O}\left(\left(\frac{a}{f_a} - \bar{\theta}_{\text{SM}}\right)^4\right), \tag{II.47}$$

which is the canonical form for an instanton induced potential. If this term is the only contribution to the axion potential, the minimum for the field a is exactly at $\langle a \rangle = \bar{\theta} f_a$ as we required to solve the strong CP problem exactly.

II.3.4 Axion Diphoton Coupling and Experimental Searches

In order to get a prediction for the axion-diphoton coupling, which we can use to constrain the axion mass, we need to express the diphoton coupling in the same basis as the potential. Thus, we transform up- and down-quark anomalously with PQ charges X'_u and X'_d and obtain

$$G_{a\gamma\gamma} \to \frac{e^2}{8\pi^2}\frac{1}{f_a}\left(\frac{\mathcal{A}_{\gamma\gamma}}{\mathcal{A}_{gg}} - \frac{2}{3}\frac{4m_d + m_u}{m_d + m_u}\right), \quad \frac{\mathcal{A}^{\text{KSVZ}}_{\gamma\gamma}}{\mathcal{A}^{\text{KSVZ}}_{gg}} = 6Y_q^2, \quad \frac{\mathcal{A}^{\text{DFSZ}}_{\gamma\gamma}}{\mathcal{A}^{\text{DFSZ}}_{gg}} = \frac{8}{3}. \tag{II.48}$$

The change in $G_{a\gamma\gamma}$ is only a leading order approximation and is sensitive to higher order QCD corrections as well as instanton calculations.

Figure II.1 shows the canonical DFSZ axion line in the $\{m_a, G_{a\gamma\gamma}\}$ plane, where we used the results from reference [54],

$$\Lambda_{\text{QCD}} = 75.5(5)\ \text{MeV}, \quad G_{a\gamma\gamma} = \frac{e^2}{8\pi^2}\frac{1}{f_a}\left(\frac{\mathcal{A}_{\gamma\gamma}}{\mathcal{A}_{gg}} - 1.92(4)\right), \tag{II.49}$$

which also include higher order QCD corrections.

There are multiple ways to search for the anomalous axion-diphoton coupling in experiments and through astrophysical observations. Experiments which are primarily dedicated to the search for axions make use of the Primakoff effect [55], in which the application of a strong magnetic field can convert axions into photons and vice versa. In the laboratory this can be achieved by Light-shining-through-walls experiments [56–61], where one magnetic field converts a beam of light into axions which then can pass through a light-absorbing barrier ("wall") and get reconverted by a second magnetic field and hence could be measured.

On the other hand, there are experiments which aim for detecting axions from natural sources, and therefore only need to reconvert the axions into photons by applying a magnetic field. There are two main examples for this kind of experiments, Helioscopes and Haloscopes [62]. The goal of Helioscopes [63–65] is to find axions which are produced in the sun. Hence, the respective experiments track the apparent movement of the sun while being shielded from sunlight. Haloscopes instead search for axions which are present in the Dark Matter Halo [66–101]. Thus, Haloscopes rely on axions contributing to the local Dark Matter density, i.e. through the axion misalignment mechanism [102–104].

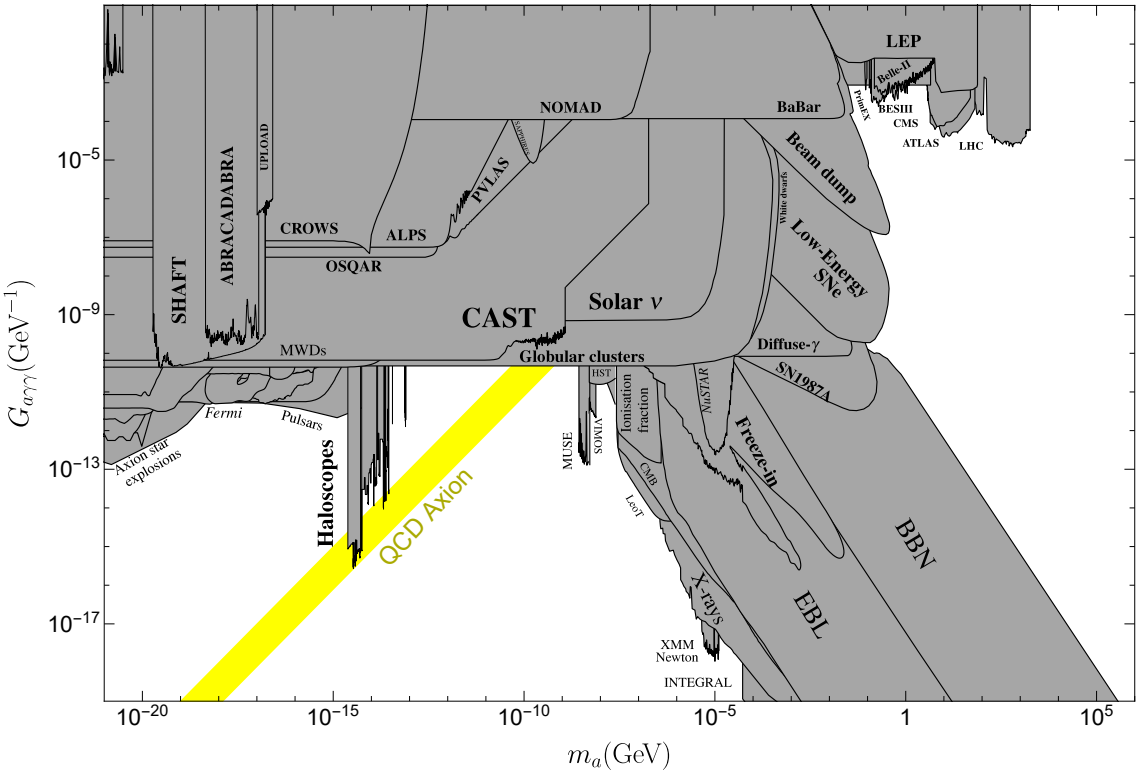

Figure II.1: Expected QCD axion band for $\Lambda_{\mathrm{QCD}} = 75.5(5)$ MeV in the axion mass vs. diphoton coupling parameter space. The band corresponds to the possible region which is motivated by both KSVZ and DFSZ models. The constraints are extracted from reference [53] and are explained in more detail in the main text.

Heavier axions can be probed in collider and beam dump experiments [105–121]. In collider experiments axions can be produced as intermediate particles, leaving an analysis of the decay products. Beam dump experiments on the other hand, search for axions as long-lived particles which decays within a dedicated decay volume. Shielding devices separate the long-lived particles from SM particles in order to obtain a clean signal.

Finally, there is a large variety of constraints which are based on astrophysical [122–186] and cosmological [187–189] observations. These mainly indirect measurements involve diverse radiation and neutrinos emitting sources as, for example, globular clusters or supernovae. The cosmological bounds rely on our understanding of the cosmic history including information about big bang nucleosynthesis (BBN) as well as CMB data.

Taking all these constraints into account, Figure II.1 gives an impression of how much parameter space is still open for experimental searches and theoretical motivation. While there are many motivations for finding axion-like particles over the full $\{m_a, G_{a\gamma\gamma}\}$ range, it is more difficult to motivate QCD axions apart from the canonical coupling band. Multiple proposals in this direction have been shown references [190–197].

In principle we can deviate from the canonical band by either modifying the axion potential to move to different axion masses, or changing the axion couplings, moving along the $G_{a\gamma\gamma}$-axis. In this thesis we are going to present novel approaches in both directions. The first part will be about exotic axion potentials based on the work in references [1,3,5], while the second part deals with exotic axion couplings as presented in references [2,4].

Part I

Exotic Axion Potential

CHAPTER III

Axion Potential and Goldstone Basis

The first part of this thesis is dedicated to the axion potential V_{axion}. As we discussed in section II.3, the QCD axion potential is given at leading order by

$$V_{\text{axion}} = -\Lambda_{\text{QCD}}^4 \cos\left(\frac{a}{f_a} - \bar{\theta}_{\text{SM}}\right) + \mathcal{O}\left(\left(\frac{a}{f_a} - \bar{\theta}_{\text{SM}}\right)^4\right), \quad \Lambda_{\text{QCD}}^4 = \frac{m_d m_u}{(m_d + m_u)^2} m_\pi^2 f_\pi^2 . \tag{III.1}$$

Nevertheless, corrections from QCD, instantons and additional PQ breaking operators can change this picture drastically. While QCD and instantons give mainly a correction to Λ_{QCD}, the implications from additional PQ breaking operators are more severe. In particular, these operators move the minimum out of the CP conserving phase of QCD, spoiling the axion solution of the strong CP problem. This is known as the quality problem of the axion [23].

Both types of corrections lead to additional mixing effects between neutral Goldstone bosons. The QCD and instanton corrections mainly couple global Goldstone bosons as the axion a to the pions π^0 of chiral symmetry breaking. Additional PQ breaking terms lead to a mixing between different global Goldstones as well as Goldstone bosons of gauge symmetries, like the φ^0.

In this chapter we provide with a general description of a theory with multiple complex scalar fields, focusing on the angular Lagrangian $\mathcal{L}_{\text{ang}}$ for which we disregard radial degrees of freedom. With this description we can find a basis in which we can distinguish between neutral Goldstone bosons of spontaneously broken $U(1)$ gauge symmetries, spontaneously broken global $U(1)$ symmetries and pseudo Goldstone bosons of explicitly broken global $U(1)$ symmetries.

In section III.1 we present a generalized scalar Lagrangian and point out linear transformations to obtain a useful basis. We demonstrate the procedure for the vanilla DFSZ model. Afterwards, in section III.2, we derive the parametric dependence from additional effects coming from fermion interactions and $SU(N)$ instantons.

III.1 Generalized Scalar Lagrangian and Goldstone Basis

We start our discussion of the angular Lagrangian by constructing a generalized version of a scalar Lagrangian containing N_Φ complex scalars $\Phi_{\mathtt{i}}$. The kinetic and potential terms of this theory then read

$$\mathcal{L}_{\text{scalar}} \supset \sum_{\mathtt{i}} |D_{\mathtt{i},\mu}\Phi_{\mathtt{i}}|^2 - \sum_{\mathtt{a}} \lambda_{\mathtt{a}} \Lambda^4 \left(\prod_{\mathtt{i}} \left(\frac{\Phi_{\mathtt{i}}}{\Lambda}\right)^{n_{\mathtt{a}}^{\mathtt{i}}} \left(\frac{\Phi_{\mathtt{i}}^*}{\Lambda}\right)^{\bar{n}_{\mathtt{a}}^{\mathtt{i}}}\right) + \text{h.c.}\,, \tag{III.2}$$

where $\mathtt{a}$ runs over all terms in the potential with corresponding dimensionless coupling $\lambda_{\mathtt{a}}$ and mass scale Λ.

We impose a $U(1)^{N_A}$ gauge symmetry on our theory with N_A being the number of corresponding gauge bosons $A_{\mathtt{I},\mu}$. Hence, the covariant derivative of a scalar $\Phi_{\mathtt{i}}$ is given by

$$D_{\mathtt{i},\mu} = \partial_\mu - i \sum_{\mathtt{I}} g_{\mathtt{I}} Q^{\mathtt{i}}_{\mathtt{I}} A_{\mathtt{I},\mu} \,, \tag{III.3}$$

with $g_{\mathtt{I}}$ being the gauge coupling of gauge field $A_{\mathtt{I},\mu}$ and $Q^{\mathtt{i}}_{\mathtt{I}}$ being the charge of the scalar field under the respective gauge symmetry. In general, the $U(1)$ gauge symmetries can be subgroups of $SU(N)$ symmetries, but since we are only interested in neutral Goldstone bosons we disregard further $SU(N)$ gauge bosons.

The terms in the scalar potential are characterized by their dimension and total $U(1)$ charges,

$$d_{\mathtt{a}} \equiv \sum_{\mathtt{i}} \left(n^{\mathtt{i}}_{\mathtt{a}} + \bar{n}^{\mathtt{i}}_{\mathtt{a}}\right) \leq 4 \,, \quad Q_{\mathtt{I},\mathtt{a}} \equiv \sum_{\mathtt{i}} \left(n^{\mathtt{i}}_{\mathtt{a}} - \bar{n}^{\mathtt{i}}_{\mathtt{a}}\right) Q^{\mathtt{i}}_{\mathtt{I}} \,. \tag{III.4}$$

In order to preserve gauge invariance we require $Q_{\mathtt{I},\mathtt{a}} = 0$ for each gauge symmetry.

Since the $U(1)$ gauge symmetries can be in general subgroups of $SU(N)$ symmetries, we forbid kinetic mixing of the field strength tensors, such that there is only a mass mixing between the gauge bosons and the mass basis can be found by performing an orthogonal rotation,

$$\mathcal{G}_{\text{gauge}} \supset U(1)^{N_A} \xrightarrow{O(N_A)} U(1)^{N_A^m} \times U(1)^{N_A^0} \xrightarrow{m_{\mathtt{I}}} U(1)^{N_A^0} \,, \tag{III.5}$$

$$\sum_{\mathtt{I}} g_{\mathtt{I}} Q^{\mathtt{i}}_{\mathtt{I}} A_{\mathtt{I},\mu} = \sum_{m_{\mathtt{I}} \neq 0} g_{\mathtt{I}} Q^{\mathtt{i}}_{\mathtt{I}} A_{\mathtt{I},\mu} + \sum_{m_{\mathtt{J}} = 0} g_{\mathtt{J}} Q^{\mathtt{i}}_{\mathtt{J}} A_{\mathtt{J},\mu} \,, \tag{III.6}$$

where N_A^m corresponds to the number of massive gauge bosons and N_A^0 to the number of massless gauge bosons. In the SM this orthogonal transformation corresponds to the mixing between the Z boson and the photon through the weak mixing angle. We discuss possible deviations through kinetic mixing in section VII.1.3.

In order to match pseudoscalar degrees of freedom of the complex scalars with longitudinal modes of the massive gauge bosons, we parametrize the complex fields non-linearly in their radial and angular modes,

$$\Phi_{\mathtt{i}} = \frac{v_{\mathtt{i}} + \phi_{\mathtt{i}}}{\sqrt{2}} \exp\left(i \frac{a_{\mathtt{i}}}{v_{\mathtt{i}}}\right) \,, \tag{III.7}$$

where $\phi_{\mathtt{i}}$ represent the radial modes, $a_{\mathtt{i}}$ the angular modes and $v_{\mathtt{i}} = \sqrt{2}\langle|\Phi_i|\rangle$ the vevs set by the scalar potential.

Disregarding for now the explicit symmetry breaking by the scalar potential, we can perform a corresponding orthogonal transformation on the angular modes,

$$\mathcal{G}_{\text{global}} \supset U(1)^{N_\Phi} \xrightarrow{O(N_\Phi)} U(1)^{N_\varphi} \times U(1)^{N_a} \times U(1)^{N_\Phi^0} \xrightarrow{v_{\mathtt{i}}} U(1)^{N_\Phi^0} \,, \tag{III.8}$$

where N_Φ^0 denotes the number of complex scalars with vanishing vev $v_{\mathtt{i}} = 0$, N_φ the number of Goldstone bosons which get absorbed as longitudinal modes of the gauge fields and N_a the number of global Goldstone bosons with decay constants $f_{\mathtt{K}}$.

Without loss of generality we assume that all spontaneously broken gauge symmetries follow a Higgs mechanism ($N_A^m = N_\varphi$) and that all vevs are non-vanishing ($N_\Phi^0 = 0$), such

that the orthogonal transformation can be written as

$$\frac{a_{\mathtt{i}}}{v_{\mathtt{i}}} = \sum_{m_{\mathtt{I}}\neq 0} g_{\mathtt{I}} Q_{\mathtt{I}}^{\mathtt{i}} \frac{\varphi_{\mathtt{I}}^0}{m_{\mathtt{I}}} + \sum_{\mathtt{K}} Q_{\mathtt{K}}^{\mathtt{i}} \frac{a_{\mathtt{K}}}{f_{\mathtt{K}}} \,. \tag{III.9}$$

The corresponding rotation matrix and orthogonality conditions are given by

$$R^T_{\mathtt{iI}} = \frac{g_{\mathtt{I}} Q_{\mathtt{I}}^{\mathtt{i}} v_{\mathtt{i}}}{m_{\mathtt{I}}} \,, \quad R^T_{\mathtt{iK}} = \frac{Q_{\mathtt{K}}^{\mathtt{i}} v_{\mathtt{i}}}{f_{\mathtt{K}}} \,, \tag{III.10}$$

$$\delta_{\mathtt{IJ}} = \sum_{\mathtt{i}} \frac{g_{\mathtt{I}} Q_{\mathtt{I}}^{\mathtt{i}} v_{\mathtt{i}}}{m_{\mathtt{I}}} \frac{g_{\mathtt{J}} Q_{\mathtt{J}}^{\mathtt{i}} v_{\mathtt{i}}}{m_{\mathtt{J}}} \,, \quad \delta_{\mathtt{KL}} = \sum_{\mathtt{i}} \frac{Q_{\mathtt{K}}^{\mathtt{i}} v_{\mathtt{i}}}{f_{\mathtt{K}}} \frac{Q_{\mathtt{L}}^{\mathtt{i}} v_{\mathtt{i}}}{f_{\mathtt{L}}} \,, \quad 0 = \sum_{\mathtt{i}} \frac{g_{\mathtt{I}} Q_{\mathtt{I}}^{\mathtt{i}} v_{\mathtt{i}}}{m_{\mathtt{I}}} \frac{Q_{\mathtt{K}}^{\mathtt{i}} v_{\mathtt{i}}}{f_{\mathtt{K}}} \,. \tag{III.11}$$

From $m_{\mathtt{I}}^2 = g_{\mathtt{I}}^2 \sum_{\mathtt{i}} (Q_{\mathtt{I}}^{\mathtt{i}})^2 v_{\mathtt{i}}^2$ we can deduce that the gauge charges to massless gauge bosons vanish for $v_{\mathtt{i}} \neq 0$, such that the angular part of the kinetic terms becomes

$$\begin{aligned} \sum_{\mathtt{i}} |D_{\mathtt{i},\mu} \Phi_{\mathtt{i}}|^2 &= \sum_{\mathtt{i}} \frac{(v_{\mathtt{i}} + \phi_{\mathtt{i}})^2}{2} \left(\sum_{\mathtt{I}} g_{\mathtt{I}} Q_{\mathtt{I}}^{\mathtt{i}} \left(A_{\mathtt{I},\mu} - \frac{\partial_\mu \varphi_{\mathtt{I}}^0}{m_{\mathtt{I}}} \right) - \sum_{\mathtt{K}} Q_{\mathtt{K}}^{\mathtt{i}} \frac{a_{\mathtt{K}}}{f_{\mathtt{K}}} \right)^2 \\ &\overset{\phi_{\mathtt{i}} \to 0}{\longrightarrow} \sum_{\mathtt{I}} \frac{m_{\mathtt{I}}^2}{2} \left(A_{\mathtt{I},\mu} - \frac{\partial_\mu \varphi_{\mathtt{I}}^0}{m_{\mathtt{I}}} \right)^2 + \sum_{\mathtt{K}} \frac{1}{2} (\partial_\mu a_{\mathtt{K}})^2 \,. \end{aligned} \tag{III.12}$$

We notice, that indeed the fields $\varphi_{\mathtt{I}}^0$ get absorbed as longitudinal modes for the massive gauge bosons $A_{\mathtt{I},\mu}$ while the fields $a_{\mathtt{K}}$ represent scalar Goldstone bosons for the spontaneously broken $U(1)^{N_a}$ symmetry.

We call the new basis the Goldstone basis in order to emphasize that this is neither the so-called Higgs basis, nor the mass basis of the global Goldstones $a_{\mathtt{K}}$. The Higgs basis describes the basis in which each radial mode is aligned to a gauge boson mass. It coincides with the Goldstone basis, if the charges of the complex scalars are of equal magnitude ($|Q_{\mathtt{I}}^{\mathtt{i}}| = |Q_{\mathtt{I}}^{\mathtt{j}}|$).

In order to switch to the physical mass basis we consider the angular potential where we parametrize the couplings in their non-linear form $\lambda_{\mathtt{a}} = |\lambda_{\mathtt{a}}| \exp(-i\theta_{\mathtt{a}})$,

$$\begin{aligned} V\Big|_{\phi_{\mathtt{i}}\to 0} &= \sum_{\mathtt{a}} 2|\lambda_{\mathtt{a}}|\Lambda^4 \left(\prod_{\mathtt{i}} \left(\frac{v_{\mathtt{i}}}{\sqrt{2}\Lambda} \right)^{n_{\mathtt{a}}^{\mathtt{i}} + \bar{n}_{\mathtt{a}}^{\mathtt{i}}} \right) \cos\left(\sum_{\mathtt{i}} \left(n_{\mathtt{a}}^{\mathtt{i}} - \bar{n}_{\mathtt{a}}^{\mathtt{i}} \right) \frac{a_{\mathtt{i}}}{v_{\mathtt{i}}} - \theta_{\mathtt{a}} \right) \\ &= \sum_{\mathtt{a}} \frac{|\lambda_{\mathtt{a}}|}{2} \left(\sqrt{2}\Lambda \right)^{4-d_{\mathtt{a}}} \left(\prod_{\mathtt{i}} (v_{\mathtt{i}})^{n_{\mathtt{a}}^{\mathtt{i}} + \bar{n}_{\mathtt{a}}^{\mathtt{i}}} \right) \cos\left(\sum_{\mathtt{K}} Q_{\mathtt{K},\mathtt{a}} \frac{a_{\mathtt{K}}}{f_{\mathtt{K}}} - \theta_{\mathtt{a}} \right) . \end{aligned} \tag{III.13}$$

We notice, that the Goldstone bosons $\varphi_{\mathtt{I}}^0$ of the gauge symmetries drop out due to the vanishing total gauge charge and that terms which are only sensitive to the absolute values of the complex scalars $|\Phi_{\mathtt{i}}|$ do not contribute to the angular potential, since they have $n_{\mathtt{a}}^{\mathtt{i}} = \bar{n}_{\mathtt{a}}^{\mathtt{i}}$ for each scalar.

In the special case where the terms in the angular potential contain orthogonal linear combinations of global Goldstone bosons, we can write $Q_{\mathtt{K},\mathtt{a}} \equiv Q_{\mathtt{a}} \delta_{\mathtt{Ka}}$ and the Goldstone basis aligns with the mass basis.

III.1.1 Application to DFSZ Model

In the case of the DFSZ Model we have three complex scalar fields H_u, H_d and Φ, one massive neutral gauge boson Z_μ and one term in the scalar potential with coupling μ_A

which breaks the global symmetry explicitly. Hence, we have three pseudoscalar degrees of freedom, the longitudinal mode φ^0 of the Z_μ, a heavy pseudo Goldstone boson A from the explicitly broken global symmetry and a massless Goldstone boson of the remaining global PQ symmetry, the axion a. We discuss the QCD induced potential which furthermore breaks the PQ symmetry in section III.2.

In order to identify the linear combinations of angular modes which represent the heavy pseudoscalar A and the axion a we first perform an orthogonal transformation on the initial global $U(1)^3$ in the unbroken phase,

$$U(1)_{H_u} \times U(1)_{H_d} \times U(1)_\Phi \xrightarrow{O(3)} U(1)_Y \times U(1)_{\text{PQ}} \times U(1)_Z \xrightarrow{\mu_A} U(1)_Y \times U(1)_{\text{PQ}}\,, \quad \text{(III.14)}$$

where we align one linear combination with the $U(1)_Y$ gauge symmetry of hypercharge and one with a global $U(1)_Z$ symmetry which is explicitly broken by the term proportional to μ_A. The alignment with $U(1)_Y$ instead of the spontaneously broken subgroup of $U(1)_Y \times SU(2)_L$ is sufficient since the charged Goldstone bosons $\varphi^\pm$ do not mix with the chargeless fields and the T_3 charges of the Higgs components in the broken phase match the respective hypercharges.

We parametrize the orthogonal rotation matrix by three angles β_1, β_2 and β_3. Abbreviating sine and cosine by s_{β_i} and c_{β_i} we can write

$$\begin{pmatrix} \varphi^0 \\ a \\ A \end{pmatrix} = \begin{pmatrix} s_{\beta_1} c_{\beta_3} & -c_{\beta_1} c_{\beta_3} & -s_{\beta_3} \\ c_{\beta_1} c_{\beta_2} - s_{\beta_1} s_{\beta_2} s_{\beta_3} & s_{\beta_1} c_{\beta_2} + c_{\beta_1} s_{\beta_2} s_{\beta_3} & -s_{\beta_2} c_{\beta_3} \\ c_{\beta_1} s_{\beta_2} + s_{\beta_1} c_{\beta_2} s_{\beta_3} & s_{\beta_1} s_{\beta_2} - c_{\beta_1} c_{\beta_2} s_{\beta_3} & c_{\beta_2} c_{\beta_3} \end{pmatrix} \begin{pmatrix} a_u \\ a_d \\ a_\Phi \end{pmatrix}, \quad \text{(III.15)}$$

where we can now evaluate the mixing angles under the use of equation (III.10),

$$s_{\beta_3} = -\frac{g_Y Y_\Phi v_\Phi}{m_Z} = 0 \quad \Rightarrow \quad c_{\beta_3} = 1 \quad \text{(III.16)}$$

$$t_{\beta_1} = -\frac{g_Y Y_u v_u}{m_Z} \frac{m_Z}{g_Y Y_d v_d} = \frac{v_u}{v_d} \quad \Leftrightarrow \quad v_u s_{\beta_1}^{-1} = v = v_d c_{\beta_1}^{-1} \quad \text{(III.17)}$$

$$t_{\beta_2} = -\frac{X_\Phi v_\Phi}{f_a} \frac{f_A}{Z_\Phi v_\Phi} = \frac{X}{Z_\Phi} \frac{f_A}{f_a} \quad \Leftrightarrow \quad f_a X^{-1} s_{\beta_2}^{-1} = v_\Phi = f_A Z_\Phi^{-1} c_{\beta_2}^{-1}\,, \quad \text{(III.18)}$$

with Z_Φ being the charge of Φ under $U(1)_Z$. We can choose Z_Φ freely, since it normalizes the decay constant f_A of the heavy pseudoscalar.

Under the requirement that the axion has to be mainly composed out of the angular mode a_Φ in order to ensure a high PQ breaking scale $f_a \gg f_A, v$, we choose for the charge normalization

$$Z_\Phi \equiv \frac{f_A^2}{f_a^2} X \quad \Rightarrow \quad \tan\beta_2 = \frac{f_a}{f_A} \gg 1\,. \quad \text{(III.19)}$$

Since the opposite case, in which a_Φ mainly mixes into A is already ruled out [198], we will treat $f_A^2/f_a^2 \ll 1$ as a small parameter for the remainder of this thesis.

Finally, we can use $X_u + X_d = X$ and the orthogonality conditions from equation (III.11) to find a relation between f_a and the SM vev v.

$$0 = \frac{g_Y Y_u v_u}{m_Z} \frac{X_u v_u}{f_a} + \frac{g_Y Y_d v_d}{m_Z} \frac{X_d v_d}{f_a} \quad \Leftrightarrow \quad X_u = c_{\beta_1}^2 X\,, \quad X_d = s_{\beta_1}^2 X\,, \quad \text{(III.20)}$$

$$c_{\beta_1} c_{\beta_2} = \frac{X_u v_u}{f_a} = \frac{c_{\beta_1}^2 X s_{\beta_1} v}{f_a} \quad \Leftrightarrow \quad f_a c_{\beta_2} = X v s_{\beta_1} c_{\beta_1}\,, \quad \text{(III.21)}$$

where we get a large scale separation for $\beta_2 \to \pi/2$ and $\beta_1 \to \pi/4$.

III.2 Scalar Potential from Fermion Condensates

Another contribution to the angular potential comes from Yukawa interactions to fermions which form a condensate of the form $\langle\bar{\psi}^j\psi^j\rangle = v_j^3$. This condensate breaks the chiral symmetry of the fermions ψ^j. The corresponding pions form a matrix valued field

$$\mathbf{\Sigma}^\psi = \frac{f_\psi}{2}\exp\left(2i\frac{\pi^a t^a}{f_\psi}\right), \quad \Sigma^\psi_{jj} \equiv \frac{f_\psi}{2}\exp\left(i\frac{\pi_j^0}{f_\psi}\right) + \mathcal{O}\left(\left(\frac{\pi_j^0}{f_\psi}\right)^2\right), \tag{III.22}$$

where t^a represent the generators of the chiral symmetry, f_ψ the decay constant of the pions and π_j^0 the neutral pions from the diagonal entries of the pion matrix.

Using this notation and neglecting flavor-changing effects we can express the Yukawa potential by

$$\begin{aligned}\mathcal{L}_{\text{Yukawa}} &= -\sum_{\mathtt{b}} y_{\mathtt{b}}\Lambda^4\left(\prod_{\mathtt{i}}\left(\frac{\Phi_{\mathtt{i}}}{\Lambda}\right)^{n_{\mathtt{b}}^{\mathtt{i}}}\left(\frac{\Phi_{\mathtt{i}}^*}{\Lambda}\right)^{\bar{n}_{\mathtt{b}}^{\mathtt{i}}}\right)\left(\prod_j\left(\frac{\bar{\psi}_L^j\psi_R^j}{\Lambda^3}\right)^{\tilde{n}_{\mathtt{b}}^j}\right) + \text{h.c.}\\ &\to -\sum_{\mathtt{b}} y_{\mathtt{b}}\Lambda^4\left(\prod_{\mathtt{i}}\left(\frac{\Phi_{\mathtt{i}}}{\Lambda}\right)^{n_{\mathtt{b}}^{\mathtt{i}}}\left(\frac{\Phi_{\mathtt{i}}^*}{\Lambda}\right)^{\bar{n}_{\mathtt{b}}^{\mathtt{i}}}\right)\left(\prod_j\left(\frac{\Sigma^\psi_{jj}}{f_\psi}\right)^{\tilde{n}_{\mathtt{b}}^j}\left(\frac{v_j^3}{\Lambda^3}\right)^{\tilde{n}_{\mathtt{b}}^j}\right) + \text{h.c.}\,,\end{aligned} \tag{III.23}$$

where $\mathtt{b}$ runs over all Yukawa interactions and vector-like masses and $y_{\mathtt{b}}$ represent the corresponding Yukawa couplings.

The expressions for the dimension and total charges of the operators extend to

$$d_{\mathtt{b}} \equiv \sum_{\mathtt{i}}\left(n_{\mathtt{b}}^{\mathtt{i}} + \bar{n}_{\mathtt{b}}^{\mathtt{i}}\right) + 3\sum_j \tilde{n}_{\mathtt{b}}^j \le 4\,, \quad Q_{\mathtt{I},\mathtt{b}} \equiv \sum_{\mathtt{i}}\left(n_{\mathtt{b}}^{\mathtt{i}} - \bar{n}_{\mathtt{b}}^{\mathtt{i}}\right)Q_{\mathtt{I}}^{\mathtt{i}} + 2\sum_j \tilde{n}_{\mathtt{b}}^j Q_{\mathtt{I},A}^j\,, \tag{III.24}$$

where we require $Q_{\mathtt{I},\mathtt{b}} = 0$ for gauge symmetries.

We can remove the Goldstone bosons of the gauge fields by performing an axial transformation of the fermions

$$\psi^j \to \exp\left(i\sum_{\mathtt{I}} g_{\mathtt{I}} Q_{\mathtt{I},A}^j \frac{\varphi_{\mathtt{I}}^0}{m_{\mathtt{I}}}\gamma_5\right)\psi^j\,. \tag{III.25}$$

Expressing the Yukawa couplings non-linearly by $y_{\mathtt{b}} = |y_{\mathtt{b}}|\exp(-i\theta_{\mathtt{b}})$ the angular potential extends to

$$\begin{aligned}V\Big|_{\phi_{\mathtt{i}}\to 0} &= \sum_{\mathtt{b}} 2|y_{\mathtt{b}}|\Lambda^4\left(\prod_{\mathtt{i}}\left(\frac{v_{\mathtt{i}}}{\sqrt{2}\Lambda}\right)^{n_{\mathtt{b}}^{\mathtt{i}}+\bar{n}_{\mathtt{b}}^{\mathtt{i}}}\right)\left(\prod_j\left(\frac{v_j^3}{2\Lambda^3}\right)^{\tilde{n}_{\mathtt{b}}^j}\right)\\ &\qquad\times\cos\left(\sum_{\mathtt{i}}\left(n_{\mathtt{b}}^{\mathtt{i}} - \bar{n}_{\mathtt{b}}^{\mathtt{i}}\right)\frac{a_{\mathtt{i}}}{v_{\mathtt{i}}} + \sum_j \tilde{n}_{\mathtt{b}}^j\left(\frac{\pi_j^0}{f_\psi} + 2\sum_{\mathtt{I}} g_{\mathtt{I}} Q_{\mathtt{I},A}^j\frac{\varphi_{\mathtt{I}}^0}{m_{\mathtt{I}}}\right) - \theta_{\mathtt{b}}\right)\\ &= \sum_{\mathtt{b}}\frac{|y_{\mathtt{b}}|}{2}\left(\sqrt{2}\Lambda\right)^{4-d_{\mathtt{b}}}\left(\prod_{\mathtt{i}}\left(v_{\mathtt{i}}\right)^{n_{\mathtt{b}}^{\mathtt{i}}+\bar{n}_{\mathtt{b}}^{\mathtt{i}}}\right)\left(\prod_j\left(\sqrt{2}v_j^3\right)^{\tilde{n}_{\mathtt{b}}^j}\right)\\ &\qquad\times\cos\left(\sum_{\mathtt{K}} Q_{\mathtt{K},\mathtt{b}}\frac{a_{\mathtt{K}}}{f_{\mathtt{K}}} + \sum_j \tilde{n}_{\mathtt{b}}^j\left(\frac{\pi_j^0}{f_\psi} - 2\sum_{\mathtt{K}} Q_{\mathtt{K},A}^j\frac{a_{\mathtt{K}}}{f_{\mathtt{K}}}\right) - \theta_{\mathtt{b}}\right).\end{aligned} \tag{III.26}$$

We see, that the dependence on the gauge Goldstone bosons $\varphi^0_{\mathtt{I}}$ again drops out due to $Q_{\mathtt{I},\mathtt{b}} = 0$ and that we have an additional term in the cosine which leads to a mass mixing between the global Goldstone bosons $a_{\mathtt{K}}$ and the neutral pions π^0_j.

From the Yukawa interaction we can now deduce the fermion mass m_j, defined by

$$\mathcal{L}_{\text{Yukawa}}\Big|_{\phi_{\mathtt{i}}\to 0} \supset -\sum_j m_j \bar{\psi}^j \exp\left(-2i\sum_{\mathtt{K}} Q^j_{\mathtt{K},A}\frac{a_{\mathtt{K}}}{f_{\mathtt{K}}}\gamma_5\right)\psi^j + \mathcal{O}\left(\theta_{\mathtt{b}}, Q_{\mathtt{K},\mathtt{b}}\right), \tag{III.27}$$

$$\Rightarrow \quad m_j = \sum_{\mathtt{b}} \tilde{n}^j_{\mathtt{b}} \frac{|y_{\mathtt{b}}|}{\sqrt{2}}\left(\sqrt{2}\Lambda\right)^{4-d_{\mathtt{b}}}\left(\prod_{\mathtt{i}}(v_{\mathtt{i}})^{n^{\mathtt{i}}_{\mathtt{b}}+\bar{n}^{\mathtt{i}}_{\mathtt{b}}}\right), \quad \tilde{n}^j_{\mathtt{b}} \in \{0,1\}. \tag{III.28}$$

We notice, that only the global Goldstone bosons have a coupling in the mass sector of the fermions, which we will make use of in the ALP-EFT description in section V.1.

Hence, the mass mixing potential for π^0_j and $a_{\mathtt{K}}$ is given by

$$V_{\text{mix}} = \sum_{j,\mathtt{K}} \frac{\pi^0_j}{f_\psi}\frac{a_{\mathtt{K}}}{f_{\mathtt{K}}} 2 Q^j_{\mathtt{K},A} v_j^3 m_j + \mathcal{O}\left(\theta_{\mathtt{b}}, Q_{\mathtt{K},\mathtt{b}}\right). \tag{III.29}$$

We neglect $\theta_{\mathtt{b}}$, which will be absorbed by the minima of the fields $a_{\mathtt{K}}$, as well as $Q_{\mathtt{K},\mathtt{b}}$, since in this thesis we do not consider Yukawa interactions which break global symmetries explicitly.

III.2.1 Scalar Potential from $SU(N)$ Instantons

In the case that the fermion condensate is induced by the confinement of an $SU(N)$ symmetry, we obtain corrections to the angular potential induced by instanton effects. We recall the gauge sector of the $SU(N)$ Lagrangian from section II.2,

$$\mathcal{L}_{\text{gauge}} \supset -\frac{1}{4}F^a_{\mu\nu}F^{a\mu\nu} + \frac{g^2}{32\pi^2}\theta F^a_{\mu\nu}\tilde{F}^{a\mu\nu}, \tag{III.30}$$

where g is the corresponding gauge coupling and θ a CP violating phase. We remove the couplings to global Goldstone bosons $a_{\mathtt{K}}$ from the Yukawa potential via a fermion transformation

$$\psi^j \to \exp\left(i\sum_{\mathtt{K}} Q^j_{\mathtt{K},A}\frac{a_{\mathtt{K}}}{f_{\mathtt{K}}}\gamma_5\right)\psi^j, \quad \mathcal{A}_{\mathtt{K}QQ} \equiv -\sum_j Q^j_{\mathtt{K},A}, \tag{III.31}$$

where $\mathcal{A}_{\mathtt{K}QQ}$ represent the corresponding anomaly coefficients as defined in equation (II.8).

The $SU(N)$ Lagrangian proportional to θ then changes to

$$\mathcal{L}^\theta_{\text{gauge}} \to -\frac{g^2}{32\pi^2}\left(2\sum_{\mathtt{K}}\mathcal{A}_{\mathtt{K}QQ}\frac{a_{\mathtt{K}}}{f_{\mathtt{K}}} - \theta\right)F^a_{\mu\nu}\tilde{F}^{a\mu\nu} \tag{III.32}$$

$$\to K^4\left(\prod_{m_j\lesssim v_j} K^{-3}\det\left(\bar{\psi}^j_L\psi^j_R\right)\right)\exp\left(-i\left(2\sum_{\mathtt{K}}\mathcal{A}_{\mathtt{K}QQ}\frac{a_{\mathtt{K}}}{f_{\mathtt{K}}} - \theta\right)\right) + \text{h.c.}, \tag{III.33}$$

where we replaced the $F\tilde{F}$ interaction by the t'Hooft determinantal operator from instantons [199, 200], with K being the corresponding effective instanton amplitude [199–201].

This induces an angular potential from instantons of the form

$$\begin{aligned} V_{\text{inst}} &= \sum_{\mathsf{c}} K^4 \left(\prod_{m_j \lesssim v_j} \left(\frac{\Sigma^{\psi}_{jj}}{f_\psi} \right)^{\tilde{n}^j_{\mathsf{c}}} \left(\frac{v_j^3}{K^3} \right)^{\tilde{n}^j_{\mathsf{c}}} \left(\frac{m_j \Lambda_j^2}{K^3} \right)^{\hat{n}^j_{\mathsf{c}}} \left(\delta_{\tilde{n}^j_{\mathsf{c}} \hat{n}^j_{\mathsf{c}}} - 1 \right) \right) \\ &\quad \times \exp\left(-i \left(2 \sum_{\mathsf{K}} \mathcal{A}_{\mathsf{K}QQ} \frac{a_{\mathsf{K}}}{f_{\mathsf{K}}} - \theta \right) \right) + \text{h.c.} \\ &= \sum_{\mathsf{c}} 2K^{4-3N^0_\psi} \left(\prod_{m_j \lesssim v_j} \left(\frac{v_j^3}{2} \right)^{\tilde{n}^j_{\mathsf{c}}} \left(m_j \Lambda_j^2 \right)^{\hat{n}^j_{\mathsf{c}}} \left(\delta_{\tilde{n}^j_{\mathsf{c}} \hat{n}^j_{\mathsf{c}}} - 1 \right) \right) \qquad \text{(III.34)} \\ &\quad \times \cos\left(2 \sum_{\mathsf{K}} \mathcal{A}_{\mathsf{K}QQ} \frac{a_{\mathsf{K}}}{f_{\mathsf{K}}} - \sum_{m_j \lesssim v_j} \tilde{n}^j_{\mathsf{c}} \frac{\pi^0_j}{f_\psi} - \theta \right), \qquad \text{(III.35)} \end{aligned}$$

where λ_j defines a cut-off scale for the instanton size integration, c runs over all contributing instanton diagrams and N^0_ψ denotes the number of light fermions, defined via

$$N^0_\psi \equiv \sum_{m_j \lesssim v_j} \left(\tilde{n}^j_{\mathsf{c}} + \hat{n}^j_{\mathsf{c}} \right) . \qquad \text{(III.36)}$$

The instanton potential now also introduces a mass mixing of the global Goldstone bosons to the pions of an approximate global $SU(N^0_\psi)$ symmetry. This mixing can be suppressed, if the instanton contribution to the pion mass is much smaller than the contribution from the fermion masses.

III.2.2 Application to DFSZ Model

In the DFSZ model, the PQ symmetry is broken by the quark condensate v_χ,

$$U(1)_Y \times U(1)_{\text{PQ}} \xrightarrow{v_\chi} U(1)_Y \, . \qquad \text{(III.37)}$$

This explicit breaking of the global PQ symmetry can be evaluated in two different ways, via the Yukawa induced quark masses of the chiral Lagrangian $\mathcal{L}_{\text{chiral}}$ or through instanton effects.

In the vanilla QCD axion calculation from section II.3 we used chiral transformations to shift the axion interaction into the first generation quark mass matrix. In this case, where we have

$$\theta_{\mathsf{b}} = 0 \, , \quad Q_{\mathsf{K},\mathsf{b}} = 0 \, , \quad 2Q^j_{\mathsf{K},A} = 1 - \frac{m_j}{m_u + m_d} \, , \quad \pi^0_j = (\delta_{ju} - \delta_{jd}) \pi^0 \, , \qquad \text{(III.38)}$$

the mass mixing between the axion a and the neutral pion π^0 in equation (III.29) cancels and we recover the leading order axion potential with $m_a^2 f_a^2 = \Lambda^4_{\text{QCD}}$ from equation (III.1). Higher order QCD corrections include further neutral mesons and therefore change the potential and mass mixing.

On the other hand, if we calculate the axion potential through instanton effects we obtain additional corrections, which can have a strong impact on the $\{m_a, f_a\}$ parameter space. The starting point for the instanton calculation for the QCD axion is the anomalous $SU(3)_C$ Lagrangian,

$$\mathcal{L}_{agg} \supset -\frac{g_s^2}{32\pi^2} \left(\frac{a}{f_a} - \bar{\theta}_{\text{SM}} \right) G^a_{\mu\nu} \tilde{G}^{a\mu\nu} \, , \qquad \text{(III.39)}$$

where we can make use of the axion shift symmetry by shifting $a \to a + \bar{\theta}_{\rm SM} f_a$ to define $\langle a \rangle = 0$ as the CP conserving phase of QCD.

At the QCD confinement scale there are three light quarks, the up-, down- and strange-quark (u, d, s). These three quarks respect an approximate global $U(3)_L \times U(3)_R$ symmetry which gets broken by the quark condensate v_χ^3. The associated Goldstone bosons which are neutral in all quantum numbers are the pion $\pi^0 \sim \bar{u}u - \bar{d}d$ as well as the mesons $\eta \sim \bar{u}u + \bar{d}d - 2\bar{s}s$ and $\eta' \sim \bar{u}u + \bar{d}d + \bar{s}s$ with their respective decay constants f_π, f_η and $f_{\eta'}$.

We now construct the potential of the neutral Goldstone bosons following the procedure from subsection III.2.1. We neglect the mixing with the η meson as well as mixing effects induced by the strange quark which are suppressed by $1/m_s$ compared to $1/m_u$ and $1/m_d$. Including the mass contributions to m_π and $m_{\eta'}$ from the chiral Lagrangian leads to an instanton induced potential of

$$\begin{aligned} V_{\rm inst}^{\rm DFSZ} = &-2K^{-5}\left(\frac{v_\chi^9}{6}\cos\left(\frac{a}{f_a} - 2\frac{\eta'}{f_{\eta'}}\right) + \frac{v_\chi^6}{4}\sum_{j=u,d} m_j \Lambda_j^2 \cos\left(\frac{a}{f_a} - \frac{\eta'}{f_{\eta'}} - (\delta_{ju} - \delta_{jd})\frac{\pi^0}{f_\pi}\right)\right) \\ &- m_u v_\chi^3 \cos\left(\frac{\eta'}{f_{\eta'}} + \frac{\pi^0}{f_\pi}\right) - m_d v_\chi^3 \cos\left(\frac{\eta'}{f_{\eta'}} - \frac{\pi^0}{f_\pi}\right). \end{aligned} \tag{III.40}$$

From this potential we can now derive a mass mixing matrix between the fields a, η' and π^0.

In the following we present our calculation from reference [1], where we reproduced and extended the discussion in [201]. Under the use of the abbreviations

$$\begin{aligned} m_\pm = m_d \pm m_u\,, \quad \mu = \frac{m_u m_d}{m_u + m_d}\,, \quad \Lambda_{\eta'}^4 = \frac{v_\chi^9}{4K^5}\,, \\ \mu\Lambda_{\rm inst}^3 = (m_u\Lambda_u^2 + m_d\Lambda_d^2)\frac{v_\chi^6}{4K^5}\,, \quad 0 \approx m_u\Lambda_u^2 - m_d\Lambda_d^2\,, \end{aligned} \tag{III.41}$$

we obtain the mass contribution[1]

$$V_{\rm inst}^{\rm DFSZ} \supset \frac{1}{2}\begin{pmatrix} a & \eta' & \pi^0 \end{pmatrix} \begin{pmatrix} \frac{\Lambda_{\eta'}^4 + 2\mu\Lambda_{\rm inst}^3}{f_a^2} & -\frac{2\Lambda_{\eta'}^4 + 2\mu\Lambda_{\rm inst}^3}{f_a f_{\eta'}} & 0 \\ -\frac{2\Lambda_{\eta'}^4 + 2\mu\Lambda_{\rm inst}^3}{f_a f_{\eta'}} & \frac{m_+ v_\chi^3 + 4\Lambda_{\eta'}^4 + 2\mu\Lambda_{\rm inst}^3}{f_{\eta'}} & -\frac{m_- v_\chi^3}{f_{\eta'} f_\pi} \\ 0 & -\frac{m_- v_\chi^3}{f_{\eta'} f_\pi} & \frac{m_+ v_\chi^3 + 2\mu\Lambda_{\rm inst}^3}{f_\pi^2} \end{pmatrix} \begin{pmatrix} a \\ \eta' \\ \pi^0 \end{pmatrix}, \tag{III.42}$$

which is hierarchical in the decay constants f_a, $f_{\eta'}$ and f_π.

The diagonalization of the mass matrix at leading order in $1/f_a$ leads to the pseudoscalar mass relations

$$\begin{aligned} m_{\pi,\eta'}^2 = &\frac{m_+ v_\chi^3 + 4\Lambda_{\eta'}^4 + 2\mu\Lambda_{\rm inst}^3}{2f_{\eta'}^2} + \frac{m_+ v_\chi^3 + 2\mu\Lambda_{\rm inst}^3}{2f_\pi^2} \\ &\mp \sqrt{\left(\frac{m_+ v_\chi^3 + 4\Lambda_{\eta'}^4 + 2\mu\Lambda_{\rm inst}^3}{2f_{\eta'}^2} - \frac{m_+ v_\chi^3 + 2\mu\Lambda_{\rm inst}^3}{2f_\pi^2}\right)^2 + \frac{m_-^2 v_\chi^6}{f_{\eta'}^2 f_\pi^2}}\,, \end{aligned} \tag{III.43}$$

[1] We refer in reference [1] to this calculation as the KSVZ case, since we assume a more general axion Lagrangian, in which we have not necessarily shifted the axion couplings into $\mathcal{L}_{agg}$.

$$m_a^2 f_a^2 = \Lambda_{\eta'}^4 + 2\mu\Lambda_{\rm inst}^3 - \frac{(m_+ v_\chi^3 + 2\mu\Lambda_{\rm inst}^3)\left(2\Lambda_{\eta'}^4 + 2\mu\Lambda_{\rm inst}^3\right)^2}{(m_+ v_\chi^3 + 4\Lambda_{\eta'}^4 + 2\mu\Lambda_{\rm inst}^3)(m_+ v_\chi^3 + 2\mu\Lambda_{\rm inst}^3) - (m_- v_\chi^3)^2}\,, \tag{III.44}$$

which we now further expand in different limiting cases.

For this purpose we define a parameter

$$\Delta_m^2 \equiv \frac{m_+ v_\chi^3 + 4\Lambda_{\eta'}^4 + 2\mu\Lambda_{\rm inst}^3}{f_{\eta'}^2} - \frac{m_+ v_\chi^3 + 2\mu\Lambda_{\rm inst}^3}{f_\pi^2}\,, \tag{III.45}$$

which for small $K \ll v_\chi$ becomes large as it scales as $\Delta_m \to 4\Lambda_{\eta'}^4/f_{\eta'}^2$.

Using a series representation of the square root in equation (III.43) allows us to express the masses via

$$m_{\eta'}^2 = \frac{m_+ v_\chi^3 + 4\Lambda_{\eta'}^4 + 2\mu\Lambda_{\rm inst}^3}{f_{\eta'}^2} + \frac{\Delta_m^2}{2}\sum_{k=1}^{\infty}\binom{1/2}{k}\left(\frac{4m_-^2 v_\chi^6}{\Delta_m^4 f_\pi^2 f_{\eta'}^2}\right)^k\,, \tag{III.46}$$

$$m_\pi^2 = \frac{m_+ v_\chi^3 + 2\mu\Lambda_{\rm inst}^3}{f_\pi^2} - \frac{\Delta_m^2}{2}\sum_{k=1}^{\infty}\binom{1/2}{k}\left(\frac{4m_-^2 v_\chi^6}{\Delta_m^4 f_\pi^2 f_{\eta'}^2}\right)^k\,, \tag{III.47}$$

such that the limit $\Lambda_{\eta'} \gg m_u, m_d$ is given by dropping the last term containing the series.

Similarly, we can rewrite the relation for the axion from equation (III.44) using a series of the form

$$\begin{aligned} m_a^2 f_a^2 =& \frac{(m_+ v_\chi^3 + 2\mu\Lambda_{\rm inst}^3)^2 - m_-^2 v_\chi^6}{4(m_+ v_\chi^3 + 2\mu\Lambda_{\rm inst}^3)} \\ &- \frac{(4\mu^2\Lambda_{\rm inst}^6 + m_+^2 v_\chi^6 - m_-^2 v_\chi^6)^2}{16\Lambda_{\eta'}^4(m_+ v_\chi^3 + 2\mu\Lambda_{\rm inst}^3)^2}\sum_{k=0}^{\infty}\left(\frac{m_-^2 v_\chi^6 - (m_+ v_\chi^3 + 2\mu\Lambda_{\rm inst}^3)^2}{4\Lambda_{\eta'}^4(m_+ v_\chi^3 + 2\mu\Lambda_{\rm inst}^3)}\right)^k\,. \end{aligned} \tag{III.48}$$

Again, we obtain the limit $\Lambda_{\eta'} \gg m_u, m_d$ by dropping the term which contains the series.

Under the use of the leading order expressions from equations (III.47) and (III.48), we can express the axion mass relation by

$$m_a^2 f_a^2 = \frac{m_\pi^4 f_\pi^4 - m_-^2 v_\chi^6}{4m_\pi^2 f_\pi^2} = \Lambda_{\rm QCD}^4\left(1 + \frac{m_-^2}{m_+}\frac{\Lambda_{\rm inst}^3(m_+ v_\chi^3 + \mu\Lambda_{\rm inst}^3)}{m_{\pi^0}^4 f_\pi^4}\right)\,. \tag{III.49}$$

We see, that the leading expression gets corrected by a small factor proportional to the quark mass difference. Under the use of the experimental values [202]

$$\begin{aligned} f_{\pi^0} &\approx 131 \ \ \text{MeV}, & f_{\eta'} &\approx 121 \ \ \text{MeV}, \\ m_{\pi^0} &= 134.9768(5) \ \ \text{MeV}, & m_{\eta'} &= 957.78(6) \ \ \text{MeV}, \\ m_u &= 2.16^{+0.5}_{-0.26} \ \ \text{MeV}\,, & m_d &= 4.67^{+0.48}_{-0.17} \ \ \text{MeV}\,, \end{aligned} \tag{III.50}$$

we can derive the mass scales $v_\chi = 336.3$MeV, $\Lambda_{\eta'} = 239.3$ MeV and $\Lambda_{\rm inst} = 261.7$ MeV. This provides an estimate of the small correction factor of $m_a^2 f_a^2 = \Lambda_{\rm QCD}^4(1 + 0.037)$.

CHAPTER IV

Anarchic Axion

Every QCD axion model suffers from having a quality problem [23], meaning that additional PQ-breaking operators move the axion minimum out of the CP conserving phase of QCD. This is especially problematic since Planck mass suppressed operators are expected break global symmetries in general [203–205].

In this chapter, we show that such additional operators also drastically change the behavior in the $\{m_a, G_{a\gamma\gamma}\}$ plane, allowing for heavier and much lighter axions than usual. Therefore, we first show the general concept in section IV.1 and possible operators which generate this behavior in section IV.2. Finally, we present in section IV.3 a UV completion which relaxes the quality problem. While the general concept was published in reference [3], the UV completion is treated in a follow-up work [5].

IV.1 Light Axion from additional PQ breaking Operator

In this section we demonstrate the modified $\{m_a, G_{a\gamma\gamma}\}$ behavior in the DFSZ model from an additional PQ breaking operator that has a linear dependence on f_a. We start with the angular potential of the DFSZ model,

$$V_{\text{ang}}^{\text{DFSZ}} = -\frac{|\mu_A|}{\sqrt{2}} v_u v_d v_\Phi \cos\left(\frac{1}{N_g}\frac{A}{f_A}\left(1+\frac{f_A^2}{f_a^2}\right) - \theta_A\right) - \Lambda_{\text{QCD}}^4 \cos\left(\frac{a}{f_a} + \frac{A}{f_A} - \bar{\theta}_{\text{SM}}\right), \tag{IV.1}$$

where we expressed $\mu_A = |\mu_A| \exp(-i\theta_A)$ in its non-linear form.

To this angular potential we add a PQ breaking operator of the form

$$V_{\text{ang}}^{\text{break}} = -\Lambda_{\text{QCD}}^4 N_g^2 \frac{f_a}{f_{\text{max}}} \cos\left(\frac{1}{N_g}\left(\frac{a}{f_a} + x\frac{A}{f_A}\right) - \theta_x\right), \tag{IV.2}$$

where the factor f_{max} depends on the mechanism which generates this term and marks the maximal f_a for which $V_{\text{ang}}^{\text{break}}$ has a smaller axion mass contribution than the PQ anomaly. The parameters x and θ_x depend on the mechanism as well and symbolize the dependence on the pseudoscalar A and the phase of the additional operator, respectively. The factors of N_g stem from the normalization of f_a and f_{max}.

We take advantage of the initial shift symmetry in order to move the constant phase offsets into $V_{\text{ang}}^{\text{break}}$. The corresponding transformations read

$$A \to A + \frac{N_g \theta_A f_A}{1+\frac{f_A^2}{f_a^2}}, \quad a \to a + \bar{\theta}_{\text{SM}} f_a - \frac{N_g \theta_A f_a}{1+\frac{f_A^2}{f_a^2}}, \tag{IV.3}$$

such that the CP conserving phase is at $\langle A\rangle = 0 = \langle a\rangle$.

The resulting angular potential, where we also replaced v_u, v_d and v_Φ by the expressions obtained in subsection III.1.1 is then given by

$$V_{\text{ang}} \to -\frac{|\mu_A|}{\sqrt{2}} v f_a f_A N_g^2 \left(1+\frac{f_A^2}{f_a^2}\right)^{-1} \cos\left(\frac{1}{N_g}\frac{A}{f_A}\left(1+\frac{f_A^2}{f_a^2}\right)\right) - \Lambda_{\text{QCD}}^4 \cos\left(\frac{a}{f_a}+\frac{A}{f_A}\right) - \Lambda_{\text{QCD}}^4 N_g^2 \frac{f_a}{f_{\max}} \cos\left(\frac{1}{N_g}\left(\frac{a}{f_a}+x\frac{A}{f_A}\right) - \theta_x + \frac{\bar{\theta}_{\text{SM}}}{N_g} - \frac{(1-x)\theta_A}{1+\frac{f_A^2}{f_a^2}}\right). \tag{IV.4}$$

We see that the dependence on θ_A drops out for $x = 1$, hence any deviation from $\langle A\rangle = 0$ would be absorbed by a corresponding shift of θ_A, leaving only $\langle a\rangle \neq 0$ in this case.

In general, we can combine the different phases to a parameter $\bar{\theta}$ and can express the residual PQ anomaly in the minimum of a and A by an effective phase $\bar{\theta}_{\text{eff}}$. These two phases are defined by

$$N_g\bar{\theta} \equiv \bar{\theta}_{\text{SM}} - N_g\theta_x - N_g\frac{(1-x)\theta_A}{1+\frac{f_A^2}{f_a^2}}, \quad N_g\bar{\theta}_{\text{eff}} \equiv -\frac{\langle a\rangle}{f_a} - \frac{\langle A\rangle}{f_A}, \tag{IV.5}$$

where we defined both parameters with an additional factor of N_g to account for the full 2π period of θ_x and θ_A.

For a sufficiently large $|\mu_A| \gg \Lambda_{\text{QCD}}$, the mass of the heavy pseudoscalar is dominantly given by the μ_A term,

$$m_A^2 = \frac{|\mu_A|}{\sqrt{2}} v \frac{f_a}{f_A}\left(1+\frac{f_A^2}{f_a^2}+\mathcal{O}\left(\frac{\Lambda_{\text{QCD}}}{|\mu_A|}\right)\right). \tag{IV.6}$$

Consequently, the mixing between A and a in the mass basis is negligibly small and the minimum of A is only set by the μ_A term to $\langle A\rangle = 0$, independently of the choice of x.

Hence, we can treat the axion potential separately from the heavy pseudoscalar by setting $A \to 0$,

$$V_{\text{axion}} = V_{\text{ang}}\Big|_{A\to 0} = -\Lambda_{\text{QCD}}^4 \cos\left(\frac{a}{f_a}\right) - \Lambda_{\text{QCD}}^4 N_g^2 \frac{f_a}{f_{\max}} \cos\left(\frac{1}{N_g}\frac{a}{f_a}+\bar{\theta}\right). \tag{IV.7}$$

This potential equals the potential in equation (III.1) of the vanilla axion model for $f_{\max} \to \infty$. Since the phases of the two terms differ by $\bar{\theta}$ the minimum of a gets moved out of the CP conserving phase by $\langle a\rangle = -N_g\bar{\theta}_{\text{eff}} f_a$.

In order to find the resulting shift in $\langle a\rangle$ we determine the minimum of the potential with respect to the axion a,

$$\frac{\partial V_{\text{axion}}}{\partial a}\bigg|_{a\to\langle a\rangle} = 0 \quad \Rightarrow \quad \sin\left(-N_g\bar{\theta}_{\text{eff}}\right) + N_g\frac{f_a}{f_{\max}}\sin\left(\bar{\theta}-\bar{\theta}_{\text{eff}}\right) = 0, \tag{IV.8}$$

$$\frac{\partial^2 V_{\text{axion}}}{\partial^2 a}\bigg|_{a\to\langle a\rangle} = m_a^2 \quad \Rightarrow \quad \cos\left(-N_g\bar{\theta}_{\text{eff}}\right) + \frac{f_a}{f_{\max}}\cos\left(\bar{\theta}-\bar{\theta}_{\text{eff}}\right) = \frac{m_a^2 f_a^2}{\Lambda_{\text{QCD}}^4}. \tag{IV.9}$$

We can make use of these relations to constrain the physically allowed parameter space. Substituting $\bar{\theta}$ leaves us with

$$\left(1-\frac{1}{N_g^2}\right)\cos^2(N_g\bar{\theta}_{\text{eff}}) - 2\frac{m_a^2 f_a^2}{\Lambda_{\text{QCD}}^4}\cos\left(N_g\bar{\theta}_{\text{eff}}\right) + \frac{m_a^4 f_a^4}{\Lambda_{\text{QCD}}^8} - \frac{f_a^2}{f_{\max}^2} + \frac{1}{N_g^2} = 0, \tag{IV.10}$$

which depends on the deviation of $m_a^2 f_a^2$ from Λ_{QCD}^4 and of f_a from $f_{\max}$.

We display the allowed parameter space in $m_a^2 f_a^2/\Lambda_{\rm QCD}^4$ and $f_{\rm max}/f_a$ in Figure IV.1 for different values of $\bar{\theta}_{\rm eff}$. It shows that we can either deviate from the canonical DFSZ line to heavier axion masses for small $\bar{\theta}$ and $f_a > f_{\rm max}$, or to much lighter axion masses for $\bar{\theta} \to \pi$ and $f_a \to f_{\rm max}$. On the other hand, for $f_a \ll f_{\rm max}$ we recover $m_a^2 f_a^2 = \Lambda_{\rm QCD}^4$. This also implies, that in the absence of $V_{\rm ang}^{\rm break}$ ($f_{\rm max} \to \infty$) we restore the canonical axion solution as expected.

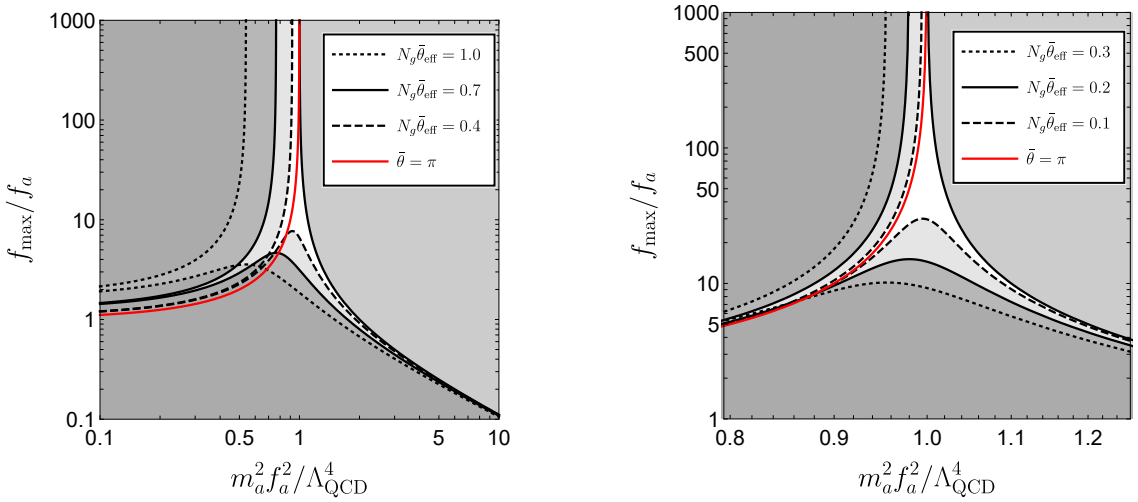

Figure IV.1: Deviation from the canonical axion mass relation in the anarchic axion model. The allowed parameter space is shown in white for different residual strong CP phases $\bar{\theta}_{\rm eff}$ compared to the axion mass relation in the $\bar{\theta} = \pi$ case. The left panel shows higher values of $\bar{\theta}_{\rm eff}$ while the right panel represents a zoomed-in version with lower values of $\bar{\theta}_{\rm eff}$.

The maximal extend of a line of constant $\bar{\theta}$ is sensitive to the effective CP violating phase, which is constrained by $N_g\bar{\theta}_{\rm eff} < 10^{-10}$ [14]. This residual phase can be determined from equation (IV.8) and reads for $\bar{\theta}$ close to π

$$\bar{\theta}_{\rm eff} = \frac{2(\pi - \bar{\theta})}{-1 + \sqrt{1 + \frac{4 m_a^2 f_{\rm max}^2}{\Lambda_{\rm QCD}^4}}} + \mathcal{O}\left((\pi - \bar{\theta})^2\right) . \tag{IV.11}$$

Since the deviation of $\bar{\theta}$ from π is now of the same order of magnitude as the effective CP violating parameter $\bar{\theta}_{\rm eff}$ we only get lighter axion masses for an accidentally small difference of $\bar{\theta}$ and π. We see this behavior in Figure IV.1 as the allowed parameter space approaches the $\bar{\theta} = \pi$ line for smaller $\bar{\theta}_{\rm eff}$. In section IV.3, we show a model extension that naturally leads to such a small difference and therefore prevents the reintroduction of a fine-tuning problem.

In order to see the corresponding behavior in the $\{m_a, G_{a\gamma\gamma}\}$ plane, we solve equation (IV.9) for $1/f_a$,

$$\frac{1}{f_a} = -\frac{\cos\left(\bar{\theta} - \bar{\theta}_{\rm eff}\right)}{2 f_{\rm max} \cos\left(N_g \bar{\theta}_{\rm eff}\right)} + \sqrt{\frac{m_a^2}{\Lambda_{\rm QCD}^4 \cos\left(N_g \bar{\theta}_{\rm eff}\right)} + \left(\frac{\cos\left(\bar{\theta} - \bar{\theta}_{\rm eff}\right)}{2 f_{\rm max} \cos\left(N_g \bar{\theta}_{\rm eff}\right)}\right)^2} . \tag{IV.12}$$

From this equation we see, that for $\bar{\theta} \to \pi$ and $m_a \to 0$ the $1/f_a$ dependence reaches a constant. For a vanishing $\bar{\theta}_{\rm eff}$ this constant is exactly $1/f_{\rm max}$.

Neglecting the mixing between A and a of order $\mathcal{O}(\Lambda_{\rm QCD}/|\mu_A|)$, the axion diphoton coupling stays in its canonical form, such that we get new model lines for different $f_{\rm max}$, shown in Figure IV.2. We see that the model lines branch off close to $f_a \approx f_{\rm max}$ and reach $m_a \to 0$ for $f_a \to f_{\rm max}$. Lines of light axions are already excluded for $f_{\rm max} \lesssim 10^7$ GeV by astrophysical bounds and helioscope experiments such as CAST [63, 64].

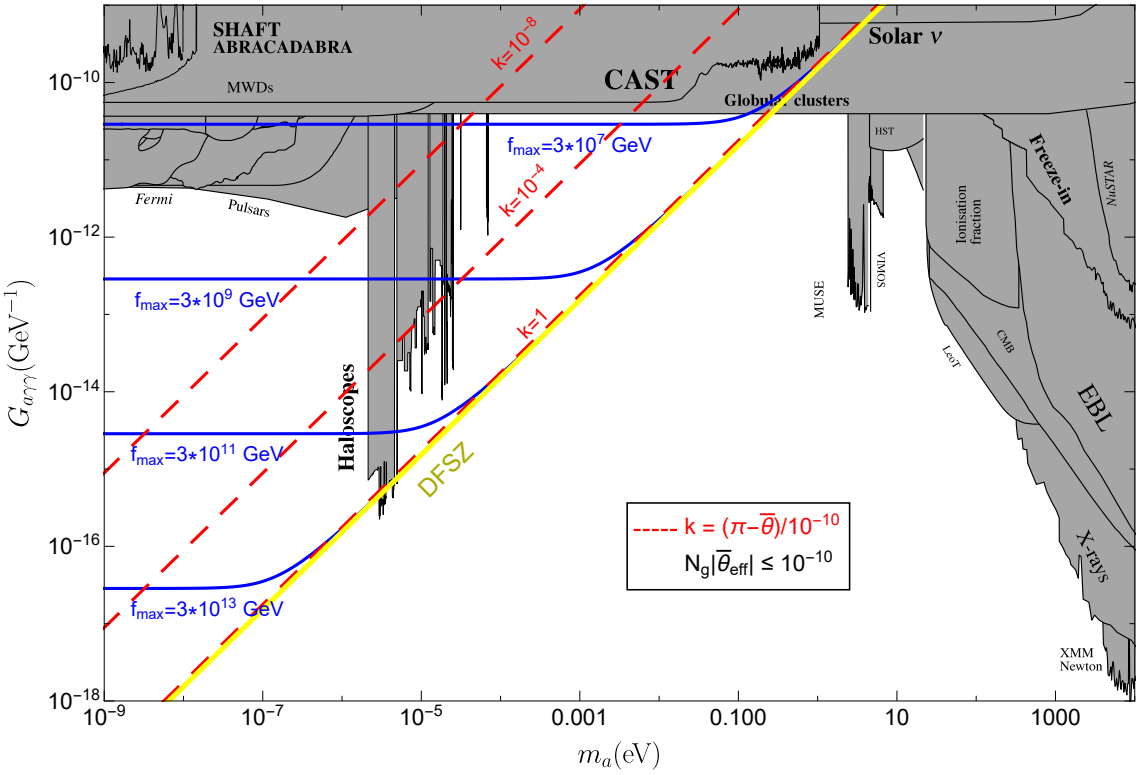

Figure IV.2: Deviations from the canonical DFSZ axion line in the $\{m_a, G_{a\gamma\gamma}\}$ plane. We show the axion mass relations for $\bar{\theta}$ close to π for different values of $f_{\rm max}$ in comparison to the canonical DFSZ line. The dashed lines show the maximal deviations from π to not spoil the nEDM bound of $N_g|\bar{\theta}_{\rm eff}| \leq 10^{-10}$. The limits are extracted from reference [53].

For 10^7 GeV $\lesssim f_{\rm max} \lesssim 10^{11}$ GeV the model lines for light axions reach a region that is relevant for Haloscope experiments and telescope-based searches. Our approach not only shows that additional PQ breaking operators change the QCD axion line drastically but also constrains the maximal extend of the canonical DFSZ line for an additional PQ breaking term in the Lagrangian to $f_a \lesssim f_{\rm max}$. In the next section, we discuss how we can generate such an additional potential.

IV.2 Operators with Anarchic Axion Solution

In order to construct a PQ breaking term of the form of $V_{\rm ang}^{\rm break}$ in equation (IV.2), we can make use of the various options which we presented in Chapter III. This includes a term in the scalar potential which explicitly breaks the PQ symmetry. We show such an example in subsection IV.2.1. Additionally, we can generate $V_{\rm ang}^{\rm break}$ from a fermion condensate through either the Yukawa interaction in subsection IV.2.2 or $SU(N)$ instantons in subsection IV.2.3.

IV.2.1 Explicit soft breaking Term

In the DFSZ model the axion as the Goldstone boson of the spontaneously broken PQ symmetry is composed of the angular modes of the complex scalars H_u, H_d, and Φ. Hence, we can define an additional operator which breaks the PQ symmetry explicitly by adding a new term in the scalar potential,

$$V_{\text{soft}}^{\text{break}} = -\mu_B^2 H_u H_d + \text{h.c.} = -\left(1+\frac{h_u}{v_u}\right)\left(1+\frac{h_d}{v_d}\right)|\mu_B|^2 v_u v_d \cos\left(\frac{a_u}{v_u}+\frac{a_d}{v_d}-2\theta_B\right), \tag{IV.13}$$

which describes a soft PQ breaking since it is proportional to a complex mass scale $\mu_B = |\mu_B|\exp(-i\theta_B)$.

We reexpress the vevs and angular modes in terms of the physical scales f_a, f_A, v and the fields a and A under the use of the mixing angles $\tan\beta_1 = v_u/v_d$ and $\tan\beta_2 = f_a/f_A$ (see subsection III.1.1). The angular potential is then given by

$$V_{\text{ang}}^{\text{break}} \to -|\mu_B|^2 N_g f_a v \cos\beta_2 \cos\left(\frac{1}{N_g}\left(\frac{a}{f_a}+\frac{A}{f_A}\right)-2\theta_B\right) \tag{IV.14}$$

where the amplitude of the term is naturally suppressed by $\cos\beta_2 \ll 1$.

The corresponding model dependent parameters read

$$x = 1\,, \quad \theta_x = 2\theta_B\,, \quad f_{\max} = \frac{N_g \Lambda_{\text{QCD}}^4}{|\mu_B|^2 v\cos\beta_2}\,. \tag{IV.15}$$

We notice, that since $x = 1$ the dependence of θ_A drops out and the minimum of the heavy pseudoscalar is exactly at $\langle A\rangle = 0$.

From the plateau region, where we have $f_a \lesssim f_{\max}$, we can find a constraint on the magnitude of μ_B,

$$|\mu_B|^2 \sin(2\beta_1) \lesssim 2\frac{N_g^2 \Lambda_{\text{QCD}}^4}{v^2} \approx 10^{-8}\ \text{GeV}^2\,. \tag{IV.16}$$

Especially in the case of a large scale separation between v and f_a ($\beta_1 \to \pi/4$) we get $|\mu_B| \lesssim 10^{-4}$ GeV.

IV.2.2 PQ breaking from Yukawa Interactions

The appearance of a fermion condensate can enter in two different ways into the scalar potential. The first option is through a Yukawa interaction with one of the complex scalars. The second option is through instanton effects which we discuss in the next subsection.

We add a fermion ψ which does not transform under the SM gauge group but has chiral $\mathbb{Z}_n$ charges with a difference of 1. We then can write down a Yukawa interaction of the form

$$V_{\text{Yukawa}}^{\text{break}} = y_\psi \bar{\psi}_L \Phi \psi_R + \text{h.c.} \to \frac{|y_\psi|}{\sqrt{2}} v_\psi^3 v_\Phi \cos\left(\frac{a_\Phi}{v_\Phi}-\theta_\psi\right), \tag{IV.17}$$

with coupling $y_\psi = |y_\psi|\exp(-i\theta_\psi)$. This term leads to an angular potential for the axion via the angular mode a_Φ of the complex scalar field Φ with

$$V_{\text{ang}}^{\text{break}} = -\frac{|y_\psi|}{\sqrt{2}} v_\psi^3 \frac{N_g f_a}{\sqrt{1+\frac{f_A^2}{f_a^2}}} \cos\left(\frac{1}{N_g}\left(\frac{a}{f_a}-\frac{f_A^2}{f_a^2}\frac{A}{f_A}\right)+\theta_\psi-\pi\right), \tag{IV.18}$$

where we replaced a_Φ and v_Φ according to subsection III.1.1. We see, that $V_{\text{ang}}^{\text{break}}$ has a linear dependence on f_a which is crucial for the deviation in the $\{m_a, G_{a\gamma\gamma}\}$ plane.

The related model dependent parameter are then given by

$$x = -\frac{f_A^2}{f_a^2}\,, \quad \theta_x = \pi - \theta_\psi\,, \quad f_{\max} = \sqrt{2}\frac{N_g \Lambda_{\rm QCD}^4}{|y_\psi| v_\psi^3}\sqrt{1+\frac{f_A^2}{f_a^2}}\,, \tag{IV.19}$$

where now only the large parameter μ_A ensures the decoupling of A from the axion potential. The experimental limits from Figure IV.2 now set a constraint on $f_{\max} \gtrsim 10^7$ GeV which can be converted for a $\mathcal{O}(1)$ Yukawa coupling into a limit on the fermion condensate $v_\psi \lesssim 10^{-7}$ GeV.

IV.2.3 PQ breaking from $SU(N)$ Instantons

We now consider the case that the complex scalar field couples to N_ψ fermions ψ^j, which are singlets under the SM gauge group but transform under an additional $SU(N)$ gauge group. We then can calculate the operator which breaks the PQ symmetry explicitly through instanton effects.

We start by extending the Yukawa Lagrangian for multiple fermions ψ^j,

$$\mathcal{L}_{\rm Yukawa}^{\rm break} \supset -\sum_j y_j \bar{\psi}_L^j \Phi \psi_R^j + \text{h.c.} = -\sum_j \frac{|y_j|}{\sqrt{2}}(v_\Phi + h_\Phi)\bar{\psi}^j \exp\left(i, \left(\frac{a_\Phi}{v_\Phi} - \theta_j\right)\gamma_5\right)\psi^j\,, \tag{IV.20}$$

with Yukawa couplings $y_j \equiv |y_j|\exp(-i\theta_j)$. The Yukawa interactions induce fermions masses of $m_j = |y_j| v_\Phi/\sqrt{2}$.

We then use a chiral transformation of the form

$$\psi^j \to \exp\left(-\frac{i}{2}\left(\frac{a_\Phi}{v_\Phi} - \frac{i}{2}\theta_j\right)\gamma_5\right)\psi^j \tag{IV.21}$$

in order to shift the axion coupling into the anomalous θ term of $SU(N)$,

$$\mathcal{L}_{\rm gauge}^\theta = \frac{g^2}{32\pi^2}\theta F_{\mu\nu}^a \tilde{F}^{a\mu\nu} \to -\frac{g^2}{32\pi^2}\left(N_\psi \frac{a_\Phi}{v_\Phi} - \sum_j \theta_j - \theta\right) F_{\mu\nu}^a \tilde{F}^{a\mu\nu}\,. \tag{IV.22}$$

The factor N_ψ appears since all fermions ψ^j which transform under $SU(N)$ contribute. The total CP violating θ parameter also shifts by the sum of complex phases θ_j.

We assume that only one fermion ψ^0 has a mass below the confinement scale $m_\psi \leq v_\psi$. Hence, we can use equation (III.35) with $N_\psi^0 = 1$ to obtain the corresponding instanton potential

$$V_{\rm inst}^{\rm break} = -K\left(v_\psi^3 + 2 m_\psi \Lambda_\psi^2\right)\cos\left(N_\psi \frac{a_\Phi}{v_\Phi} - \sum_j \theta_j - \theta\right), \tag{IV.23}$$

with instanton amplitude K and Λ_ψ being a cut-off in the instanton size integration. Since ψ^0 is the only light fermion, we do not have an approximate global $SU(N_\psi^0)$ symmetry and therefore no associated pions.

Reexpressing the fermion mass m_ψ as well as the angular mode a_Φ and vev v_Φ of the complex terms in terms of the axion a, the pseudoscalar A and the associated decay constants, the resulting angular potential reads

$$V_{\rm ang}^{\rm break} = -K\left(v_\psi^3 + \sqrt{2}|y_\psi|\Lambda_\psi^2 \frac{N_g f_a}{\sqrt{1+\frac{f_A^2}{f_a^2}}}\right)\cos\left(\frac{N_\psi}{N_g}\left(\frac{a}{f_a} - \frac{f_A^2}{f_a^2}\frac{A}{f_A}\right) + \sum_j \theta_j + \theta\right). \tag{IV.24}$$

We notice, that we not only generate a PQ breaking operator linear in f_a but also get a constant correction to m_a of order $Kv_\psi^3/\Lambda_{\rm QCD}^4$. This dependence opens up the parameter space allowing for higher and lower axion masses, as shown in Figure IV.3.

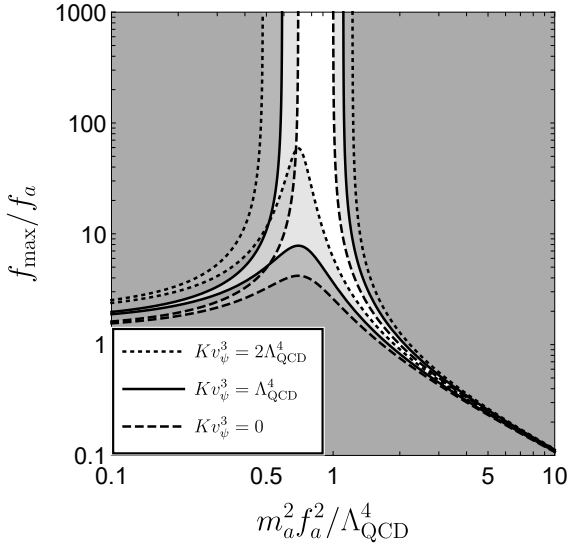

Figure IV.3: Deviation from the canonical axion mass relation for an instanton induced additional PQ breaking. We show the allowed parameter space in white for a fixed $N_g\bar{\theta}_{\rm eff} = 0.8$. The different regions are obtained for a variation of the constant instanton contribution Kv_ψ^3 from the PQ anomaly $\Lambda_{\rm QCD}^4$.

The figure is based on a modified version of equation (IV.10), taking into account the correction proportional to $Kv_\psi^3/\Lambda_{\rm QCD}^4$ as well as the multiplicity N_ψ of the fermions,

$$\left(1-\frac{N_\psi^2}{N_g^2}\right)\cos^2(N_g\bar{\theta}_{\rm eff})-2\frac{m_a^2 f_a^2}{\Lambda_{\rm QCD}^4}\cos\big(N_g\bar{\theta}_{\rm eff}\big)+\frac{m_a^4 f_a^4}{\Lambda_{\rm QCD}^8}-\left(N_\psi^2\frac{f_a}{f_{\rm max}}+\frac{N_\psi^2}{N_g^2}\frac{Kv_\psi^3}{\Lambda_{\rm QCD}^4}\right)^2+\frac{N_\psi^2}{N_g^2}=0\,. \tag{IV.25}$$

It becomes evident, that not only the parameter space opens up, but also that the $f_{\rm max}/f_a$ ratio gets shifted to smaller values for increasing $Kv_\psi^3/\Lambda_{\rm QCD}^4$.

Thus, the maximal decay constant $f_{\rm max}$ is defined in the limit where the constant piece vanishes and is given by

$$f_{\rm max} = \frac{N_g\Lambda_{\rm QCD}^4}{\sqrt{2}|y_\psi|K\Lambda_\psi^2}\sqrt{1+\frac{f_A^2}{f_a^2}}\,. \tag{IV.26}$$

For $f_{\rm max} \gtrsim 10^7$ GeV this sets an upper limit on the parameters $2|y_\psi|K\Lambda_\psi^2 \lesssim 10^{-7}$ GeV. This is consistent with the assumption, that the Yukawa coupling $|y_\psi|$ is associated with the only light fermion which transforms under $SU(N)$, keeping $f_{\rm max}$ large.

IV.3 UV Completion with natural light Axion Solution

In Figure IV.2 we saw that in order to achieve a lighter axion than usual, the phase $\bar{\theta}$ has to be closely aligned with π, such that light axion solutions would still have a quality problem. In our work [5] we aim to find a UV completion that avoids this problem.

For this purpose we can embed our model into a Nelson-Barr solution [50, 51] of the strong CP problem. Nelson-Barr models regard CP as a conserved symmetry in the UV,

such that the strong CP phase is parametrically zero and can only emerge radiatively or through higher dimensional operators. Including an axion in our case allows for a second solution of Nelson-Barr with a strong CP phase of π in the UV. This second case coincides with our light axion construction.

Since the SM also includes a CP violating phase in the weak sector, a viable Nelson-Barr extension must incorporate a mechanism that violates CP spontaneously. This spontaneous CP violation (SCPV) are minimally realizable by adding a vector-like quark q and an additional complex scalar Φ_C, as was shown in [206]. The corresponding field content is depicted in Table IV.1.

	$SU(3)_C$	$SU(2)_L$	$U(1)_Y$	$\mathbb{Z}_n$	$U(1)_{PQ}$
Q_L^i	3	2	1/6	0	X_Q
u_R^i	3	1	2/3	1	X_Q-X_u
d_R^i	3	1	-1/3	0	X_Q-X_d
L_L^i	1	2	-1/2	0	X_L
e_R^i	1	1	-1	0	X_L-X_d
H_u	1	2	-1/2	n-1	X_u
H_d	1	2	1/2	0	X_d
Φ	1	1	0	1	-X
q_L	3	1	2/3 - δ_{qd}	$n/2 + \delta_{qu}$	X_q
q_R	3	1	2/3 - δ_{qd}	$n/2 + \delta_{qu}$	X_q
Φ_C	1	1	0	$n/2$	0

Table IV.1: Field content of the Nelson-Barr extension in the anarchic axion model. We add a vector-like quark q and a complex scalar Φ_C to the field content of the DFSZ model. The quark can either have up-type charges ($\delta_{qu} = 1$, $\delta_{qd} = 0$) or down-type charges ($\delta_{qu} = 0$, $\delta_{qd} = 1$).

In addition to our requirement of $n > 4$ to secure the DFSZ model, we also assume that n represents an even number which is necessary to generate SCPV. This becomes clear by investigating the scalar Lagrangian of the NB extension,

$$\begin{aligned}\mathcal{L}^{\text{NB}}_{\text{scalar}} \supset & \mathcal{L}^{\text{DFSZ}}_{\text{scalar}} + |\partial_\mu \Phi_C|^2 - \mu_C^2 |\Phi_C|^2 - \lambda_C |\Phi_C|^4 \\ & - \lambda_{uC} |H_u|^2 |\Phi_C|^2 - \lambda_{dC} |H_d|^2 |\Phi_C|^2 - \lambda_{\Phi C} |\Phi|^2 |\Phi_C|^2 \\ & - \left(\tilde{\mu}_C^2 + \tilde{\lambda}_C |\Phi_C|^2 + \tilde{\lambda}_{uC} |H_u|^2 + \tilde{\lambda}_{dC} |H_d|^2 + \tilde{\lambda}_{\Phi C} |\Phi|^2 \right) \Phi_C^2 - \lambda'_C \Phi_C^4 + \text{h.c.}\,,\end{aligned} \tag{IV.27}$$

where the last line only appears for even n and induces a complex vev $\langle \Phi_C \rangle \equiv v_C \exp(-i\theta_C)/\sqrt{2}$ for the scalar field Φ_C including a CP violating phase θ_C.

In order to move the CP violating phase into the weak sector of the SM, we choose the vector-like quark either being up-type ($\delta_{qu} = 1$, $\delta_{qd} = 0$) or down-type ($\delta_{qu} = 0$, $\delta_{qd} = 1$), such that the Yukawa Lagrangian becomes

$$\mathcal{L}^{\text{NB}}_{\text{Yukawa}} \supset \mathcal{L}^{\text{DFSZ}}_{\text{Yukawa}} - \bar{q}_L \left(y_C^i \Phi_C + \tilde{y}_C^i \Phi_C^* \right) \left(\delta_{qu} u_R^i + \delta_{qd} d_R^i \right) - \mu_q \bar{q}_L q_R + \text{h.c.}\,. \tag{IV.28}$$

This choice however, not only opens up a decay channel for the additional quark but it also introduces an off-diagonal mass mixing term proportional to the Yukawa couplings y_C^i and $\tilde{y}_C^i$ in addition to a vector-like mass μ_q of the quark.

Since the Nelson-Barr construction assures CP to be a conserved symmetry in the UV, the couplings can only depend on phases which are multiples of π: $y_C^i \equiv |y_C^i| \exp\left(-ik_C^i \pi\right)$, $\tilde{y}_C^i \equiv |\tilde{y}_C^i| \exp\left(-i\tilde{k}_C^i \pi\right)$ and $\mu_q \equiv |\mu_q| \exp(-ik_q\pi)$, with $\{k_C^i, \tilde{k}_C^i, k_q\} \in \mathbb{Z}$. The corresponding quark mass matrix then reads

$$\mathcal{L}_{\text{Yukawa}}^{\text{NB}} \supset -\begin{pmatrix}\bar{\mathbf{u}}_L & \bar{\mathbf{d}}_L & \bar{q}_L\end{pmatrix} \begin{pmatrix} \mathbf{Y}_u \frac{v_u}{\sqrt{2}} & 0 & \delta_{qu}\left(\mathbf{y}_C e^{-i\theta_C} + \tilde{\mathbf{y}}_C e^{i\theta_C}\right)\frac{v_C}{\sqrt{2}} \\ 0 & \mathbf{Y}_d \frac{v_d}{\sqrt{2}} & \delta_{qd}\left(\mathbf{y}_C e^{-i\theta_C} + \tilde{\mathbf{y}}_C e^{i\theta_C}\right)\frac{v_C}{\sqrt{2}} \\ 0 & 0 & |\mu_q| e^{-ik_q\pi} \end{pmatrix} \begin{pmatrix}\mathbf{u}_R \\ \mathbf{d}_R \\ q_R\end{pmatrix} + \text{h.c.}\,. \tag{IV.29}$$

From this Lagrangian we can extract the four dimensional Yukawa matrices $\mathbf{Y}_{qf}$ for both up- and down-type quarks, $f \in \{u, d\}$. The Yukawa matrices and their hermitian products $\mathbf{Y}_{qf}^\dagger \mathbf{Y}_{qf}$ read

$$\mathbf{Y}_{qf} \equiv \begin{pmatrix} \mathbf{Y}_f & \delta_{qf}\frac{\sqrt{2}}{v_f}\mathbf{m}_C \\ 0 & \frac{\sqrt{2}}{v_f}|\mu_q| e^{-ik_q\pi} \end{pmatrix}, \quad \mathbf{Y}_{qf}^\dagger \mathbf{Y}_{qf} = \frac{2}{v_f^2}\begin{pmatrix} \frac{v_f^2}{2}\mathbf{Y}_f^\dagger \mathbf{Y}_f & \delta_{qf}\frac{v_f}{\sqrt{2}}\mathbf{Y}_f^\dagger \mathbf{m}_C \\ \delta_{qf}\frac{v_f}{\sqrt{2}}\mathbf{m}_C^\dagger \mathbf{Y}_f & \left(|\mu_q|^2 + \delta_{qf}|\mathbf{m}_C|^2\right) \end{pmatrix}, \tag{IV.30}$$

where we used $\mathbf{m}_C \equiv (\mathbf{y}_C e^{-i\theta_C} + \tilde{\mathbf{y}}_C e^{i\theta_C})v_C/\sqrt{2}$ as a short-hand.

Assuming $|\mu_q|^2 + |\mathbf{m}_C|^2 \gg v^2$, we can now find the three-dimensional Yukawa matrices in the DFSZ model $\mathbf{Y}_f^{\text{DFSZ}}$ by diagonalizing equation (IV.30), which leads to

$$\left(\mathbf{Y}_f^{\text{DFSZ}}\right)^\dagger \mathbf{Y}_f^{\text{DFSZ}} = \mathbf{Y}_f^\dagger \mathbf{Y}_f - \delta_{qf}\frac{\mathbf{Y}_f^\dagger \mathbf{m}_C \mathbf{m}_C^\dagger \mathbf{Y}_f}{|\mu_q|^2 + |\mathbf{m}_C|^2}\,. \tag{IV.31}$$

We notice that we only get a correction for those quarks which couple directly to q ($\delta_{qf} = 1$).

Since the Nelson-Barr construction forbids CP violation in the UV, the Yukawa matrices $\mathbf{Y}_f$ are purely real, such that a complex phase only enters through the SCPV phase θ_C in $\mathbf{m}_C$. We transform the SM quarks according to subsection II.2.2 using $U(3)$ matrices to obtain real and diagonal Yukawa matrices $\mathbf{Y}_{D,f}^{\text{DFSZ}}$,

$$\mathbf{f}_L \to \mathbf{U}_f \mathbf{f}_L\,, \quad \mathbf{f}_R \to \mathbf{V}_f \mathbf{f}_R\,, \quad \mathbf{U}_f^\dagger \mathbf{U}_f = \mathbb{1} = \mathbf{V}_f^\dagger \mathbf{V}_f\,, \quad \mathbf{Y}_{D,f}^{\text{DFSZ}} = \mathbf{U}_f^\dagger \mathbf{Y}_f^{\text{DFSZ}} \mathbf{V}_f\,. \tag{IV.32}$$

This then leads to the CKM matrix $\mathbf{V}_{\text{CKM}} \equiv \mathbf{U}_u^\dagger \mathbf{U}_d$, which contains a CP violating phase as expected, since either the up-type or down-type quarks have a complex Yukawa matrix before the transformation.

In order to determine the CP violating phase of QCD we only need to take into account the quark sector which couples to the heavy quark q, since the Yukawa matrix of the other sector is purely real. Since the parameter θ_{QCD} is also forbidden by CP conservation in the Nelson-Barr model, the parameter $\bar{\theta}_{\text{SM}}$ changes to

$$\bar{\theta}_{\text{SM}} \to -\sum_{f=u,d} \delta_{qf} \arg\left(\det(\mathbf{Y}_{qf})\right) = k_q \pi\,, \tag{IV.33}$$

such that the $\bar{\theta}$ parameter from equation (IV.5) is given by $N_g \bar{\theta}_{\text{NB}} \equiv k_q \pi$. Strictly speaking are all CP phases discretized as $k\pi$ with $k \in \mathbb{Z}$, but we can absorb all integers k into k_q without loss of generality.

In addition to the $k_q\pi$ phase we need to take corrections from higher dimensional operators as well as radiative corrections into account. As it was pointed out by reference [207]

dimension-5 operators contributing to a strong CP phase are given by

$$\mathcal{L}^{d=5}_{\text{Yukawa}} \supset -\frac{y_{qC}}{\Lambda}\Phi_C^2 \bar{q}_L q_R - \sum_{f=u,d} \delta_{qf} \frac{y^i_{fC}}{\Lambda} \Phi_C \bar{Q}^i_L H_f q_R + \text{h.c.}\,. \tag{IV.34}$$

Hence, we get a correction to $\bar{\theta}_{\text{NB}}$ of $N_g \Delta\bar{\theta}_{\text{NB}} \sim \theta_C v_C/\Lambda$. One obtains a comparable contribution from radiative corrections that involves multi-scalar interactions from equation (IV.27).

We can now compute the residual CP violating phase under the use of equation (IV.11). For small axion masses it reads

$$|\bar{\theta}_{\text{eff}}| = \Delta\bar{\theta}_{\text{NB}} \frac{\Lambda^4_{\text{QCD}}}{m_a^2 f_{\text{max}}^2} \leq 10^{-10} \quad \Leftrightarrow \quad \frac{m_a^2 f_a^2}{\Lambda^4_{\text{QCD}}} \gtrsim \frac{\theta_C v_C}{|\bar{\theta}_{\text{eff}}|\Lambda} \frac{f_a}{f_{\text{max}}}\,. \tag{IV.35}$$

Hence, for f_a close to f_{max}, $v < v_C = 1$ TeV and a Planck suppressed higher dimension-5 operator ($\Lambda = M_{\text{Pl}}$) we can deviate from the canonical axion mass relation by six orders of magnitude, $m_a^2 f_a^2 \gtrsim 10^{-6}\Lambda^4_{\text{QCD}}$.

Since $\bar{\theta}_{\text{NB}}$ now only takes discrete values, we need to specify the generation of the $V^{\text{break}}_{\text{ang}}$ in more detail to obtain the light axion solution. We show this necessity based on an instanton induced PQ breaking operator as was introduced in subsection IV.2.3.

In particular, one cannot choose the number of fermions N_ψ freely anymore. This becomes evident as the respective version of equation (IV.9) now contains factors of N_ψ,

$$\left.\frac{\partial^2 V_{\text{axion}}}{\partial^2 a}\right|_{a\to\langle a\rangle} = m_a^2 \quad \Rightarrow \quad \cos\!\left(-N_g\bar{\theta}_{\text{eff}}\right) + \frac{f_a}{f_{\text{max}}}\cos\!\left(\frac{N_\psi}{N_g}k_q\pi - N_\psi\bar{\theta}_{\text{eff}}\right) = \frac{m_a^2 f_a^2}{\Lambda^4_{\text{QCD}}}\,, \tag{IV.36}$$

where the $\bar{\theta}$ dependence was replaced by the discretized version containing k_q.

In Figure IV.4 we show the allowed parameter space for $N_\psi \in \{1,2,3,4\}$ accounting for the deviations of $m_a^2 f_a^2$ from Λ^4_{QCD} and f_a from f_{max}. We also depicted the discretized model lines achievable for different k_q. We notice that we can only reach the light axion solution for an odd number of $SU(N)$ fermions.

In conclusion, we showed that one indeed can obtain light axion solutions without reintroducing a fine-tuning problem. However, we only reach extreme deviations for suppressed higher-order corrections like Planck suppressed dimension-5 operators. We leave the construction of mechanisms which relax these bounds further for future work.

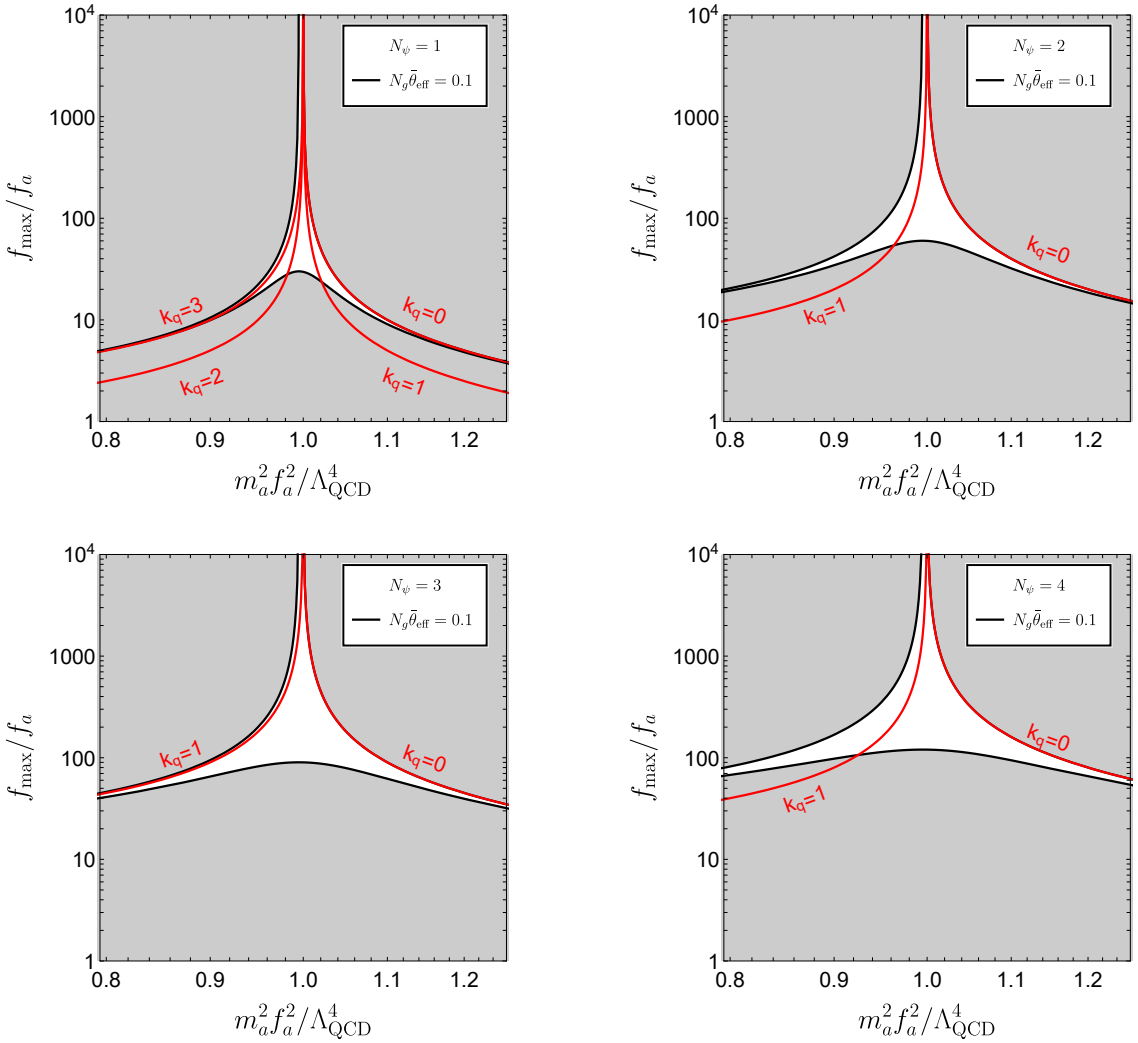

Figure IV.4: Deviation from the canonical axion mass relation for an instanton induced additional PQ breaking with Nelson-Barr extension. We show the allowed parameter space in white for a fixed $N_g\bar{\theta}_{\rm eff} = 0.1$ and $Kv_\psi^3 \ll \Lambda^4_{\rm QCD}$ and vary N_ψ between the panels. The red lines show the expected mass relations for different classes of k_q denoted by their lowest possible value.

Part II

Exotic Axion Couplings

CHAPTER V

Axion Couplings and ALP-EFT Basis

In the second part of this thesis we investigate various modifications of axion couplings. For this discussion we first establish in section V.1 a general ALP-EFT basis which includes all possible linear axion couplings to fermions, scalars and gauge bosons up to $\mathcal{O}(1/f_a)$. Afterwards we calculate in section V.2 the respective Wilson coefficients from integrating out heavy fermion. The results of this chapter are mainly published in [2].

In Chapter III we saw already that in the flavor-conserving case the global Goldstone bosons couple to the mass sector of the fermions,

$$\mathcal{L}_{\text{Yukawa}}\Big|_{\phi_{\mathtt{i}}\to 0} \supset -\sum_j m_j \bar{\psi}_j \exp\left(-2i\sum_{\mathtt{K}} Q^j_{\mathtt{K},A}\frac{a_{\mathtt{K}}}{f_{\mathtt{K}}}\gamma_5\right)\psi_j\,, \tag{V.1}$$

where we set the focus for this chapter on the axion $a_{\mathtt{K}} \equiv a$ with the corresponding PQ charges $Q_{\mathtt{K},A} \equiv X_A$. Further global Goldstone bosons as the A from the DFSZ model will be regarded as much heavier and therefore decouple from the particle spectrum.

In order to take effects into account which can change the flavor of the fermions, we express the parameters as vectors and matrices in flavor space. The vector Ψ then contains all fermion flavors and $\mathbf{M}^\psi$ represents the fermion mass matrix. Expressing also the PQ charges as vector-like and axial charge matrices, $\mathbf{X}^\psi_V$ and $\mathbf{X}^\psi_A$, the axion couplings in the fermion mass sector become

$$\mathcal{L}^\psi_{\mathbf{M}} \supset -\bar{\Psi}\exp\left(i(\mathbf{X}^\psi_V - \mathbf{X}^\psi_A\gamma_5)\frac{a}{f_a}\right)\mathbf{M}^\psi\exp\left(-i(\mathbf{X}^\psi_V + \mathbf{X}^\psi_A\gamma_5)\frac{a}{f_a}\right)\Psi\,. \tag{V.2}$$

We notice that in the flavor-conserving case the dependence on the vector-like charges cancels and we recover equation (V.1).

Expanding $\mathcal{L}^\psi_{\mathbf{M}}$ in leading order in $1/f_a$ leads to the canonical expression

$$\begin{aligned}\mathcal{L}^\psi_{\mathbf{M}} &\supset i\frac{a}{f_a}\left(\bar{\Psi}[\mathbf{M}^\psi, \mathbf{X}^\psi_V]\Psi + \bar{\Psi}\{\mathbf{M}^\psi, \mathbf{X}^\psi_A\}\gamma_5\Psi\right) + \mathcal{O}\left(\frac{1}{f_a^2}\right)\\ &= i\frac{a}{f_a}\sum_{ij}\left((m_i - m_j)\bar{\psi}_i X^{ij}_V\psi_j + (m_i + m_j)\bar{\psi}_i X^{ij}_A\gamma_5\psi_j\right) + \mathcal{O}\left(\frac{1}{f_a^2}\right)\,.\end{aligned} \tag{V.3}$$

In the following section we use the axion interaction in the mass sector of the fermions as a starting point to obtain the full ALP-EFT basis.

V.1 Generalized ALP-EFT Basis and Fermion Transformations

In this section we construct a general ALP-EFT basis for the axion field up to $\mathcal{O}(1/f_a)$. We start by identifying interactions which are induced by chiral transformations of fermion fields and add terms from the scalar Lagrangian in subsection V.1.1. Finally we apply the general description in subsection V.1.2 to the DFSZ model.

First we need the most general fermionic Lagrangian at dimension 4 including the exponential axion coupling in the fermion mass sector from equation (V.2). It involves gauge interaction in unitary gauge as well as Yukawa interactions of all fermions and reads

$$\begin{aligned}\mathcal{L}^\psi \supset & i\bar{\Psi}\gamma^\mu\partial_\mu\Psi + \sum_{\mathtt{I}} g_{\mathtt{I}}\bar{\Psi}A_{\mathtt{I},\mu}\gamma^\mu(\mathbf{Q}^\psi_{\mathtt{I},V} + \mathbf{Q}^\psi_{\mathtt{I},A}\gamma_5)\Psi - \sum_{\mathtt{i}}\frac{\phi_{\mathtt{i}}}{\sqrt{2}}\bar{\Psi}\mathbf{Y}^\psi_{\mathtt{i}}\Psi \\ & - \bar{\Psi}\exp\left(i(\mathbf{X}^\psi_V - \mathbf{X}^\psi_A\gamma_5)\frac{a}{f_a}\right)\mathbf{M}^\psi\exp\left(-i(\mathbf{X}^\psi_V + \mathbf{X}^\psi_A\gamma_5)\frac{a}{f_a}\right)\Psi\,, \end{aligned} \tag{V.4}$$

where the matrices $\mathbf{Y}^\psi_{\mathtt{i}}$ represent the Yukawa interactions to the real scalar fields $\phi_{\mathtt{i}}$. We neglect angular scalar fields besides the axion as they are either absorbed by the gauge fields in unitary gauge or are assumed to be much heavier.

The charge matrices $\mathbf{Q}^\psi_{\mathtt{I},V}$ and $\mathbf{Q}^\psi_{\mathtt{I},A}$ represent the couplings of the fermions to the respective gauge groups labeled by index $\mathtt{I}$. The gauge interactions are further specified by their gauge couplings $g_{\mathtt{I}}$ and gauge bosons $A_{\mathtt{I},\mu} = A^a_{\mathtt{I},\mu}t^a_{\mathtt{I}}$ in unitary gauge, with $t^a_{\mathtt{I}}$ being the corresponding generators. In case of an $SU(N)$ symmetry the charge matrices comprise unitary matrices as the CKM matrix in case of the SM $SU(2)_L$ gauge group.

From $\mathcal{L}^\psi$ we can deduce general ALP-EFT terms by performing a chiral transformation on the fermions of the form

$$\Psi \to \exp\left(i(\mathbf{X}^\psi_V + \mathbf{X}^\psi_A\gamma_5)\frac{a}{f_a}\right)\Psi, \quad \bar{\Psi} \to \bar{\Psi}\exp\left(-i(\mathbf{X}^\psi_V - \mathbf{X}^\psi_A\gamma_5)\frac{a}{f_a}\right). \tag{V.5}$$

The resulting Lagrangian can then be used to write down a basis for which the physical observables are invariant under the given chiral transformation.

Among other terms, the transformation in equation (V.5) leads to an anomaly in the gauge sector due to the regularization in the Jacobian factor of the path integral following Fujikawa's method [47]. The anomaly appears as a flavor changing generalization of equation (II.8) with anomaly coefficients given by

$$\begin{aligned}\mathcal{A}_{\mathtt{PQIJ}} &= \sum_{i,j,k} T(R_{\mathtt{I}k})(X^{ij}_R Q^{ik}_{\mathtt{I}R}Q^{kj}_{\mathtt{J}R} - X^{ij}_L Q^{ik}_{\mathtt{I}L}Q^{kj}_{\mathtt{J}L}) \\ &= 2\sum_{i,j,k} T(R_{\mathtt{I}k})(X^{ij}_V(Q^{ik}_{\mathtt{I}V}Q^{kj}_{\mathtt{J}A} + Q^{ik}_{\mathtt{I}A}Q^{kj}_{\mathtt{J}V}) + X^{ij}_A(Q^{ik}_{\mathtt{I}V}Q^{kj}_{\mathtt{J}V} + Q^{ik}_{\mathtt{I}A}Q^{kj}_{\mathtt{J}A}))\,, \end{aligned} \tag{V.6}$$

where $T(R_{\mathtt{I}k})$ again is defined as the Dynkin index [48] via $\mathrm{tr}\left[T^a_R T^b_R\right] \equiv T(R)\delta^{ab}$ and $R_{\mathtt{I}k}$ denotes the representation of fermion k under gauge group $\mathtt{I}$.

The transformed Lagrangian then contains

$$\begin{aligned}\mathcal{L}^\psi \to & \, i\bar{\Psi}\gamma^\mu\partial_\mu\Psi - \frac{\partial_\mu a}{f_a}\bar{\Psi}\gamma^\mu(\mathbf{X}^\psi_V + \mathbf{X}^\psi_A\gamma_5)\Psi - \bar{\Psi}\mathbf{M}^\psi\Psi + \frac{a}{f_a}\sum_{\mathtt{I},\mathtt{J}}\mathcal{A}_{\mathtt{PQIJ}}\frac{g_{\mathtt{I}}g_{\mathtt{J}}}{(4\pi)^2}F^a_{\mathtt{I}\mu\nu}\tilde{F}^{a,\mu\nu}_{\mathtt{J}} \\ & + \sum_{\mathtt{I}} g_{\mathtt{I}}\bar{\Psi}A_{\mathtt{I},\mu}\gamma^\mu\exp\left(-i(\mathbf{X}^\psi_V + \mathbf{X}^\psi_A\gamma_5)\frac{a}{f_a}\right)(\mathbf{Q}^\psi_{\mathtt{I}V} + \mathbf{Q}^\psi_{\mathtt{I}A}\gamma_5)\exp\left(i(\mathbf{X}^\psi_V + \mathbf{X}^\psi_A\gamma_5)\frac{a}{f_a}\right)\Psi \end{aligned}$$

$$-\sum_{\mathtt{i}}\frac{\phi_{\mathtt{i}}}{\sqrt{2}}\bar{\Psi}\exp\left(-i(\mathbf{X}_V^\psi-\mathbf{X}_A^\psi\gamma_5)\frac{a}{f_a}\right)\mathbf{Y}_{\mathtt{i}}^\psi\exp\left(i(\mathbf{X}_V^\psi+\mathbf{X}_A^\psi\gamma_5)\frac{a}{f_a}\right)\Psi\,, \tag{V.7}$$

involving the derivative coupling of the axion to the PQ current as well as the the anomalous axion coupling to gauge bosons.

Expanding the gauge and Yukawa interaction at leading order in $1/f_a$ leads to

$$\begin{aligned}\mathcal{L}^\psi_{\text{gauge}}&\supset\sum_{\mathtt{I}}g_{\mathtt{I}}A_{\mathtt{I},\mu}\left(\bar{\Psi}\gamma^\mu(\mathbf{Q}^\psi_{\mathtt{I}V}+\mathbf{Q}^\psi_{\mathtt{I}A}\gamma_5)\Psi+i\frac{a}{f_a}\bar{\Psi}\gamma^\mu[\mathbf{Q}^\psi_{\mathtt{I}V}+\mathbf{Q}^\psi_{\mathtt{I}A}\gamma_5,\mathbf{X}^\psi_V+\mathbf{X}^\psi_A\gamma_5]\Psi\right)\,,\\ \mathcal{L}^\psi_{\text{Yukawa}}&\supset\sum_{\mathtt{i}}\frac{v_{\mathtt{i}}+\phi_{\mathtt{i}}}{\sqrt{2}}\left(-\bar{\Psi}\mathbf{Y}^\psi_{\mathtt{i}}\Psi-i\frac{a}{f_a}\bar{\Psi}[\mathbf{Y}^\psi_{\mathtt{i}},\mathbf{X}^\psi_V]\Psi-i\frac{a}{f_a}\bar{\Psi}\{\mathbf{Y}^\psi_{\mathtt{i}},\mathbf{X}^\psi_A\}\gamma_5\Psi\right)\,.\end{aligned} \tag{V.8}$$

We notice that the gauge bosons acquire a new coupling proportional to the commutator of gauge charges and PQ charges, which vanishes in the flavor-conserving limit.

After pointing out the axion couplings which are generated through fermion transformations, we can write down the full fermion-related axion Lagrangian with generalized coefficients at order $1/f_a$,

$$\begin{aligned}\mathcal{L}^\psi_{\text{axion}}\supset&-\frac{\partial_\mu a}{2f_a}\bar{\Psi}\gamma^\mu(\mathbf{C}^\psi_{1V}+\mathbf{C}^\psi_{1A}\gamma_5)\Psi+\frac{a}{f_a}\sum_{\mathtt{I},\mathtt{J}}C_3^{\mathtt{I}\mathtt{J}}\frac{g_{\mathtt{I}}g_{\mathtt{J}}}{(4\pi)^2}F^a_{\mathtt{I}\mu\nu}\tilde{F}^{a,\mu\nu}_{\mathtt{J}}\\&+\frac{i}{2}\frac{a}{f_a}\bar{\Psi}[\mathbf{M}^\psi,\mathbf{C}^\psi_{2V}]\Psi+\frac{i}{2}\frac{a}{f_a}\bar{\Psi}\{\mathbf{M}^\psi,\mathbf{C}^\psi_{2A}\}\gamma_5\Psi\\&+\frac{i}{2}\frac{a}{f_a}\sum_{\mathtt{i}}\frac{\phi_{\mathtt{i}}}{\sqrt{2}}\bar{\Psi}[\mathbf{Y}^\psi_{\mathtt{i}},\mathbf{C}^\psi_{\mathtt{i}V}]\Psi+\frac{i}{2}\frac{a}{f_a}\sum_{\mathtt{i}}\frac{\phi_{\mathtt{i}}}{\sqrt{2}}\bar{\Psi}\{\mathbf{Y}^\psi_{\mathtt{i}},\mathbf{C}^\psi_{\mathtt{i}A}\}\gamma_5\Psi\\&-\frac{i}{2}\frac{a}{f_a}\sum_{\mathtt{I}}g_{\mathtt{I}}\bar{\Psi}A^{\mathtt{I}}_\mu\gamma^\mu[\mathbf{Q}^\psi_{\mathtt{I}V}+\mathbf{Q}^\psi_{\mathtt{I}A}\gamma_5,\mathbf{C}^\psi_{\mathtt{I}V}+\mathbf{C}^\psi_{\mathtt{I}A}\gamma_5]\Psi+\mathcal{O}\left(\frac{1}{f_a^2}\right)\,.\end{aligned} \tag{V.9}$$

This set of operators describes a closed basis under chiral fermion transformations and is needed to fully calculate the Wilson coefficients in an effective theory where we integrate out heavy fermions. The operators in the EFT then follow the same pattern, but also include terms from the scalar Lagrangian, which we show in the next subsection.

Applying a chiral fermion transformation of the form of equation (V.5) changes the coefficients in equation (V.9) according to

$$\begin{aligned}&\mathbf{C}^\psi_{1V/A}\to\mathbf{C}^\psi_{1V/A}+2\mathbf{X}^\psi_{V/A}\,,\quad\mathbf{C}^\psi_{2V/A}\to\mathbf{C}^\psi_{2V/A}-2\mathbf{X}^\psi_{V/A}\,,\\&\mathbf{C}^\psi_{\mathtt{i}V/A}\to\mathbf{C}^\psi_{\mathtt{i}V/A}-2\mathbf{X}^\psi_{V/A}\,,\quad\mathbf{C}^\psi_{\mathtt{I}V/A}\to\mathbf{C}^\psi_{\mathtt{I}V/A}-2\mathbf{X}^\psi_{V/A}\,,\\&C_3^{\mathtt{I}\mathtt{J}}\to C_3^{\mathtt{I}\mathtt{J}}+\mathcal{A}_{\text{PQ}\mathtt{I}\mathtt{J}}\,.\end{aligned} \tag{V.10}$$

We will see in section V.2 that these transformation properties assure that the effective theory is invariant under chiral fermion transformations.

V.1.1 ALP-EFT Terms from Scalar Potential

The Lagrangian in equation (V.9) does not comprise all axion couplings in the EFT at order $1/f_a$, since integrating out heavy fermions also mediates axion interactions to scalars and gauge bosons which originate at tree-level from the kinetic part of the scalar Lagrangian.

We recall from equation (III.12) the expression for the kinetic terms in the Goldstone basis in unitary gauge,

$$\mathcal{L}^{\phi}_{\text{kin}} \supset \sum_{\mathtt{i}} |D_{\mathtt{i},\mu}\Phi_{\mathtt{i}}|^2 = \sum_{\mathtt{i}} \frac{(v_{\mathtt{i}}+\phi_{\mathtt{i}})^2}{2} \left(\sum_{m_{\mathtt{I}}\neq 0} g_{\mathtt{I}} Q^{\mathtt{i}}_{\mathtt{I}} A_{\mathtt{I},\mu} - \sum_{\mathtt{K}} Q^{\mathtt{i}}_{\mathtt{K}} \frac{a_{\mathtt{K}}}{f_{\mathtt{K}}} \right)^2$$
$$\supset -\frac{\partial_\mu a}{f_a} \sum_{\mathtt{i}} X_{\mathtt{i}} \left(2v_{\mathtt{i}}\phi_{\mathtt{i}} + \phi^2_{\mathtt{i}}\right) \sum_{m_{\mathtt{I}}\neq 0} g_{\mathtt{I}} Q^{\mathtt{i}}_{\mathtt{I}} A_{\mathtt{I},\mu} + \mathcal{O}\left(\frac{1}{f_a^2}\right), \quad \text{(V.11)}$$

where we again set the focus on the axion $a_{\mathtt{K}} \equiv a$ with PQ charges $Q^{\mathtt{i}}_{\mathtt{K}} \equiv X_{\mathtt{i}}$. The orthogonality conditions assure that there is no tree-level mixing between the axion and the gauge bosons.

The resulting axion interaction can then be generalized by introducing a set of coefficients $C_4^{\mathtt{Ii}}$, defined by

$$\mathcal{L}^{\phi}_{\text{axion}} \supset -\frac{\partial_\mu a}{f_a} \sum_{\mathtt{I},\mathtt{i}} C_4^{\mathtt{Ii}} g_{\mathtt{I}} A_{\mathtt{I},\mu} \left(v_{\mathtt{i}}\phi_{\mathtt{i}} + \frac{\phi^2_{\mathtt{i}}}{2} \right) + \mathcal{O}\left(\frac{1}{f_a^2}\right), \quad \text{(V.12)}$$

which is by construction invariant under chiral fermion transformations. Finally, the full axion coupling basis at $1/f_a$ is given by $\mathcal{L}_{\text{axion}} = \mathcal{L}^{\psi}_{\text{axion}} + \mathcal{L}^{\phi}_{\text{axion}}$.

V.1.2 Application to DFSZ Model

After we introduced a full basis for axion couplings we can apply our derivation to the DFSZ axion model at tree-level. In the Higgs basis we only generate axion couplings to fermions via the mixing of angular modes in the Yukawa interactions,

$$\mathcal{L}_{\text{axion}} \supset \frac{1}{2}(\partial_\mu a)^2 - \sum_{i\in \text{SM}} m_i \left(1+\frac{h}{v}\right) \bar{\psi}_i \exp\left(-2iX^i_A \frac{a}{f_a}\gamma_5\right) \psi_i + \mathcal{O}\left(A, H^0, H^\pm\right), \quad \text{(V.13)}$$

where we neglect terms proportional to A, H^0 and $H^\pm$, assuming that these fields are much heavier then the electroweak scale and therefore decouple from the particle spectrum. We note that we do not have a C_4^{Zh} coupling in the Higgs basis at tree-level, since the alignment of h with the SM vev v allows us to apply the orthogonality conditions of the angular mixing to the Higgs couplings.

We then can generate the other terms of the axion interaction basis by performing the chiral transformation from equation (II.38),

$$u^i \to \exp\left(-i\frac{X_u}{2}\frac{a}{f_a}\gamma_5\right) u^i, \quad d^i \to \exp\left(-i\frac{X_d}{2}\frac{a}{f_a}\gamma_5\right) d^i, \quad e^i \to \exp\left(-i\frac{X_d}{2}\frac{a}{f_a}\gamma_5\right) e^i.$$

This transformation results in the canonical DFSZ axion Lagrangian at order $1/f_a$,

$$\begin{aligned}\mathcal{L}_{\text{axion}} \to & \frac{1}{2}(\partial_\mu a)^2 + \frac{\partial_\mu a}{f_a} J^\mu_{\text{PQ}} - \frac{g_s^2}{32\pi^2}\left(2X\mathcal{A}_{gg}\frac{a}{f_a} - \bar{\theta}\right) G^a_{\mu\nu}\tilde{G}^{a\mu\nu} \\ & - X\mathcal{A}_{\gamma\gamma}\frac{e^2}{(4\pi)^2}\frac{a}{f_a}F_{\mu\nu}\tilde{F}^{\mu\nu} - X\mathcal{A}_{\gamma Z}\frac{e^2}{s_W c_W}\frac{1}{(4\pi)^2}\frac{a}{f_a}Z_{\mu\nu}\tilde{F}^{\mu\nu} \\ & - X\mathcal{A}_{ZZ}\frac{e^2}{s_W^2 c_W^2}\frac{1}{(4\pi)^2}\frac{a}{f_a}Z_{\mu\nu}\tilde{Z}^{\mu\nu} - X\mathcal{A}_{WW}\frac{g_L^2}{(4\pi)^2}\frac{a}{f_a}W_{\mu\nu}\tilde{W}^{\mu\nu} \\ & + i\frac{a}{f_a}\frac{e}{\sqrt{2}s_W}(W^-_\mu(X_d J^{+\mu}_W - X_u J^{+\mu}_{W,l}) + \text{h.c.}) + \mathcal{O}\left(A, H^0, H^\pm\right), \end{aligned} \quad \text{(V.14)}$$

where we added with respect to equation (II.41) the couplings to the heavy SM fields Z_μ and $W_\mu^\pm$ proportional to the respective normalized anomaly coefficients $\mathcal{A}_{\mathtt{IJ}} \equiv \mathcal{A}_{\mathrm{PQ}\mathtt{IJ}}/X$. We see that since the charged current interactions are flavor-violating, we generate a commutator interaction as defined in equation (V.8), which does not depend on the leptons in the $J^{+\mu}_{W,l}$ current, since neutrinos are not charged under PQ.

In Chapter VII we show that we can generate exotic interactions like an effective C^{eff}_{Zh} coupling by integrating out heavy fermions. For this purpose we present in the next section a calculation of the ALP-EFT Wilson coefficients.

V.2 Calculation of ALP-EFT Wilson Coefficients

In this section we provide with general calculations of Wilson coefficients in an ALP-EFT where we integrate out heavy fermions. The interactions of the heavy fermions can be flavor-changing and are given by the terms defined in equations (V.4) and (V.9).

The resulting effective operators are then represented by the full ALP-EFT basis consisting of the terms in equations (V.9) and (V.12). Especially the terms with coefficients $C_3^{\mathtt{IJ}}$ and $C_4^{\mathtt{Ii}}$ are newly generated from only having fermion couplings in the UV. Hence, we show the calculation for an effective axion coupling to two gauge bosons in subsection V.2.1 and to one gauge boson and one scalar in subsection V.2.2.

Finally, we discuss in subsection V.2.3 additional contributions to axion interactions with SM fermions from integrating out heavy fermions and scalars, leading to effective $\mathbf{C}_1$ and $\mathbf{C}_2$ terms. We do not discuss effective contributions to the vertices in $\mathcal{L}^{\psi}_{\mathrm{gauge}}$ and $\mathcal{L}^{\psi}_{\mathrm{Yukawa}}$, which describe interactions of four particles and do not play a role in our phenomenological studies.

V.2.1 Loop-induced Axion Coupling to Gauge Bosons

We start our discussion on fermion loop induced axion couplings by considering the anomalous axion couplings to gauge bosons. It is given for $U(1)$ gauge bosons by

$$\mathcal{L}^{\mathrm{eff}}_{\mathrm{axion}} \supset -C^{\mathrm{eff}}_{\mathtt{IJ}} \frac{g_{\mathtt{I}} g_{\mathtt{J}}}{(4\pi)^2} \frac{a}{f_a} F_{\mathtt{I}\mu\nu} \tilde{F}^{\mu\nu}_{\mathtt{J}} \,, \tag{V.15}$$

where we define the Wilson coefficient $C^{\mathrm{eff}}_{\mathtt{IJ}}$ excluding the loop factor of $(4\pi)^{-2}$, in order to match the parametrics with the tree-level $C_3^{\mathtt{IJ}}$ term. This is motivated by the fact that an anomalous fermion transformation can shift the UV coupling entirely from the fermion sector in the gauge sector, which therefore has to match with the one-loop contribution.

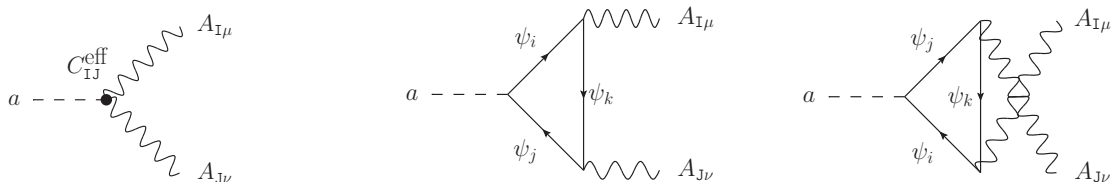

Figure V.1: Effective vertex and one-loop diagrams for anomalous coupling of an axion to two gauge bosons. The loop consists of three fermions ψ_i, ψ_j and ψ_k connecting an axion a with two gauge bosons $A_{\mathtt{I},\mu}$ and $A_{\mathtt{J},\nu}$.

In order to determine the Wilson coefficient we calculate the triangle diagrams shown in Figure V.1. We consider three flavors of fermions ψ_i, ψ_j and ψ_k with masses m_i, m_j and

m_k, which have in general flavor violating couplings to the axion and the gauge bosons defined by the corresponding coupling coefficients and charge matrices.

We consider three limiting cases. In the first limit we consider the fermion masses being much larger than the boson masses, $m_i, m_j, m_k \gg m_a, m_{\mathtt{I}}, m_{\mathtt{J}}$. The resulting Wilson coefficient reads

$$\begin{aligned}
C_{\mathtt{IJ}}^{\text{eff}} =& C_3^{\mathtt{IJ}} - 2\sum_{i,j,k} N_k \frac{C_0(0,0,0,m_i,m_j,m_k)}{\lambda(m_a^2,m_{\mathtt{I}}^2,m_{\mathtt{J}}^2)}\times \\
&\times \Bigg((m_i+m_j)(C_{1A}^{ij}+C_{2A}^{ij})\Bigg((Q_{\mathtt{I}V}^{ik}Q_{\mathtt{J}V}^{kj} - Q_{\mathtt{I}A}^{ik}Q_{\mathtt{J}A}^{kj}) m_k m_a^2 (m_a^2 - m_{\mathtt{I}}^2 - m_{\mathtt{J}}^2) \\
&+ (Q_{\mathtt{I}V}^{ik}Q_{\mathtt{J}V}^{kj} + Q_{\mathtt{I}A}^{ik}Q_{\mathtt{J}A}^{kj})(m_i m_{\mathtt{J}}^2 (m_a^2 + m_{\mathtt{I}}^2 - m_{\mathtt{J}}^2) + m_j m_{\mathtt{I}}^2 (m_a^2 - m_{\mathtt{I}}^2 + m_{\mathtt{J}}^2))\Bigg) \\
&+ (m_i - m_j)(C_{1V}^{ij}+C_{2V}^{ij})\Bigg((Q_{\mathtt{I}A}^{ik}Q_{\mathtt{J}V}^{kj} - Q_{\mathtt{I}V}^{ik}Q_{\mathtt{J}A}^{kj}) m_k m_a^2 (m_a^2 - m_{\mathtt{I}}^2 - m_{\mathtt{J}}^2) \\
&+ (Q_{\mathtt{I}V}^{ik}Q_{\mathtt{J}A}^{kj} + Q_{\mathtt{I}A}^{ik}Q_{\mathtt{J}V}^{kj})(m_i m_{\mathtt{J}}^2 (m_a^2 + m_{\mathtt{I}}^2 - m_{\mathtt{J}}^2) - m_j m_{\mathtt{I}}^2 (m_a^2 - m_{\mathtt{I}}^2 + m_{\mathtt{J}}^2))\Bigg)\Bigg) \\
&- \sum_{i,j,k} N_k \Bigg(C_{1A}^{ij}(Q_{\mathtt{I}V}^{ik}Q_{\mathtt{J}V}^{kj} + Q_{\mathtt{I}A}^{ik}Q_{\mathtt{J}A}^{kj}) + C_{1V}^{ij}(Q_{\mathtt{I}V}^{ik}Q_{\mathtt{J}A}^{kj} + Q_{\mathtt{I}A}^{ik}Q_{\mathtt{J}V}^{kj})\Bigg) + \mathcal{O}\left(\frac{m_{a,\mathtt{I},\mathtt{J}}^2}{m_{i,k,j}^2}\right),
\end{aligned} \tag{V.16}$$

with N_k being the multiplicity of the fermions accounting for the number of colors and flavors. The function λ represents the Källén function, while the function C_0 denotes the three-point Passarino-Veltman function [208], given in the heavy fermion limit by

$$\begin{aligned}
C_0(m_{b_1}^2, m_{b_2}^2, m_{b_3}^2, m_{f_1}, m_{f_2}, m_{f_3}) &= C_0(0,0,0,m_{f_1},m_{f_2},m_{f_3}) + \frac{1}{m_{f_2}^2}\mathcal{O}\left(\frac{m_{b_1,b_2,b_3}^2}{m_{f_1,f_2,f_3}^2}\right) \\
&= \frac{1}{m_{f_2}^2}\left(\frac{\ln\left(\frac{m_{f_1}^2}{m_{f_2}^2}\right)}{\left(1-\frac{m_{f_3}^2}{m_{f_1}^2}\right)\left(1-\frac{m_{f_1}^2}{m_{f_2}^2}\right)} + \frac{\ln\left(\frac{m_{f_3}^2}{m_{f_2}^2}\right)}{\left(1-\frac{m_{f_1}^2}{m_{f_3}^2}\right)\left(1-\frac{m_{f_3}^2}{m_{f_2}^2}\right)} + \mathcal{O}\left(\frac{m_{b_1,b_2,b_3}^2}{m_{f_1,f_2,f_3}^2}\right)\right),
\end{aligned} \tag{V.17}$$

with boson masses m_{b_i} and fermion masses m_{f_i}.

From equation (V.16) we see, that the result is indeed invariant under a chiral fermion transformation as defined in equation (V.5). In order to obtain the result for $SU(N)$ gauge bosons, which necessarily requires $\mathtt{I} = \mathtt{J}$ to conserve the respective color charge, we just replace the number of colors by the Dynkin index $T(R_{I\mathtt{k}})$.

The second limit is characterized by the flavor conserving limit with $i = j = k \equiv f$. The Wilson coefficient in this limit is given by

$$\begin{aligned}
\left(C_{\mathtt{IJ}}^{\text{eff}}\right)_f = C_3^{\mathtt{IJ}} - 2\sum_f N_f \Bigg(\Bigg(& C_{1A}^f (Q_{\mathtt{I}V}^f Q_{\mathtt{J}V}^f + Q_{\mathtt{I}A}^f Q_{\mathtt{J}A}^f) + 2\Bigg(C_{1A}^f + C_{2A}^f\Bigg)\times \\
&\times \Bigg(Q_{\mathtt{I}V}^f Q_{\mathtt{J}V}^f m_f^2 C_0(m_a^2, m_{\mathtt{I}}^2, m_{\mathtt{J}}^2, m_f, m_f, m_f) - \frac{Q_{\mathtt{I}A}^f Q_{\mathtt{J}A}^f m_f^2}{\lambda(m_a^2, m_{\mathtt{I}}^2, m_{\mathtt{J}}^2)}\times \\
&\times \Bigg((m_a^4 - (m_{\mathtt{I}}^2 - m_{\mathtt{J}}^2)^2) C_0(m_a^2, m_{\mathtt{I}}^2, m_{\mathtt{J}}^2, m_f, m_f, m_f) + 4m_a^2 B_0(m_a^2, m_f, m_f) \\
&- 2(m_a^2 + m_{\mathtt{I}}^2 - m_{\mathtt{J}}^2) B_0(m_{\mathtt{I}}^2, m_f, m_f) - 2(m_a^2 - m_{\mathtt{I}}^2 + m_{\mathtt{J}}^2) B_0(m_{\mathtt{J}}^2, m_f, m_f)\Bigg)\Bigg)\Bigg).
\end{aligned} \tag{V.18}$$

The result now depends on the two-point Passarino-Veltman function B_0 [208]. The $1/\epsilon$ divergence in B_0 from dimensional regularization cancels in this case due to a vanishing prefactor for the constant pieces of the B_0 functions.

Finally, we have the limit for the SM W bosons, in which the axion coupling is flavor-conserving ($i = j \equiv f$) and the gauge couplings are left-handed to gauge bosons with equal masses ($\mathtt{I} = \mathtt{J} \equiv W$). In this case, the Wilson coefficient reads

$$C_{WW}^{\text{eff}} = \sum_{f,k} N_f Q_{WL}^{fk} Q_{WL}^{kf} \left(4 \frac{m_f^2 (C_{1A}^f + C_{2A}^f)}{m_a^2 - 4m_W^2} \left(B_0(m_a^2, m_f, m_f) - B_0(m_W^2, m_f, m_k) \right.\right.$$
$$\left.\left. + (m_W^2 - m_f^2 + m_k^2) C_0(m_a^2, m_W^2, m_W^2, m_f, m_f, m_k) \right) - C_{1A}^f \right) + C_3^{WW} \,, \quad \text{(V.19)}$$

where the charge matrices $\mathbf{Q}_{WL}$ represent the CKM matrix $\mathbf{V}_{\text{CKM}}$. The divergence in B_0 again cancels and the result is finite.

V.2.2 Loop-induced Axion Coupling to Scalar and Gauge Boson

In this subsection we discuss the interaction of an axion to a gauge boson $A_{\mathtt{I}\mu}$ and a real scalar field $\phi_{\mathtt{i}}$, which is induced by a fermion loop. Although this interaction is not part of the fermion-related axion interactions at tree-level, it generically is generated through the scalar Lagrangian from equation (V.11).

We write down the effective Lagrangian analogously to the $C_4^{\mathtt{Ii}}$ interaction from equation (V.12),

$$\mathcal{L}_{\text{axion}}^{\text{eff}} \supset -C_{\mathtt{Ii}}^{\text{eff}} g_{\mathtt{I}} v_{\mathtt{i}} \phi_{\mathtt{i}} A_{\mathtt{I},\mu} \frac{\partial^\mu a}{f_a} \,, \quad \text{(V.20)}$$

where we neglect the $\phi_{\mathtt{i}}^2$ interactions, since it is a four-point vertex which does not play a role in our phenomenological studies.

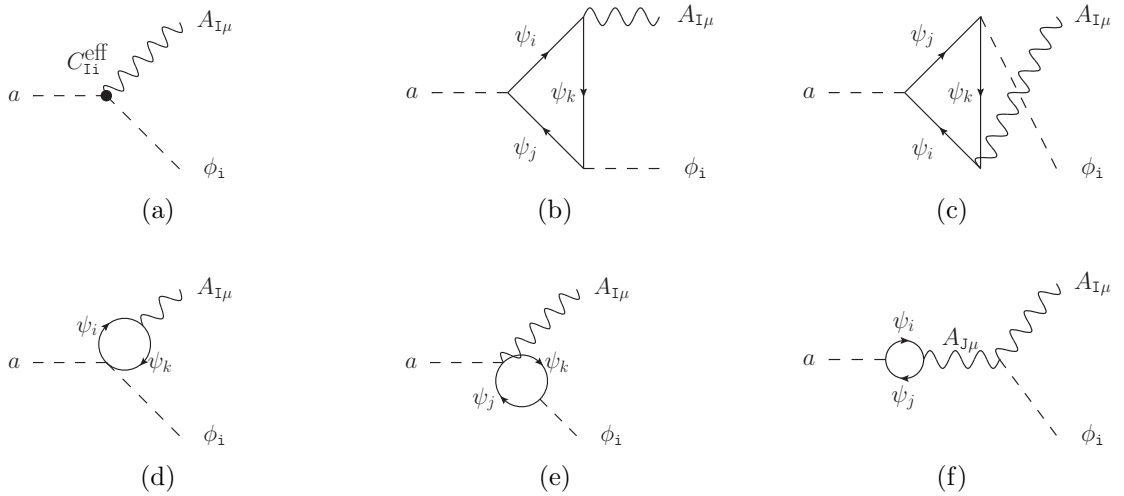

Figure V.2: Effective vertex and one-loop diagrams for coupling of an axion to a gauge boson and a scalar. The loop consists of three fermions ψ_i, ψ_j and ψ_k connecting an axion a with one gauge boson $A_{\mathtt{I},\mu}$ and a scalar $\phi_{\mathtt{i}}$.

We find five one-loop diagrams involving up to three flavors of fermions ψ_i, ψ_j and ψ_k with masses m_i, m_j and m_k. These diagrams are shown in Figure V.2. The first two loop-diagrams in subfigures V.2b and V.2c show the usual triangle contribution from three-point

fermion interactions. Diagrams V.2d and V.2e include the four-point contact interactions in the gauge and Yukawa sector including flavor-violating commutator interactions.

The last diagram in subfigure V.2f shows an additional contribution from an off-shell internal gauge boson line. The diagram cancels as soon as the internal gauge boson is on-shell due to the orthogonality relations from the mixing of angular fields. We remark that the effective coupling has also been studied in reference [209] to analyze the CP properties of a new scalar, but since we additionally account for flavor-violating fermion interactions we include Figure V.2e as an additional diagram.

In the limit where we have fermions which are much heavier then the external bosons, $m_i, m_j, m_k \gg m_a, m_{\mathtt{I}}, \mathtt{i}$, the Wilson coefficient for the acion-scalar-gauge boson coupling is given by

$$\begin{aligned}
C_{\mathtt{Ii}}^{\text{eff}} =& C_4^{\mathtt{Ii}} + \frac{1}{(4\pi)^2}\frac{1}{\sqrt{2}v_{\mathtt{i}}}\sum_{i,j,k} N_k \Bigg(2\frac{C_0(0,0,0,m_i,m_j,m_k)}{\lambda(m_a^2,m_{\mathtt{i}}^2,m_{\mathtt{I}}^2)}\times \\
&\times (m_i+m_j)((C_{1A}^{ji}+C_{2A}^{ji})Q_{\mathtt{I}A}^{ik}Y_{\mathtt{i}}^{kj} + (C_{1A}^{ij}+C_{2A}^{ij})Y_{\mathtt{i}}^{jk}Q_{\mathtt{I}A}^{ki})\times \\
&\times \Big(m_{\mathtt{I}}^2(m_{\mathtt{I}}^2 - m_a^2 - m_{\mathtt{i}}^2)(m_i - m_j)(m_j+m_k) - \lambda(m_a^2,m_{\mathtt{i}}^2,m_{\mathtt{I}}^2)(m_i m_k + m_j^2)\Big) \\
&- 2(m_i+m_j)((C_{1A}^{ji}+C_{2A}^{ji})Q_{\mathtt{I}A}^{ik}Y_{\mathtt{i}}^{kj} + (C_{1A}^{ij}+C_{2A}^{ij})Y_{\mathtt{i}}^{jk}Q_{\mathtt{I}A}^{ki})B_0(0,m_k,m_i) \\
&+ (m_j-m_k)((C_{1A}^{ji}+C_{\mathtt{I}A}^{ji})Q_{\mathtt{I}A}^{ik}Y_{\mathtt{i}}^{kj} + (C_{1A}^{ij}+C_{\mathtt{I}A}^{ij})Y_{\mathtt{i}}^{jk}Q_{\mathtt{I}A}^{ki})B_0(0,m_j,m_k) \\
&- \sum_{\mathtt{J},\mathtt{j}}(m_i+m_j)((C_{1A}^{ji}+C_{2A}^{ji})Q_{\mathtt{J}A}^{ik}Y_{\mathtt{j}}^{kj} + (C_{1A}^{ij}+C_{2A}^{ij})Y_{\mathtt{j}}^{jk}Q_{\mathtt{J}A}^{ki})B_0(0,m_i,m_j) \\
&\times \frac{g_{\mathtt{J}}^2 Q_{\mathtt{I}}^{\mathtt{i}} Q_{\mathtt{J}}^{\mathtt{i}} v_{\mathtt{i}} v_{\mathtt{j}}}{m_{\mathtt{J}}^2}\Bigg) + \mathcal{O}\left(\frac{m_{a,\mathtt{I},\mathtt{i}}^2}{m_{i,k,j}^2}\right),
\end{aligned} \tag{V.21}$$

where we used the scalar coupling to two gauge bosons from equation (V.11). The result is again invariant under a chiral transformation as defined in equation (V.5).

The two-point Passarino-Veltman function B_0 in the heavy fermion limit is given by

$$\begin{aligned}
B_0(m_b^2, m_{f_1}, m_{f_2}) &= B_0(0, m_{f_1}, m_{f_2}) + \mathcal{O}\left(\frac{m_b^2}{m_{f_1}^2, m_{f_2}^2}\right) \\
&= \frac{1}{\epsilon} - \gamma_E + \ln(4\pi) + \ln\left(\frac{\mu^2}{m_{f_1}m_{f_2}}\right) + 1 - \frac{1}{2}\frac{m_{f_1}^2+m_{f_2}^2}{m_{f_1}^2-m_{f_2}^2}\ln\left(\frac{m_{f_1}^2}{m_{f_2}^2}\right) + \mathcal{O}\left(\frac{m_b^2}{m_{f_1}^2, m_{f_2}^2}\right),
\end{aligned} \tag{V.22}$$

where the divergent piece does not cancel trivially in this case. In order to find the cancellation we extract the divergent piece from equation (V.21),

$$\begin{aligned}
C_{\mathtt{Ii}}^{\text{eff}} =& \frac{1}{(4\pi)^2}\frac{1}{\sqrt{2}v_{\mathtt{i}}}\frac{1}{\epsilon}\Bigg(\mathcal{T}_-\Big(\mathbf{Y}_{\mathtt{i}}, \mathbf{M}, \mathbf{Q}_{\mathtt{I}A}, \mathbf{C}_{2A} - \mathbf{C}_{\mathtt{I}A}\Big) + \mathcal{T}_+\Big(\mathbf{Y}_{\mathtt{i}}, \mathbf{M}, \mathbf{Q}_{\mathtt{I}A}, \mathbf{C}_{1A} + \mathbf{C}_{2A}\Big) \\
&- \sum_{\mathtt{J},\mathtt{j}} \frac{g_{\mathtt{J}}^2 Q_{\mathtt{I}}^{\mathtt{i}} Q_{\mathtt{J}}^{\mathtt{i}} v_{\mathtt{i}} v_{\mathtt{j}}}{m_{\mathtt{J}}^2}\mathcal{T}_+\Big(\mathbf{Y}_{\mathtt{j}}, \mathbf{M}, \mathbf{Q}_{\mathtt{J}A}, \mathbf{C}_{1A} + \mathbf{C}_{2A}\Big)\Bigg) + \mathcal{O}(\epsilon^0),
\end{aligned} \tag{V.23}$$

where $\mathcal{T}_-$ and $\mathcal{T}_+$ represent the traces of commutator and anti-commutator relations, given by

$$\mathcal{T}_+(\mathbf{A},\mathbf{B},\mathbf{C},\mathbf{D}) = \text{Tr}[\{\mathbf{A},\mathbf{C}\}\{\mathbf{B},\mathbf{D}\}] + \text{Tr}[\{\mathbf{B},\mathbf{C}\}\{\mathbf{A},\mathbf{D}\}], \tag{V.24}$$

$$\mathcal{T}_-(\mathbf{A},\mathbf{B},\mathbf{C},\mathbf{D}) = \text{Tr}[\{\mathbf{A},\mathbf{C}\}\{\mathbf{B},\mathbf{D}\}] - \text{Tr}[\{\mathbf{B},\mathbf{C}\}\{\mathbf{A},\mathbf{D}\}] = \text{Tr}[[\mathbf{B},\mathbf{A}][\mathbf{C},\mathbf{D}]]. \tag{V.25}$$

We notice, that we need the contribution from diagram V.2f to be able to cancel the $\mathcal{T}_+$ term, while the $\mathcal{T}_-$ term cancels for vanishing commutators.

Applying the orthogonality conditions from angular mixing, we can replace

$$\frac{g_{\mathtt{J}} Q_{\mathtt{I}}^{\mathtt{i}} v_{\mathtt{j}}}{m_{\mathtt{J}}} = \delta_{\mathtt{IJ}} \delta_{\mathtt{ij}} \,, \tag{V.26}$$

such that the $\mathcal{T}_+$ terms cancel exactly and we are left with

$$C_{\mathtt{Ii}}^{\text{eff}} = \frac{1}{(4\pi)^2} \frac{1}{\sqrt{2} v_{\mathtt{i}}} \frac{1}{\epsilon} \mathcal{T}_- \left(\mathbf{Y}_{\mathtt{i}}, \mathbf{M}, \mathbf{Q}_{\mathtt{I}A}, \mathbf{C}_{2A} - \mathbf{C}_{\mathtt{I}A} \right) + \mathcal{O}(\epsilon^0) \,. \tag{V.27}$$

This contribution cancels in the case where the Yukawa matrices commute with the mass matrix, $[\mathbf{Y}_{\mathtt{i}}, \mathbf{M}] = 0$, and the divergence vanishes.

V.2.3 Loop-induced Axion Coupling to Fermions

Lastly, we discuss the loop-induced axion interaction to fermions. This coupling provides the leading contribution for fermions which are not charged under the PQ symmetry and therefore do not have a tree-level coupling to axions. The effective Lagrangian for this case is given by

$$\mathcal{L}_{\text{axion}}^{\text{eff}} \supset -\frac{\partial_\mu a}{2 f_a} \bar{f}^i \left(C_{V,ij}^{\text{eff}} + C_{A,ij}^{\text{eff}} \right) f^j \,, \tag{V.28}$$

where f^i and f^j now represent light fermions with masses m_i and m_j. Alternatively, we can replace this interaction by an axion coupling in the mass sector of the fermions.

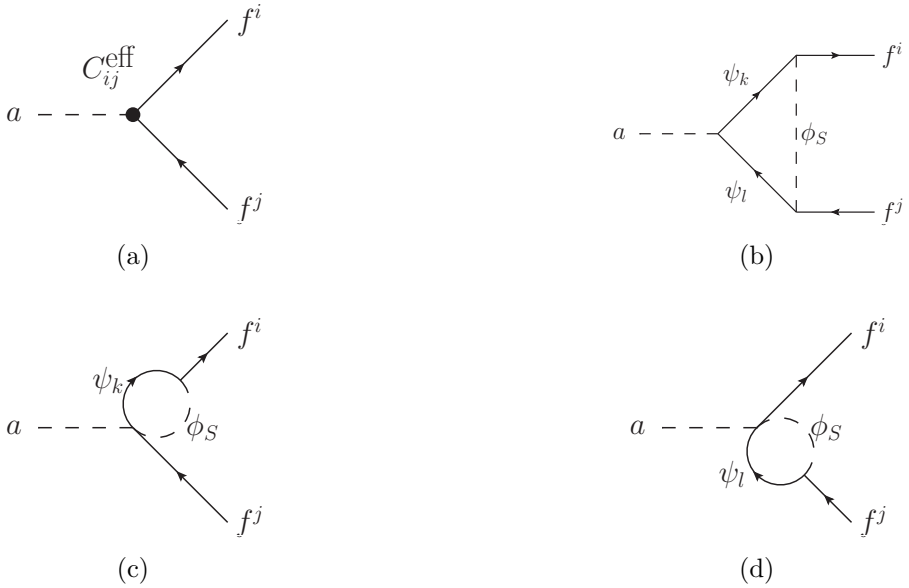

Figure V.3: Effective vertex and one-loop diagrams for anomalous coupling of an axion to two fermions. The loop consists of up to two fermions ψ_k, ψ_l and a scalar ϕ_S connecting an axion a with two fermions f^i and f^j.

In order to calculate the Wilson coefficients $\mathbf{C}_V^{\text{eff}}$ and $\mathbf{C}_A^{\text{eff}}$ we close a loop containing two heavy fermion flavors ψ^k and ψ^l and one heavy real scalar field ϕ_S. The corresponding diagrams are shown in Figure V.3. In addition to the triangle diagram in subfigure V.3b, we get two diagrams with loop corrections on each outgoing fermion-line due to the four-point contact interaction defined in equation (V.9).

Since we are interested in effective interactions to the SM fields and do not want to generate any $SU(2)_L$ anomalies, we couple the heavy scalar to right-handed light fermions and left-handed heavy fermions,

$$\mathcal{L}_{\text{Yukawa}} \supset -y_S^{ki}\bar{\psi}_L^k \phi_S f_R^i + \text{h.c.}\,, \tag{V.29}$$

where we assume the Yukawa matrix $\mathbf{Y}_S$ to be purely real. The corresponding masses for the heavy fields are denoted by m_k, m_l and m_S, respectively.

Since the effective interaction is only mediated to right-handed light fermions, we get matching expressions for both, vector-like coefficient $\mathbf{C}_V^{\text{eff}}$ and the axial coefficient $\mathbf{C}_A^{\text{eff}}$. In the limit where we integrate out the heavy fermions and scalar the Wilson coefficients read

$$\begin{aligned}
C_{V/A,ij}^{\text{eff}} =& C_{1V/A}^{ij} - \frac{1}{(4\pi)^2}\sum_{k,l}\frac{N_k}{2} y_S^{ik} y_S^{lj}\Bigg(8\left(C_{1A}^{kl}+C_{2A}^{kl}\right) m_k m_l C_0(0,0,0,m_k,m_l,m_S) \\
&+\left(C_{1V}^{kl}+C_{2V}^{kl}-C_{1A}^{kl}-C_{2A}^{kl}\right)\Bigg((m_k^2-4m_k m_l+m_l^2)C_0(0,0,0,m_k,m_l,m_S) \\
&\quad + m_k^2 C_0(0,0,0,m_k,m_k,m_S) + m_l^2 C_0(0,0,0,m_l,m_l,m_S)\Bigg) \\
&+\left(C_{1V}^{kl}+C_{SV}^{kl}-C_{1A}^{kl}-C_{SA}^{kl}\right)\Bigg(1 - B_0(0,m_k,m_S) - B_0(0,m_l,m_S) \\
&\quad + m_k^2 C_0(0,0,0,m_k,m_k,m_S) + m_l^2 C_0(0,0,0,m_l,m_l,m_S)\Bigg)\Bigg) + \mathcal{O}\left(\frac{m_{a,i,j}^2}{m_{S,k,l}^2}\right).
\end{aligned} \tag{V.30}$$

From the transformation properties in equation (V.10) we can deduce that the coefficients are invariant under the chiral transformation defined in equation (V.5). We further notice, that in the flavor-conserving axion limit ($\psi^k = \psi^l$) the dependence on the vector-like couplings drops out. This matches our expectations since the tree-level vector-like axion couplings cancel in this case.

The divergence in the two-point Passarino-Veltman functions B_0 only vanishes if the contributions from diagrams V.3c and V.3d cancel the contribution from the derivative interaction. This holds true in the case that the heavy fermions ψ^k and ψ^l acquire their axion couplings originally in the mass sector.

CHAPTER VI

Chiral Enhancement of Axion Couplings

In the previous chapter we saw that we can modify axion couplings in the framework of an EFT, where we integrate out fields which are much heavier than the energy scale of interest. The focus of this chapter is on the axion couplings to SM fermions which get an additional contribution from heavy fermions and scalars. Since the SM fermions are chiral, the heavy fields couple differently to left- and right-handed states. An increase in the fermion coupling is therefore called chiral enhancement.

In general, Chiral enhancement describes a loop correction to a fermionic coupling which is enhanced by the ratio of a heavy scale and the fermion mass. Such types of corrections are usually used to explain discrepancies between theoretical expectations and experimental measurements such as in the muon anomalous magnetic dipole moment [210]. In the case of axion models, chiral enhancement mainly interferes with flavor effects as well as the properties of the additional field content.

To demonstrate this, we first show in the concept of chiral enhancement within axion models section VI.1. Afterwards in section VI.2, we present the corresponding effective couplings and flavor effects. In section VI.3 we embed the chiral enhancement into the DFSZ model with a DM scalar and constrain our parameter space according to DM bounds. Finally, we discuss in section VI.4 additional effects accounting for neutrino masses.

VI.1 Chiral Enhancement in Axion Models

In this section we discuss the possibility and implications of having corrections through chiral enhancement in an axion model. Even though these corrections are generally considered to be sub-dominant effects, chiral enhancement gets interesting in axion physics as it can compete with the tree-level coupling in DFSZ models and even provide the dominant contribution in KSVZ models. We demonstrate this fact in a model with a heavy fermion F and a gauge singlet scalar S.

The tree-level coupling to SM fermions f and the heavy fermion F can be parameterized by

$$\mathcal{L}_{\text{axion}} \supset -\sum_{f\in\text{SM}} \frac{C^0_{aff}}{2f_a}(\partial_\mu a)\bar{f}\gamma^\mu\gamma_5 f - \frac{C^0_{aFF}}{2f_a}(\partial_\mu a)\bar{F}\gamma^\mu\gamma_5 F\,, \tag{VI.1}$$

where a represents the axion field with decay constant f_a and dimensionless couplings C^0_{aff} and C^0_{aFF}.

We consider the heavy fermion F getting its mass from the complex scalar Φ in a KSVZ-like manner, where the angular mode of Φ is dominantly represented by the axion. Assuming the fermion $F \in \{E, U, D\}$ having the same quantum numbers as one of the right-handed SM fermions ($f \in \{e, u, d\}$), the Yukawa couplings of F and S read

$$\mathcal{L}^{FS}_{\text{Yukawa}} \supset -y_F \bar{F}_L \Phi F_R - y_S^i \bar{F}_L S f_R^i - y_{\text{eff}}^{ij} \bar{f}_L^i S f_R^j + \text{h.c.}\,, \tag{VI.2}$$

where y_{eff}^{ij} needs to be generated through a dimension-5 interaction of the form $\bar{Q}_L^i H_d S d_R^j$, $\bar{Q}_L^i H_u S u_R^j$ or $\bar{L}_L^i H_d S e_R^j$, respectively.

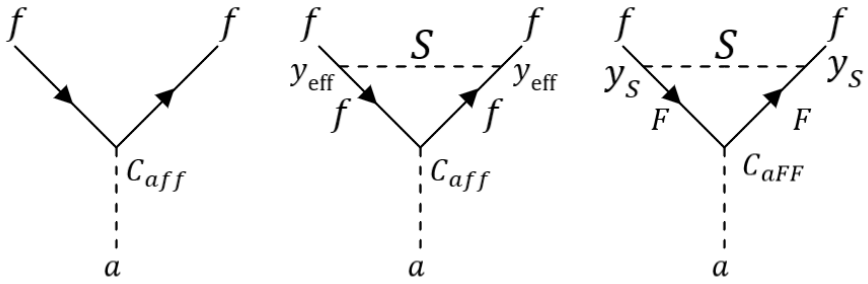

Figure VI.1: Feynman diagrams for axion couplings to SM fermions.

The tree-level coupling of the axion to the SM fermions as well as the one-loop corrections induced by S are shown in Figure VI.1. We split the total coupling at one-loop into three parts,

$$C_{aff}^{\text{tot}} \equiv C_{aff}^0 + C_{aff}^f + C_{aff}^F\,, \tag{VI.3}$$

where C_{aff}^f stands for the one-loop correction with the SM fermion in the loop and C_{aff}^F with the heavy fermion in the loop. The parametric dependence is given by

$$C_{aff}^f = \frac{|y_{\text{eff}}|^2}{4\pi^2} C_{aff}^0 \frac{m_f^2}{m_S^2}\left(1 + \ln\frac{m_f^2}{m_S^2}\right) + \mathcal{O}\left(\frac{m_f^4}{m_S^4}\right)\,, \tag{VI.4}$$

$$C_{aff}^F = \frac{|y_S|^2}{4\pi^2} C_{aFF}^0 \frac{m_F^2}{m_S^2}\left(1 + \ln\frac{m_F^2}{m_S^2}\right) + \mathcal{O}\left(\frac{m_f^4}{m_S^4}, \frac{m_F^4}{m_S^4}\right)\,. \tag{VI.5}$$

Here, we can see that in the DFSZ-case ($C_{aff}^0 \neq 0$) the correction from the heavy fermion is enhanced compared to the correction with only having f by a factor m_F^2/m_f^2. For large Yukawa couplings $|y_S| \sim 4\pi/3$ it even competes with the tree-level coupling. In the KSVZ-case ($C_{aff}^0 = 0$) the effective one-loop contribution from the heavy F gives the leading contribution, since the tree-level contribution vanishes.

In the next section we set up C_{aff}^F in a more general way and include flavor-changing interactions. In section VI.3, we also account for the case $m_F \gg m_S$ which leads to even larger contributions.

VI.2 Effective Axion Interactions and Flavor Effects

In this section we calculate the effective interactions of the axion a to gauge bosons and SM fermions. In addition to the canonical DFSZ contribution, the couplings to gauge bosons are determined by integrating out the heavy fermion F in a KSVZ-like manner as presented in subsection V.2.1. The couplings to SM fermions are enhancend by their

Yukawa interactions with the heavy fermion F and the heavy scalar S which are both integrated out according to our calculation in subsection V.2.3.

We present the resulting EFT interactions in subsections VI.2.1 and VI.2.2. In subsection VI.2.2 we also show that the effective axion fermion interactions involve in general flavor changing effects. These effects are strongly constrained [106, 211, 212] and therefore narrow down the available parameter space for chiral enhancement.

VI.2.1 Axion-Gauge Boson Interactions

We start with the axion gauge boson couplings which are induced at one-loop order by integrating out the heavy fermion F. The corresponding Feynman diagrams are shown in Figure V.1, replacing the fields $\psi_{i,j,k}$ with F. Since F does not couple to the $SU(2)_L$ gauge group we only generate effective couplings to the neutral bosons γ, Z and the gluon g, given by

$$\mathcal{L}^F_{\text{axion}} \supset - C^F_{a\gamma\gamma}\frac{a}{f_a}F_{\mu\nu}\tilde{F}^{\mu\nu} - C^F_{aZ\gamma}\frac{a}{f_a}Z_{\mu\nu}\tilde{F}^{\mu\nu} - C^F_{aZZ}\frac{a}{f_a}Z_{\mu\nu}\tilde{Z}^{\mu\nu} - C^F_{agg}\frac{a}{f_a}G^a_{\mu\nu}\tilde{G}^{a\mu\nu}\,. \tag{VI.6}$$

The superscript F denotes that we integrated out the heavy fermion.

In order to calculate the effective coefficients we express the axion couplings to F in terms of the Yukawa interaction to the complex scalar Φ,

$$\mathcal{L}^F_{\text{Yukawa}} \supset -y_F\bar{F}_L\Phi F_R + \text{h.c.} = -m_F\left(1+\frac{h_\Phi}{v_\Phi}\right)\bar{F}\exp\left(iX\left(\frac{a}{f_a}+\frac{A}{f_A}\right)\gamma_5\right)F, \tag{VI.7}$$

where we re-expressed the angular mode a_Φ according to the procedure from subsection III.1.1. In this basis we do not generate anomalous axion couplings to gauge bosons at tree-level.

Taking the mass of F to be proportional to the axion decay constant f_a which is in usual axion models well above the weak scale, we neglect all terms of order $\mathcal{O}(1/m_F^2)$. Using our calculation from subsection V.2.1 the coefficients then read

$$\begin{aligned} C^F_{a\gamma\gamma} &= X\frac{Y_F^2}{(4\pi)^2}e^2\,, \quad C^F_{aZ\gamma} = X\frac{Y_F^2}{(4\pi)^2}\frac{e^2}{s_W c_W}\,, \quad C^F_{aZZ} = X\frac{Y_F^2}{(4\pi)^2}\frac{e^2}{s_W^2 c_W^2}\,, \\ C^F_{agg} &= X\frac{1-\delta_{FE}}{2}\frac{g_s^2}{(4\pi)^2}\,. \end{aligned} \tag{VI.8}$$

We see, that the induced coupling to gluons vanishes in the case of heavy electron ($F = E$). The loop-induced couplings lead to a small shift of the DFSZ axion line in the $\{m_a, G_{a\gamma\gamma}\}$-plane, since we effectively add a KSVZ model on top of the DFSZ construction.

VI.2.2 Axion-Fermion Interactions and Flavor Effects

In addition to the canonical axion-fermion couplings, we generate also one-loop contributions for the SM fermions which couple to the heavy fermion F and the real scalar S via a right-handed Yukawa interaction. Since the mass of the scalar m_S is a free parameter, we can take it to be at a scale well above the electroweak scale. This allows us to integrate out the scalar, leading to a chirally enhanced effective axion-fermion coupling. The respective Feynman diagrams for this process are shown in Figure V.3, after replacing the fields $\psi_{k,l}$ with F and ϕ_S with S.

This can be added to the effective Lagrangian analogously to our discussion of subsection V.2.3 as a derivative coupling to the axion via an effective PQ current

$$\mathcal{L}^{S}_{\text{axion}} \supset -\frac{\partial_\mu a}{2f_a}\bar{\mathbf{f}}\gamma^\mu(\mathbf{C}^{S,V}_{aff}+\mathbf{C}^{S,A}_{aff}\gamma_5)\mathbf{f}\,. \tag{VI.9}$$

Here, the superscript S for the effective coupling matrices $\mathbf{C}^{S}_{aff}$ symbolizes that we integrated out the scalar S. We split the coupling matrices into a vector-like part $\mathbf{C}^{S,V}_{aff}$ and an axial part $\mathbf{C}^{S,A}_{aff}$.

Since S only couples to right-handed SM fermions, the vector-like and axial parts of the PQ current have the same charge. Again, we neglect all terms of order $\mathcal{O}(1/m_F^2)$ as well as $\mathcal{O}(1/m_S^2)$. For now, we also neglect terms which are sensitive to the difference between m_F and m_S. The resulting effective charge matrix in the mass basis of the SM fermions reads

$$\mathbf{C}^{S,V}_{aff}=\mathbf{C}^{S,A}_{aff}\equiv-\mathbf{X}^m_f\,,\quad \left(X^m_f\right)^{ij}=X\frac{y^i_S y^j_S}{8\pi^2}+\mathcal{O}\left(1-\frac{m_F^2}{m_S^2}\right)\,. \tag{VI.10}$$

It depends dominantly on the couplings y^i_S of the SM fermions to the real scalar. We see that for each flavor-diagonal axion-fermion coupling we also generate the corresponding mixed couplings between different flavors.

In order to further study the flavor structure we include the PQ current in the covariant derivative of the respective right-handed fermion $f\in\{e,u,d\}$. In matrix form regarding flavor space and mass basis of the fermions this reads

$$\mathbf{D}^m_{f,\mu}=\partial_\mu\mathbb{1}-iY_f g_Y B_\mu\mathbb{1}-i(1-\delta_{fe})g_s\lambda^a G^a_\mu\mathbb{1}-i\frac{(\partial_\mu a)}{f_a}\mathbf{X}^m_f\,, \tag{VI.11}$$

where only the PQ current is flavor-changing.

Going back to gauge basis via the transformation from subsection II.2.2

$$f_R\to\mathbf{V}^\dagger_f f_R\,,\quad \mathbf{X}_f=\mathbf{V}_f\mathbf{X}^m_f\mathbf{V}^\dagger_f\,, \tag{VI.12}$$

we recover flavor-diagonal gauge interactions, but have flavor-changing Higgs-Yukawa interactions. The PQ current is also still flavor-changing due to the dependence on the fermion-scalar interactions. Hence, there is no basis where Yukawa interactions and PQ current are generically flavor-diagonal at the same time.

The combined flavor effects of the Higgs Yukawa interactions and the PQ interactions can be seen by performing a chiral transformations on the fermions following the description in section V.1 with

$$f\to\exp\left(\frac{i}{2}(\mathbf{X}_f+\mathbf{X}_f\gamma_5)\frac{a}{f_a}\right)f,\quad \bar{f}\to\bar{f}\exp\left(-\frac{i}{2}(\mathbf{X}_f-\mathbf{X}_f\gamma_5)\frac{a}{f_a}\right)\,. \tag{VI.13}$$

This is equivalent to a transformation of only the right-handed fields, yielding

$$\begin{aligned}\mathcal{L}&\supset-\frac{v+h}{\sqrt{2}}\bar{f}_L\mathbf{Y}_f\exp\left(i\frac{a}{f_a}\mathbf{X}_f\right)f_R+\text{h.c.}\\&=-\frac{v+h}{\sqrt{2}}\left(\bar{f}\mathbf{Y}_f f+i\frac{a}{f_a}\bar{f}[\mathbf{Y}_f,\mathbf{X}_f]f+i\frac{a}{f_a}\bar{f}\{\mathbf{Y}_f,\mathbf{X}_f\}f\right)+\mathcal{O}\left(\frac{1}{f_a^2}\right)\,.\end{aligned} \tag{VI.14}$$

We see again, that we can not diagonalize the Yukawa coupling to the Higgs and to the axion at the same time.

The resulting flavor changing effects in equation (VI.10) are strongly constrained as shown in references [106, 211, 212]. Hence, for the flavor changing couplings between two SM fermions with flavor indices $i \neq j$ we take a conservative limit

$$X\frac{y_S^i y_S^j}{8\pi^2} \lesssim 10^{-8}\frac{f_a}{\text{TeV}} = 10^{-8} X \sin\beta_2 \frac{\sqrt{2}}{y_F}\frac{m_F}{\text{TeV}} \quad \Leftrightarrow \quad \frac{y_S^i y_S^j}{m_F} \lesssim \frac{1}{y_F} 10^{-9}\ \text{GeV}^{-1}\,, \tag{VI.15}$$

where we rewrite f_a in terms of v_Φ following subsection III.1.1 with $\beta_2 \to \pi/2$ for a large scale separation $f_a \gg v$.

VI.3 Chiral Enhancement and Dark Matter

Having introduced the concept of chiral enhancement in axion models, we now want to estimate the impact of such an enhancement within the DFSZ model. For this purpose we add a heavy fermion F and a heavy gauge singlet scalar S to the field content of the DFSZ model. Again we choose the quantum numbers of the heavy fermion $F \in \{E, U, D\}$ to be aligned with the quantum numbers of one of the right-handed SM fields, $f \in \{e, u, d\}$.

The corresponding field content is presented in Table VI.1, where the $\mathbb{Z}_n$ charges with $4 < n \in 2\mathbb{N}$ are chosen in such a way that for $m_F > m_S$ the fermion F can decay into SM fermions while the decay of the scalar S is forbidden. Thus, the heavy scalar serves as a DM candidate. The full Lagrangian of this model is given by

$$\begin{aligned}\mathcal{L}_{\text{DM}}^{\text{DFSZ}} \supset & \mathcal{L}^{\text{DFSZ}} + \frac{1}{2}(\partial_\mu S)^2 + i\bar{F}\not{D}_F F - y_F \bar{F}_L \Phi F_R - y_S^i \bar{F}_L S f_R^i + \text{h.c.} \\ & - \frac{1}{2}S^2\left(m_S^2 + \lambda_S S^2 + \lambda_{HS}(h^2 + 2vh) + \lambda_{\Phi S}(h_\Phi^2 + 2v_\Phi h_\Phi) + \mathcal{O}\left(H^0, H^\pm\right)\right)\,,\end{aligned} \tag{VI.16}$$

where h_Φ was defined in equation (II.30) as the radial mode of Φ and h describes the radial mode of the two Higgs doublets from equation (II.40) which is aligned with the SM Higgs field. We neglect the couplings to the heavy DFSZ fields H^0 and $H^\pm$. Note, that a tree-level coupling of S to the pseudoscalars a and A is forbidden due to the $\mathbb{Z}_n$ symmetry.

	$SU(3)_C$	$SU(2)_L$	$U(1)_Y$	$\mathbb{Z}_n$	$U(1)_{PQ}$
Q_L^i	3	2	1/6	0	X_Q
u_R^i	3	1	2/3	1	X_Q-X_u
d_R^i	3	1	-1/3	0	X_Q-X_d
L_L^i	1	2	-1/2	0	X_L
e_R^i	1	1	-1	0	X_L-X_d
H_u	1	2	-1/2	n-1	X_u
H_d	1	2	1/2	0	X_d
Φ_A	1	1	0	1	-X
F_L	R_F	1	Y_F	$n/2 + \delta_{FU}$	X_F
F_R	R_F	1	Y_F	$(n-2)/2 + \delta_{FU}$	X_F+X
S	1	1	0	$n/2$	0

Table VI.1: Field content of the DFSZ model with an additional heavy fermion F and a DM scalar S. The $SU(3)_C$ representations R_F and hypercharges Y_F of the additional fermion correspond to one of the right-handed SM fermions.

Since the heavy scalar contributes to the DM relic density, we obtain further limits on the Yukawa couplings y_S^i. On one hand, the Yukawa coupling controls the rate for pair

annihilation of the heavy scalar into SM particles in the early universe. If this process is not efficient enough, the relic abundance of S exceeds the measured value for DM in the energy budget of the universe. Thus, this provides a lower limit on y_S^i as we present in subsection VI.3.1.

On the other hand, experiments dedicated for direct DM detection provide an upper bound on interactions between DM and SM particles. We discuss the corresponding constraints on y_S^i from the LUX-ZEPLIN (LZ) and XENONnT experiments [213–215] in subsection VI.3.2. Afterwards, we show our estimates on chiral enhancement for quarks in subsection VI.3.3 and for charged leptons in subsection VI.3.4.

VI.3.1 Relic Abundance

From cosmological observations like rotation curves of galaxies and the cosmic microwave background (CMB) we know that 26.8% of the energy density of the universe is given by cold Dark Matter [39]. The term "cold" refers to a non-relativistic particle species which is mainly characterized by its mass, whereas "dark" signifies that the particles do not transform under the SM gauge group. Furthermore, DM has to be stable on cosmological time scales.

In our model, the scalar field S fulfills the requirements on a DM candidate as it is a heavy gauge singlet and cannot decay due to the $\mathbb{Z}_n$ symmetry. We can estimate its fraction of the energy density of the universe by defining the corresponding density parameter

$$\Omega_S \equiv \frac{\rho_S}{\rho_c} = \frac{m_S n_S}{\rho_c} = \frac{8\pi m_S n_S}{3H^2 M_{\mathrm{Pl}}^2} \,. \tag{VI.17}$$

Here, ρ_S describes the energy density of S which is given by the mass m_S times the number density n_S since we assume the scalar to be non-relativistic. The critical energy density ρ_c describes the energy density of an entirely flat universe. We express ρ_c in terms of the Planck Mass M_{Pl} and the Hubble parameter H which measures the expansion of the universe [216, 217].

The behavior of the number density n_S is sensitive to the pair annihilation rate of S into SM particles as it moves the particles into a state of thermal equilibrium. This behavior can be described using a Boltzmann equation of the form [218]

$$\frac{d}{dt} n_S + 3H n_S = -\langle \sigma v \rangle \left(n_S^2 - \bar{n}_S^2 \right) \,, \tag{VI.18}$$

where $\bar{n}_S$ denotes the number density in thermal equilibrium and $\langle \sigma v \rangle$ describes the thermal average of the pair annihilation cross section σ times the velocity v.

As soon as the pair annihilation rate becomes smaller than the expansion rate of the universe, the scalar S decouples from thermal equilibrium. This is called thermal freeze-out and occurs when

$$\bar{n}_S \langle \sigma v \rangle = H \,, \tag{VI.19}$$

where the left-hand side describes the pair annihilation rate and the right-hand side the expansion rate of the universe given by H.

Following the standard freeze-out calculation as, for example, shown in reference [218] we obtain for the DM relic abundance Ω_{DM} and the freeze-out condition the expressions

$$h^2 \Omega_{\mathrm{DM}} \gtrsim \frac{x_S}{\sqrt{g_*}} \frac{1.07 \times 10^9 \ \mathrm{GeV}^{-1}}{M_{\mathrm{Pl}} \langle \sigma v \rangle} \,, \quad \sqrt{x_S} e^{-x_S} = 2\pi^3 \sqrt{\frac{8}{45}} \frac{\sqrt{g_*}}{m_S M_{\mathrm{Pl}} \langle \sigma v \rangle} \,, \tag{VI.20}$$

with h being the scaling factor for the Hubble parameter ($H = 100h\text{kms}^{-1}\text{Mpc}^{-1}$), g_* describing the number of relativistic degrees of freedom and $x_S = m_S/T_S$ expressing the dependence on the freeze-out temperature T_S. The total DM relic abundance is determined from CMB data using the ΛCDM model and is given by $h^2\Omega_{\text{DM}} = 0.12 \pm 0.012$ [42].

In order to find the dependence of the freeze-out temperature T_S on the DM mass m_S we express $\langle\sigma v\rangle$ in terms of the relic density and rewrite the freeze-out condition as

$$\delta_S \equiv x_S^{3/2} - e^{x_S} g_* h^2 \Omega_{\text{DM}} \frac{2.4436 \times 10^{-8}\ \text{GeV}}{m_S} = 0\,. \tag{VI.21}$$

This equation does not have an analytical solution for x_S. Hence, we approximate the solution in our mass range of interest using a graphical approach. In Figure VI.2 we show δ_S for DM masses between $m_S = 1$ GeV and $m_S = 10^6$ GeV. We assume that freeze-out occurs at temperatures above the electroweak symmetry breaking scale, such that all SM particles are relativistic with $g_* = 106.75$.

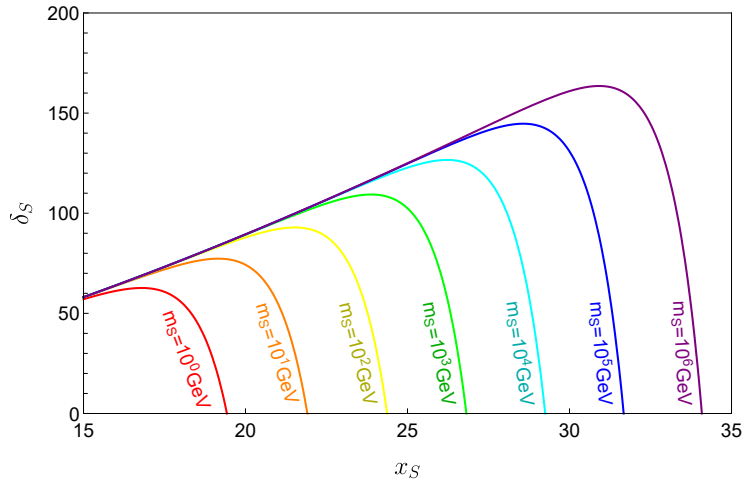

Figure VI.2: Graphical determination of the freeze-out temperature T_S for different DM masses m_S. The zeroes of the lines represent values of $x_S = m_S/T_S$ for which the freeze-out condition $\delta_S = 0$ is fulfilled.

The zeroes of δ_S represent values of $x_S = m_S/T_S$ for which the freeze-out condition $\delta_S = 0$ is fulfilled. Since the zeroes in Figure VI.2 are relatively even distributed we approximate x_S with a logarithmic dependence on m_S,

$$x_S \approx \left(19.4645 + 1.0606 \ln\left(\frac{m_S}{\text{GeV}}\right)\right)\,. \tag{VI.22}$$

With this expression we can find a lower limit on the thermally averaged cross section

$$\langle\sigma v\rangle \geq \frac{x_S}{\sqrt{g_*}} \frac{1.07 \times 10^9\ \text{GeV}^{-1}}{M_{\text{Pl}} h^2 \Omega_{\text{DM}}} \approx \left(1.3759 + 0.0750 \ln\left(\frac{m_S}{\text{GeV}}\right)\right) \times 10^{-9}\ \text{GeV}^{-2}\,, \tag{VI.23}$$

for which the pair annihilation is efficient enough to not overproduce DM particles.

In our model the annihilation cross section is mainly mediated through the interaction of S with the Higgs and the SM fermions. We show the contributing Feynman diagrams in Figure VI.3. The channels which are mediated by the Higgs are sensitive to the coupling λ_{HS} and are given by [219–221]

$$\langle\sigma v\rangle_{ff}^{H} \simeq \frac{N_c^f \lambda_{HS}^2 m_f^2 (m_S^2 - m_f^2)}{4\pi m_S^2 \left[(4m_S^2 - m_h^2)^2 + m_h^2 \Gamma_h^2\right]} \sqrt{1 - \frac{m_f^2}{m_S^2}}, \tag{VI.24}$$

$$\langle\sigma v\rangle^H_{VV} \simeq \frac{\delta_V \lambda_{HS}^2 (4m_S^4 - 4m_S^2 m_V^2 + 3m_V^4)}{8\pi m_S^2 \left[(4m_S^2 - m_h^2)^2 + m_h^2 \Gamma_h^2\right]} \sqrt{1 - \frac{m_V^2}{m_S^2}}, \tag{VI.25}$$

$$\langle\sigma v\rangle^H_{hh} \simeq \frac{\lambda_{HS}^2 \left(4m_S^4 - m_h^4 - \lambda_{HS} v^2 (4m_S^2 - m_h^2)\right)^2}{8\pi m_S^2 (m_h^2 - 2m_S^2)^2 \left[(4m_S^2 - m_h^2)^2 + m_h^2 \Gamma_h^2\right]} \sqrt{1 - \frac{m_h^2}{m_S^2}}\,, \tag{VI.26}$$

where Γ_h symbolizes the total decay width of the Higgs, $f \in \{e, u, d\}$ denotes SM fermions with color multiplicity N_C^f and $V \in \{Z, W\}$ represents SM gauge bosons with $\delta_W = 1$ and $\delta_Z = 1/2$.

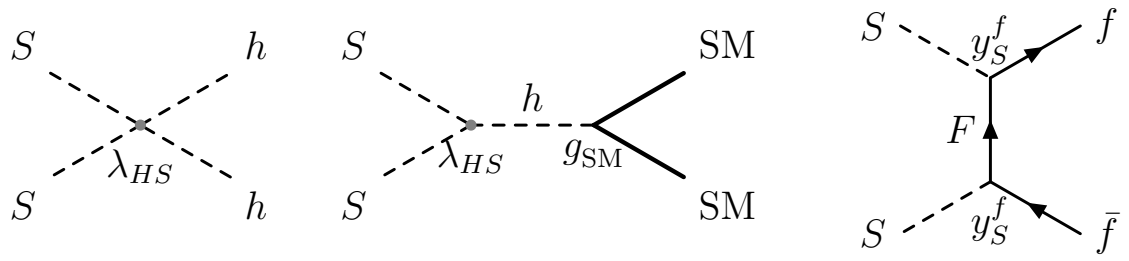

Figure VI.3: Feynman diagrams for DM matter pair annihilation into SM particles.

Analogously we can find the annihilation cross section for the last diagram which is mediated through the heavy fermion F, leading to

$$\langle\sigma v\rangle^F_{ff} \simeq \frac{N_c^f \left(y_S^f\right)^4}{4\pi\, m_F^2} \left(1 - \frac{m_f^2}{m_S^2}\right)^{3/2}. \tag{VI.27}$$

Summing over all contributions, the total thermally averaged annihilation cross section reads

$$\langle\sigma v\rangle = \langle\sigma v\rangle^H_{hh} + \sum_V \langle\sigma v\rangle^H_{VV} + \sum_f \left(\langle\sigma v\rangle^H_{ff} + \langle\sigma v\rangle^F_{ff}\right). \tag{VI.28}$$

Assuming λ_{HS} to be sufficiently small ($\lambda_{HS} \lesssim 10^{-3}$), we can neglect the Higgs contributions and find an estimate of the Yukawa couplings y_S^f.

After applying the limit from equation (VI.23) to one fermion flavor f, we can use the flavor limit from equation (VI.15) to find a bound on the Yukawa couplings of the other flavors $i \neq f$,

$$\frac{\left(y_S^f\right)^4}{m_F^2} \gtrsim \frac{4\pi}{N_c^f} 10^{-9}\ \text{GeV}^{-2} \quad \Rightarrow \quad \frac{\left(y_S^i\right)^4}{m_F^2} = \frac{\left(y_S^i y_S^f\right)^4}{m_F^4} \frac{m_F^2}{\left(y_S^f\right)^4} \lesssim \frac{N_c^f}{4\pi y_F^2} 10^{-27}\ \text{GeV}^{-2}. \tag{VI.29}$$

We see that the flavor limit leads to a strong suppression of the other Yukawa couplings, such that we only can have one sizable Yukawa coupling at a time.

VI.3.2 Direct Detection Constraints

Dark Matter direct detection experiments like XENONnT and LUX-ZEPLIN [213–215] provide constrains on the scattering cross section σ_{nS} between DM particles and nucleons. The tree-level scattering is again mediated via the Higgs and Yukawa interactions as

depicted in the last two diagrams in Figure VI.3. The corresponding cross sections read

$$\sigma_{nS}^{H} = \frac{\lambda_{HS}^2}{4\pi m_h^4} \frac{m_n^4 f_n^2}{(m_S + m_n)^2}, \tag{VI.30}$$

$$\sigma_{nS}^{Fq} = \frac{\left(y_S^q\right)^4}{4\pi m_F^2 m_q^2} \frac{m_n^4 (f_q^n)^2}{(m_S + m_n)^2}, \tag{VI.31}$$

where $m_n \approx 0.939$ GeV refers to the average nucleon mass, f_q^n represents the individual fraction of quark q in a nucleon and $f_n = \sum_q f_q^n$ the total quark fraction in a nucleon.

We approximate the quark fractions following references [222–224] by

$$f_u^n \approx 0.02\,, \quad f_d^n \approx 0.045\,, \quad f_s^n \approx 0.043\,, \quad f_c^n = f_b^n = f_t^n \approx 0.06\,, \tag{VI.32}$$

such that the total quark fraction is given by $f_n \approx 0.3$.

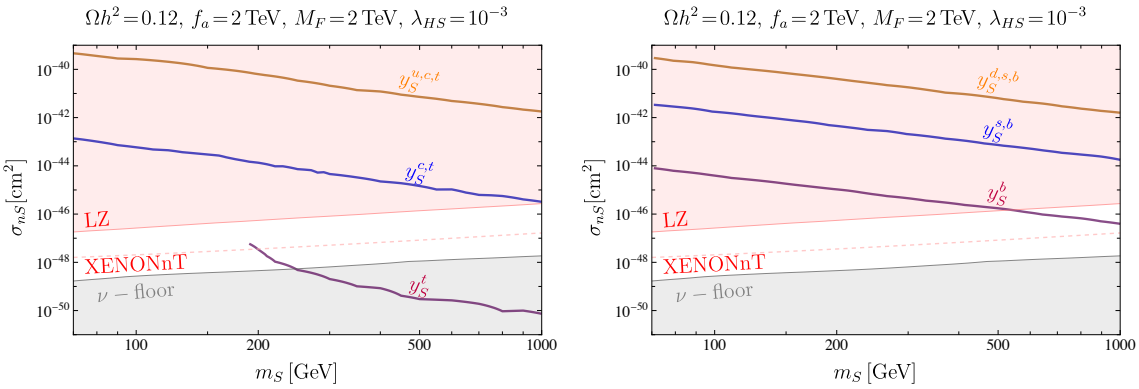

Figure VI.4: DM direct detection limits on DM-nucleon cross sections with chirally enhanced quark couplings. The light red region is excluded by the LUX-ZEPLIN experiment, while the red dashed line shows the 20 ton-year projection for XENONnT [213–215]. The superscript in the Yukawa coupling denotes which DM Yukawa couplings are non-zero. The left panel uses non-zero Yukawa couplings of up-type quarks and the right panel of down-type quarks. The calculation was performed under the use of `micrOMEGAS-5.3` [11]. The figure is taken from reference [4].

Figure VI.4 shows the limits from the LZ experiment in the light red region and the 20 ton-year projection from the XENONnT experiment for different quarks coupling to the DM scalar with Yukawa couplings y_S^q. We depict the total DM-nucleon cross section

$$\sigma_{nS} = \sigma_{nS}^{H} + \sum_q \sigma_{nS}^{Fq}\,, \tag{VI.33}$$

where we again assume that the contribution of the Higgs boson is negligible due to a small coupling $\lambda_{HS} = 10^{-3}$.

Under the assumption that we can only switch on one Yukawa coupling at a time, we get a bound on the Yukawa couplings of

$$\frac{\left(y_S^q\right)^4}{m_F^2} \lesssim \frac{4\pi m_q^2 (m_S + m_n)^2}{\left(f_q^n\right)^2 m_n^4} \sigma_{nS}^{\text{exp}}\,, \tag{VI.34}$$

where σ_{nS}^{exp} symbolizes the limits obtained by the experiments.

We can also find a limit on the DM-cross section in the case of chirally enhanced axion lepton couplings. But since leptons do not contribute to the nucleonic cross section, we only get a contribution from σ_{nS}^{H}, such that the bound depends entirely on λ_{HS}. In Figure VI.5 we show the case for $\lambda_{HS} = 10^{-3}$ as an example.

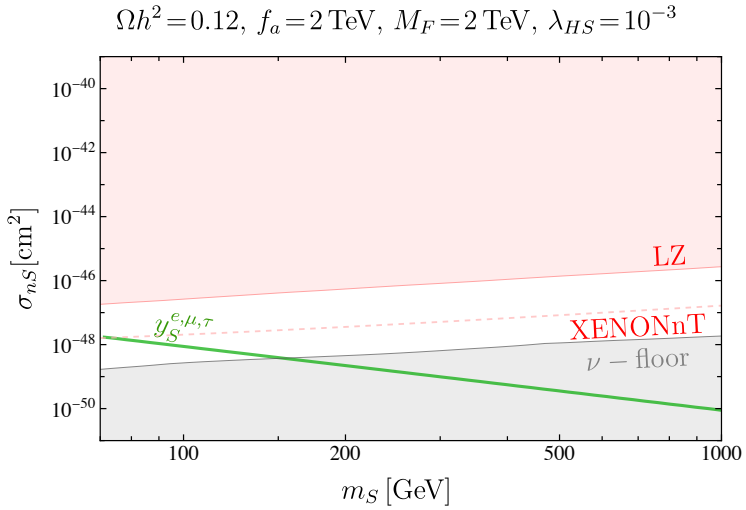

Figure VI.5: DM direct detection limits on DM-nucleon cross sections with chirally enhanced lepton couplings. The light red region is excluded by the LUX-ZEPLIN experiment, while the red dashed line shows the 20 ton-year projection for XENONnT [213–215]. The superscript in the Yukawa coupling denotes which DM Yukawa couplings are non-zero. The calculation was performed using `micrOMEGAS-5.3` [11]. The figure is taken from reference [4].

VI.3.3 Chiral Enhancement of Axion Quark Couplings

We now make use of the DM bounds from the previous sections to establish an estimate on the chiral enhancement of quark couplings. Neglecting all terms of order $\mathcal{O}(m_f^2/m_S^2)$ and $\mathcal{O}(m_f^2/m_F^2)$ but keeping now further dependences on the heavy masses, the total coefficient for the pseudoscalar axion quark couplings reads

$$C_{aqq}^{\text{tot}} = C_{aqq}^{0} + C_{aqq}^{S,A} = -X_{u/d} - X\frac{\left(y_S^q\right)^2}{4\pi^2}\left(\frac{m_F^2}{m_F^2 - m_S^2} + \frac{m_F^2 m_S^2 \ln\left(\frac{m_S^2}{m_F^2}\right)}{\left(m_F^2 - m_S^2\right)^2}\right), \tag{VI.35}$$

where the tree-level coupling is given for up-type quarks as $X_u = \cos^2\beta_1 X$ and for down-type quarks as $X_d = \sin^2\beta_1 X$ with $\tan\beta_1 = v_d/v_u$ as shown in subsection III.1.1. Hence, the chiral enhancement for up-type quarks is larger at $\beta_1 \to \pi/2$ and for down-type quarks at $\beta_1 \to 0$. The vector-like axion quark coupling does not play a role here as we only consider flavor conserving couplings due to the smallness of flavor-changing couplings.

We extract the limits on the DM Yukawa couplings from relic abundance and direct detection as presented in equations (VI.23) and (VI.34), leading to

$$\frac{4\pi}{3}\frac{x_S}{\sqrt{g_*}}\frac{1.07\times 10^9\ \text{GeV}^{-1}}{M_{\text{Pl}}h^2\Omega_{\text{DM}}}\left(1-\frac{m_q^2}{m_S^2}\right)^{-3/2} \lesssim \frac{\left(y_S^q\right)^4}{m_F^2} \lesssim \frac{4\pi m_q^2(m_S+m_n)^2}{\left(f_q^n\right)^2 m_n^4}\sigma_{nS}^{\text{exp}}. \tag{VI.36}$$

We see that small quark mass are stronger constrained by the direct detection experiments than large quark masses. The heavy fermion mass on the other hand relaxes the direct detection bound for higher values, but increases the lower bound from relic abundance.

We show the resulting parameter space for different quarks in Figure VI.6, where we also account for an upper limit at which the Yukawa couplings become non-perturbative. The heavy fermion mass is taken to be $m_F = 50$ TeV for all quarks besides the up-quark, where we show the case for $m_F = 100$ TeV. The high values are motivated by the fact, that F has to be heavier than S to forbid direct decays of the heavy scalar. As expected, we see that the parameter space for light quarks is much more constrained than for heavy quarks due to the direct detection bounds which are sensitive too the quark mass.

The mixing angle β_1 is taken to be $\beta_1 = 0.45\pi$ for up-type quarks and $\beta_1 = 0.05\pi$ for down-type quarks to get a sizable chiral enhancement of order $\mathcal{O}(10)$. In fact, for up-type quarks this represents a natural choice as this angle corresponds to the case where the SM Higgs Yukawa couplings to top- and bottom-quark are of the same size. On the other hand, the limit for the down-type quarks is more difficult to construct, since the top-quark would need a larger SM Yukawa coupling. Hence, we conclude that chiral enhancement is more preferable for up-type quarks than down-type quarks.

Finally, we notice that for any non-zero Yukawa coupling y_S^i the limits from relic abundance and direct DM searches overlap, leading to a lower bound on the DM mass m_S. For example, assuming an enhanced axion-charm quark interaction $C_{acc}^{\text{tot}} > C_{acc}^0$ with $m_F = 50$ TeV and $\beta_1 = 0.45\pi$, we obtain a lower limit of $m_S > 1$ TeV.

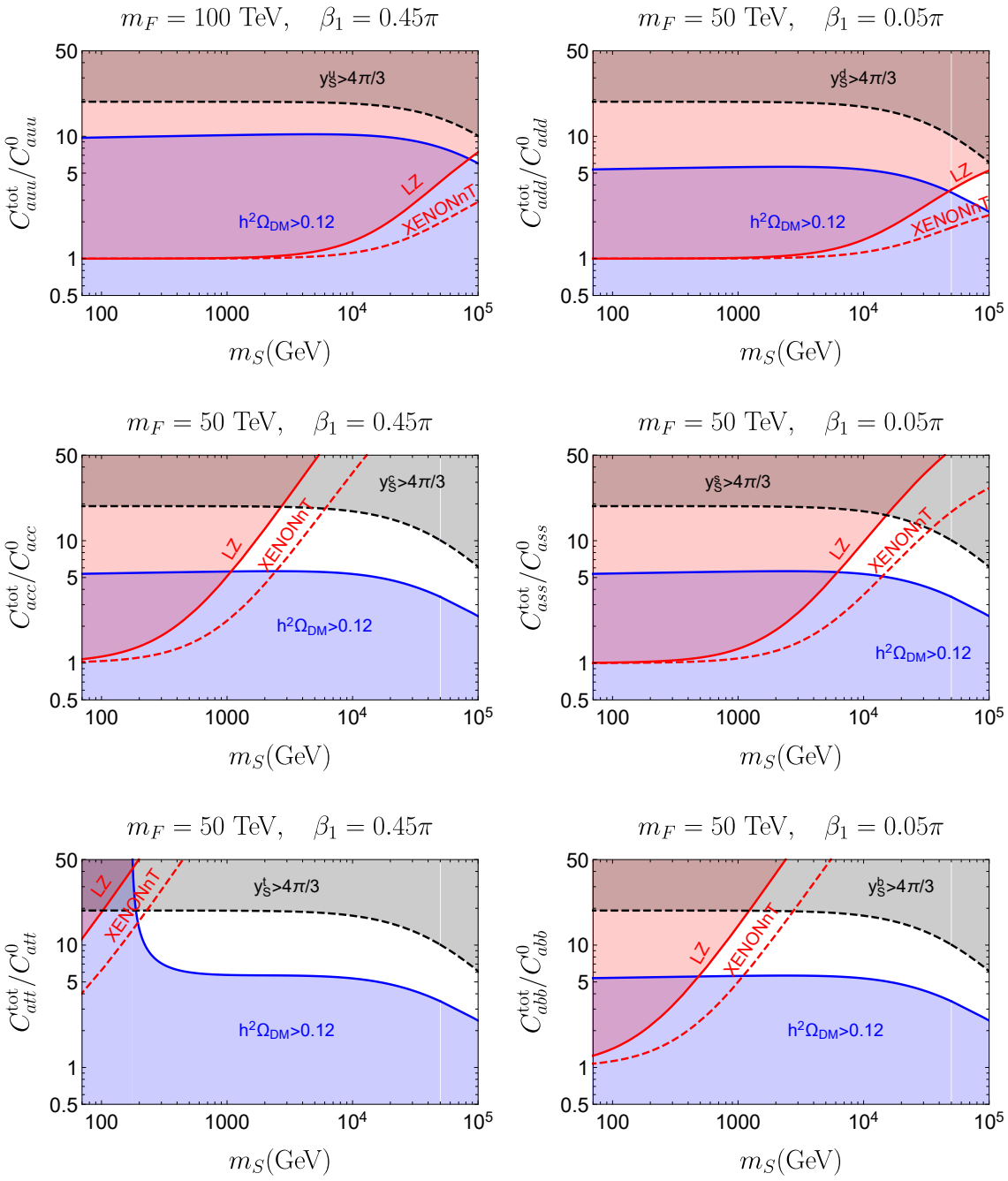

Figure VI.6: Chiral enhancement of axion couplings to quarks. The red region is excluded by the LUX-ZEPLIN experiment, while the red dashed line shows the 20 ton-year projection for XENONnT [213–215]. In the blue region the scalar S would provide an overabundance of DM and in the gray region the Yukawa couplings become non-perturbative. The left panels use non-zero Yukawa couplings of up-type quarks and the right panels of down-type quarks.

VI.3.4 Chiral Enhancement of Axion Lepton Couplings

In the case of leptons the tree-level axion lepton coupling is given by $C^0_{all} = -X_d$ as it was the case for down-like quarks. However, in contrast to down-type quarks the chiral enhancement is less constrained. This has multiple reasons. On one hand, the direct detection constraints are weaker, since they are only sensitive to the Higgs coupling λ_{HS}.

On the other hand, we could have also chosen a $\mathbb{Z}_n$ charge of 1 for the right-handed charged leptons, such that they would receive their mass contribution from H_u. This case is called the flipped two Higgs-doublet model [52] in which the tree-level coupling to leptons becomes $C^0_{all} = -X_u$, leaving the chiral enhancement preferable to all charged leptons. Figure VI.7 shows the corresponding parameter space for $m_F = 50$ TeV, $\beta_1 = \pi/8$ and $\lambda_{HS} = 10^{-2}$.

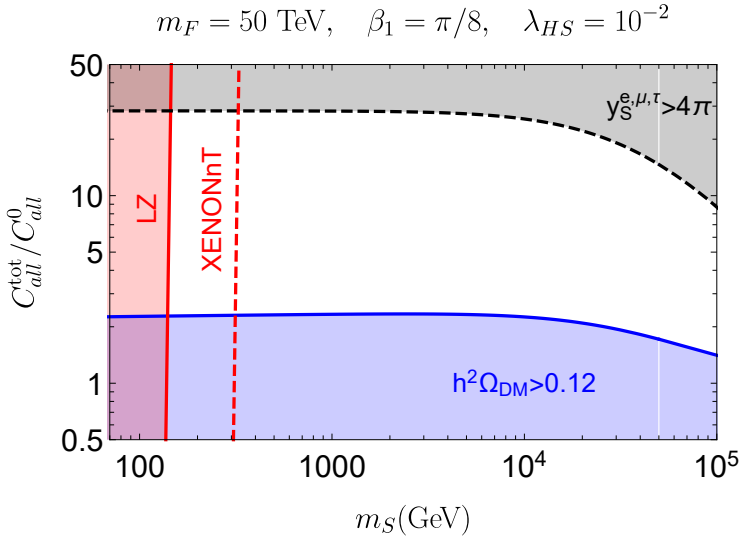

Figure VI.7: Chiral enhancement of axion couplings to leptons. The red region is excluded by the LUX-ZEPLIN experiment, while the red dashed line shows the 20 ton-year projection for XENONnT [213–215]. In the blue region the scalar S would provide an overabundance of DM and in the gray region the Yukawa couplings become non-perturbative.

VI.4 Chiral Enhancement and Neutrino Masses

In the previous sections we showed how the axion couplings to quarks and charged leptons are enhanced in presence of new heavy fields. In this section we briefly investigate axion couplings to neutrinos and possible chiral enhancement factors from heavy right-handed neutrinos.

In order to be able to explain the phenomenon of neutrino oscillation [44] we need to include a mass term for the neutrinos in our theory. Such a mass term can be written down using the SM (or DFSZ) field content at dimension five via the Weinberg operator [225]

$$\mathcal{L}_\nu \supset \frac{C_\nu}{\Lambda_\nu} \left(\bar{L}_L H_u\right)^c H_u^* L_L + \text{h.c.}\,. \tag{VI.37}$$

We can find a UV completion for this operator by introducing right-handed fermion fields ν_R^i which are gauge singlet under the SM gauge group. We show the extended field content in Table VI.2.

	$SU(3)_C$	$SU(2)_L$	$U(1)_Y$	$\mathbb{Z}_n$	$U(1)_{PQ}$
Q_L^i	3	2	1/6	$(n-1)/2$	X_Q
u_R^i	3	1	2/3	$(n+1)/2$	X_Q-X_u
d_R^i	3	1	-1/3	$(n-1)/2$	X_Q-X_d
L_L^i	1	2	-1/2	$(n-1)/2$	X_L
e_R^i	1	1	-1	$(n-1)/2$	X_L-X_d
H_u	1	2	-1/2	n-1	X_u
H_d	1	2	1/2	0	X_d
Φ_A	1	1	0	1	-X
ν_R^i	1	1	0	$(n+1)/2$	X_L-X_u

Table VI.2: Field content of the DFSZ model with three additional right-handed neutrinos ν_R^i.

The $\mathbb{Z}_n$ charges allow for two Yukawa couplings for the right-handed neutrinos, one being the usual Higgs coupling which is the same as for the other SM fermions and the other one being a coupling to the complex scalar Φ involving the charge conjugated field $\bar{\nu}_R^c = \overline{(\nu_R)^c} = \overline{(\nu^c)_L}$. The full Lagrangian is given by

$$\mathcal{L}_\nu^{\text{DFSZ}} \supset \mathcal{L}^{\text{DFSZ}} + \bar{\nu}_R^i i\partial\!\!\!/ \nu_R^i - y_\nu^{ij} \bar{L}_L^i H_u \nu_R^j - y_N^{ij} \bar{\nu}_R^{c,i} \Phi^* \nu_R^j + \text{h.c.}\,, \tag{VI.38}$$

where the term proportional to the Yukawa coupling y_ν^{ij} leads to a Dirac mass while the term proportional to y_N^{ij} provides a Majorana mass for the neutrinos. Since the last term includes the field Φ with vev $v_\Phi \gg v$, we expect the right handed-field to be much heavier than the left-handed fields.

In order to find the mass basis of the neutrinos, we first diagonalize the matrix $\mathbf{Y}_\nu$ analogously to the procedure in the SM,

$$\nu_L \to \mathbf{U}_\nu \nu_L\,, \quad \nu_R \to \mathbf{V}_\nu \nu_R\,, \quad \mathbf{U}_\nu^\dagger \mathbf{U}_\nu = \mathbb{1} = \mathbf{V}_\nu^\dagger \mathbf{V}_\nu\,, \quad \mathbf{Y}_{D,\nu} = \mathbf{U}_\nu^\dagger \mathbf{Y}_\nu \mathbf{V}_\nu\,. \tag{VI.39}$$

Together with the same transformations for the charged leptons we now get a mixing matrix in the weak sector $\mathbf{V}_{\text{PMNS}} \equiv \mathbf{U}_\nu^\dagger \mathbf{U}_e$ which is responsible for neutrino oscillation.

Assuming $y_N^{ij} = y_N^i \delta^{ij}$ for simplicity, we find two mass eigenstates for the neutrinos,

$$\nu^i = (\nu_L^{c,i} - \nu_L^i) + \frac{1}{2} \frac{y_{D,\nu}^i X s_{\beta_1} v}{y_N^i f_a} (\nu_R^{c,i} - \nu_R^i) + \mathcal{O}\left(\frac{v^2}{f_a^2}\right)\,, \tag{VI.40}$$

$$N^i = (\nu_R^{c,i} + \nu_R^i) + \frac{1}{2} \frac{y_{D,\nu}^i X s_{\beta_1} v}{y_N^i f_a} (\nu_L^{c,i} + \nu_L^i) + \mathcal{O}\left(\frac{v^2}{f_a^2}\right)\,, \tag{VI.41}$$

with s_{β_1} being the sine of the mixing angle between v_u and v_d. The corresponding masses are up to $\mathcal{O}(v^2/f_a^2)$

$$m_{N^i} = y_N^i \frac{f_a}{X\sqrt{2}} + \frac{1}{4} \frac{(y_{D,\nu}^i)^2}{y_N^i} \frac{X s_{\beta_1}^2 v^2}{\sqrt{2} f_a}\,, \quad m_{\nu^i} = \frac{1}{4} \frac{(y_{D,\nu}^i)^2}{y_N^i} \frac{X s_{\beta_1}^2 v^2}{\sqrt{2} f_a}\,. \tag{VI.42}$$

The fields ν^i correspond to the observed neutrino states with direct couplings to the $SU(2)_L$ gauge bosons, while the couplings of the heavy fields N^i to the gauge bosons are suppressed by an additional factor of $\sqrt{m_\nu^i/(m_N^i - m_\nu^i)} \sim v/f_a$.

Now, we can write down the couplings of the pseudoscalar a in the mass basis of the fermions, where we expand in large f_a, dropping all terms of order $\mathcal{O}(1/f_a^2)$. The corresponding Lagrangian reads

$$\begin{aligned}\mathcal{L}^{\nu}_{\text{axion}} \supset & - iXm_N^i \frac{a}{f_a}\bar{N}^i\gamma_5 N^i + iXm_\nu^i \frac{a}{f_a}\bar{\nu}^i\gamma_5\nu^i \\ & - iX(m_N^i - m_\nu^i)\frac{a}{f_a}\sqrt{\frac{m_\nu^i}{m_N^i - m_\nu^i}}(\bar{\nu}^i N^i - \bar{N}^i\nu^i)\,. \end{aligned} \tag{VI.43}$$

We already see that loop-effects from the neutrino couplings are either suppressed by m_ν^i or their corresponding couplings to gauge bosons. It also shows that although the heavy neutrinos N^i have a strong coupling to the axion, the axion couplings to the light neutrinos ν^i are not enhanced.

VI.4.1 Effective Couplings from Neutrino Interactions

Having introduced the tree-level axion couplings to neutrinos, we discuss the effective couplings induced by neutrino effects. Since the neutrinos only couple to the weak bosons Z, W^+ and W^- and charged leptons l the effective couplings are

$$\mathcal{L}_{\text{EFT}} \supset C^N_{aZZ}\frac{a}{f_a}Z_{\mu\nu}\tilde{Z}^{\mu\nu} + C^N_{aWW}\frac{a}{f_a}W_{\mu\nu}\tilde{W}^{\mu\nu} - \frac{\partial_\mu a}{2f_a}\bar{l}\gamma^\mu(\mathbf{C}^{N,V}_{all} + \mathbf{C}^{N,A}_{all}\gamma_5)l\,. \tag{VI.44}$$

The superscript N denotes that we integrated out the heavy neutrinos. The corresponding diagrams are shown in Figure VI.8.

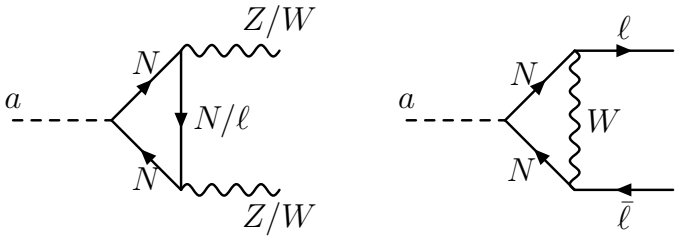

Figure VI.8: Feynman diagrams for effective couplings induced by heavy right-handed neutrinos.

Although the heavy neutrinos N^i have a mass proportional to the axion decay constant and have therefore a large coupling to the axion at tree-level, the corresponding couplings to the gauge bosons are each suppressed by at least one power of v/f_a. On the other hand the light neutrinos have a mass which is already suppressed by a factor v^2/f_a^2. Hence the effective couplings are all suppressed by

$$C^N_{aZZ} \sim \frac{1}{(4\pi)^2}\frac{e^2}{s_W^2 c_W^2}\frac{v^2}{f_a^2}\,, \quad C^N_{aWW} \sim \frac{1}{(4\pi)^2}\frac{e^2}{s_W^2}\frac{v^2}{f_a^2}\,, \quad \mathbf{C}^{N,V}_{all} = -\mathbf{C}^{N,A}_{all} \sim \frac{1}{(4\pi)^2}\frac{e^2}{s_W^2}\frac{v^2}{f_a^2}\,. \tag{VI.45}$$

This means that although we have predestined candidates for a loop induced axion-W boson coupling as well as chirally enhanced charged lepton couplings of the same size, these couplings are much smaller than the couplings induced by the heavy fermion F in the previous model. In addition, the flavor-violating couplings induced by the heavy neutrinos are suppressed by the unitarity of the PMNS matrix.

CHAPTER VII

Axion Couplings in gauged U(1)' Extensions

In this chapter we study the interplay between the axion and additional $U(1)'$ gauge bosons. It mainly follows our discussion in reference [2]. In the SM there are two residual global symmetries, baryon number $U(1)_B$ and lepton number $U(1)_L$. Since both of these symmetries are anomalous, they are expected to be violated through non-perturbative effects. Only their combination $U(1)_{B-L}$ does not generate an anomaly.

In order to protect either $U(1)_B$ or $U(1)_L$, we can associate it to a $U(1)'$ gauge symmetry, introducing a new electrically neutral gauge bosons, called Z'. This additional gauge field receives a contribution from the hypercharge gauge boson through kinetic mixing which is consistent with gauge invariance. The kinetic mixing is induced by additional heavy fermions which are needed to cancel the $U(1)' \times SU(2)_L^2$ and $U(1)' \times U(1)_Y^2$ gauge anomalies and are therefore called anomalons.

Here, we present the implications on axion physics in the case of a DFSZ model in combination with a gauged $U(1)_B$ symmetry with gauge coupling g_B. While the SM sector consists of two Higgs fields to enable axion couplings to SM fermions, the additional sector also includes two complex scalars which spontaneously break the PQ symmetry as well as baryon number. This leads to a non-trivial mixing between the axion and the longitudinal mode of the Z'.

This connection between the angular fields reduces the parameter spaces in the mass coupling planes as the $\{m_a, f_a^{-1}\}$ and $\{m_{Z'}, g_B\}$ spaces are no longer independent. We constrain our parameters by applying collider limits from ATLAS and CMS and present our results in the $\{m_a, G_{a\gamma\gamma}\}$ parameter space.

In the following we start in section VII.1 by setting up the model and discussing the mixing of the angular fields. Afterwards, in section VII.2 we describe our theory in an ALP-EFT framework, where we integrate out the heavy fermions. Finally, in section VII.3 we present our phenomenological studies which are based on collider experiments.

VII.1 Model

We start with the construction of the model in general, followed by a more detailed description of the different particle sectors. To construct a DFSZ model with a gauged $U(1)_B$ extension, we first take the canonical two-Higgs doublet model with Higgs fields H_u, H_d and add two complex scalar fields Φ_1 and Φ_2. These two complex scalars are singlets under the SM gauge group but are charged under $U(1)_B$ with baryon numbers $B_1 = -3$ and $B_2 = 3$.

We assume that both additional scalars acquire a non-vanishing vev, such that they not only fulfill the role of the complex scalar Φ in the DFSZ model, but also break $U(1)_B$ spontaneously. Hence, the Z' becomes massive and the angular modes of Φ_1 and Φ_2 provide both the axion degree of freedom as well as the longitudinal mode of the Z'.

Of the SM fields only the quarks have a baryon number $B_q = 1/3$, such that we need fermionic anomalon fields which cancel the $U(1)_B \times SU(2)_L^2$ and $U(1)_B \times U(1)_Y^2$ gauge anomalies. We adapt the respective field content from references [226,227] which introduce six chiral anomalon fields L'_L, L'_R, E'_L, E'_R, N'_L and N'_R.

Table VII.1 shows the complete fermionic and scalar field content. We introduce a discrete $\mathbb{Z}_4$ symmetry, which is mainly needed to define the Yukawa couplings in the two-Higgs doublet model and to protect the global PQ symmetry, as we discussed in subsection II.3.2.

	$SU(3)_C$	$SU(2)_L$	$U(1)_Y$	$U(1)_B$	$\mathbb{Z}_4$	$U(1)_{PQ}$
Q_L^i	3	2	1/6	1/3	0	X_Q
u_R^i	3	1	2/3	1/3	1	X_Q-X_u
d_R^i	3	1	-1/3	1/3	0	X_Q-X_d
L_L^i	1	2	-1/2	0	0	X_L
e_R^i	1	1	-1	0	0	X_L-X_d
H_u	1	2	-1/2	0	3	X_u
H_d	1	2	1/2	0	0	X_d
L'_L	1	2	-1/2	-1	0	X'
L'_R	1	2	-1/2	2	3	X'-X_2
E'_L	1	1	-1	2	3	X'-X_d-X_2
E'_R	1	1	-1	-1	0	X'-X_d
N'_L	1	1	0	2	0	X'-X_u-X_2
N'_R	1	1	0	-1	1	X'-X_u
Φ_1	1	1	0	-3	2	$-X_1$
Φ_2	1	1	0	3	3	$-X_2$

Table VII.1: Field content for a DFSZ-like model with gauged baryon number. In addition to the SM fermions we have two Higgs doublets H_u and H_d for electroweak symmetry breaking (EWSB), two Higgs fields Φ_1 and Φ_2 for breaking baryon number and heavy anomalon fields which cancel gauge anomalies. Besides the SM charges, we assign baryon number and a $\mathbb{Z}_4$ charge. The PQ charge results from the global symmetry of the Lagrangian.

Hence, the scalar Lagrangian of our model involving all complex scalars is given by

$$\begin{aligned}\mathcal{L}_{\text{scalar}} \supset & \sum_{\mathtt{i}=u,d} |D_{\mathtt{i},\mu} H_{\mathtt{i}}|^2 + \sum_{\mathtt{i}=1,2} |D_{\mathtt{i},\mu} \Phi_{\mathtt{i}}|^2 - \sum_{\mathtt{i},\mathtt{j}=u,d} \lambda_{\mathtt{ij}} \left(|H_{\mathtt{i}}|^2 - \frac{v_{\mathtt{i}}^2}{2}\right)\left(|H_{\mathtt{j}}|^2 - \frac{v_{\mathtt{j}}^2}{2}\right) \\ & - \sum_{\mathtt{i},\mathtt{j}=1,2} \lambda_{\mathtt{ij}} \left(|\Phi_{\mathtt{i}}|^2 - \frac{v_{\mathtt{i}}^2}{2}\right)\left(|\Phi_{\mathtt{j}}|^2 - \frac{v_{\mathtt{j}}^2}{2}\right) - \sum_{\mathtt{i},\mathtt{j}} \lambda_{\mathtt{ij}} \left(|H_{\mathtt{i}}|^2 - \frac{v_{\mathtt{i}}^2}{2}\right)\left(|\Phi_{\mathtt{j}}|^2 - \frac{v_{\mathtt{j}}^2}{2}\right) \\ & - \lambda_A \left(H_u^T H_d \Phi_1 \Phi_2 + \text{h.c.}\right) \ , \end{aligned} \tag{VII.1}$$

where we contract $SU(2)_L$ indices implicitly. The last term proportional to λ_A fulfills the role of the μ_A term in the vanilla axion model, separating the axion from the heavy pseudoscalar A. We discuss this in more detail in subsection VII.1.1.

The $\mathbb{Z}_4$ charges of the anomalons are chosen in such a way, that they get mass contributions through Yukawa couplings with the Higgs doublets and the complex scalar Φ_2. The corresponding Yukawa Lagrangian reads

$$\begin{aligned}\mathcal{L}_{\text{Yukawa}} \supset & - y_u^{ij} \bar{Q}_L^i H_u u_R^j - y_d^{ij} \bar{Q}_L^i H_d d_R^j - y_e^{ij} \bar{L}_L^i H_d e_R^j \\ & - y_L \bar{L}'_R \Phi_2 L'_L - y_E \bar{E}'_L \Phi_2 E'_R - y_N \bar{N}'_L \Phi_2 N'_R \\ & - y_1 \bar{L}'_L H_d E'_R - y_2 \bar{L}'_R H_d E'_L - y_3 \bar{L}'_L H_u N'_R - y_4 \bar{L}'_R H_u N'_L + \text{h.c.}\,. \end{aligned} \tag{VII.2}$$

The Yukawa interactions not only generate fermion masses but also mediate axion couplings to the anomalon sector, such that we induce corrections to axion couplings by integrating out the heavy fermions. Since the Yukawa interactions also induce a mass mixing between the anomalons, the axion couplings will change the flavor of the heavy fields. We demonstrate this in subsection VII.1.2.

Finally, in subsection VII.1.3 we show that the anomalons also fulfill a trace-condition which allows for a finite loop-induced kinetic mixing term

$$\mathcal{L}_{\text{kin-mix}} \supset \frac{\epsilon_{\text{eff}}}{2} B_{\mu\nu} K^{\mu\nu}\,, \tag{VII.3}$$

where K_μ describes the $U(1)_B$ gauge boson before diagonalization and canonical normalization of the gauge boson mass basis. In principle, we could also write down a kinetic mixing at tree-level, but since the $U(1)$ gauge groups generally can be subgroups of $SU(N)$ symmetries in the UV we forbid a tree-level kinetic mixing.

In the following we include a more detailed discussion of the model setup from reference [2] which was written by the author of this thesis. The discussion consists of three parts: In subsection VII.1.1 we present the scalar sector, where we define the Goldstone basis taking into account the mixing of angular fields. Subsequently, we discuss the mixing between anomalon fields in subsection VII.1.2 leading to flavor-violating axion couplings. In the last subsection VII.1.3 we then show the impact of kinetic mixing on the interactions involving the gauge fields.

VII.1.1 Scalar Sector

To define the Goldstone basis of the angular fields, we parameterize the complex fields via

$$\begin{aligned} H_u = \frac{1}{\sqrt{2}} \exp\left(i\frac{\varphi_u^a \sigma^a}{v_u}\right) \begin{pmatrix} v_u + h_u \\ 0 \end{pmatrix}\,, \quad H_d = \frac{1}{\sqrt{2}} \exp\left(i\frac{\varphi_d^a \sigma^a}{v_d}\right) \begin{pmatrix} 0 \\ v_d + h_d \end{pmatrix}\,, \\ \Phi_1 = \frac{v_1 + h_1}{\sqrt{2}} \exp\left(i\frac{a_1}{v_1}\right)\,, \quad \Phi_2 = \frac{v_2 + h_2}{\sqrt{2}} \exp\left(i\frac{a_2}{v_2}\right)\,. \end{aligned} \tag{VII.4}$$

Here, $v_{\mathtt{i}}$ denote the vevs of the scalar fields, $h_{\mathtt{i}}$ are the radial modes, and $a_{\mathtt{i}}$ and $\varphi_{\mathtt{i}}^a$ are angular modes, while σ^a denote the Pauli matrices as generators of $SU(2)_L$. We define $a_u \equiv \varphi_u^3$, $a_d \equiv -\varphi_d^3$ as neutral angular modes of H_u and H_d. The vevs which spontaneously break $SU(2)_L \times U(1)_Y$ and $U(1)_B$ are $v \equiv \sqrt{v_u^2 + v_d^2}$ and $v' \equiv \sqrt{v_1^2 + v_2^2}$, respectively, with $\tan\beta \equiv v_u/v_d$ and $\tan\beta' \equiv v_1/v_2$.

Since the PQ symmetry is orthogonal to the gauge $U(1)$ symmetries, we have the relations

$$0 = \sum_{\{H_{\mathtt{i}}\}} Y_{\mathtt{i}} X_{\mathtt{i}} v_{\mathtt{i}}^2\,, \quad 0 = \sum_{\{\Phi_{\mathtt{i}}\}} B_{\mathtt{i}} X_{\mathtt{i}} v_{\mathtt{i}}^2\,, \quad X^2 v_a^2 = \sum_{\{H_{\mathtt{i}}, \Phi_{\mathtt{i}}\}} X_{\mathtt{i}}^2 v_{\mathtt{i}}^2\,. \tag{VII.5}$$

Together with the requirement of $X \equiv X_u + X_d = X_1 + X_2$ to keep the λ_A term PQ invariant, the PQ charges of the scalar fields evaluate to

$$X_u = X\cos^2\beta\ , \quad X_d = X\sin^2\beta\ , \quad X_1 = X\cos^2\beta'\ , \quad X_2 = X\sin^2\beta'\ . \tag{VII.6}$$

Consequently, the PQ symmetry is spontaneously broken by the effective scale v_a, where

$$v_a \equiv \sqrt{v^2\sin^2\beta\cos^2\beta + v'^2\sin^2\beta'\cos^2\beta'}\,, \quad \tan\gamma \equiv \frac{v\sin\beta\cos\beta}{v'\sin\beta'\cos\beta'}\,. \tag{VII.7}$$

The PQ charge normalization X is then fixed by the axion decay constant $f_a \equiv X v_a$.

To identify the axion a, the heavy $SU(2)$ pseudoscalar A, and the two Goldstones φ^0, φ_B for the longitudinal Z and Z' bosons, we perform the following orthogonal transformation,

$$\begin{pmatrix} a \\ A \\ \varphi^0 \\ \varphi_B \end{pmatrix} = \begin{pmatrix} c_\beta s_\gamma & s_\beta s_\gamma & -c_{\beta'}c_\gamma & -s_{\beta'}c_\gamma \\ c_\beta c_\gamma & s_\beta c_\gamma & c_{\beta'}s_\gamma & s_{\beta'}s_\gamma \\ -s_\beta & c_\beta & 0 & 0 \\ 0 & 0 & -s_{\beta'} & c_{\beta'} \end{pmatrix} \begin{pmatrix} a_u \\ a_d \\ a_1 \\ a_2 \end{pmatrix}\ , \tag{VII.8}$$

where the φ^0 and φ_B Goldstones are easily identified as aligning with the Higgs basis of each sector. The shorthand notation of s and c represents cosine and sine. We remark that for $v \ll v'$, $\gamma \approx 0$, we reproduce the invisible axion of the DFSZ model which is dominantly composed of a_1 and a_2 SM gauge singlets. We can also reproduce the Weinberg-Wilczek model [17, 18] by considering the other limit, $v \gg v'$, $\gamma \approx \pi/2$.

The heavy pseudoscalar A gets a mass from the λ_A term given by

$$m_A^2 = \frac{\lambda_A}{2}\frac{v_a^2}{s_\beta c_\beta s_{\beta'} c_{\beta'}}\ . \tag{VII.9}$$

A mass for the axion is only induced by instanton effects, which are quantified by the topological susceptibility χ [54]

$$\chi = m_a^2 f_a^2\ , \quad \chi_{\rm QCD} = \Lambda_{\rm QCD}^4 = \frac{m_u m_d}{(m_u+m_d)^2} m_\pi^2 f_\pi^2\ . \tag{VII.10}$$

For an ALP, χ remains a free parameter, while a vanilla QCD axion demands $\chi = \chi_{\rm QCD}$, although recent studies have demonstrated that χ can be enhanced by non-QCD sources and still preserve the axion solution to the strong CP problem [1, 193, 194, 196]. As long as λ_A is sufficiently large, the basis rotation in equation (VII.8) coincides with the mass basis of a and A.

For the CP even Higgs bosons, we perform the orthogonal transformation to the Higgs basis in the alignment limit, giving

$$\begin{pmatrix} h \\ H_0 \\ h' \\ H_0' \end{pmatrix} \equiv \begin{pmatrix} s_\beta & c_\beta & 0 & 0 \\ c_\beta & -s_\beta & 0 & 0 \\ 0 & 0 & s_{\beta'} & c_{\beta'} \\ 0 & 0 & c_{\beta'} & -s_{\beta'} \end{pmatrix} \begin{pmatrix} h_u \\ h_d \\ h_1 \\ h_2 \end{pmatrix}\ . \tag{VII.11}$$

We will assume that the Higgs basis is aligned with the mass basis and neglect further scalar mixing, since our focus is the phenomenology of the light axion and Z' boson. Large deviations from the alignment limit are also strongly constrained by Higgs observables [228, 229].

VII.1.2 Fermion Sector

In this section, we calculate the anomalon masses and couplings to the axion and other scalars. From equation (VII.2), the masses of the anomalons arise from the vevs v_2, v_u and v_d, where we parameterize the Yukawa couplings by $y_k = |y_k| \exp i\delta_k$. After accounting for rephasing freedom, we have two complex phases signifying CP violation which we shift into the Yukawa terms with H_u and H_d,

$$\begin{aligned}\mathcal{L}_{\text{anom}} \supset &- |y_L| \bar{L}'_R \Phi_2 L'_L - |y_E| \bar{E}'_L \Phi_2 E'_R - |y_1| e^{i\delta_{12}} \bar{L}'_L H_d E'_R - |y_2| e^{-i\delta_{12}} \bar{L}'_R H_d E'_L \\ &- |y_N| \bar{N}'_L \Phi_2 N'_R - |y_3| e^{i\delta_{34}} \bar{L}'_L H_u N'_R - |y_4| e^{-i\delta_{34}} \bar{L}'_R H_u N'_L + \text{h.c.} \,, \end{aligned} \tag{VII.12}$$

where the physical complex phases δ_{12} and δ_{34} are given by

$$\delta_{12} = \frac{\delta_1 - \delta_2 + \delta_L - \delta_E}{2} \,, \quad \delta_{34} = \frac{\delta_3 - \delta_4 + \delta_L - \delta_N}{2} \,. \tag{VII.13}$$

The induced mass parameters are

$$\begin{gathered} m_L = \frac{|y_L|}{\sqrt{2}} c_{\beta'} v' \,, \quad m_E = \frac{|y_E|}{\sqrt{2}} c_{\beta'} v' \,, \quad m_N = \frac{|y_N|}{\sqrt{2}} c_{\beta'} v' \,, \\ m_1 = \frac{|y_1|}{\sqrt{2}} c_{12} c_\beta v \,, \quad m_2 = \frac{|y_2|}{\sqrt{2}} c_{12} c_\beta v \,, \quad m_3 = \frac{|y_3|}{\sqrt{2}} c_{34} s_\beta v \,, \quad m_4 = \frac{|y_4|}{\sqrt{2}} c_{34} s_\beta v \,, \end{gathered} \tag{VII.14}$$

where $c_{12} \equiv \cos\delta_{12}$ and $c_{34} \equiv \cos\delta_{34}$ reflect the impact of the CP violating phases. We introduce the shorthand notation

$$m_{ij} \equiv \frac{m_i + m_j}{2} \,, \quad \Delta_{ij} \equiv \frac{m_i - m_j}{m_i + m_j} \,, \quad t_{ij} \equiv \tan\delta_{ij} \,, \tag{VII.15}$$

after which the mass mixing matrices become

$$\begin{aligned}\mathcal{L}_{\text{anom}} \supset &- \begin{pmatrix} \bar{e}'_L & \bar{E}'_L \end{pmatrix} \begin{pmatrix} m_L & m_{12}(1+\Delta_{12})(1+it_{12}) \\ m_{12}(1-\Delta_{12})(1-it_{12}) & m_E \end{pmatrix} \begin{pmatrix} e'_R \\ E'_R \end{pmatrix} \\ &- \begin{pmatrix} \bar{\nu}'_L & \bar{N}'_L \end{pmatrix} \begin{pmatrix} m_L & m_{34}(1+\Delta_{34})(1+it_{34}) \\ m_{34}(1-\Delta_{34})(1-it_{34}) & m_N \end{pmatrix} \begin{pmatrix} \nu'_R \\ N'_R \end{pmatrix} + \text{h.c.} \,. \end{aligned} \tag{VII.16}$$

For $v' \gg v$, the off-diagonal terms are at least suppressed by v/v_a. The Δ_{12} and Δ_{34} terms are also suppressed by the difference in the Yukawa couplings, which is generally negligible unless the couplings are hierarchical, and so we will assume $\Delta_{12} = \Delta_{34} = 0$ for the remainder of this work.

The CP violation is encoded via the tangent of the CP violating phases and will cause mixing between the axion a and the SM Higgs h. Since we are aligned in the Higgs basis, we will set $t_{12} = t_{34} = 0$ and leave a study of small deviations inducing mixing between a and h to future work.

After these simplifying assumptions, we can now rotate the symmetric mass matrices of the anomalons in equation (VII.16) using α_E and α_N mixing angles defined via

$$\begin{pmatrix} E_1 \\ E_2 \end{pmatrix} = \begin{pmatrix} \cos\alpha_E & \sin\alpha_E \\ -\sin\alpha_E & \cos\alpha_E \end{pmatrix} \begin{pmatrix} e' \\ E' \end{pmatrix} \,, \quad \begin{pmatrix} N_1 \\ N_2 \end{pmatrix} = \begin{pmatrix} \cos\alpha_N & \sin\alpha_N \\ -\sin\alpha_N & \cos\alpha_N \end{pmatrix} \begin{pmatrix} \nu' \\ N' \end{pmatrix} \,. \tag{VII.17}$$

The masses of E_1, E_2, N_1 and N_2 are given by

$$m_{E_{1,2}} = m_{LE} \left(1 \mp \sqrt{\Delta_{LE}^2 + \frac{m_{12}^2}{m_{LE}^2}} \right) \,, \quad m_{N_{1,2}} = m_{LN} \left(1 \mp \sqrt{\Delta_{LN}^2 + \frac{m_{34}^2}{m_{LN}^2}} \right) \,, \tag{VII.18}$$

using the shorthand notations in equation (VII.15).

We now evaluate the couplings of the axion field a and the SM Higgs field h to the anomalons. The couplings to the axion are at order $1/f_a$

$$\begin{aligned}\mathcal{L}_{\text{anom, } a} \supset\ & iX_2\frac{a}{f_a}\cos(2\alpha_E)(m_{E_1}\bar{E}_1\gamma_5 E_1 - m_{E_2}\bar{E}_2\gamma_5 E_2)\\ &+ iX_2\frac{a}{f_a}\sin(2\alpha_E)\frac{m_{E_1}+m_{E_2}}{2}(\bar{E}_1\gamma_5 E_2 + \bar{E}_2\gamma_5 E_1)\\ &+ iX_2\frac{a}{f_a}\cos(2\alpha_N)(m_{N_1}\bar{N}_1\gamma_5 N_1 - m_{N_2}\bar{N}_2\gamma_5 N_2)\\ &+ iX_2\frac{a}{f_a}\sin(2\alpha_N)\frac{m_{N_1}+m_{N_2}}{2}(\bar{N}_1\gamma_5 N_2 + \bar{N}_2\gamma_5 N_1)\\ &+ iX_d\frac{a}{f_a}\sin(2\alpha_E)\frac{m_{E_1}-m_{E_2}}{2}(\bar{E}_1 E_2 - \bar{E}_2 E_1)\\ &+ iX_u\frac{a}{f_a}\sin(2\alpha_N)\frac{m_{N_1}-m_{N_2}}{2}(\bar{N}_1 N_2 - \bar{N}_2 N_1)\ .\end{aligned} \tag{VII.19}$$

Here, we see that the terms proportional to X_2 are the canonical axial couplings proportional to fermion masses, while the remaining terms proportional to X_d or X_u scale as the difference of fermion masses and arise generically in flavor violating axion models, as we discussed in section V.1.

Separately, the interactions of the SM Higgs h to the anomalons are

$$\begin{aligned}\mathcal{L}_{\text{anom, } h} \supset\ & \sin(2\alpha_E)\frac{m_{E_1}-m_{E_2}}{2}\frac{h}{v}(\cos(2\alpha_E)(\bar{E}_1 E_2 + \bar{E}_2 E_1) - \sin(2\alpha_E)(\bar{E}_1 E_1 - \bar{E}_2 E_2))\\ &+ \sin(2\alpha_N)\frac{m_{N_1}-m_{N_2}}{2}\frac{h}{v}(\cos(2\alpha_N)(\bar{N}_1 N_2 + \bar{N}_2 N_1) - \sin(2\alpha_N)(\bar{N}_1 N_1 - \bar{N}_2 N_2))\ .\end{aligned} \tag{VII.20}$$

At dimension 5 we also get mixed operators

$$\begin{aligned}\mathcal{L}_{\text{anom, } a, h} \supset\ & iX_d\sin(2\alpha_E)\frac{m_{E_1}-m_{E_2}}{2}\frac{h}{v}\frac{a}{f_a}(\bar{E}_1 E_2 - \bar{E}_2 E_1)\\ &+ iX_u\sin(2\alpha_N)\frac{m_{N_1}-m_{N_2}}{2}\frac{h}{v}\frac{a}{f_a}(\bar{N}_1 N_2 - \bar{N}_2 N_1)\ .\end{aligned} \tag{VII.21}$$

The last two terms are due to the fact that the interactions of the axion proportional to X_u and X_d are induced by the Higgs doublets and are needed for a complete set of operators at order $1/f_a$. In the case with CP violation, the linear Higgs interactions would mix with the linear axion interactions proportional to X_u and X_d.

VII.1.3 Gauge Sector

Finally, we discuss the Z and Z' interactions, which necessarily includes the kinetic mixing effect in equation (VII.3). The effective kinetic mixing parameter ϵ_{eff} is determined by calculating the one-loop contribution to the two point interaction between the hypercharge gauge field B_μ and baryon number gauge field K_μ, giving

$$\mathcal{L} \supset \frac{\epsilon_{\text{eff}}}{2}B_{\mu\nu}K^{\mu\nu} + \frac{m_{\text{eff}}^2}{2}B_\mu K^\mu\ , \tag{VII.22}$$

where m_{eff} corresponds to a possible mass mixing. The mass mixing vanishes if all fermions in the loop are vector-like under one of the $U(1)$ gauge symmetries [227]. The divergence in

the two-point loop diagram is cancelled after imposing the trace condition on the mediator fermions,

$$\sum_f N_f (Y_V^f B_V^f + Y_A^f B_A^f) = 0 \ , \tag{VII.23}$$

where N_f denotes the multiplicity factor of fermion f. In the unbroken phase of electroweak symmetry, we can consider the SM fermions to be massless, such that the only remaining contribution comes from the anomalons. For m_L^2 , $m_E^2 \gg p^2$ the effective kinetic mixing parameter reads

$$\begin{aligned}\epsilon_{\text{eff}} &= \frac{g_Y g_B}{(4\pi)^2}\frac{4}{3}\sum_{f\in\{L',E',N'\}}(Y_V^f B_V^f + Y_A^f B_A^f)\left(\frac{5}{3}+\ln\left(\frac{m_f^2}{p^2}\right)+\mathcal{O}\left(\frac{p^2}{m_f^2}\right)\right)\\ &= -\frac{e g_B}{c_W}\frac{1}{(4\pi)^2}\frac{2}{3}\left(\frac{10}{3}+\ln\left(\frac{m_L^2}{p^2}\right)+\ln\left(\frac{m_E^2}{p^2}\right)+\mathcal{O}\left(\frac{p^2}{m_L^2, m_E^2}\right)\right) .\end{aligned} \tag{VII.24}$$

The large logarithms in ϵ_{eff} roughly cancel the loop factor such that the dominant parametric dependence is given by $\epsilon_{\text{eff}} \approx e g_B c_W^{-1}$. In the following we will see that we get new interactions proportional to ϵ_{eff}.

We recall from Ref. [230] that kinetic mixing is removed by shifting the gauge fields into a diagonal and canonically normalized basis, using the replacement rules

$$Z_\mu^{\text{SM}} = Z_\mu - \epsilon_{\text{eff}} s_W \frac{m_{Z'}^2}{m_{Z'}^2 - m_Z^2} Z'_\mu + \mathcal{O}\left(\epsilon_{\text{eff}}^2\right) \ , \tag{VII.25}$$

$$K_\mu = Z'_\mu - \epsilon_{\text{eff}} s_W \frac{m_Z^2}{m_Z^2 - m_{Z'}^2} Z_\mu + \mathcal{O}\left(\epsilon_{\text{eff}}^2\right) \tag{VII.26}$$

to shift to the mass basis. Assuming $m_K > m_{Z,\text{SM}}$, the corresponding masses are

$$m_Z = m_{Z,\text{SM}}\left(1 + \frac{\epsilon_{\text{eff}}^2}{2}\frac{s_W^2 m_{Z,\text{SM}}^2}{m_{Z,\text{SM}}^2 - m_K^2} + \mathcal{O}(\epsilon_{\text{eff}}^4)\right) , \tag{VII.27}$$

$$m_{Z'} = m_K\left(1 + \frac{\epsilon_{\text{eff}}^2}{2}\frac{(m_K^2 - c_W^2 m_{Z,\text{SM}}^2)}{m_K^2 - m_{Z,\text{SM}}^2} + \mathcal{O}(\epsilon_{\text{eff}}^4)\right) , \tag{VII.28}$$

with s_W, c_W being sine and cosine of the weak angle θ_W. We see that the mass correction only appears at order ϵ_{eff}^2 and is hence typically negligible.

We apply the shifts to the gauge bosons in equations (VII.25) and (VII.26) and obtain for the scalar Lagrangian

$$\begin{aligned}\mathcal{L}_{\text{scalar}}^{d\leq 4} \supset & \frac{1}{2}\partial_\mu h \partial^\mu h + \frac{1}{2}\partial_\mu H_0 \partial^\mu H_0 + \frac{1}{2}\partial_\mu h' \partial^\mu h' + \frac{1}{2}\partial_\mu H_0' \partial^\mu H_0' - V(h, H_0, h', H_0')\\ &+ \frac{1}{2}\partial_\mu a \partial^\mu a + \frac{1}{2}\partial_\mu A \partial^\mu A - \frac{m_A^2}{2}A^2 + \frac{1}{s_\gamma^2 c_\gamma^2}\frac{m_A^2}{v_a^2}\frac{A^4}{4!}\\ &+ \frac{1}{8}\frac{e^2}{s_W^2 c_W^2}\left((h+v)^2 + H_0^2\right)\left(Z_\mu - \epsilon_{\text{eff}} s_W \frac{m_{Z'}^2}{m_{Z'}^2 - m_Z^2} Z'_\mu\right)\left(Z^\mu - \epsilon_{\text{eff}} s_W \frac{m_{Z'}^2}{m_{Z'}^2 - m_Z^2} Z'^\mu\right)\\ &+ \frac{9}{2}g_B^2\left((h'+v')^2 + H_0'^2\right)\left(Z'_\mu - \epsilon_{\text{eff}} s_W \frac{m_Z^2}{m_Z^2 - m_{Z'}^2} Z_\mu\right)\left(Z'^\mu - \epsilon_{\text{eff}} s_W \frac{m_Z^2}{m_Z^2 - m_{Z'}^2} Z^\mu\right)\\ &- \frac{e}{s_W c_W} H_0 \left(Z_\mu - \epsilon_{\text{eff}} s_W \frac{m_{Z'}^2}{m_{Z'}^2 - m_Z^2} Z'_\mu\right)(s_\gamma \partial^\mu a + c_\gamma \partial^\mu A)\end{aligned}$$

$$+ 6 g_B H_0' \left(Z_\mu' - \epsilon_{\text{eff}} s_W \frac{m_Z^2}{m_Z^2 - m_{Z'}^2} Z_\mu \right) (c_\gamma \partial^\mu a - s_\gamma \partial^\mu A) + \mathcal{O}\left(\epsilon_{\text{eff}}^2\right) \ , \tag{VII.29}$$

where φ^0 is absorbed by Z_μ^{SM}, φ_B by K_μ, and A is the only angular mode which gets a mass from the term proportional to λ_A as defined in (VII.9).

Finally, we discuss the gauge interactions of the anomalons. Following Ref. [230], the interactions of the neutral gauge bosons are given at $\mathcal{O}(\epsilon_{\text{eff}})$ by[1].

$$\begin{aligned}\mathcal{L}_{\text{gauge}} \supset\ & e A_\mu J_Q^\mu + \frac{e}{\sqrt{2} s_W} (W_\mu^- J_W^{+\mu} + \text{h.c.}) + Z_\mu \left(\frac{e}{s_W c_W} J_Z^\mu - \epsilon_{\text{eff}} s_W g_B \frac{m_Z^2}{m_Z^2 - m_{Z'}^2} J_B^\mu \right) \\ & + Z_\mu' \left(g_B J_B^\mu + \epsilon_{\text{eff}} e J_Q^\mu - \epsilon_{\text{eff}} \frac{e}{c_W} \frac{m_{Z'}^2}{m_{Z'}^2 - m_Z^2} J_Z^\mu \right) \ ,\end{aligned} \tag{VII.30}$$

with the gauge currents given by

$$J_Q^\mu \supset - (\bar{E}_1 \gamma^\mu E_1 + \bar{E}_2 \gamma^\mu E_2) \ , \tag{VII.31}$$

$$J_W^{+\mu} \supset (c_E c_N \bar{E}_1 \gamma^\mu N_1 + c_E s_N \bar{E}_1 \gamma^\mu N_2 + s_E c_N \bar{E}_2 \gamma^\mu N_1 + s_E s_N \bar{E}_2 \gamma^\mu N_2) \ , \tag{VII.32}$$

$$\begin{aligned}J_Z^\mu \supset & \frac{1}{2} ((2 s_W^2 - c_E^2) \bar{E}_1 \gamma^\mu E_1 + (2 s_W^2 - s_E^2) \bar{E}_2 \gamma^\mu E_2 - s_E c_E (\bar{E}_1 \gamma^\mu E_2 + \bar{E}_2 \gamma^\mu E_1)) \\ & + \frac{1}{2} (c_N^2 \bar{N}_1 \gamma^\mu N_1 + s_N^2 \bar{N}_2 \gamma^\mu N_2 + s_N c_N (\bar{N}_1 \gamma^\mu N_2 + \bar{N}_2 \gamma^\mu N_1)) \ ,\end{aligned} \tag{VII.33}$$

$$\begin{aligned}J_B^\mu \supset & \frac{1}{2} (\bar{E}_1 \gamma^\mu E_1 + \bar{E}_2 \gamma^\mu E_2 + \bar{N}_1 \gamma^\mu N_1 + \bar{N}_2 \gamma^\mu N_2) \\ & + \frac{3}{2} (\cos(2\alpha_E) (\bar{E}_1 \gamma^\mu \gamma_5 E_1 - \bar{E}_2 \gamma^\mu \gamma_5 E_2) + \sin(2\alpha_E) (\bar{E}_1 \gamma^\mu \gamma_5 E_2 + \bar{E}_2 \gamma^\mu \gamma_5 E_1)) \\ & + \frac{3}{2} (\cos(2\alpha_N) (\bar{N}_1 \gamma^\mu \gamma_5 N_1 - \bar{N}_2 \gamma^\mu \gamma_5 N_2) + \sin(2\alpha_N) (\bar{N}_1 \gamma^\mu \gamma_5 N_2 + \bar{N}_2 \gamma^\mu \gamma_5 N_1)) \ .\end{aligned} \tag{VII.34}$$

There are two extreme cases: $\alpha_i \to 0$ corresponds to minimal mixing, while $\alpha_i \to \pi/4$ describes maximal mixing. In the minimal mixing case, we recover flavor-conserving axion and Z' couplings, while in the maximal mixing case, the axion, Z and Z' bosons all change the flavor of the anomalons. Another feature is given by the fact that the anomalons give rise to new contributions to the Higgs decay to two gauge bosons which are not excluded [232].

VII.2 Effective Theory and Wilson Coefficients

In order to study the phenomenology of our model at collider scales we describe the couplings of the axion in an ALP-EFT framework where we integrate out the heavy anomalons, while keeping the SM fermions dynamically. In addition, we need to deviate from the DFSZ axion band to higher masses, $m_a^2 f_a^2 \gg \Lambda_{\text{QCD}}^4$. This can be either achieved by enhancing χ for the QCD axion through non-QCD sources [1, 193, 194, 196] or by a free topological susceptibility in case of an ALP.

In both cases we assume that the QCD contribution is negligible, such that we can work in the ALP-EFT basis in which we do not use the axion digluon coupling for the axion mass generation and neglect QCD corrections to the axion diphoton coupling. The axion

[1] In contrast to Refs. [227, 231], our convention for g_B in this work uses $\mathcal{L} = \frac{1}{3} g_B Z_\mu' (\bar{q} \gamma^\mu q)$, and thus our g_B is half the value used in Refs. [227, 231].

Lagrangian consists of an effective contribution from integrating out the anomalons as well as an SM contribution and reads

$$\begin{aligned}\mathcal{L}_{\text{axion}} \supset &+ \frac{1}{2}(\partial_\mu a)(\partial^\mu a) - \frac{m_a^2}{2}a^2 + \frac{\partial_\mu a}{f_a}J^\mu_{\text{PQ,SM}} - C^{\text{eff}}_{Zh}\frac{v}{f_a}hZ_\mu\partial^\mu a - C^{\text{eff}}_{Z'h}\frac{v}{f_a}hZ'_\mu\partial^\mu a \\ &+ \left(C^{\text{SM}}_{\gamma\gamma} + C^{\text{eff}}_{\gamma\gamma}\right)\frac{e^2}{(4\pi)^2}\frac{a}{f_a}F_{\mu\nu}\tilde{F}^{\mu\nu} + \left(C^{\text{SM}}_{Z\gamma} + C^{\text{eff}}_{Z\gamma}\right)\frac{e^2}{s_W c_W}\frac{1}{(4\pi)^2}\frac{a}{f_a}Z_{\mu\nu}\tilde{F}^{\mu\nu} \\ &+ \left(C^{\text{SM}}_{ZZ} + C^{\text{eff}}_{ZZ}\right)\frac{e^2}{s_W^2 c_W^2}\frac{1}{(4\pi)^2}\frac{a}{f_a}Z_{\mu\nu}\tilde{Z}^{\mu\nu} + \left(C^{\text{SM}}_{Z'\gamma} + C^{\text{eff}}_{Z'\gamma}\right)\frac{g_B e}{(4\pi)^2}\frac{a}{f_a}Z'_{\mu\nu}\tilde{F}^{\mu\nu} \\ &+ \left(C^{\text{SM}}_{Z'Z'} + C^{\text{eff}}_{Z'Z'}\right)\frac{g_B^2}{(4\pi)^2}\frac{a}{f_a}Z'_{\mu\nu}\tilde{Z}'^{\mu\nu} + \left(C^{\text{SM}}_{Z'Z} + C^{\text{eff}}_{Z'Z}\right)\frac{g_B e}{s_W c_W}\frac{1}{(4\pi)^2}\frac{a}{f_a}Z'_{\mu\nu}\tilde{Z}^{\mu\nu} \\ &+ \left(C^{\text{SM}}_{WW} + C^{\text{eff}}_{WW}\right)\frac{g_L^2}{(4\pi)^2}\frac{a}{f_a}W_{\mu\nu}\tilde{W}^{\mu\nu} + C^{\text{SM}}_{gg}\frac{g_s^2}{(4\pi)^2}\frac{a}{f_a}G^a_{\mu\nu}\tilde{G}^{a\mu\nu} \\ &+ i\frac{a}{f_a}\frac{e}{\sqrt{2}s_W}(W^-_\mu(X_d J^{+\mu}_W - X_u J^{+\mu}_{W,l}) + \text{h.c.}) + \mathcal{O}\left(h', H_0, H_0', A, H^\pm\right) , \end{aligned} \tag{VII.35}$$

where we neglect contributions from other scalars, which we assume to be much heavier than the collider scale.

Under the use of our calculations of the Wilson coefficients in the heavy fermion limit in equations (V.16) and (V.21) we obtain

$$C^{\text{eff}}_{\gamma\gamma} = -\frac{8}{3}Xs^2_{\beta'}\frac{\Delta_E}{\Sigma_E^3}\cos(2\alpha_E)\frac{m_a^2}{f_a^2} + \mathcal{O}\left(\frac{1}{f_a^3}\right) , \tag{VII.36}$$

$$C^{\text{eff}}_{\gamma Z} = -\frac{Xs^2_{\beta'}}{4} , \quad C^{\text{eff}}_{ZZ} = -\frac{Xs^2_{\beta'}}{4}(1-2s_W^2) , \quad C^{\text{eff}}_{WW} = -\frac{Xs^2_{\beta'}}{2} , \tag{VII.37}$$

$$C^{\text{eff}}_{hZ'} = -\frac{Xs^2_{\beta'}}{2}(\Sigma_M^2 + \Delta_M^2)\left(1 - 6\frac{m_{Z'}^2(m_a^2 + m_h^2 - m_{Z'}^2)}{\lambda(m_{Z'}^2, m_a^2, m_h^2)}\right) , \tag{VII.38}$$

$$C^{\text{eff}}_{\gamma Z'} = -\frac{\epsilon_{\text{eff}}e}{g_B c_W}\frac{m_{Z'}^2}{m_{Z'}^2 - m_Z^2}C^{\text{eff}}_{\gamma Z} , \quad C^{\text{eff}}_{hZ} = -\frac{g_B\epsilon_{\text{eff}}s_W^2 c_W}{e}\frac{m_Z^2}{m_Z^2 - m_{Z'}^2}C^{\text{eff}}_{hZ'} , \tag{VII.39}$$

$$C^{\text{eff}}_{ZZ'} = -\frac{\epsilon_{\text{eff}}e}{g_B c_W}\frac{m_{Z'}^2}{m_{Z'}^2 - m_Z^2}C^{\text{eff}}_{ZZ} , \quad C^{\text{eff}}_{Z'Z'} = \left(-\frac{\epsilon_{\text{eff}}e}{g_B c_W}\frac{m_{Z'}^2}{m_{Z'}^2 - m_Z^2}\right)^2 C^{\text{eff}}_{ZZ} + \mathcal{O}\left(\epsilon^3_{\text{eff}}\right) , \tag{VII.40}$$

where we drop all terms of order $1/f_a$, ϵ^2_{eff}, Δ_E^2, Δ_N^2 and Δ_{EN}^2, if not mentioned otherwise.

The parameters Σ and Δ decribe mass sums and differences and are given by

$$\Sigma_M = \frac{m_{12} + m_{34}}{v} = \frac{1}{2}\left(\frac{|y_1| + |y_2|}{\sqrt{2}}c_{12}c_\beta + \frac{|y_3| + |y_4|}{\sqrt{2}}c_{34}s_\beta\right) \approx \frac{c_\beta + s_\beta}{\sqrt{2}} , \tag{VII.41}$$

$$\Delta_M = \frac{m_{12} - m_{34}}{v} = \frac{1}{2}\left(\frac{|y_1| + |y_2|}{\sqrt{2}}c_{12}c_\beta - \frac{|y_3| + |y_4|}{\sqrt{2}}c_{34}s_\beta\right) \approx \frac{c_\beta - s_\beta}{\sqrt{2}} , \tag{VII.42}$$

$$\Sigma_E = \frac{m_{E_1} + m_{E_2}}{f_a} = \frac{2m_{LE}}{f_a} = \frac{|y_L| + |y_E|}{\sqrt{2}}\frac{c_\gamma}{Xs_{\beta'}} \approx \frac{4\pi}{3}\frac{\sqrt{2}}{Xs_{\beta'}} , \tag{VII.43}$$

$$\Sigma_N = \frac{m_{N_1} + m_{N_2}}{f_a} = \frac{2m_{LN}}{f_a} = \frac{|y_L| + |y_N|}{\sqrt{2}}\frac{c_\gamma}{Xs_{\beta'}} \approx \frac{4\pi}{3}\frac{\sqrt{2}}{Xs_{\beta'}} , \tag{VII.44}$$

$$\Delta_E = \frac{m_{E_1} - m_{E_2}}{f_a} = -\frac{1}{\sin(2\alpha_E)}\frac{2m_{12}}{f_a} = -\frac{v}{f_a}\frac{\Sigma_M + \Delta_M}{\sin(2\alpha_E)} \approx -\frac{v}{f_a}\frac{\sqrt{2}c_\beta}{\sin(2\alpha_E)} , \tag{VII.45}$$

$$\Delta_N = \frac{m_{N_1} - m_{N_2}}{f_a} = -\frac{1}{\sin(2\alpha_N)}\frac{2m_{34}}{f_a} = -\frac{v}{f_a}\frac{\Sigma_M - \Delta_M}{\sin(2\alpha_N)} \approx -\frac{v}{f_a}\frac{\sqrt{2}s_\beta}{\sin(2\alpha_N)} , \tag{VII.46}$$

$$\Delta_{EN} = \Sigma_E - \Sigma_N = \frac{2m_{LE} - 2m_{LN}}{f_a} = \frac{|y_E| - |y_N|}{\sqrt{2}} \frac{c_\gamma}{X s_{\beta'}} \,. \tag{VII.47}$$

Here, we further assumed that the Yukawa couplings $|y_L|$, $|y_E|$ and $|y_N|$ are $4\pi/3$, while the other Yukawa couplings are of order 1. As it was motivated previously, we used the small angle approximation for the angles γ, δ_{12} and δ_{34}.

We highlight that the axion diphoton coupling is significantly suppressed due to the opposite sign in the flavor-conserving interactions of the charged anomalons. This is remarkable as it is in contrast to usual QCD axion models where the diphoton and digluon couplings are dominating. In fact, in our model the coefficients $C^{\text{eff}}_{\gamma Z}$, C^{eff}_{ZZ} and C^{eff}_{WW} become the most important axion gauge boson couplings for energies above $2m_t$ where the SM contributions to the axion couplings to photons and gluons decrease. We discuss this in more detail in section VII.3.

We also notice that the coupling of the axion to the Higgs and the SM Z boson is proportional to the effective kinetic mixing parameter ϵ_{eff}. This meets our expectations as in absence of kinetic mixing the orthogonality conditions from angular mixing forbid the respective term in the Lagrangian.

Lastly, we point out that the Z' mass as well as the anomalon masses implicitly depend on the axion decay constant f_a, since in the invisible axion limit, as described in subsection VII.1.1, f_a is mainly composed out of v' with $f_a = X c_\gamma^{-1} v' s_{\beta'} c_{\beta'}$. The mass relations of the Z' and the anomalons are then given by

$$m_{Z'} = 3 g_B v' = \frac{3 c_\gamma g_B f_a}{X s_{\beta'} c_{\beta'}} \,, \quad m_{\text{anom}} \equiv \frac{\Sigma_{E,N} \pm \Delta_{E,N}}{2} f_a \approx \frac{4\pi}{3} \frac{f_a}{X s_{\beta'} \sqrt{2}} \,. \tag{VII.48}$$

We find that in order to obtain a Z' mass which is lighter than the anomalons but allows for a sizable gauge coupling g_B we need to consider the limit $\beta' \to \pi/4$. Substituting the PQ charge normalization of the DFSZ model and taking the small angle approximation for γ then leads to $m_{Z'} \approx 36 g_B f_a$ and $m_{\text{anom}} \approx 8\pi f_a$.

Hence, we are left with two independent parameters for the QCD axion, g_B and f_a, and a third parameter χ for an ALP. We can trade χ or f_a to have a free axion mass m_a or analogously g_B or f_a to obtain a free Z' mass $m_{Z'}$. Having established the parameters in the EFT, we proceed in the next section discussing the phenomenological implications of our model.

VII.3 Phenomenology

We have seen in equation (VII.35) that the effective Lagrangian contains new exotic operators involving the axion, the Z' boson as well as heavy SM particles. These operators are of particular interest for collider experiments which cover energy scales in the GeV to TeV range.

In order to find constraints on our model parameter from collider experiments we investigate different production and decay channels and compare the results with existing narrow resonance searches at the LHC. The analysis includes the calculation of the branching ratios of the possible two-body decays as well as a simulation of the collider events using `MadGraph5_aMC@NLO` [10]. We provide an exemplary calculation of a narrow resonance cross section in section A in the appendix.

First, in subsection VII.3.1, we constrain the $\{m_{Z'}, g_B\}$ parameter space by looking at different Z' decays. Afterwards, we discuss in subsection VII.3.2 possible axion decays and present our results in the $\{m_a, G_{a\gamma\gamma}\}$-plane.

VII.3.1 Collider Constraints for the Z' Boson

The phenomenology of the Z' gauge boson is mainly determined by its mass $m_{Z'}$ and gauge coupling g_B. We can find constraints on these parameters from collider experiments by varying the mass in the accessible energy range while comparing the expected cross sections for a given gauge coupling with the actual experimental limits. We focus on narrow resonance searches, since we expect the total decay width of the Z' to be much smaller than its mass. In this narrow width approximation, the cross section is dictated by the branching ratios of the different Z' decays.

In order to find the most relevant production processes as well as interesting decay channels, we first determine partial two-body decay widths and set up the corresponding branching ratios. Since the quarks are the only particles in the SM which transform under $U(1)_B$, we expect the corresponding decay widths to be dominating,

$$\Gamma_{Z'\to\bar{q}q} = \frac{N_q^2 g_B^2 B_q^2 m_{Z'}}{12\pi}\sqrt{1-2\frac{m_q^2}{m_{Z'}^2}}\left(1+2\frac{m_q^2}{m_{Z'}^2}\right), \tag{VII.49}$$

where B_q denotes the baryon number of quark q, m_q its mass and N_q its multiplicity.

The coupling to other SM particles is only induced via kinetic mixing or integrating out the heavy anomalons. In case of SM leptons the tree-level coupling is mediated by the mixing of the Z' with the photon and the Z boson. Hence, the decay width to two leptons with mass m_l is controlled by the electric charge Q_l and the $SU(2)_L$ isospin charge $T_3^l = \pm 1/2$ associated to the third generator,

$$\begin{aligned}\Gamma_{Z'\to\bar{l}l} = &\frac{e^2\epsilon_{\text{eff}}^2 m_{Z'}}{12\pi c_W^2}\left(1-\frac{m_Z^2}{m_{Z'}^2}\right)^{-2}\left(\left(Q_l s_W^2\right)^2 - T_3^l Q_l s_W^2 + \frac{1}{2}\left(T_3^l\right)^2\right)\sqrt{1-2\frac{m_l^2}{m_{Z'}^2}}\\ &\times\left(1+2\frac{m_l^2}{m_{Z'}^2}\frac{(Q_l s_W^2)^2 - T_3^l Q_l s_w^2 - (T_3^l)^2/4}{(Q_l s_W^2)^2 - T_3^l Q_l s_w^2 + (T_3^l)^2/2}\right).\end{aligned} \tag{VII.50}$$

We notice, that $\Gamma_{Z'\to\bar{l}l}$ is suppressed by the square of the effective kinetic mixing parameter ϵ_{eff} and has a resonance at $m_{Z'} \approx m_Z$.

The Z' decay widths involving the axion can be derived from the effective operators in equation (VII.35), while for the Z' decays into gauge bosons we use the procedure presented in reference [232].

Especially the decay of the Z' into a photon and a Z boson can be calculated analogously to [232] by interchanging the role of the Z' and the Z,

$$\begin{aligned}\Gamma_{Z'\to\gamma Z} =&\frac{3}{2048\pi^5}\frac{e^4 g_B^2}{s_W^2 c_W^2}\frac{m_Z^2}{m_{Z'}}\left(1-\frac{m_Z^4}{m_{Z'}^4}\right)\\ &\Bigg|-\sum_q 2T_3^q Q_q B_q\left(\frac{m_{Z'}^2}{m_{Z'}^2-m_Z^2}\left(B_0(m_{Z'}^2,m_q,m_q)-B_0(m_Z^2,m_q,m_q)\right)\right.\\ &\qquad\left.+2m_q^2\frac{m_{Z'}^2}{m_Z^2}C_0(0,m_Z^2,m_{Z'}^2,m_q,m_q,m_q)\right)\\ &+\left(\frac{m_{Z'}^2}{m_{Z'}^2-m_Z^2}\left(B_0(m_{Z'}^2,m_{\text{anom}},m_{\text{anom}})-B_0(m_Z^2,m_{\text{anom}},m_{\text{anom}})\right)\right.\\ &\qquad\left.\left.+2m_{\text{anom}}^2 C_0(0,m_Z^2,m_{Z'}^2,m_{\text{anom}},m_{\text{anom}},m_{\text{anom}})\right)\right|^2,\end{aligned} \tag{VII.51}$$

where we neglect corrections of order $\mathcal{O}(\Delta_E^2,\ \Delta_N^2,\ \Delta_{EN}^2)$.

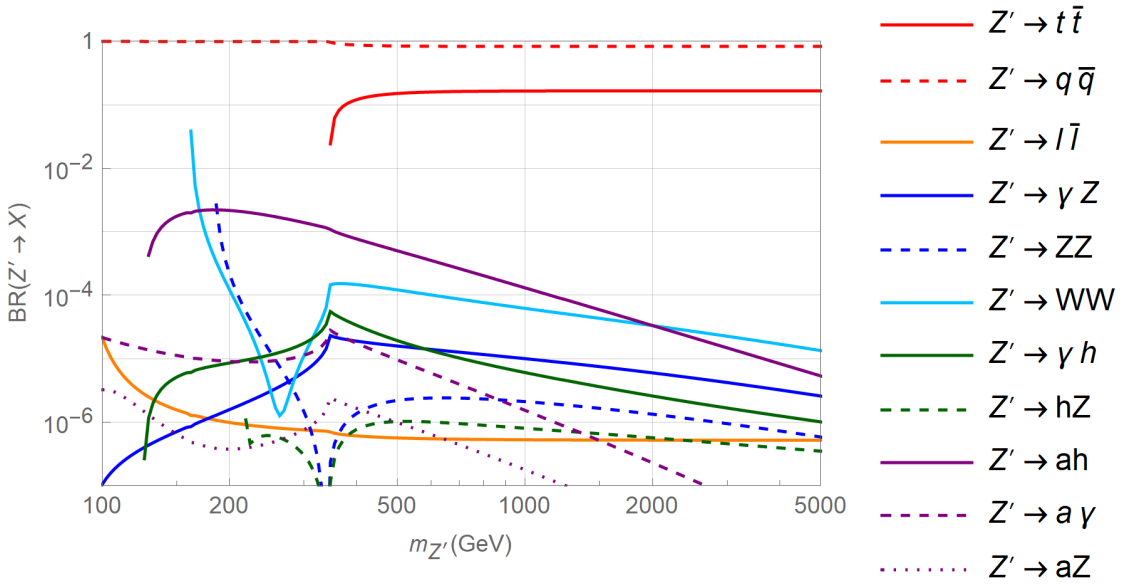

Figure VII.1: Branching ratios of two-body decays of the Z' gauge boson for $m_{Z'}$ between 100 GeV and 5 TeV. The ALP mass is fixed at $m_a = 1$ GeV and the gauge coupling at $g_B = 0.5$. The figure is taken from reference [2] and was created by the author.

In Figure VII.1 we show the branching ratios of two-body decays of the Z' for a varying $m_{Z'}$ between 100 GeV and 5 TeV, while keeping the gauge coupling fixed at $g_B = 0.5$. The axion mass is taken to be $m_a = 1$ GeV. We display the decay into two top quarks separately from the other quarks. We see that the most dominant decay is into two quarks as we expected, while the decay into leptons is heavily suppressed.

The exotic decays $Z' \to ah$, $Z' \to WW$, $Z' \to \gamma Z$ and $Z' \to \gamma h$ represent the most important sub-dominant contributions. The decay into axion and Higgs can only appear in a model construction like ours, with non-trivial mixing effects between the axion and the Z'. The decays into SM particles are tested by ATLAS and CMS and can therefore be used to constrain our parameter space.

For this purpose we simulate detector events in the respective decay channels using `MadGraph5_aMC@NLO` [10] and compare the results with the published LHC limits [233–235]. We then exclude regions in the parameter space which are not consistent with the experimental results.

We show the excluded regions in Figure VII.2, where we display for comparison the limits from dijet resonance searches [227]. We also include a limit on the charged anomalon masses, $m_{\text{anom}} < 90$ GeV from the ALEPH and L3 collaborations [236,237], which is linked to the Z' mass via their dependence on f_a as shown in equations (VII.18) and (VII.48).

While the $Z' \to h\gamma$ and $Z' \to WW$ channels can only probe unrealistically large gauge couplings of order $\mathcal{O}(10)$, the $Z' \to Z\gamma$ constraint competes with the dijet limit at low masses. The enhanced sensitivity in the $Z' \to Z\gamma$ channel reflects a better efficiency and a smaller background for signal photon and leptons. The limits get weaker with increasing Z' mass since the corresponding branching ratios in Figure VII.1 fall off for higher masses as the $Z' \to \bar{t}t$ channel opens up.

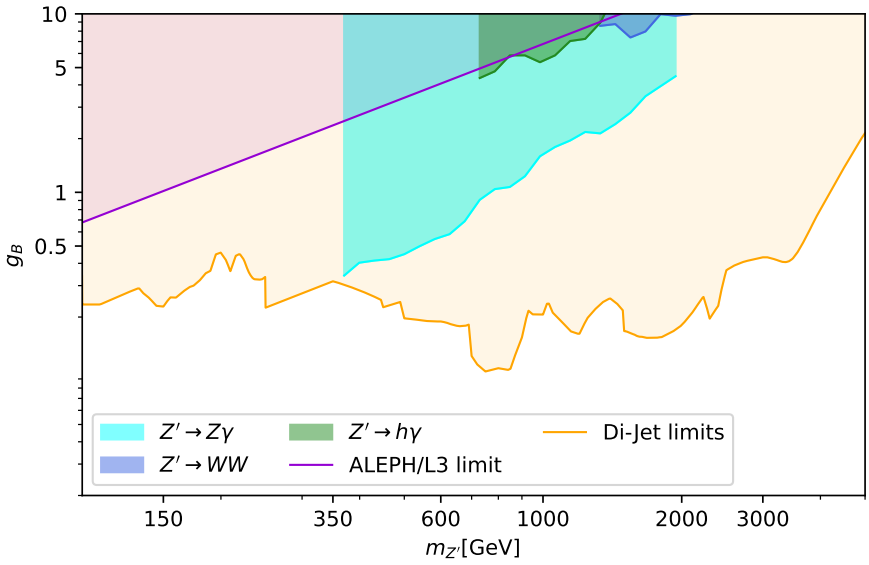

Figure VII.2: Excluded regions in the $\{m_{Z'}, g_B\}$ parameter space from narrow resonance searches in the $Z\gamma$ [233], $h\gamma$ [234] and WW [235] channels. Shown are also a limit on the anomalon masses, $m_{\text{anom}} < 90$ GeV excluded from searches by ALEPH and L3 collaborations [236, 237], as well as constraints from dijet resonance searches [227]. The figure is taken from reference [2].

VII.3.2 Collider Constraints for the Axion

In case of the axion phenomenology we are mainly interested in constraining the $\{m_a, f_a^{-1}\}$ parameter space, which provides information about the topological susceptibility χ and therefore the underlying axion or ALP model. In order to exclude parameter space based on existing collider searches we first compute the branching ratios of the axion two-body decays and simulate the cross section for different decay channels. We compare the cross sections with the experimental limits and present our results in the $\{m_a, G_{a\gamma\gamma}\}$-plane.

The branching ratios are dictated by the operators of the EFT basis defined in equation (VII.35) and are shown in Figure VII.3 for a varying axion mass. We set the axion decay constant to $f_a = 500$ GeV and the Z' mass to $m_{Z'} = 1$ TeV. Consequently, the gauge coupling g_B and the effective kinetic mixing parameter ϵ_{eff} are fixed as well. Again, we display the decay into two top quarks separately from the other quarks.

We see that for small axion masses the decays into SM fermions, gluons and photons are most dominant as it is true for most QCD axion models. In addition, the exotic $a \to hZ$ decay channel becomes enhanced near the top threshold providing approximately 10% of the total decay width. Since this decay is only induced through kinetic mixing effects, this channel serves as an exciting opportunity for discovery.

Above the top threshold the decays $a \to WW$, $a \to ZZ$ and $a \to \gamma Z$ become more important, since they are induced by integrating out the anomalons, while the axion diphoton and the axion digluon couplings cancel out at high energies. The $a \to hZ'$ decay mode is suppressed by the Z' mass and therefore does not play a big role. The corresponding branching ratio has a minimum at $m_a^2 = m_h^2 + 4m_{Z'}^2 + \sqrt{16m_h^2 m_{Z'}^2 + 9m_{Z'}^4}$ as the Wilson coefficient in equation (VII.38) changes sign at this point.

We make use of the branching ratios by simulating collider events in different decay

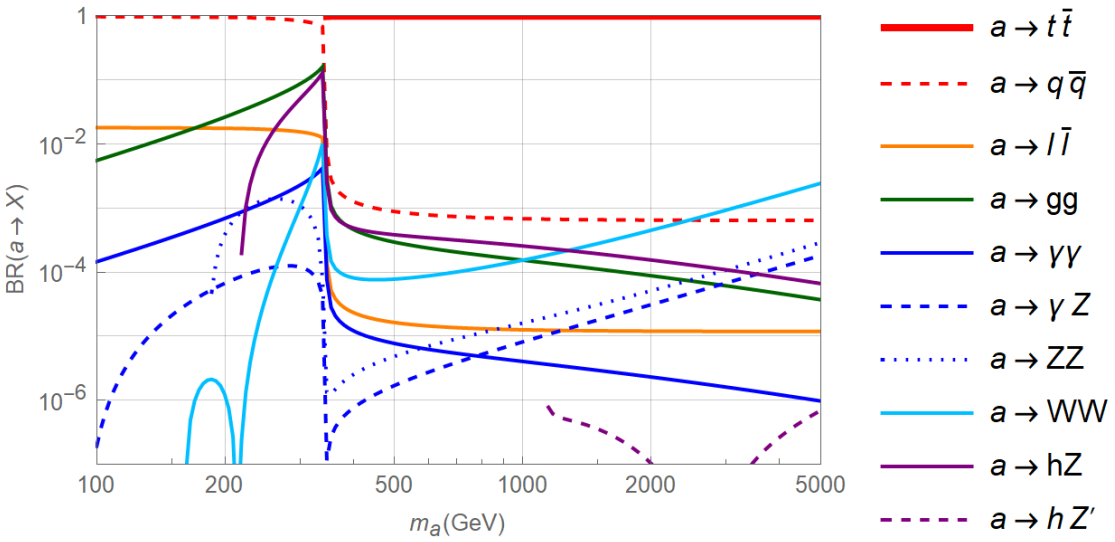

Figure VII.3: Branching ratios of two-body decays of the axion for m_a between 100 GeV and 5 TeV. The Z' mass is fixed at $m_{Z'} = 1$ TeV and the ALP decay constant at $f_a = 500$ GeV. The figure is taken from reference [2] and was created by the author.

channels using `MadGraph5_aMC@NLO` [10]. We then compare the result with the LHC limits published in references [233, 235, 238, 239]. Figure VII.4 shows the excluded regions in the $\{m_a, f_a^{-1}\}$ parameter space for which the simulated cross section is not consistent with the experimental limits.

In addition to the collider constraints we display the limit on charged anomalon masses, $m_{\text{anom}} < 90$ GeV from the ALEPH and L3 collaborations [236, 237] for the mixing angles $\beta = 0.05$ and $\beta' = \pi/4$. The anomalon masses directly depend on f_a as shown in equations (VII.18) and (VII.48). We also show two lines of constant $m_a f_a$ with $\chi = (10^2 \text{ GeV})^4$ and $\chi = (10^3 \text{ GeV})^4$.

We see that the diphoton channel gives the strongest constraints. This is reasonable, since the $\gamma\gamma$ resonance searches are more sensitive than the other channels and at the top threshold there is still a significant contribution to the axion diphoton coupling from SM particles. In contrast, the $\gamma\gamma$ constraints get weaker for higher axion masses as the effective contribution from anomalons cancels out.

Finally, we study the impact of our results on the $\{m_a, G_{a\gamma\gamma}\}$ parameter space. For this purpose we first express the axion diphoton coupling through

$$G_{a\gamma\gamma} = \sum_{f \in \text{SM}, E_{1,2}} \frac{2e^2}{\pi^2 f_a} N_f Q_f^2 X_A^f \frac{m_f^2}{m_a^2} \ln\left(\frac{2m_f^2 - m_a^2 + \sqrt{m_a^4 - 4m_a^2 m_f^2}}{2m_f^2}\right)^2 , \qquad \text{(VII.52)}$$

where the axial PQ charges $X_A^{E_{1,2}}$ of the charged anomalons are extracted from equation (VII.19). We disregard possible corrections from mass mixing with pions since we are interested in axions and ALPs with enhanced masses $m_a^2 f_a^2 \gg \Lambda_{\text{QCD}}^4$.

Figure VII.5 shows the $\{m_a, G_{a\gamma\gamma}\}$-plane for axion masses between $m_a = 10^{-2}$ GeV and $m_a = 10^6$ GeV. We convert our results from Figure VII.4 to the $G_{a\gamma\gamma}$ coupling and display for comparison the canonical limits extracted from reference [53]. In addition we show four lines of constant topological susceptibility. The dashed lines represent the model lines without threshold corrections through the quark masses.

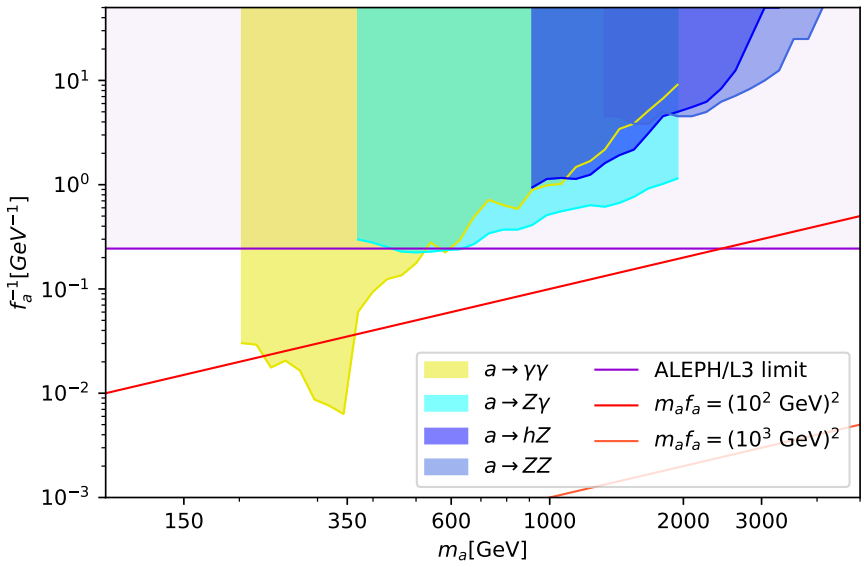

Figure VII.4: Excluded regions in the $\{m_a, f_a^{-1}\}$ parameter space from narrow resonance searches in the $\gamma\gamma$ [238], $Z\gamma$ [233], ZZ [235] and hZ [239] channels. Shown are also a limit on the anomalon masses, $m_{\text{anom}} < 90$ GeV excluded from searches by ALEPH and L3 collaborations [236, 237], as well as lines of different $m_a f_a$ relations. The figure is taken from reference [2].

The behavior of the model lines reflects the mass thresholds of the quarks and shows a smaller diphoton coupling at higher energies due to the cancellation effects in the anomalon induced couplings. We notice, that our limits from the diphoton resonance are stronger than the canonical bounds in this channel around the top threshold but weaker for higher axion masses. In fact, for our model the decay channels $a \to Z\gamma$, $a \to hZ$ and $a \to ZZ$ compete with the diphoton limits and become even more important for axion masses larger than 1 TeV.

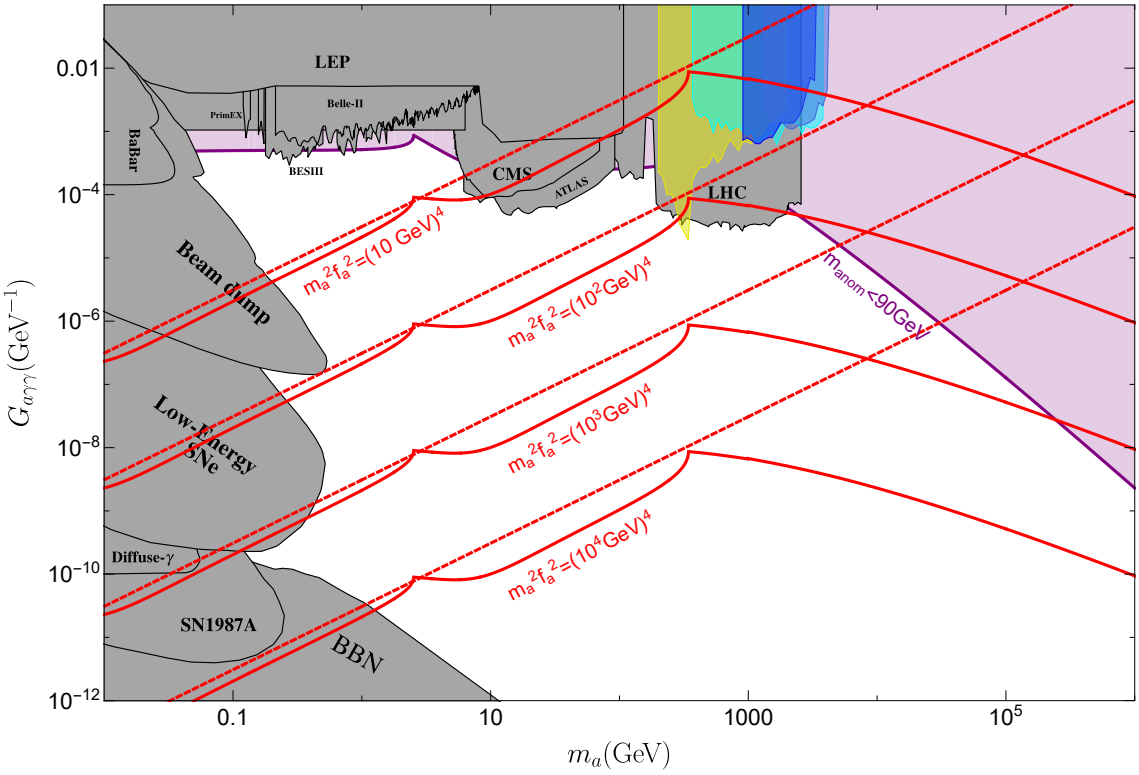

Figure VII.5: Implications of an additional $U(1)_B$ gauge symmetry in the $\{m_a, G_{a\gamma\gamma}\}$ parameter space for axion masses between $m_a = 10^{-2}$ GeV and $m_a = 10^6$ GeV. Displayed are four lines of constant topological susceptibility with $\chi \in \{(10\ \mathrm{GeV})^4, (10^2\ \mathrm{GeV})^4, (10^3\ \mathrm{GeV})^4, (10^4\ \mathrm{GeV})^4\}$, where the dashed lines represent the model without threshold corrections through quark masses. We extract the canonical constraints from reference [53] and overlay our limits from Figure VII.4.

Epilogue

CHAPTER VIII

Conclusion and Outlook

In this thesis we worked out various phenomenological implications in DFSZ axion models taking into account consequences from several observations and theoretical expectations which can not be described within the SM. Our goal was to identify effects that lead to a better accessibility of the DFSZ axion in experimental searches, including dedicated axion experiments like Haloscopes and Helioscopes as well as collider and DM experiments.

In the prologue we pointed out that the challenges in axion physics comprise an extensive possible mass range with a decrease in the coupling strength of axion-SM interactions for small axion masses. This decrease in the coupling strength is due to an inverse proportionality to the axion decay constant f_a in combination with a constant axion mass relation $m_a^2 f_a^2 = \Lambda_{\text{QCD}}^4$. We concluded that we can find deviations from the standard procedure either in the axion potential which fixes m_a or in the axion interactions themselves.

We started in part I by discussing possible modifications of the axion potential. For this purpose we introduced in Chapter III a general description of the angular scalar potential involving the pseudoscalar degrees of freedom of complex scalar fields. We pointed out three contributions to the angular potential. The first contribution originated from complex scalar fields with non-vanishing vevs in the scalar Lagrangian and led to a mixing between neutral Goldstone bosons of gauge symmetries and global Goldstone bosons like the axion.

Secondly, the angular potential consisted of terms that were induced by a fermionic condensate. In general, the fermion condensate entered through the Yukawa interactions with the complex scalar fields. The third contribution was induced by fermion condensates that are generated by the confinement of an $SU(N)$ gauge symmetry. Here, we used instanton calculus to find corrections in the potential. It turned out that in the standard axion case the correction was of order $\mathcal{O}(1\%)$ and therefore negligible.

We then used the results from Chapter III in Chapter IV to find a procedure in which additional PQ-breaking operators led to a branch-off point in the $\{m_a, G_{a\gamma\gamma}\}$-plane at which the axion decay constant saturated at a model dependent value f_{max}. This value not only provided an estimate of the maximal extent of the expected $G_{a\gamma\gamma}$ line in presence of an additional PQ-breaking operator, but also allowed for much lighter axion masses with $m_a^2 f_a^2 \ll \Lambda_{\text{QCD}}^4$. This corresponds to an enhancement in the axion-diphoton coupling for small axion masses, reaching for 10^7 GeV $\lesssim f_{\text{max}} \lesssim 10^{11}$ GeV the preferred region of Haloscope and Helioscope searches.

Following the procedure from the previous chapter, we were able to identify several constructions which naturally provide f_{max} in our range of interest. On the other hand, in order to achieve a sizable deviation from the canonical DFSZ line, we needed a CP

violating parameter $\bar{\theta} \approx \pi$ in the UV to not generate a residual CP phase $\bar{\theta}_{\text{eff}}$ that was in conflict with current nEDM measurements. We solved this problem with a Nelson-Barr-like UV completion, leading to a deviation of $m_a^2 f_a^2 \gtrsim 10^{-6}\Lambda_{\text{QCD}}^4$ in presence of Planck mass suppressed operators.

In part II we discussed modifications of the axion couplings using an EFT approach. For this purpose we constructed in Chapter V a general ALP-EFT basis accounting for anomalous fermion transformations and flavor changing effects. We identified operators which do not appear in the flavor-conserving limit, including a five-dimensional commutator interaction between the axion, two fermions, and a gauge boson. Subsequently, we calculated the Wilson coefficients of effective three-point interactions, where we integrate out heavy fermions and scalars. We presented our results for axion couplings to two gauge boson, one gauge boson and one scalar, and two fermions.

The effective axion-fermion vertices played a role in Chapter VI in the context of chiral enhancement. Here, we compared the tree-level axion-fermion coupling to the one-loop contribution from integrating out a heavy DM scalar S and a heavy fermion F. We observed that the effective one-loop contribution led to an enhancement in the total axion-fermion interaction proportional to the Yukawa couplings between S, F and SM fermions. We constrained these couplings using collider limits on flavor-violating axion interactions and DM bounds on the scalar S.

We found out that the flavor limits led to a large hierarchy between the individual Yukawa couplings, allowing for only one sizable y_S^i at a time. Furthermore, after applying limits on m_S from DM relic abundance and DM direct detection, we concluded that chiral enhancement of order $\mathcal{O}(10-100)$ appears preferably for heavy up-type quarks as well as for charged leptons. In addition, we noticed that any non-zero chiral enhancement implied a lower limit of m_S as a result of an overlap between the two DM limits.

Afterwards, we briefly discussed possible enhancement factors in models with neutrino masses. In general, heavy right-handed neutrinos are predestined candidates for generating chiral enhancement, since they have a large coupling to the axion and a chiral coupling to leptons through a W interaction. However, this W interaction is suppressed by the light-neutrino mass, since W bosons only couple to right-handed neutrinos through their mixing with their left-handed counterparts. This leads to a large suppression in the chiral enhancement of order v/f_a.

Finally, we studied in Chapter VII new effects in axion models with an additional $U(1)_B$ gauge symmetry. The model contained a new gauge boson Z' and heavy fermionic anomalon fields to cancel gauge anomalies. After integrating out the anomalons and accounting for kinetic mixing effects between the gauge bosons, we obtained new exotic operators involving the axion, the Z' boson and heavy SM fields. In particular, kinetic mixing effects induced a three-point interaction between axion, Higgs and Z boson which provides up to $\mathcal{O}(10\%)$ of the total axion decay width but vanishes in canonical axion models.

Another peculiarity of our model were cancellation effects in the effective axion-diphoton coupling from integrating out the anomalons. We simulated collider events in different axion and Z' channels and compared our results with narrow resonance searches at the LHC. We found out that due to the suppression in the axion-diphoton coupling, the decay channels $a \to Z\gamma$, $a \to hZ$ and $a \to ZZ$ provided the strongest bounds in the $\{m_a, f_a^{-1}\}$ parameter space for axion masses above 1 TeV.

In summary, we discovered new ways to search for DFSZ axions that are accessible for experiments in the near future but lie outside of the canonical expectation range. On one hand, we obtained enhancement effects in the axion-diphoton and axion-fermion

couplings which generically arose from the interplay of the DFSZ axion model with Planck-mass suppressed operators and heavy DM particles. On the other hand, we found new operators describing axion interactions with heavy SM particles and additional fields from other BSM theories such as right-handed neutrinos, DM scalars or Z' gauge bosons.

In this thesis, we were able to answer the question of whether generic BSM features modify the DFSZ axion solution to the strong CP problem towards a better accessibility in experiments. Nevertheless, there are still open problems that are inspirational for future research. One remaining question is whether we can reach arbitrarily small axion masses from PQ-breaking effects which do not interfere with radiative corrections and Planck-suppressed operators. Secondly, chiral enhancement effects could only affect individual axion-fermion couplings with a preference for charged leptons and heavy up-type quarks. Here, we can ask the question of finding a different description which also allows for multiple enhanced interactions at the same time including also light quarks and neutrinos. Finally, we found new interactions between the axion and the Higgs boson, which can be even better constrained at future colliders and therefore motivate more extensive studies at collider experiments.

Appendix

A Decay Widths and Cross Sections

In this section we want to recap the procedure of calculating decay widths and cross section to estimate observables for collider searches. This summary was prepared by the author for a previous work and is mainly based on the textbooks [240, 241]. We start with the decay width of the axion/ALP or analogously for a gauge boson which can be calculated by

$$\Gamma(\mathcal{A} \to \mathcal{F}) = \frac{1}{2m_{\mathcal{A}}} \int d\Pi_{\mathcal{F}} |\mathcal{M}_{\mathcal{A}\to\mathcal{F}}|^2, \tag{IX.1}$$

where $\mathcal{A}$ stands for the decaying particle and $\mathcal{F}$ for the final state. Here, the Lorentz-invariant phase space element is given by

$$d\Pi_{\mathcal{F}} = \prod_{j\in\mathcal{F}} \frac{d^3p_j}{(2\pi)^3} \frac{1}{2E_j} \delta^4(p_{\mathcal{A}} - \sum_{j\in\mathcal{F}} p_j). \tag{IX.2}$$

For a two-particle final state this Lorentz-invariant phase space becomes

$$\int d\Pi_2 = \int \frac{d\Omega_{\text{CM}}}{4\pi} \frac{1}{8\pi} \frac{2|\vec{p}|}{E_{\text{CM}}}, \tag{IX.3}$$

where $|\vec{p}|$ is the absolute value of the three-momenta of the outgoing particles $\mathcal{B}$ and $\mathcal{C}$ in the center-of-mass frame (CM) of the initial particles. Since there is only one decaying particle, the center-of-mass energy is given by $E_{\text{CM}} = m_{\mathcal{A}}$. For all external particles being on-shell ($p_{\mathcal{A}}^2 = m_{\mathcal{A}}^2$, $p_{\mathcal{B}}^2 = m_{\mathcal{B}}^2$, $p_{\mathcal{C}}^2 = m_{\mathcal{C}}^2$), $|\vec{p}|$ can be calculated by

$$m_{\mathcal{A}} = E_{\text{CM}} = E_{\mathcal{B}} + E_{\mathcal{C}} = \sqrt{|\vec{p}|^2 + m_{\mathcal{B}}^2} + \sqrt{|\vec{p}|^2 + m_{\mathcal{C}}^2} \tag{IX.4}$$

$$\Leftrightarrow |\vec{p}| = \frac{\sqrt{\lambda(m_{\mathcal{A}}^2, m_{\mathcal{B}}^2, m_{\mathcal{C}}^2)}}{2m_{\mathcal{A}}}. \tag{IX.5}$$

Hence, the Lorentz-invariant phase space becomes

$$\int d\Pi_2 = \frac{1}{8\pi} \frac{\sqrt{\lambda(m_{\mathcal{A}}^2, m_{\mathcal{B}}^2, m_{\mathcal{C}}^2)}}{m_{\mathcal{A}}^2} \int \frac{d\Omega_{\text{CM}}}{4\pi} = \frac{1}{8\pi} \frac{\sqrt{\lambda(m_{\mathcal{A}}^2, m_{\mathcal{B}}^2, m_{\mathcal{C}}^2)}}{m_{\mathcal{A}}^2}. \tag{IX.6}$$

Next, we calculate the squared matrix element which is defined by

$$|\mathcal{M}_{\mathcal{A}\to\mathcal{F}}|^2 = \frac{1}{d_{\mathcal{A}}} \sum_{\text{pol.}} \mathcal{M}_{\mathcal{A}\to\mathcal{F}} \mathcal{M}^*_{\mathcal{A}\to\mathcal{F}}, \tag{IX.7}$$

with $d_{\mathcal{A}}$ being the number of degrees of freedom for the incoming particle. Furthermore, the sum going over all polarizations of the external gauge bosons. Inserting the effective couplings $c_{\text{eff}} \equiv C_{12}^{\text{eff}} g_1 g_2 (4\pi)^2$ from subsection V.2.1 gives with $d_a = 1$

$$\begin{aligned} |\mathcal{M}_{a\to A_1A_2}|^2 &= \sum_{\text{pol.}} \left(2\frac{c_{\text{eff}}}{f_a}\epsilon^{\mu\nu\alpha\beta} p_{1\alpha} p_{2\beta} \epsilon^*_{1\mu} \epsilon^*_{2\nu}\right)\left(2\frac{c_{\text{eff}}}{f_a}\epsilon^{\rho\sigma\gamma\delta} p_{1\gamma} p_{2\delta} \epsilon_{1\rho} \epsilon_{2\sigma}\right) \\ &= 4\frac{c_{\text{eff}}^2}{f_a^2}\epsilon^{\mu\nu\alpha\beta}\epsilon^{\rho\sigma\gamma\delta} p_{1\alpha} p_{2\beta} p_{1\gamma} p_{2\delta} \left(\sum_{\text{pol.}} \epsilon^*_{1\mu}\epsilon_{1\rho}\right)\left(\sum_{\text{pol.}} \epsilon^*_{2\nu}\epsilon_{2\sigma}\right). \end{aligned} \tag{IX.8}$$

The polarization sum yields for massless gauge bosons

$$\sum_{\text{pol.}} \epsilon^*_\mu \epsilon_\nu = -g_{\mu\nu} \tag{IX.9}$$

and for massive gauge bosons

$$\sum_{\text{pol.}} \epsilon^*_\mu \epsilon_\nu = -g_{\mu\nu} + \frac{p_\mu p_\nu}{m^2}. \tag{IX.10}$$

Since there are ϵ-tensors in the matrix element, the additional term in equation (IX.10) vanishes and equation (IX.9) holds true for all gauge bosons. Therefore, the squared matrix element becomes under the use of `Package X` [8]

$$\begin{aligned} |\mathcal{M}_{a\to A_1A_2}|^2 &= 4\frac{c_{\text{eff}}^2(p^2,p_1^2,p_2^2)}{f_a^2}\epsilon^{\mu\nu\alpha\beta}\epsilon^{\rho\sigma\gamma\delta} p_{1\alpha} p_{2\beta} p_{1\gamma} p_{2\delta} (-g_{\mu\rho})(-g_{\nu\sigma}) \\ &= 2\frac{c_{\text{eff}}^2(p^2,p_1^2,p_2^2)}{f_a^2}\lambda(p^2,p_1^2,p_2^2). \end{aligned} \tag{IX.11}$$

Having gauge bosons in the initial state changes the result only by factors of d_1 and d_2, since $C_0(p^2,p_1^2,p_2^2,m_f^2,m_f^2,m_f^2)$ is symmetric under interchanging p^2, p_1^2 and p_2^2 and, therefore, $c_{\text{eff}}(p^2,p_1^2,p_2^2)$ is also symmetric. This is true as well for $\lambda(p^2,p_1^2,p_2^2)$. Hence, the general expression for the triangle diagram with one external axion/ALP and two external gauge bosons is

$$|\mathcal{M}_{\mathcal{A}\to\mathcal{BC}}|^2 = \frac{2}{d_{\mathcal{A}}}\frac{c_{\text{eff}}^2(p_{\mathcal{A}}^2,p_{\mathcal{B}}^2,p_{\mathcal{C}}^2)}{\mu^2}\lambda(p_{\mathcal{A}}^2,p_{\mathcal{B}}^2,p_{\mathcal{C}}^2). \tag{IX.12}$$

Inserting the previous expressions into the decay width (IX.1) and using the on-shell condition ($p_{\mathcal{A}}^2 = m_{\mathcal{A}}^2$, $p_{\mathcal{B}}^2 = m_{\mathcal{B}}^2$, $p_{\mathcal{C}}^2 = m_{\mathcal{C}}^2$) leads to

$$\begin{aligned} \Gamma(\mathcal{A}\to\mathcal{BC}) &= \frac{1}{2m_{\mathcal{A}}}\int d\Pi_2 |\mathcal{M}_{\mathcal{A}\to\mathcal{BC}}|^2 = \frac{1}{2m_{\mathcal{A}}}|\mathcal{M}_{\mathcal{A}\to\mathcal{BC}}|^2 \int d\Pi_2 \\ &= \frac{1}{2m_{\mathcal{A}}}\frac{2}{d_{\mathcal{A}}}\frac{c_{\text{eff}}^2(m_{\mathcal{A}}^2,m_{\mathcal{B}}^2,m_{\mathcal{C}}^2)}{\mu^2}\lambda(m_{\mathcal{A}}^2,m_{\mathcal{B}}^2,m_{\mathcal{C}}^2)\frac{1}{8\pi}\frac{\sqrt{\lambda(m_{\mathcal{A}}^2,m_{\mathcal{B}}^2,m_{\mathcal{C}}^2)}}{m_{\mathcal{A}}^2} \\ &= \frac{c_{\text{eff}}^2(m_{\mathcal{A}}^2,m_{\mathcal{B}}^2,m_{\mathcal{C}}^2)}{d_{\mathcal{A}}8\pi\mu^2 m_{\mathcal{A}}^3}(\lambda(m_{\mathcal{A}}^2,m_{\mathcal{B}}^2,m_{\mathcal{C}}^2))^{3/2} \end{aligned} \tag{IX.13}$$

for the triangle coupling.

A.1 Production Cross Section for Axions/ALPs

In order to get predictions for hadron colliders like the LHC, the production cross section for an axion/ALP has to be evaluated. Since for high energies the parton distribution function (PDF) of the gluon gives the largest contribution in proton-proton collision, the partonic cross section for two gluons in the initial state has to be calculated. The full process would be $gg \to a \to A_1 A_2$. This is displayed in Figure IX.1.

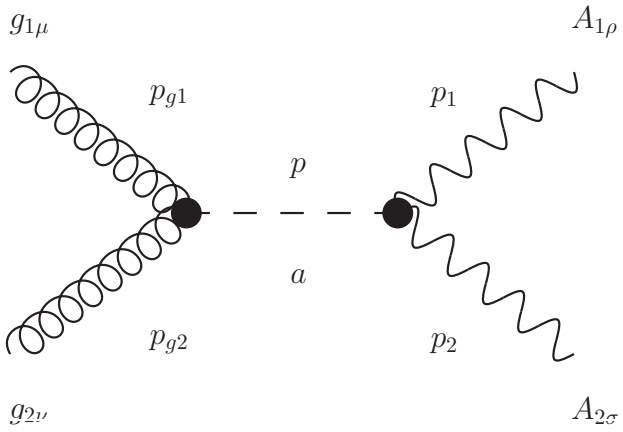

Figure IX.1: Feynman diagram for the s-channel cross section of two incoming gluons g_1 and g_2 with momenta p_{g1} and p_{g2} and two outgoing gauge bosons A_1 and A_2 with momenta p_1 and p_2. Inbetween an axion/ALP a with momentum p is produced. The vertices are the effective couplings from section V.2.

The axion/ALP can be treated as an unstable particle with the total decay width being much smaller than its real pole mass $\Gamma_{\text{tot}} \ll m_P$. These assumptions lead to an imaginary part in the propagator

$$iG(p^2) = \frac{i}{p^2 - m_P^2 + i m_P \Gamma_{\text{tot}}}. \tag{IX.14}$$

In the squared matrix element this gives a Breit-Wigner distribution, which can be approximated for $\Gamma_{\text{tot}} \ll m_P$ by the so-called narrow-width approximation

$$\left| \frac{i}{p^2 - m_P^2 + i m_P \Gamma_{\text{tot}}} \right|^2 = \frac{1}{(p^2 - m_P^2)^2 + (m_P \Gamma_{\text{tot}})^2} \approx \frac{\pi}{m_P \Gamma_{\text{tot}}} \delta(p^2 - m_P^2). \tag{IX.15}$$

The matrix element for the process in Figure IX.1 is

$$i\mathcal{M}_{gg \to A_1 A_2} = i\mathcal{M}_{gg \to a} \frac{i}{p^2 - m_a^2 + i m_a \Gamma_{\text{tot}}} i\mathcal{M}_{a \to A_1 A_2} \tag{IX.16}$$

and, therefore, the squared matrix element gives

$$|\mathcal{M}_{gg \to A_1 A_2}|^2 \approx |\mathcal{M}_{gg \to a}|^2 \frac{\pi}{m_a \Gamma_{\text{tot}}} \delta(p^2 - m_a^2) |\mathcal{M}_{a \to A_1 A_2}|^2. \tag{IX.17}$$

Similar to the decay width, the cross section of a process $\mathcal{AB} \to \mathcal{F}$ with $\mathcal{A}$,$\mathcal{B}$ being the initial particles and $\mathcal{F}$ being the final state is defined by

$$\sigma(\mathcal{AB} \to \mathcal{F}) = \frac{1}{2E_\mathcal{A} 2E_\mathcal{B} |\vec{v}_\mathcal{A} - \vec{v}_\mathcal{B}|} \int d\Pi_\mathcal{F} |\mathcal{M}_{\mathcal{AB} \to \mathcal{F}}|^2, \tag{IX.18}$$

with $\vec{v} \equiv \vec{p}/E$. Hence, the partonic cross section for $gg \to a \to A_1 A_2$ is given by

$$\hat{\sigma}(gg \to A_1 A_2) \approx \frac{1}{2E_{g_1} 2E_{g_2} |\vec{v}_{g_1} - \vec{v}_{g_2}|} \int d\Pi_2 |\mathcal{M}_{gg\to a}|^2 \frac{\pi}{m_a \Gamma_{\text{tot}}} \delta(p^2 - m_a^2) |\mathcal{M}_{a \to A_1 A_2}|^2. \tag{IX.19}$$

The external gluons/gauge bosons are on-shell, while the internal axion/ALP can be taken to be on-shell as well due to the δ-function. With this,

$$p_{g_1}^2 = p_{g_2}^2 = 0, \quad p^2 = m_a^2, \quad p_1^2 = m_1^2, \quad p_2^2 = m_2^2, \tag{IX.20}$$

the squared matrix elements do not depend on the momenta anymore and the partonic cross section can be re-expressed using equation (IX.13) by

$$\begin{aligned} \hat{\sigma}(gg \to A_1 A_2) &\approx \frac{1}{2E_{g_1} 2E_{g_2} |\vec{v}_{g_1} - \vec{v}_{g_2}|} |\mathcal{M}_{gg\to a}|^2 2\pi \delta(p^2 - m_a^2) \frac{\Gamma(a \to A_1 A_2)}{\Gamma_{\text{tot}}} \\ &:= \hat{\sigma}(gg \to a) BR(a \to A_1 A_2), \end{aligned} \tag{IX.21}$$

where the branching ratio of the decay $a \to A_1 A_2$ is defined by

$$BR(a \to A_1 A_2) = \frac{\Gamma(a \to A_1 A_2)}{\Gamma_{\text{tot}}}. \tag{IX.22}$$

The squared matrix elements of $gg \to a$ and $a \to gg$ are related in the following way

$$|\mathcal{M}_{gg\to a}|^2 = \frac{1}{d_g^2} |\mathcal{M}_{a\to gg}|^2 = \frac{1}{16^2} 2m_a 8\pi \frac{m_a^2}{\sqrt{\lambda(m_a^2, 0, 0)}} \Gamma(a \to gg) = \frac{\pi m_a}{16} \Gamma(a \to gg) \tag{IX.23}$$

with $d_g = 2(N_C^2 - 1) = 2(3^2 - 1) = 16$ for $N_C = 3$ colors. Thus, the partonic production cross section for an axion/ALP is given by

$$\hat{\sigma}(gg \to a) = \frac{\pi^2 m_a \Gamma(a \to gg)}{32 E_{g_1} E_{g_2} |\vec{v}_{g_1} - \vec{v}_{g_2}|} \delta(\hat{s} - m_a^2) \tag{IX.24}$$

$$\approx \frac{\pi BR(a \to gg)}{32 E_{g_1} E_{g_2} |\vec{v}_{g_1} - \vec{v}_{g_2}|} \frac{(m_a \Gamma_{\text{tot}})^2}{(\hat{s} - m_a^2)^2 + (m_a \Gamma_{\text{tot}})^2} \tag{IX.25}$$

and, therefore, the total production cross section for a proton-proton collision is

$$\sigma(pp \to a) = \int_0^1 dx_1 \int_0^1 dx_2 f_g(x_1) f_g(x_2) \hat{\sigma}(gg \to a), \tag{IX.26}$$

with $f_g(x)$ being the parton distribution function for the gluons. x denotes the Bjorken variable and gives the fraction of the proton momentum P, which contributes in the cross section via the gluons $p_g = xP$. For the center-of-mass energy being much larger than the proton mass $\sqrt{s} \gg m_p$, the partonic squared center-of-mass energy is given by

$$\hat{s} = (x_1 P_1 + x_2 P_2)^2 = x_1^2 m_p^2 + x_2^2 m_p^2 + x_1 x_2 (s - 2m_p^2) \approx x_1 x_2 s. \tag{IX.27}$$

In the center-of-mass frame of the protons ($P_1 = (E, \vec{p})$ and $P_2 = (E, -\vec{p})$), the denominator in equation (IX.24) simplifies to

$$E_{g_1} E_{g_2} |\vec{v}_{g_1} - \vec{v}_{g_2}| = x_1 x_2 E^2 \left| \frac{2\vec{p}}{E} \right| \approx x_1 x_2 2E^2 = x_1 x_2 \frac{s}{2}. \tag{IX.28}$$

Hence, the partonic cross section becomes

$$\hat{\sigma}(gg \to a) = \frac{\pi BR(a \to gg)}{16 x_1 x_2 s} \frac{(m_a \Gamma_{\text{tot}})^2}{(x_1 x_2 s - m_a^2)^2 + (m_a \Gamma_{\text{tot}})^2}. \tag{IX.29}$$

Finally, we remark that the calculation for the Z' works analogously by interchanging the scalar propagator by a vector propagator.

List of Figures

Appendix

List of Tables

List of Abbreviations

ΛCDM	Standard Model of cosmology
ALP	axion-like particle
BBN	BigBang Nucleosynthesis
BR	branching ratio
BSM	beyond the Standard Model
C	charge conjugation
CDM	cold dark matter
CKM	Cabibbo-Kobayashi-Maskawa matrix
CMB	cosmic microwave background
DFSZ	Dine-Fischler-Srednicki-Zhitnitsky
DM	dark matter
EDM	electric dipole moment
EFT	effective field theory
EWSB	electroweak symmetry breaking
GR	general relativity
KSVZ	Kim-Shifman-Vainshtein-Zakharov
P	parity inversion
PDF	parton distribution function
PMNS	Pontecorvo–Maki–Nakagawa–Sakata matrix
PQ	Peccei-Quinn
QCD	quantum chromodynamics
QED	quantum electrodynamics
QFT	quantum field theory
SCPV	spontaneous CP violation
SM	Standard Model of particle physics
SSI	small size instantons
UV	ultraviolet
vev	vacuum expectation value
WIMP	weakly interacting massive particles

List of Experiments

CERN - Conseil europeén pour la recherche nucléaire

LHC - Large Hadron Collider since 2010

- ATLAS - A Toroidal LHC Apparatus
- CMS - Compact Muon Solenoid

LEP - Large Electron-Positron Collider 1989 - 2000

- ALEPH - Apparatus for LEP Physics
- L3 - Third LEP Experiment

Axion Experiments

Haloscopes

- ADMX - Axion Dark Matter Experiment
- ABRACADABRA - A Broadband/Resonant Approach to Cosmic Axion Detection with an Amplifying B-field Ring Apparatus
- SHAFT - Search for Halo Axions with Ferromagnetic Toroids

Helioscopes

- CAST - CERN Axion Solar Telescope
- IAXO - International Axion Observatory

LSW - Light-shining-through-wall

- ALPS - Any Light Particle Search
- CROWS - CERN Resonant WISP Search

Further Experiments

Dark Matter Direct Detection

- LUX-ZEPLIN - Collaboration of Large Underground Xenon Experiment and Zoned Proportional Scintillation in Liquid Noble Gases

- XENONnT

Neutrino Experiments

- Super-Kamiokande - Super-Kamioka Neutrino Detection Experiment

- MiniBooNE - Mini Booster Neutrino Experiment

Bibliography

[1] A. Kivel, J. Laux and F. Yu, *Supersizing axions with small size instantons*, *JHEP* **11** (2022) 088 [2207.08740].

[2] A. Kivel, J. Laux and F. Yu, *Axion couplings in gauged U(1)' extensions of the Standard Model*, *JHEP* **03** (2023) 078 [2211.12155].

[3] F. Elahi, G. Elor, A. Kivel, J. Laux, S. Najjari and F. Yu, *Lighter QCD axion from anarchy*, *Phys. Rev. D* **108** (2023) L031701 [2301.08760].

[4] J. Laux, S. Najjari and F. Yu, *in preparation*, .

[5] A. Kivel, J. Laux and F. Yu, *in preparation*, .

[6] D. Binosi, J. Collins, C. Kaufhold and L. Theussl, *JaxoDraw: A Graphical user interface for drawing Feynman diagrams. Version 2.0 release notes*, *Comput. Phys. Commun.* **180** (2009) 1709 [0811.4113].

[7] W. R. Inc., "Mathematica, Version 12.1."

[8] H. H. Patel, *Package-X: A Mathematica package for the analytic calculation of one-loop integrals*, *Comput. Phys. Commun.* **197** (2015) 276 [1503.01469].

[9] A. Alloul, N. D. Christensen, C. Degrande, C. Duhr and B. Fuks, *FeynRules 2.0 - A complete toolbox for tree-level phenomenology*, *Comput. Phys. Commun.* **185** (2014) 2250 [1310.1921].

[10] J. Alwall, R. Frederix, S. Frixione, V. Hirschi, F. Maltoni, O. Mattelaer et al., *The automated computation of tree-level and next-to-leading order differential cross sections, and their matching to parton shower simulations*, *JHEP* **07** (2014) 079 [1405.0301].

[11] G. Alguero, G. Belanger, S. Kraml and A. Pukhov, *Co-scattering in micrOMEGAs: A case study for the singlet-triplet dark matter model*, *SciPost Phys.* **13** (2022) 124 [2207.10536].

[12] ATLAS collaboration, *Observation of a new particle in the search for the Standard Model Higgs boson with the ATLAS detector at the LHC*, *Phys. Lett. B* **716** (2012) 1 [1207.7214].

[13] CMS collaboration, *Observation of a New Boson at a Mass of 125 GeV with the CMS Experiment at the LHC*, *Phys. Lett. B* **716** (2012) 30 [1207.7235].

[14] C. Abel et al., *Measurement of the Permanent Electric Dipole Moment of the Neutron*, *Phys. Rev. Lett.* **124** (2020) 081803 [2001.11966].

[15] R. D. Peccei and H. R. Quinn, *CP Conservation in the Presence of Instantons*, *Phys. Rev. Lett.* **38** (1977) 1440.

[16] R. D. Peccei and H. R. Quinn, *Constraints Imposed by CP Conservation in the Presence of Instantons*, *Phys. Rev.* **D16** (1977) 1791.

[17] S. Weinberg, *A New Light Boson?*, *Physical Review Letters* **40** (1978) 223.

[18] F. Wilczek, *Problem of Strong P and T Invariance in the Presence of Instantons*, *Phys. Rev. Lett.* **40** (1978) 279.
[19] J. E. Kim, *Weak Interaction Singlet and Strong CP Invariance*, *Phys. Rev. Lett.* **43** (1979) 103.
[20] M. A. Shifman, A. I. Vainshtein and V. I. Zakharov, *Can Confinement Ensure Natural CP Invariance of Strong Interactions?*, *Nucl. Phys.* **B166** (1980) 493.
[21] A. R. Zhitnitsky, *On Possible Suppression of the Axion Hadron Interactions. (In Russian)*, *Sov. J. Nucl. Phys.* **31** (1980) 260.
[22] M. Dine, W. Fischler and M. Srednicki, *A Simple Solution to the Strong CP Problem with a Harmless Axion*, *Phys. Lett. B* **104** (1981) 199.
[23] M. Kamionkowski and J. March-Russell, *Planck scale physics and the Peccei-Quinn mechanism*, *Phys. Lett. B* **282** (1992) 137 [hep-th/9202003].
[24] E. Rutherford, *The scattering of alpha and beta particles by matter and the structure of the atom*, *Phil. Mag. Ser. 6* **21** (1911) 669.
[25] H. Yukawa, *On the Interaction of Elementary Particles I*, *Proc. Phys. Math. Soc. Jap.* **17** (1935) 48.
[26] E. Fermi, *Tentativo di una teoria dell'emissione dei raggi beta*, *Ric. Sci.* **4** (1933) 491.
[27] E. Fermi, *An attempt of a theory of beta radiation. 1.*, *Z. Phys.* **88** (1934) 161.
[28] C. M. G. Lattes, H. Muirhead, G. P. S. Occhialini and C. F. Powell, *Processes involving charged mesons*, *Nature* **159** (1947) 694.
[29] C. L. Cowan, F. Reines, F. B. Harrison, H. W. Kruse and A. D. McGuire, *Detection of the free neutrino: A Confirmation*, *Science* **124** (1956) 103.
[30] M. Gell-Mann, *A Schematic Model of Baryons and Mesons*, *Phys. Lett.* **8** (1964) 214.
[31] G. Zweig, *An SU(3) model for strong interaction symmetry and its breaking. Version 1*, .
[32] S. L. Glashow, *Partial Symmetries of Weak Interactions*, *Nucl. Phys.* **22** (1961) 579.
[33] C. S. Wu, E. Ambler, R. W. Hayward, D. D. Hoppes and R. P. Hudson, *Experimental Test of Parity Conservation in β Decay*, *Phys. Rev.* **105** (1957) 1413.
[34] F. Englert and R. Brout, *Broken Symmetry and the Mass of Gauge Vector Mesons*, *Phys. Rev. Lett.* **13** (1964) 321.
[35] P. W. Higgs, *Broken Symmetries and the Masses of Gauge Bosons*, *Phys. Rev. Lett.* **13** (1964) 508.
[36] G. S. Guralnik, C. R. Hagen and T. W. B. Kibble, *Global Conservation Laws and Massless Particles*, *Phys. Rev. Lett.* **13** (1964) 585.
[37] S. Weinberg, *A Model of Leptons*, *Phys. Rev. Lett.* **19** (1967) 1264.
[38] A. Salam, *Weak and Electromagnetic Interactions*, *Conf. Proc. C* **680519** (1968) 367.
[39] Particle Data Group collaboration, *Review of Particle Physics*, *PTEP* **2022** (2022) 083C01.
[40] I. Newton, *Philosophiæ Naturalis Principia Mathematica*. England, 1687.
[41] A. Einstein, *The foundation of the general theory of relativity.*, *Annalen Phys.* **49** (1916) 769.
[42] Planck collaboration, *Planck 2018 results. VI. Cosmological parameters*, *Astron. Astrophys.* **641** (2020) A6 [1807.06209].
[43] A. D. Sakharov, *Violation of CP Invariance, C asymmetry, and baryon asymmetry*

of the universe, *Pisma Zh. Eksp. Teor. Fiz.* **5** (1967) 32.

[44] Super-Kamiokande collaboration, *Evidence for oscillation of atmospheric neutrinos*, *Phys. Rev. Lett.* **81** (1998) 1562 [hep-ex/9807003].

[45] Muon g-2 collaboration, *Measurement of the Positive Muon Anomalous Magnetic Moment to 0.46 ppm*, *Phys. Rev. Lett.* **126** (2021) 141801 [2104.03281].

[46] S.-S. Chern and J. Simons, *Characteristic forms and geometric invariants*, *Annals Math.* **99** (1974) 48.

[47] K. Fujikawa, *Path Integral Measure for Gauge Invariant Fermion Theories*, *Phys. Rev. Lett.* **42** (1979) 1195.

[48] T. van Ritbergen, A. N. Schellekens and J. A. M. Vermaseren, *Group theory factors for Feynman diagrams*, *Int. J. Mod. Phys. A* **14** (1999) 41 [hep-ph/9802376].

[49] M. Gell-Mann, R. J. Oakes and B. Renner, *Behavior of current divergences under SU(3) x SU(3)*, *Phys. Rev.* **175** (1968) 2195.

[50] A. E. Nelson, *Naturally Weak CP Violation*, *Phys. Lett. B* **136** (1984) 387.

[51] S. M. Barr, *Solving the Strong CP Problem Without the Peccei-Quinn Symmetry*, *Phys. Rev. Lett.* **53** (1984) 329.

[52] G. C. Branco, P. M. Ferreira, L. Lavoura, M. N. Rebelo, M. Sher and J. P. Silva, *Theory and phenomenology of two-Higgs-doublet models*, *Phys. Rept.* **516** (2012) 1 [1106.0034].

[53] C. O'Hare, "cajohare/axionlimits: Axionlimits." https://cajohare.github.io/AxionLimits/, July, 2020. 10.5281/zenodo.3932430.

[54] G. Grilli di Cortona, E. Hardy, J. Pardo Vega and G. Villadoro, *The QCD axion, precisely*, *JHEP* **01** (2016) 034 [1511.02867].

[55] H. Primakoff, *Photoproduction of neutral mesons in nuclear electric fields and the mean life of the neutral meson*, *Phys. Rev.* **81** (1951) 899.

[56] K. Ehret et al., *New ALPS Results on Hidden-Sector Lightweights*, *Phys. Lett. B* **689** (2010) 149 [1004.1313].

[57] M. Betz, F. Caspers, M. Gasior, M. Thumm and S. W. Rieger, *First results of the CERN Resonant Weakly Interacting sub-eV Particle Search (CROWS)*, *Phys. Rev. D* **88** (2013) 075014 [1310.8098].

[58] OSQAR collaboration, *New exclusion limits on scalar and pseudoscalar axionlike particles from light shining through a wall*, *Phys. Rev. D* **92** (2015) 092002 [1506.08082].

[59] F. Della Valle, A. Ejlli, U. Gastaldi, G. Messineo, E. Milotti, R. Pengo et al., *The PVLAS experiment: measuring vacuum magnetic birefringence and dichroism with a birefringent Fabry–Perot cavity*, *Eur. Phys. J. C* **76** (2016) 24 [1510.08052].

[60] SAPPHIRES collaboration, *Search for sub-eV axion-like resonance states via stimulated quasi-parallel laser collisions with the parameterization including fully asymmetric collisional geometry*, *JHEP* **12** (2021) 108 [2105.01224].

[61] SAPPHIRES collaboration, *Search for sub-eV axion-like particles in a stimulated resonant photon-photon collider with two laser beams based on a novel method to discriminate pressure-independent components*, *JHEP* **10** (2022) 176 [2208.09880].

[62] P. Sikivie, *Experimental Tests of the Invisible Axion*, *Phys. Rev. Lett.* **51** (1983) 1415.

[63] CAST collaboration, *An Improved limit on the axion-photon coupling from the CAST experiment*, *JCAP* **04** (2007) 010 [hep-ex/0702006].

[64] CAST collaboration, *New CAST Limit on the Axion-Photon Interaction*, *Nature Phys.* **13** (2017) 584 [1705.02290].
[65] IAXO collaboration, *Physics potential of the International Axion Observatory (IAXO)*, *JCAP* **06** (2019) 047 [1904.09155].
[66] J. L. Ouellet et al., *First Results from ABRACADABRA-10 cm: A Search for Sub-μeV Axion Dark Matter*, *Phys. Rev. Lett.* **122** (2019) 121802 [1810.12257].
[67] C. P. Salemi et al., *Search for Low-Mass Axion Dark Matter with ABRACADABRA-10 cm*, *Phys. Rev. Lett.* **127** (2021) 081801 [2102.06722].
[68] S. J. Asztalos, G. Carosi, C. Hagmann, D. Kinion, K. van Bibber, M. Hotz et al., *SQUID-Based Microwave Cavity Search for Dark-Matter Axions*, *Phys. Rev. Lett.* **104** (2010) 041301 [0910.5914].
[69] ADMX collaboration, *A Search for Invisible Axion Dark Matter with the Axion Dark Matter Experiment*, *Phys. Rev. Lett.* **120** (2018) 151301 [1804.05750].
[70] ADMX collaboration, *Extended Search for the Invisible Axion with the Axion Dark Matter Experiment*, *Phys. Rev. Lett.* **124** (2020) 101303 [1910.08638].
[71] ADMX collaboration, *Search for Invisible Axion Dark Matter in the 3.3–4.2 μeV Mass Range*, *Phys. Rev. Lett.* **127** (2021) 261803 [2110.06096].
[72] ADMX collaboration, *Piezoelectrically Tuned Multimode Cavity Search for Axion Dark Matter*, *Phys. Rev. Lett.* **121** (2018) 261302 [1901.00920].
[73] ADMX collaboration, *Dark matter axion search using a Josephson Traveling wave parametric amplifier*, *Rev. Sci. Instrum.* **94** (2023) 044703 [2110.10262].
[74] N. Crisosto, P. Sikivie, N. S. Sullivan, D. B. Tanner, J. Yang and G. Rybka, *ADMX SLIC: Results from a Superconducting LC Circuit Investigating Cold Axions*, *Phys. Rev. Lett.* **124** (2020) 241101 [1911.05772].
[75] S. Lee, S. Ahn, J. Choi, B. R. Ko and Y. K. Semertzidis, *Axion Dark Matter Search around 6.7 μeV*, *Phys. Rev. Lett.* **124** (2020) 101802 [2001.05102].
[76] J. Jeong, S. Youn, S. Bae, J. Kim, T. Seong, J. E. Kim et al., *Search for Invisible Axion Dark Matter with a Multiple-Cell Haloscope*, *Phys. Rev. Lett.* **125** (2020) 221302 [2008.10141].
[77] CAPP collaboration, *First Results from an Axion Haloscope at CAPP around 10.7 μeV*, *Phys. Rev. Lett.* **126** (2021) 191802 [2012.10764].
[78] Y. Lee, B. Yang, H. Yoon, M. Ahn, H. Park, B. Min et al., *Searching for Invisible Axion Dark Matter with an 18 T Magnet Haloscope*, *Phys. Rev. Lett.* **128** (2022) 241805 [2206.08845].
[79] J. Kim et al., *Near-Quantum-Noise Axion Dark Matter Search at CAPP around 9.5 μeV*, *Phys. Rev. Lett.* **130** (2023) 091602 [2207.13597].
[80] A. K. Yi et al., *Axion Dark Matter Search around 4.55 μeV with Dine-Fischler-Srednicki-Zhitnitskii Sensitivity*, *Phys. Rev. Lett.* **130** (2023) 071002 [2210.10961].
[81] C. M. Adair et al., *Search for Dark Matter Axions with CAST-CAPP*, *Nature Commun.* **13** (2022) 6180 [2211.02902].
[82] Y. Oshima, H. Fujimoto, M. Ando, T. Fujita, J. Kume, Y. Michimura et al., *First Results of Axion Dark Matter Search with DANCE*, 2303.03594.
[83] J. A. Devlin et al., *Constraints on the Coupling between Axionlike Dark Matter and Photons Using an Antiproton Superconducting Tuned Detection Circuit in a Cryogenic Penning Trap*, *Phys. Rev. Lett.* **126** (2021) 041301 [2101.11290].
[84] T. Grenet, R. Ballou, Q. Basto, K. Martineau, P. Perrier, P. Pugnat et al., *The Grenoble Axion Haloscope platform (GrAHal): development plan and first results*, 2110.14406.

[85] HAYSTAC collaboration, *Results from phase 1 of the HAYSTAC microwave cavity axion experiment*, *Phys. Rev. D* **97** (2018) 092001 [1803.03690].

[86] HAYSTAC collaboration, *A quantum-enhanced search for dark matter axions*, *Nature* **590** (2021) 238 [2008.01853].

[87] HAYSTAC collaboration, *New results from HAYSTAC's phase II operation with a squeezed state receiver*, *Phys. Rev. D* **107** (2023) 072007 [2301.09721].

[88] J. Heinze, A. Gill, A. Dmitriev, J. Smetana, T. Yan, V. Boyer et al., *First results of the Laser-Interferometric Detector for Axions (LIDA)*, 2307.01365.

[89] B. T. McAllister, G. Flower, E. N. Ivanov, M. Goryachev, J. Bourhill and M. E. Tobar, *The ORGAN Experiment: An axion haloscope above 15 GHz*, *Phys. Dark Univ.* **18** (2017) 67 [1706.00209].

[90] A. P. Quiskamp, B. T. McAllister, P. Altin, E. N. Ivanov, M. Goryachev and M. E. Tobar, *Direct search for dark matter axions excluding ALP cogenesis in the 63- to 67-μeV range with the ORGAN experiment*, *Sci. Adv.* **8** (2022) abq3765 [2203.12152].

[91] D. Alesini et al., *Galactic axions search with a superconducting resonant cavity*, *Phys. Rev. D* **99** (2019) 101101 [1903.06547].

[92] D. Alesini et al., *Search for invisible axion dark matter of mass $m_a = 43$ μeV with the QUAX–aγ experiment*, *Phys. Rev. D* **103** (2021) 102004 [2012.09498].

[93] D. Alesini et al., *Search for Galactic axions with a high-Q dielectric cavity*, *Phys. Rev. D* **106** (2022) 052007 [2208.12670].

[94] CAST collaboration, *First results of the CAST-RADES haloscope search for axions at 34.67 μeV*, *JHEP* **21** (2020) 075 [2104.13798].

[95] S. DePanfilis, A. C. Melissinos, B. E. Moskowitz, J. T. Rogers, Y. K. Semertzidis, W. U. Wuensch et al., *Limits on the abundance and coupling of cosmic axions at 4.5< m_a <5.0 μev*, *Phys. Rev. Lett.* **59** (1987) 839.

[96] A. V. Gramolin, D. Aybas, D. Johnson, J. Adam and A. O. Sushkov, *Search for axion-like dark matter with ferromagnets*, *Nature Phys.* **17** (2021) 79 [2003.03348].

[97] TASEH collaboration, *First Results from the Taiwan Axion Search Experiment with a Haloscope at 19.6 μeV*, *Phys. Rev. Lett.* **129** (2022) 111802 [2205.05574].

[98] A. Arza, M. A. Fedderke, P. W. Graham, D. F. J. Kimball and S. Kalia, *Earth as a transducer for axion dark-matter detection*, *Phys. Rev. D* **105** (2022) 095007 [2112.09620].

[99] C. Hagmann, P. Sikivie, N. S. Sullivan and D. B. Tanner, *Results from a search for cosmic axions*, *Phys. Rev. D* **42** (1990) 1297.

[100] C. A. Thomson, B. T. McAllister, M. Goryachev, E. N. Ivanov and M. E. Tobar, *Upconversion Loop Oscillator Axion Detection Experiment: A Precision Frequency Interferometric Axion Dark Matter Search with a Cylindrical Microwave Cavity*, *Phys. Rev. Lett.* **126** (2021) 081803 [1912.07751].

[101] C. A. Thomson, M. Goryachev, B. T. McAllister, E. N. Ivanov, P. Altin and M. E. Tobar, *Searching for low-mass axions using resonant upconversion*, *Phys. Rev. D* **107** (2023) 112003 [2301.06778].

[102] J. Preskill, M. B. Wise and F. Wilczek, *Cosmology of the Invisible Axion*, *Phys. Lett. B* **120** (1983) 127.

[103] L. F. Abbott and P. Sikivie, *A Cosmological Bound on the Invisible Axion*, *Phys. Lett. B* **120** (1983) 133.

[104] M. Dine and W. Fischler, *The Not So Harmless Axion*, *Phys. Lett. B* **120** (1983)

137.
[105] M. Bauer, M. Neubert and A. Thamm, *Collider Probes of Axion-Like Particles*, *JHEP* **12** (2017) 044 [1708.00443].
[106] M. Bauer, M. Neubert, S. Renner, M. Schnubel and A. Thamm, *Flavor probes of axion-like particles*, *JHEP* **09** (2022) 056 [2110.10698].
[107] ATLAS collaboration, *Measurement of light-by-light scattering and search for axion-like particles with 2.2 nb^{-1} of Pb+Pb data with the ATLAS detector*, *JHEP* **03** (2021) 243 [2008.05355].
[108] M. J. Dolan, T. Ferber, C. Hearty, F. Kahlhoefer and K. Schmidt-Hoberg, *Revised constraints and Belle II sensitivity for visible and invisible axion-like particles*, *JHEP* **12** (2017) 094 [1709.00009].
[109] CHARM collaboration, *Search for Axion Like Particle Production in 400-GeV Proton - Copper Interactions*, *Phys. Lett. B* **157** (1985) 458.
[110] E. M. Riordan et al., *A Search for Short Lived Axions in an Electron Beam Dump Experiment*, *Phys. Rev. Lett.* **59** (1987) 755.
[111] J. Blumlein et al., *Limits on neutral light scalar and pseudoscalar particles in a proton beam dump experiment*, *Z. Phys. C* **51** (1991) 341.
[112] NA64 collaboration, *Search for Axionlike and Scalar Particles with the NA64 Experiment*, *Phys. Rev. Lett.* **125** (2020) 081801 [2005.02710].
[113] Belle-II collaboration, *Search for Axion-Like Particles produced in e^+e^- collisions at Belle II*, *Phys. Rev. Lett.* **125** (2020) 161806 [2007.13071].
[114] BESIII collaboration, *Search for an axion-like particle in radiative J/ψ decays*, *Phys. Lett. B* **838** (2023) 137698 [2211.12699].
[115] CMS collaboration, *Evidence for light-by-light scattering and searches for axion-like particles in ultraperipheral PbPb collisions at $\sqrt{s_{\mathrm{NN}}} = 5.02$ TeV*, *Phys. Lett. B* **797** (2019) 134826 [1810.04602].
[116] J. Jaeckel and M. Spannowsky, *Probing MeV to 90 GeV axion-like particles with LEP and LHC*, *Phys. Lett. B* **753** (2016) 482 [1509.00476].
[117] S. Knapen, T. Lin, H. K. Lou and T. Melia, *Searching for Axionlike Particles with Ultraperipheral Heavy-Ion Collisions*, *Phys. Rev. Lett.* **118** (2017) 171801 [1607.06083].
[118] F. Capozzi, B. Dutta, G. Gurung, W. Jang, I. M. Shoemaker, A. Thompson et al., *New Constraints on ALP Electron and Photon Couplings from ArgoNeuT and the MiniBooNE Beam Dump*, 2307.03878.
[119] NOMAD collaboration, *Search for eV (pseudo)scalar penetrating particles in the SPS neutrino beam*, *Phys. Lett. B* **479** (2000) 371.
[120] PrimEx collaboration, *A New Measurement of the π^0 Radiative Decay Width*, *Phys. Rev. Lett.* **106** (2011) 162303 [1009.1681].
[121] D. Aloni, C. Fanelli, Y. Soreq and M. Williams, *Photoproduction of Axionlike Particles*, *Phys. Rev. Lett.* **123** (2019) 071801 [1903.03586].
[122] M. Escudero, C. K. Pooni, M. Fairbairn, D. Blas, X. Du and D. J. E. Marsh, *Axion Star Explosions: A New Source for Axion Indirect Detection*, 2302.10206.
[123] M. Xiao, K. M. Perez, M. Giannotti, O. Straniero, A. Mirizzi, B. W. Grefenstette et al., *Constraints on Axionlike Particles from a Hard X-Ray Observation of Betelgeuse*, *Phys. Rev. Lett.* **126** (2021) 031101 [2009.09059].
[124] BICEP/Keck collaboration, *BICEP/Keck XIV: Improved constraints on axionlike polarization oscillations in the cosmic microwave background*, *Phys. Rev. D* **105** (2022) 022006 [2108.03316].
[125] A. Keller, S. O'Brien, A. Kamdar, N. M. Rapidis, A. F. Leder and K. van Bibber,

A Model-independent Radio Telescope Dark Matter Search, *Astrophys. J.* **927** (2022) 71 [2112.03439].

[126] M. H. Chan, *Constraining the axion-photon coupling using radio data of the Bullet Cluster*, *Sci. Rep.* **11** (2021) 20087 [2109.11734].

[127] K. Kohri and H. Kodama, *Axion-Like Particles and Recent Observations of the Cosmic Infrared Background Radiation*, *Phys. Rev. D* **96** (2017) 051701 [1704.05189].

[128] D. Wouters and P. Brun, *Constraints on Axion-like Particles from X-Ray Observations of the Hydra Galaxy Cluster*, *Astrophys. J.* **772** (2013) 44 [1304.0989].

[129] M. C. D. Marsh, H. R. Russell, A. C. Fabian, B. P. McNamara, P. Nulsen and C. S. Reynolds, *A New Bound on Axion-Like Particles*, *JCAP* **12** (2017) 036 [1703.07354].

[130] C. S. Reynolds, M. C. D. Marsh, H. R. Russell, A. C. Fabian, R. Smith, F. Tombesi et al., *Astrophysical Limits on Very Light Axion-like Particles from Chandra Grating Spectroscopy of NGC 1275*, *Astrophys. J.* **890** (2020) 59 [1907.05475].

[131] J. S. Reynés, J. H. Matthews, C. S. Reynolds, H. R. Russell, R. N. Smith and M. C. D. Marsh, *New constraints on light axion-like particles using Chandra transmission grating spectroscopy of the powerful cluster-hosted quasar H1821+643*, *Mon. Not. Roy. Astron. Soc.* **510** (2021) 1264 [2109.03261].

[132] F. Capozzi, R. Z. Ferreira, L. Lopez-Honorez and O. Mena, *CMB and Lyman-α constraints on dark matter decays to photons*, *JCAP* **06** (2023) 060 [2303.07426].

[133] H. Liu, W. Qin, G. W. Ridgway and T. R. Slatyer, *Exotic energy injection in the early universe II: CMB spectral distortions and constraints on light dark matter*, 2303.07370.

[134] B. Bolliet, J. Chluba and R. Battye, *Spectral distortion constraints on photon injection from low-mass decaying particles*, *Mon. Not. Roy. Astron. Soc.* **507** (2021) 3148 [2012.07292].

[135] A. Caputo, H.-T. Janka, G. Raffelt and E. Vitagliano, *Low-Energy Supernovae Severely Constrain Radiative Particle Decays*, *Phys. Rev. Lett.* **128** (2022) 221103 [2201.09890].

[136] F. Calore, P. Carenza, C. Eckner, T. Fischer, M. Giannotti, J. Jaeckel et al., *3D template-based Fermi-LAT constraints on the diffuse supernova axion-like particle background*, *Phys. Rev. D* **105** (2022) 063028 [2110.03679].

[137] M. A. Buen-Abad, J. Fan and C. Sun, *Constraints on axions from cosmic distance measurements*, *JHEP* **02** (2022) 103 [2011.05993].

[138] Fermi-LAT collaboration, *Search for Spectral Irregularities due to Photon–Axionlike-Particle Oscillations with the Fermi Large Area Telescope*, *Phys. Rev. Lett.* **116** (2016) 161101 [1603.06978].

[139] M. Meyer and T. Petrushevska, *Search for Axionlike-Particle-Induced Prompt γ-Ray Emission from Extragalactic Core-Collapse Supernovae with the Fermi Large Area Telescope*, *Phys. Rev. Lett.* **124** (2020) 231101 [2006.06722].

[140] J. Davies, M. Meyer and G. Cotter, *Constraints on axionlike particles from a combined analysis of three flaring Fermi flat-spectrum radio quasars*, *Phys. Rev. D* **107** (2023) 083027 [2211.03414].

[141] J. L. Bernal, A. Caputo, G. Sato-Polito, J. Mirocha and M. Kamionkowski, *Seeking dark matter with γ-ray attenuation*, *Phys. Rev. D* **107** (2023) 103046 [2208.13794].

[142] A. Ayala, I. Domínguez, M. Giannotti, A. Mirizzi and O. Straniero, *Revisiting the bound on axion-photon coupling from Globular Clusters*, *Phys. Rev. Lett.* **113** (2014) 191302 [1406.6053].

[143] M. J. Dolan, F. J. Hiskens and R. R. Volkas, *Advancing globular cluster constraints on the axion-photon coupling*, *JCAP* **10** (2022) 096 [2207.03102].

[144] S. Jacobsen, T. Linden and K. Freese, *Constraining Axion-Like Particles with HAWC Observations of TeV Blazars*, 2203.04332.

[145] H.E.S.S. collaboration, *Constraints on axionlike particles with H.E.S.S. from the irregularity of the PKS 2155-304 energy spectrum*, *Phys. Rev. D* **88** (2013) 102003 [1311.3148].

[146] F. Calore, A. Dekker, P. D. Serpico and T. Siegert, *Constraints on light decaying dark matter candidates from 16 yr of INTEGRAL/SPI observations*, *Mon. Not. Roy. Astron. Soc.* **520** (2023) 4167 [2209.06299].

[147] D. Wadekar and Z. Wang, *Strong constraints on decay and annihilation of dark matter from heating of gas-rich dwarf galaxies*, *Phys. Rev. D* **106** (2022) 075007 [2111.08025].

[148] C. Dessert, A. J. Long and B. R. Safdi, *No Evidence for Axions from Chandra Observation of the Magnetic White Dwarf RE J0317-853*, *Phys. Rev. Lett.* **128** (2022) 071102 [2104.12772].

[149] C. Dessert, D. Dunsky and B. R. Safdi, *Upper limit on the axion-photon coupling from magnetic white dwarf polarization*, *Phys. Rev. D* **105** (2022) 103034 [2203.04319].

[150] M. M. Ivanov, Y. Y. Kovalev, M. L. Lister, A. G. Panin, A. B. Pushkarev, T. Savolainen et al., *Constraining the photon coupling of ultra-light dark-matter axion-like particles by polarization variations of parsec-scale jets in active galaxies*, *JCAP* **02** (2019) 059 [1811.10997].

[151] H.-J. Li, J.-G. Guo, X.-J. Bi, S.-J. Lin and P.-F. Yin, *Limits on axionlike particles from Mrk 421 with 4.5-year period observations by ARGO-YBJ and Fermi-LAT*, *Phys. Rev. D* **103** (2021) 083003 [2008.09464].

[152] H.-J. Li, X.-J. Bi and P.-F. Yin, *Searching for axion-like particles with the blazar observations of MAGIC and Fermi-LAT **, *Chin. Phys. C* **46** (2022) 085105 [2110.13636].

[153] J. W. Foster, Y. Kahn, O. Macias, Z. Sun, R. P. Eatough, V. I. Kondratiev et al., *Green Bank and Effelsberg Radio Telescope Searches for Axion Dark Matter Conversion in Neutron Star Magnetospheres*, *Phys. Rev. Lett.* **125** (2020) 171301 [2004.00011].

[154] J. Darling, *New Limits on Axionic Dark Matter from the Magnetar PSR J1745-2900*, *Astrophys. J. Lett.* **900** (2020) L28 [2008.11188].

[155] R. A. Battye, J. Darling, J. I. McDonald and S. Srinivasan, *Towards robust constraints on axion dark matter using PSR J1745-2900*, *Phys. Rev. D* **105** (2022) L021305 [2107.01225].

[156] J. W. Foster, S. J. Witte, M. Lawson, T. Linden, V. Gajjar, C. Weniger et al., *Extraterrestrial Axion Search with the Breakthrough Listen Galactic Center Survey*, *Phys. Rev. Lett.* **129** (2022) 251102 [2202.08274].

[157] R. A. Battye, M. J. Keith, J. I. McDonald, S. Srinivasan, B. W. Stappers and P. Weltevrede, *Searching for Time-Dependent Axion Dark Matter Signals in Pulsars*, 2303.11792.

[158] K. Perez, K. C. Y. Ng, J. F. Beacom, C. Hersh, S. Horiuchi and R. Krivonos, *Almost closing the νMSM sterile neutrino dark matter window with NuSTAR*,

Phys. Rev. D **95** (2017) 123002 [1609.00667].

[159] K. C. Y. Ng, B. M. Roach, K. Perez, J. F. Beacom, S. Horiuchi, R. Krivonos et al., *New Constraints on Sterile Neutrino Dark Matter from NuSTAR M31 Observations*, *Phys. Rev. D* **99** (2019) 083005 [1901.01262].

[160] B. M. Roach, S. Rossland, K. C. Y. Ng, K. Perez, J. F. Beacom, B. W. Grefenstette et al., *Long-exposure NuSTAR constraints on decaying dark matter in the Galactic halo*, *Phys. Rev. D* **107** (2023) 023009 [2207.04572].

[161] M. A. Fedderke, P. W. Graham and S. Rajendran, *Axion Dark Matter Detection with CMB Polarization*, *Phys. Rev. D* **100** (2019) 015040 [1903.02666].

[162] POLARBEAR collaboration, *Constraints on axion-like polarization oscillations in the cosmic microwave background with POLARBEAR*, 2303.08410.

[163] A. Castillo, J. Martin-Camalich, J. Terol-Calvo, D. Blas, A. Caputo, R. T. G. Santos et al., *Searching for dark-matter waves with PPTA and QUIJOTE pulsar polarimetry*, *JCAP* **06** (2022) 014 [2201.03422].

[164] T. Liu, X. Lou and J. Ren, *Pulsar Polarization Arrays*, *Phys. Rev. Lett.* **130** (2023) 121401 [2111.10615].

[165] D. Noordhuis, A. Prabhu, S. J. Witte, A. Y. Chen, F. Cruz and C. Weniger, *Novel Constraints on Axions Produced in Pulsar Polar-Cap Cascades*, 2209.09917.

[166] C. Severino and I. Lopes, *Asteroseismology: Looking for Axions in the Red Supergiant Star Alpha Ori*, *Astrophys. J.* **943** (2023) 95 [2212.01890].

[167] N. Vinyoles, A. Serenelli, F. L. Villante, S. Basu, J. Redondo and J. Isern, *New axion and hidden photon constraints from a solar data global fit*, *JCAP* **2015** (2015) 015 [1501.01639].

[168] N. H. Nguyen, E. H. Tanin and M. Kamionkowski, *Spectra of axions emitted from main sequence stars*, 2307.11216.

[169] J. Jaeckel, P. C. Malta and J. Redondo, *Decay photons from the axionlike particles burst of type II supernovae*, *Phys. Rev. D* **98** (2018) 055032 [1702.02964].

[170] S. Hoof and L. Schulz, *Updated constraints on axion-like particles from temporal information in supernova SN1987A gamma-ray data*, *JCAP* **03** (2023) 054 [2212.09764].

[171] E. Müller, F. Calore, P. Carenza, C. Eckner and M. C. D. Marsh, *Investigating the gamma-ray burst from decaying MeV-scale axion-like particles produced in supernova explosions*, *JCAP* **07** (2023) 056 [2304.01060].

[172] A. Payez, C. Evoli, T. Fischer, M. Giannotti, A. Mirizzi and A. Ringwald, *Revisiting the SN1987A gamma-ray limit on ultralight axion-like particles*, *JCAP* **02** (2015) 006 [1410.3747].

[173] G. Lucente, P. Carenza, T. Fischer, M. Giannotti and A. Mirizzi, *Heavy axion-like particles and core-collapse supernovae: constraints and impact on the explosion mechanism*, *JCAP* **12** (2020) 008 [2008.04918].

[174] A. Caputo, G. Raffelt and E. Vitagliano, *Muonic boson limits: Supernova redux*, *Phys. Rev. D* **105** (2022) 035022 [2109.03244].

[175] M. Diamond, D. F. G. Fiorillo, G. Marques-Tavares and E. Vitagliano, *Axion-sourced fireballs from supernovae*, *Phys. Rev. D* **107** (2023) 103029 [2303.11395].

[176] W. DeRocco, S. Wegsman, B. Grefenstette, J. Huang and K. Van Tilburg, *First Indirect Detection Constraints on Axions in the Solar Basin*, *Phys. Rev. Lett.* **129** (2022) 101101 [2205.05700].

[177] C. Beaufort, M. Bastero-Gil, T. Luce and D. Santos, *New solar X-ray constraints on keV Axion-Like Particles*, 2303.06968.

[178] C. Dessert, J. W. Foster and B. R. Safdi, *X-ray Searches for Axions from Super Star Clusters*, *Phys. Rev. Lett.* **125** (2020) 261102 [2008.03305].

[179] SPT-3G collaboration, *Searching for axionlike time-dependent cosmic birefringence with data from SPT-3G*, *Phys. Rev. D* **106** (2022) 042011 [2203.16567].

[180] B. D. Blout, E. J. Daw, M. P. Decowski, P. T. P. Ho, L. J. Rosenberg and D. B. Yu, *A Radio telescope search for axions*, *Astrophys. J.* **546** (2001) 825 [astro-ph/0006310].

[181] E. Todarello, M. Regis, J. Reynoso-Cordova, M. Taoso, D. Vaz, J. Brinchmann et al., *Robust bounds on ALP dark matter from dwarf spheroidal galaxies in the optical MUSE-Faint survey*, 2307.07403.

[182] D. Grin, G. Covone, J.-P. Kneib, M. Kamionkowski, A. Blain and E. Jullo, *A Telescope Search for Decaying Relic Axions*, *Phys. Rev. D* **75** (2007) 105018 [astro-ph/0611502].

[183] K. Nakayama and W. Yin, *Anisotropic cosmic optical background bound for decaying dark matter in light of the LORRI anomaly*, *Phys. Rev. D* **106** (2022) 103505 [2205.01079].

[184] P. Carenza, G. Lucente and E. Vitagliano, *Probing the blue axion with cosmic optical background anisotropies*, *Phys. Rev. D* **107** (2023) 083032 [2301.06560].

[185] M. J. Dolan, F. J. Hiskens and R. R. Volkas, *Constraining axion-like particles using the white dwarf initial-final mass relation*, *JCAP* **09** (2021) 010 [2102.00379].

[186] J. W. Foster, M. Kongsore, C. Dessert, Y. Park, N. L. Rodd, K. Cranmer et al., *Deep Search for Decaying Dark Matter with XMM-Newton Blank-Sky Observations*, *Phys. Rev. Lett.* **127** (2021) 051101 [2102.02207].

[187] D. Cadamuro and J. Redondo, *Cosmological bounds on pseudo Nambu-Goldstone bosons*, *JCAP* **02** (2012) 032 [1110.2895].

[188] P. F. Depta, M. Hufnagel and K. Schmidt-Hoberg, *Robust cosmological constraints on axion-like particles*, *JCAP* **05** (2020) 009 [2002.08370].

[189] K. Langhoff, N. J. Outmezguine and N. L. Rodd, *Irreducible Axion Background*, *Phys. Rev. Lett.* **129** (2022) 241101 [2209.06216].

[190] B. Holdom and M. E. Peskin, *Raising the Axion Mass*, *Nucl. Phys. B* **208** (1982) 397.

[191] T. Gherghetta, N. Nagata and M. Shifman, *A Visible QCD Axion from an Enlarged Color Group*, *Phys. Rev. D* **93** (2016) 115010 [1604.01127].

[192] P. Agrawal, G. Marques-Tavares and W. Xue, *Opening up the QCD axion window*, *JHEP* **03** (2018) 049 [1708.05008].

[193] P. Agrawal and K. Howe, *Factoring the Strong CP Problem*, *JHEP* **12** (2018) 029 [1710.04213].

[194] P. Agrawal and K. Howe, *A Flavorful Factoring of the Strong CP Problem*, *JHEP* **12** (2018) 035 [1712.05803].

[195] A. Hook, *Solving the Hierarchy Problem Discretely*, *Phys. Rev. Lett.* **120** (2018) 261802 [1802.10093].

[196] M. K. Gaillard, M. B. Gavela, R. Houtz, P. Quilez and R. Del Rey, *Color unified dynamical axion*, *Eur. Phys. J.* **C78** (2018) 972 [1805.06465].

[197] L. Di Luzio, B. Gavela, P. Quilez and A. Ringwald, *An even lighter QCD axion*, *JHEP* **05** (2021) 184 [2102.00012].

[198] T. W. Donnelly, S. J. Freedman, R. S. Lytel, R. D. Peccei and M. Schwartz, *Do Axions Exist?*, *Phys. Rev. D* **18** (1978) 1607.

[199] G. 't Hooft, *Symmetry Breaking Through Bell-Jackiw Anomalies*, *Phys. Rev. Lett.* **37** (1976) 8.

[200] G. 't Hooft, *How Instantons Solve the U(1) Problem*, *Phys. Rept.* **142** (1986) 357.
[201] J. E. Kim and G. Carosi, *Axions and the Strong CP Problem*, *Rev. Mod. Phys.* **82** (2010) 557 [0807.3125].
[202] Particle Data Group collaboration, *Review of Particle Physics*, *PTEP* **2020** (2020) 083C01.
[203] S. W. Hawking, *Quantum Coherence Down the Wormhole*, *Phys. Lett. B* **195** (1987) 337.
[204] S. B. Giddings and A. Strominger, *Loss of Incoherence and Determination of Coupling Constants in Quantum Gravity*, *Nucl. Phys. B* **307** (1988) 854.
[205] T. Banks and N. Seiberg, *Symmetries and Strings in Field Theory and Gravity*, *Phys. Rev. D* **83** (2011) 084019 [1011.5120].
[206] L. Bento, G. C. Branco and P. A. Parada, *A Minimal model with natural suppression of strong CP violation*, *Phys. Lett. B* **267** (1991) 95.
[207] M. Dine and P. Draper, *Challenges for the Nelson-Barr Mechanism*, *JHEP* **08** (2015) 132 [1506.05433].
[208] G. Passarino and M. J. G. Veltman, *One Loop Corrections for e+ e- Annihilation Into mu+ mu- in the Weinberg Model*, *Nucl. Phys. B* **160** (1979) 151.
[209] M. Bauer, M. Neubert and A. Thamm, *Analyzing the CP Nature of a New Scalar Particle via S->Zh Decay*, *Phys. Rev. Lett.* **117** (2016) 181801 [1610.00009].
[210] A. Czarnecki and W. J. Marciano, *The Muon anomalous magnetic moment: A Harbinger for 'new physics'*, *Phys. Rev. D* **64** (2001) 013014 [hep-ph/0102122].
[211] J. Martin Camalich, M. Pospelov, P. N. H. Vuong, R. Ziegler and J. Zupan, *Quark Flavor Phenomenology of the QCD Axion*, *Phys. Rev. D* **102** (2020) 015023 [2002.04623].
[212] L. Calibbi, D. Redigolo, R. Ziegler and J. Zupan, *Looking forward to lepton-flavor-violating ALPs*, *JHEP* **09** (2021) 173 [2006.04795].
[213] LUX-ZEPLIN collaboration, *First Dark Matter Search Results from the LUX-ZEPLIN (LZ) Experiment*, *Phys. Rev. Lett.* **131** (2023) 041002 [2207.03764].
[214] XENON collaboration, *First Dark Matter Search with Nuclear Recoils from the XENONnT Experiment*, *Phys. Rev. Lett.* **131** (2023) 041003 [2303.14729].
[215] XENON collaboration, *Physics reach of the XENON1T dark matter experiment*, *JCAP* **04** (2016) 027 [1512.07501].
[216] A. Friedmann, *On the Possibility of a world with constant negative curvature of space*, *Z. Phys.* **21** (1924) 326.
[217] E. Hubble, *A relation between distance and radial velocity among extra-galactic nebulae*, *Proc. Nat. Acad. Sci.* **15** (1929) 168.
[218] G. Bertone, D. Hooper and J. Silk, *Particle dark matter: Evidence, candidates and constraints*, *Phys. Rept.* **405** (2005) 279 [hep-ph/0404175].
[219] J. M. Cline, K. Kainulainen, P. Scott and C. Weniger, *Update on scalar singlet dark matter*, *Phys. Rev. D* **88** (2013) 055025 [1306.4710].
[220] G. Arcadi, M. Dutra, P. Ghosh, M. Lindner, Y. Mambrini, M. Pierre et al., *The waning of the WIMP? A review of models, searches, and constraints*, *Eur. Phys. J. C* **78** (2018) 203 [1703.07364].
[221] G. Arcadi, A. Djouadi and M. Raidal, *Dark Matter through the Higgs portal*, *Phys. Rept.* **842** (2020) 1 [1903.03616].
[222] J. M. Alarcon, J. Martin Camalich and J. A. Oller, *The chiral representation of the πN scattering amplitude and the pion-nucleon sigma term*, *Phys. Rev. D* **85** (2012) 051503 [1110.3797].

[223] A. Crivellin, M. Hoferichter and M. Procura, *Accurate evaluation of hadronic uncertainties in spin-independent WIMP-nucleon scattering: Disentangling two- and three-flavor effects*, *Phys. Rev. D* **89** (2014) 054021 [1312.4951].

[224] M. Hoferichter, J. Ruiz de Elvira, B. Kubis and U.-G. Meißner, *High-Precision Determination of the Pion-Nucleon σ Term from Roy-Steiner Equations*, *Phys. Rev. Lett.* **115** (2015) 092301 [1506.04142].

[225] S. Weinberg, *Baryon and Lepton Nonconserving Processes*, *Phys. Rev. Lett.* **43** (1979) 1566.

[226] B. A. Dobrescu and C. Frugiuele, *Hidden GeV-scale interactions of quarks*, *Phys. Rev. Lett.* **113** (2014) 061801 [1404.3947].

[227] B. A. Dobrescu and F. Yu, *Dijet and electroweak limits on a Z' boson coupled to quarks*, 2112.05392.

[228] ATLAS collaboration, *A detailed map of Higgs boson interactions by the ATLAS experiment ten years after the discovery*, *Nature* **607** (2022) 52 [2207.00092].

[229] CMS collaboration, *A portrait of the Higgs boson by the CMS experiment ten years after the discovery*, *Nature* **607** (2022) 60 [2207.00043].

[230] J. Liu, X.-P. Wang and F. Yu, *A Tale of Two Portals: Testing Light, Hidden New Physics at Future e^+e^- Colliders*, *JHEP* **06** (2017) 077 [1704.00730].

[231] B. A. Dobrescu and F. Yu, *Coupling-Mass Mapping of Dijet Peak Searches*, *Phys. Rev. D* **88** (2013) 035021 [1306.2629].

[232] L. Michaels and F. Yu, *Probing new $U(1)$ gauge symmetries via exotic $Z \to Z'\gamma$ decays*, *JHEP* **03** (2021) 120 [2010.00021].

[233] ATLAS collaboration, *A search for new resonances in multiple final states with a high transverse momentum Z boson in $\sqrt{s} = 13$ TeV pp collisions with the ATLAS detector*, *JHEP* **06** (2023) 036 [2209.15345].

[234] CMS collaboration, *Search for narrow $H\gamma$ resonances in proton-proton collisions at $\sqrt{s} = 13$ TeV*, *Phys. Rev. Lett.* **122** (2019) 081804 [1808.01257].

[235] ATLAS collaboration, *Search for diboson resonances in hadronic final states in 139 fb^{-1} of pp collisions at $\sqrt{s} = 13$ TeV with the ATLAS detector*, *JHEP* **09** (2019) 091 [1906.08589].

[236] L3 collaboration, *Search for heavy neutral and charged leptons in e^+e^- annihilation at LEP*, *Phys. Lett. B* **517** (2001) 75 [hep-ex/0107015].

[237] ALEPH collaboration, *Search for charginos nearly mass degenerate with the lightest neutralino in e+ e- collisions at center-of-mass energies up to 209-GeV*, *Phys. Lett. B* **533** (2002) 223 [hep-ex/0203020].

[238] ATLAS collaboration, *Search for resonances in diphoton events at $\sqrt{s}$=13 TeV with the ATLAS detector*, *JHEP* **09** (2016) 001 [1606.03833].

[239] CMS collaboration, *Search for heavy resonances decaying into two Higgs bosons or into a Higgs boson and a W or Z boson in proton-proton collisions at 13 TeV*, *JHEP* **01** (2019) 051 [1808.01365].

[240] M. E. Peskin and D. V. Schroeder, *An Introduction to quantum field theory*. Addison-Wesley, Reading, USA, 1995.

[241] M. D. Schwartz, *Quantum Field Theory and the Standard Model*. Cambridge University Press, 2014.